

CRANFIELD UNIVERSITY

WILLIAM RUST

NAO CONTROL ON MULTI-ANNUAL PERIODICITIES IN WATER  
RESOURCES AND THEIR UTILITY FOR MANAGING WATER  
RESOURCE EXTREMES

SCHOOL OF WATER, ENERGY AND ENVIRONMENT

PhD THESIS

Academic Year: 2015 - 2021

Supervisor: Ian Holman  
Associate Supervisor: Ron Corstanje  
August 2021



CRANFIELD UNIVERSITY

SCHOOL OF WATER, ENERGY AND ENVIRONMENT

PhD

Academic Year 2015 - 2021

William Rust

NAO control on multi-annual periodicities in water resources and  
their utility for managing water resource extremes

Supervisor: Ian Holman  
Associate Supervisor: Ron Corstanje  
September 2021

© Cranfield University 2021. All rights reserved. No part of this  
publication may be reproduced without the written permission of the  
copyright owner.



## ABSTRACT

Water scarcity and the hazard of drought impacts millions of people worldwide, highlighting the need for robust water resource management. Forecasting of water resources (i.e., groundwater and streamflow) aids in the planning and preparedness for water resource extremes which, in turn, can help mitigate their societal and economic impacts. With the effects of climate change expected to exacerbate certain water resource extremes, there is increased pressure to develop improved ways to estimate future water resource behaviour. Hydrometeorological conditions in Europe are modulated by the North Atlantic Oscillation with important multiannual periodicities. Existing studies have shown that the NAO can drive multiannual periodicity behaviour in water resources and influence the timing of water resource extremes such as drought. As such, it has been discussed in hydroclimate literature that these multiannual relationships may have some utility in water resource forecasting applications. However, a systematic assessment of the relationship between the NAO and wide-scale water resources, at multiannual periodicities, has yet to be undertaken for large water resource datasets. Therefore, there is limited information to develop significant relationships between catchment properties and water resource response to multiannual NAO periodicity (e.g., magnitude, or lags), which may be of value in forecasting applications. The aim of this PhD thesis is to assess the feasibility of a relationship between the NAO and water resource variables, at multiannual periodicities, for indicating water resource behaviour (including extremes), at seasonal to multiannual timescales. This has been achieved using large hydrological datasets in the UK and the wavelet transform to characterise periodicities in these records and the NAOI. This research demonstrates that a significant and wide-spread ~7-year periodicity is exhibited by most UK water resources and has a significant relationship with the NAOI. Research presented here show that the degree of influence of this ~7-year periodicity is considerable, affecting groundwater median regional groundwater level anomalies by up to 0.71sd, and median regional streamflow anomalies by up to 0.55sd. These anomalies are also comparable to the projected effects of climate change on UK

water resources. Findings demonstrate that there are notable non-stationarities of this multiannual NAO periodicity and its relation to UK water resource variables, with the ~7-year periodicity detected in water resources only being dominant since the 1970s. This has important implications for the applicability of existing water resource forecasting systems that have utilized data from this period (of a relatively stationarity frequency structure). Findings also demonstrate a second non-stationarity between the NAO and European rainfall, producing considerable uncertainties in the detection of lags between multiannual NAO periodicities and water resource response. At present, there is limited atmospheric research to explain these modes of non-stationarity in the NAO and their influence on water resources, which poses a substantial challenge to the application of these multiannual periodicities in water resource forecasting systems. Future cross-discipline work between atmospheric and hydrological sciences may be needed to account for these non-stationarities, and to better understand how the relationship between multiannual NAO periodicities and water resource response may be used in the forecasting of water resource behaviours.

Keywords:

Groundwater, Streamflow, Teleconnections, Droughts, Water Resources, Europe, United Kingdom, North Atlantic Oscillation, Wavelet Transform

## **ACKNOWLEDGEMENTS**

*Thank you to the members of my supervisory panel, Professor Ian Holman and Professor Ron Corstanje at Cranfield University, Dr Mark Cuthbert at Cardiff University and Dr John Bloomfield at the British Geology Survey, for their guidance and support throughout this project. Thanks also to my wife, Bridie, for always providing advice and being a sounding board.*

# TABLE OF CONTENTS

ABSTRACT .....	i
ACKNOWLEDGEMENTS.....	iii
LIST OF FIGURES.....	viii
LIST OF TABLES .....	xi
LIST OF EQUATIONS.....	xii
LIST OF ABBREVIATIONS .....	xiii
1 CHAPTER 1: INTRODUCTION.....	1
1.1 Management of Water Resource Extremes .....	1
1.2 Hydroclimate Indicators and the North Atlantic Oscillation.....	2
1.3 Multiannual periodicities for water resource management .....	4
1.4 Aims and Objectives .....	8
1.5 Structure of the thesis .....	9
2 CHAPTER 2: LITERATURE REVIEW .....	1
2.1 Abstract.....	1
2.2 Introduction .....	2
2.3 Generalised conceptual model of periodic climatic signal propagation to groundwater resources .....	3
2.4 Climatic variability and teleconnections .....	5
2.4.1 Measures of climatic variability.....	5
2.4.2 Teleconnection independency.....	7
2.5 Teleconnection controls on periodic weather signals.....	7
2.5.1 Atmospheric currents and storm generation.....	8
2.5.2 Oceanic currents and thermal exchange.....	9
2.5.3 Spatial distribution of periodic precipitation anomalies .....	10
2.6 Controls on periodic recharge signals.....	13
2.6.1 Land surface processes and recharge .....	13
2.6.2 Unsaturated zone influence on recharge signals .....	13
2.6.3 Spatial sensitivity of recharge signal damping.....	17
2.7 Saturated zone influence on discharge signals.....	19
2.8 Current understanding of climatic teleconnection signal control on groundwater variability .....	22
2.9 References .....	25
3 CHAPTER 3 MULTIANNUAL PERIODICITIES IN WATER RESOURCES... 26	26
3.1 Abstract.....	26
3.2 Introduction .....	27
3.3 Data and Methods.....	29
3.3.1 Groundwater data .....	29
3.3.2 Rainfall .....	30
3.3.3 Potential Evapotranspiration (PET) .....	31



3.3.4 Methods .....	31
3.4 Results.....	40
3.4.1 Time-averaged wavelet power and significance over red noise .....	40
3.4.2 Reconstructed anomaly time series .....	42
3.4.3 Percentage standard deviation.....	42
3.5 Discussion .....	0
3.5.1 Characterisation of signal presence and strength in groundwater level.....	0
3.5.2 Evidence for teleconnection control on multi-annual groundwater variability .....	1
3.5.3 Teleconnections as indicators for groundwater extremes .....	3
3.6 Conclusions .....	5
3.7 References .....	6
4 CHAPTER 4: CATCHMENT CONTROLS ON CYCLE PROPAGATION .....	7
4.1 Abstract.....	7
4.2 Introduction .....	8
4.3 Data and Methods.....	11
4.3.1 Streamflow Data.....	11
4.3.2 Catchment Rainfall Data .....	13
4.3.3 Methods .....	16
4.4 Results.....	19
4.4.1 Average wavelet power and p values.....	19
4.4.2 Spatial distribution of wavelet powers .....	22
4.4.3 Testing of hydrological pathways .....	25
4.5 Discussion .....	27
4.5.1 Detecting a teleconnection between the NAO and UK streamflow...	27
4.5.2 Controls on multi-annual signals in catchment rainfall .....	28
4.5.3 Hydrological drivers for signal strengths.....	28
4.6 Conclusions .....	32
4.7 References .....	33
5 CHAPTER 5: NON-STATIONARITY BETWEEN NAO AND EUROPEAN RAINFALL .....	35
5.1 Introduction .....	35
5.2 Data Methods .....	37
5.3 Results.....	42
5.4 Discussion and Conclusions.....	43
5.5 References .....	46
6 CHAPTER 6: IMPLICATIONS OF NONSTATIONARY NAO PERIODICITIES FOR FORECASTING OF WATER RESOURCE EXTREMES.....	47
6.1 Abstract.....	47
6.2 Introduction .....	48

6.3 Data .....	50
6.3.1 Water resource data .....	50
6.3.2 North Atlantic Oscillation data .....	52
6.4 Methods .....	54
6.4.1 Data Pre-processing .....	54
6.4.2 Quantifying wide-spread water resource extremes .....	54
6.4.3 Frequency Transformations .....	55
6.4.4 Modulation measurement .....	58
6.5 Results .....	59
6.5.1 Multiannual water resource extremes covariance with NAOI .....	59
6.5.2 Cross-wavelet phase difference .....	61
6.5.3 Modulation of dry season water resources .....	62
6.6 Discussion .....	71
6.6.1 Historical covariances between the NAOI and water resources at multiannual periodicities .....	71
6.6.2 Phase difference between NAO and water resource records at 7.5- year periodicity .....	75
6.6.3 NAO multiannual modulations on water resources in future scenarios .....	76
6.7 Conclusions .....	81
6.8 References .....	82
7 CHAPTER 7 INTEGRATED DISCUSSION .....	83
7.1 Introduction .....	83
7.2 Influence of multiannual NAO periodicities on recorded water resource behaviour .....	83
7.3 Controls on multiannual signal propagation from the NAO to water resources .....	86
7.4 Implications of multiannual periodicities in water resources for forecasting .....	88
7.4.1 Implications of findings for existing water resource forecasting systems .....	88
7.4.2 Implications of findings for the application of multiannual NAO periodicities in new forecasting systems .....	90
8 CHAPTER 8: CONCLUSIONS .....	93
9 CHAPTER 9: FUTURE WORK .....	95
10 CHAPTER 10: REFERENCE LIST .....	97
APPENDICES .....	137
Appendix A Published Articles .....	137
Appendix B Conference Papers .....	138
Appendix C Supplementary Material .....	139



## LIST OF FIGURES

- Figure 1 Generalised conceptual model of low frequency signal propagation between climatic systems and groundwater level and discharge. .... 4
- Figure 2 Correlation between Winter NAO and Precipitation and PDSI. (based on correlation coefficients from Brandimarte et al., 2010, Cullen and DeMenocal, 2000, Fowler and Kilsby, 2002, Hurrell, 1995, Lopez-Bustins et al., 2008, Luković et al., 2015, Lavers et al., 2010, López-Moreno et al., 2011, Murphy and Washington, 2001, Queralt et al., 2009, Rogers et al., 2001, Soediono, 1989, Tabari et al., 2014, Türkeş and Erlat, 2003, Uvo, 2003, Wang et al., 2015, Wilby et al., 1997). .... 11
- Figure 3 Composite plan combining NAO correlation with PPT and PDSI (Figure 1) into a 0.5° point grid, and expected damping capacity of the unsaturated zone inferred from modelled depth-to-groundwater data produced by Fan et al. (2013), where size of circles is proportional to expected damping capacity. .... 18
- Figure 4 Conceptual model of signal propagation from Teleconnection through to groundwater discharge, using the NAO in the UK as an example. .... 23
- Figure 5 Location of the observation borehole locations used in this study. Boreholes within 0.5 km of another have been displaced and denoted on a grey circle for visibility. .... 30
- Figure 6 Normalised average wavelet power spectra (left) and wavelet power significance alphas (right) for monthly groundwater levels in the 59 index boreholes (grouped by aquifer type). In the right-hand figure, boxes outlined in white are those powers that are significant over red noise to a 95% confidence interval ( $\alpha \leq 0.05$ ). .... 35
- Figure 7 Normalised average wavelet power spectra (left) and wavelet power significance alphas (right) for monthly rainfall time series for co-locations of the 59 index boreholes. In the right-hand figure, boxes outlined in white are those powers that are significant over red noise to a 95% confidence interval ( $\alpha \leq 0.05$ ). .... 36
- Figure 8 Overlaid reconstructions of the three key periodic domains found across the 59 groundwater wavelet spectra are shown. All periods (both significant and non-significant) within these bands have been displayed to allow for comparison of period strength and phase over time. Areas shaded blue represent approximate periods of significant droughts in the UK. Only reconstructions between 1955 and 2017 are shown to allow clearer comparison. .... 37
- Figure 9 Overlaid rainfall (left) and PET (right) reconstructions of the three key periodic domains are shown. All periods (both significant and non-significant) within these bands have been displayed to allow for comparison of period strength and phase over time. Areas shaded blue represent approximate

periods of significant droughts in the UK. Only reconstructions between 1955 and 2017 are shown to allow clearer comparison.....	38
Figure 10 Maps showing strength (percentage of the original time series standard deviation) and significance of the a) 1 year, b) ~7 year and c) 16-32 year periodicity bands. No periodicity strength was found to be above 60% of the original signal.....	39
Figure 11 Locations of streamflow gauges used in this study. ....	13
Figure 12 Spatial distribution of (a) baseflow index (BFI), (b) log <sub>10</sub> (GRT) and (c) standard average annual rainfall (SAAR) for each streamflow record. ....	14
Figure 13 Stacked streamflow wavelet spectra power (a, c, e) and p values (b, d, f) from the normalised monthly, winter and summer resolution data of 705 catchments. The 95 % confidence interval is shown as a dashed black line in the right column figures. The opacity of each average spectra line has been lowered to allow general trends to be identified.....	20
Figure 14 As in Figure 13 but for catchment rainfall data. ....	21
Figure 15 Spatial distribution of P7 wavelet power and significance in catchment rainfall and streamflow for winter- and summer-averaged data sets. ....	24
Figure 16 (a) Jittered scatterplots for residual wavelet powers in winter and summer, categorised by BFI; bold black points mark the average residual wavelet power for each BFI category. (b) Comparison of these median residual wavelet powers with significant changes between groups (shown as solid lines) and non-significant changes between groups (shown as dashed lines).....	26
Figure 17 As in Figure 16 but for the groundwater response times (GRTs). ....	26
Figure 18 Pearson's r correlation between NAOI and rainfall using 1991 to 2016 winter data (DJFM) .....	39
Figure 19 Cluster analysis of 10-year rolling correlation series for Western Europe. Grey lines represent the individual rolling correlation series in each cluster while the coloured lines represent the centroids (medoids) of each cluster. Dotted grey lines represent the 95% CI. ....	40
Figure 20 10 year moving correlation analysis for selected Western Europe nation-based regions. The two most dissimilar (inverse Pearson's correlation) rolling correlation series are displayed with the colours lines and their location is displayed on the inset map. Dotted grey lines represent the 95% CI.....	41
Figure 21 - Spatial and temporal distributions of water resource records; a) location of groundwater boreholes coloured by associated aquifer group, b) jitter plot of groundwater record lengths within each aquifer group, c) location	

of streamflow gauges coloured by associated regional group, d) jitter plot of streamflow record lengths within each regional group .....	53
Figure 22 - a) Significance (95% CI) contours between GWL and NAOI, b) time-averaged proportion of gwl records with a significant XWP with the NAOI (measured as a decimal fraction), c) wavelet (spectral) power of GWL drought series, d) time-averaged wavelet (spectral) power of GWL drought series, e) GWL drought coverage time series, f) temporal coverage of records.....	64
Figure 23 - a) Significance (95% CI) contours between SF and NAOI, b) time-averaged proportion of SF records with a significant XWP with the NAOI (measured as a decimal fraction),c) wavelet (spectral) power of SF drought series, d) time-averaged wavelet (spectral) power of SF drought series, e) SF drought series showing proportion of records in drought each year, f) temporal coverage of records.....	66
Figure 24 - Phase difference between the NAOI and each GWL record for the GWL record period. Results are grouped by aquifer regions. $\phi = 0$ is equivalent to an in-phase relationship and $\phi = \pm\pi$ is equivalent to an antiphase relationship.....	68
Figure 25 - Phase difference between the NAOI and each streamflow record for the streamflow record period. Results are grouped by aquifer regions. $\phi = 0$ is equivalent to an in-phase relationship and $\phi = \pm\pi$ is equivalent to an antiphase relationship.....	69
Figure 26 - Distribution of absolute mean and maximum modulation of summer groundwater level as a result of the principal cross-wavelet periodicity between the NAOI and winter Groundwater level by aquifer region .....	70
Figure 27 - Modulation of summer streamflow (relative to record standard deviation) as a result of the principal cross-wavelet periodicity between the NAOI and winter streamflow.....	71

## LIST OF TABLES

Table 1 - Synthesis of Table 3 from Jackson et al (2015). Median results from the absolute teleconnection modulation on groundwater level from Figure 3 of this paper are also presented for the mean and maximum modulation cases. NAO teleconnection modulations greater than the reported 50 <sup>th</sup> percentile climate change modulation are shaded in grey. ....	79
---	----

## LIST OF EQUATIONS

Note: Some duplicate equations are listed due to the use of published papers in this thesis.

Equation 1 – Continuous Wavelet Transform

Equation 2 – Reverse Wavelet Transform

Equation 3 – Groundwater Response Time

Equation 4 – Continuous Wavelet Transform

Equation 5 – Peters (2003) drought threshold

Equation 6 – Continuous Wavelet Transform

Equation 7- Continuous Wavelet Power

Equation 8 – Cross-Wavelet Transform

Equation 9 – Cross-Wavelet Power

Equation 10 – Wavelet Phase Difference

Equation 11 – Cross-Wavelet Reconstruction



## LIST OF ABBREVIATIONS

AMO	Atlantic Multidecadal Oscillation
AMOC	Atlantic Meridional Overturning Current
AO	Arctic Oscillation
AR1	Lag-1 Autocorrelation
BFI	Baseflow Index
CI	Confidence Interval
COI	Cone of Influence
CWP	Continuous Wavelet Power
CWT	Continuous Wavelet Transform
DJF	December, January, and February
DJFM	December, January, February, and March
DWF	Deep Water Formation
EA	East Atlantic Pattern
ENSO	El-Nino Southern Oscillation
EOF	Empirical Orthogonal Function
ET	Evapotranspiration
FP	Focal Point
GCM	Global Climate Model
GDP	Gross Domestic Product
GRT	Groundwater Response Time
GS	Gulf Stream
GWL	Groundwater Level
JJA	June, July, and August

MWU	Mann-Whitney U test
NAO	North Atlantic Oscillation
NAO-	Negative NAO phase
NAO+	Positive NAO phase
NAOI	NAO Index
NAO-P	Relationship between NAO and precipitation
NGLA	National Groundwater Level Archive
NRFA	National River Flow Archive
P1	Approximate 1-year periodicity
P7	Approximate 7-year periodicity
P16-32	16- to 32-year periodicity
PCA	Principal Component Analysis
PDO	Pacific Decadal Oscillation
PDSI	Palmer Drought Severity Index
PET	Potential Evapotranspiration
POL	Polar-Eurasian Pattern
PPT	Precipitation
QBO	Quasi-Biennial Oscillation
RBD	River Basin District
RWP	Residual Wavelet Power
SAAR	Standardised Average Annual Rainfall
SCAND	Scandinavia Pattern
sd	Standard Deviation
SF	Streamflow
SGI	Standardised Groundwater Index

SLP	Sea Level Pressure
SPI	Standardised Precipitation Index
SSA	Singular Spectrum Analysis
SST	Sea Surface Temperature
TC	Teleconnection
UK	United Kingdom
USA	United States of America
USD	United States Dollars
WT	Wavelet Transform
XWP	Cross-Wavelet Power
XWT	Cross-Wavelet Transform



# 1 CHAPTER 1: INTRODUCTION

## 1.1 Management of Water Resource Extremes

Sufficient availability of water resources is critical for the functioning of societies and ecosystems. Economies globally are dependent on water resources for drinking water supply, food production (e.g., crop irrigation or livestock), manufacturing, power generation (e.g., hydropower), transportation and recreational uses (Kloosterman, et al, 2021; Ran et al, 2016; Becker, 2016; Loucks and Beek, 2017; Mideksa and Kallbekken, 2010; Gibbons et al, 2014). For instance, water resources underpin 4 trillion USD of annual European turnover (Schellekens et al, 2018) and over 6 trillion USD of annual turnover in the United States (EPA, 2013). As such, many countries have management regimes in place to ensure water supply is resilient to changes in use, weather, and climate.

Hydrological droughts are extreme deficits of water resources, typically as a response to below-average rainfall, at a seasonal scale or greater (Mishra and Singh, 2010). Droughts can be acute (e.g., the 1975-76 drought in the UK (Rodda and Marsh, 2011), or chronic (e.g., the recent near-decadal drought in California, USA (Woodhouse et al, 2020)), and often effect a wide spatial domain with simultaneous impacts on multiple water resources (e.g., groundwater level and streamflow (Turner et al, 2021)). As such, they are one of the most impactful natural hazards on human activities (Wilhite, 2000), as well as exacerbating other hazards such as wildfires, waterborne diseases (through a degradation water quality), and ecosystem collapse (Bergstrom et al, 2021). Different geographies may be more or less resilient to the impacts of droughts, depending on the region's hydrometeorological characteristics and its dependence on certain water resources. For instance, the impact of drought has been shown to be greatest in regions that depend on agricultural industry, such as central southern Europe and southeast UK (Forzieri et al, 2018). The World Bank Group (2016) puts the average economic cost of drought at up to 6% of regional GDP per year. As a response to this, many water management practices are concerned with

understanding which water resources may be at increased risk of drought across a range of future time horizons (e.g., from a seasonal to a multiannual timescale). Being able to identify which resources may be at increased risk of drought, over time and spatially, can help inform short-term drought response measures (e.g., restrictions on certain types of water use, such as hose pipe bans), as well as long-term planning interventions (e.g., infrastructure investment or maintenance).

The challenge of managing water resources has been exacerbated by the ongoing effects of climate change on global hydroclimate processes over recent decades (Padron et al, 2020, Riedel and Webber, 2020). Projected climate change scenarios indicate that periods of water resource extremes may become greater and more common in certain regions, for instance in mid-latitude regions which are expected to experience decreased rainfall and increased warming (Cook et al 2018). Europe is expected to experience some of the greatest divergence of water resource extremes in future climate change scenarios (Forzieri, et al, 2018; Stagge et al, 2017; Rousi et al, 2021); the effects of which have already been detected in European water resource records (Stagge et al 2017). At present, drought accounts for around €9 billion of economic impact in the EU and the UK per year (Cammalleri et al, 2020). Whereas a combination of future climate change and population growth mean that drought in the region could cost more than €65 billion per annum, depending on climate change projections (Feyen et al, 2020). As a response to these pressures, there has been recent efforts to develop improved ways to forecast, project or understand future water resource behaviour and risk of extremes (Chang and Guo, 2021, Samaniego et al, 2019).

## **1.2 Hydroclimate Indicators and the North Atlantic Oscillation**

A common method for estimating current or future water resource behaviour (including extremes, such as drought) is through the use of indicators (Massmann, 2020). These are measurements of geophysical systems that exhibit a sufficient systematic or driving relationship with hydrometeorological variables, which can be used to model water resource behaviour without the need for direct

measurement. Modelling approaches can range from simple regression analysis, to more complex Earth System Models (Oschlies et al, 2016). In the case of estimating future water resource behaviour, a systematic lag between an indicator and a hydrometeorological variable can provide a short-term forecast of that variable, often at a seasonal scale (e.g., Demirel et al, 2013). An example of this is Sea Surface Temperature (SST), which has been used to forecast precipitation anomalies at a seasonal timescale in the UK (e.g., Mahmood et al, 2021). Projected indicator values may also be available from global climate models (GCM) (Eum et al, 2020) and may therefore offer a simple way to estimate likely water resource states under climate change projections.

Oscillatory atmospheric or oceanic systems (such as El Nino Southern Oscillation (ENSO), or Pacific Decadal Oscillation (PDO)) (often known as teleconnection systems) are also used to indicate broad-scale water resource behaviour, given their established modulation of meteorological processes globally (e.g., Calado et al, 2019; Ionita and Nagavcuic, 2020; Forootan et al, 2016). These systems typically span synoptic scales and can directly influence moisture transport via atmospheric and oceanic pathways (Vazquez et al, 2021, Gimeno et al, 2016). Consequently, indices of these teleconnection systems have been shown to covary with country- to continental-scale hydrometeorological behaviour (West et al, 2019; Chiew and McMahon, 2002; Kashid et al, 2010), making them favourable indicators when assessing wide-scale hydrological hazards such as drought (e.g., Forootan et al, 2018, Kim et al, 2017; Allen and Anderson, 2018). For instance, ENSO has been shown to have utility in forecasting drought conditions in Pacific regions such as west coast USA (Ryu et al, 2010), Australia (Barros and Bowden, 2008) and Asia (Lü et al, 2011), as well as further-reaching influences on water resources in Africa (Kolusu et al, 2019) and Europe (Sprouse and Vaughan, 2003).

The dominant mode of atmospheric variability in the North Atlantic region is the North Atlantic Oscillation (NAO) (Hurrel, 1995; Hurrel and Deser, 2010). The NAO represents the north-south pressure gradient in the North Atlantic which modulates moisture and heat transport to Europe via the jet stream and Gulf

Stream (López-Moreno et al., 2011; Alexander et al., 2005; Hurrell and Deser, 2010). As such, the NAO has been shown to be a dominant control on winter-time meteorological variables in Europe (such as rainfall and evapotranspiration (Trigo et al, 2002, Criado-Aldeanueva et al, 2014)), and can therefore exhibit a secondary control on hydrological variables including streamflow (Wrzesiński and Paluszkiwicz, 2011; Svensson et al 2015), groundwater level (Luque-Espinar et al 2008) and springflow (Burt and Howden, 2013). Furthermore, the NAO has been associated with hydrological extremes of flooding (e.g., Guimarães Nobre et al, 2017) and drought (e.g., Brady et al, 2019; Queralt et al, 2009). As such, the NAO index (NAOI) has been used in seasonal forecasting applications for water resources (e.g., for streamflow (Donegan et al, 2021)), or in existing early warning systems for hydrological behaviour and extremes (e.g., the UK's Hydrological Outlook (Svensson et al, 2015, Bonaccorso et al, 2015)).

### **1.3 Multiannual periodicities for water resource management**

Oscillatory ocean-atmosphere systems can exhibit multiannual periodicities as a result of planetary wave dynamics driven by changes in solar radiation (e.g., through variable solar activity or orbital cycles) (Zanchettin et al, 2008; Sagir et al, 2015) or as emergent behaviours from stochastic processes (Deser et al, 2017). These periodicities can range in length from 2 years (e.g., Quasi-Biennial Oscillation (QBO)) to multiple decades (e.g., the Atlantic Multidecadal Oscillation (AMO) (Kane, 1996; Kerr, 2000)). As such, and through their control on meteorological processes (previously discussed), these systems have been shown to influence the frequency structure of water resources globally (e.g., in the USA (e.g., Kuss and Gurdak, 2014), Europe; (e.g., Liesch and Wunsch, 2019) and Asia (e.g., Lee and Zhang 2011)). Existing research has highlighted that water resources with longer response times (such as groundwater pathways) exhibit a greater sensitivity to multiannual behaviours in teleconnection systems (e.g., Gurdak et al., 2007; Tremblay et al., 2011). For instance, Kuss and Gurdak (2011) found that groundwater levels in the USA's North Atlantic coastal plains aquifer exhibited up to 50% control (percent variance of cumulative departure



series) from multiannual periodicities in ENSO and 40% control for the Pacific Decadal Oscillation (PDO). In Europe, hydroclimate case studies on water resource records (such as groundwater level (e.g., Holman et al 2011) or streamflow (e.g., Uvo et al, 2021)) have demonstrated significant relationships with the NAOI at multiannual periodicities, covering a wide spatial domain. For instance, Liesch and Wunsch (2019) found significant covariances between 9 groundwater level boreholes in the UK, Germany, Netherlands and Denmark, and multiple atmospheric indices (including the NAOI). Furthermore, Neves et al (2019) identified significant covariances between the NAOI and groundwater level in Portugal and identified a link between this relationship and instances of wide-spread groundwater drought in the Iberian Peninsula.

Given the distribution of multiannual periodicities that have been identified in European water resource records, and their dependence on the NAO (e.g., Holman et al, 2011; Uvo et al, 2021), existing hydroclimate studies have highlighted that multiannual NAO periodicities may have some utility for indicating future water resource behaviour (e.g., Neves et al, 2019; Liesch and Wunsch, 2019). This may be possible through three methods:

1. Utilising a systematic lag between NAO periodicities and water resource response (for instance, due to catchment characteristics), to provide improvements in short- to medium-term water resource forecasts (e.g., at a seasonal scale).
2. Augmenting existing water resource projections (such as Bisselink et al, 2020 or HR Wallingford, 2020) with indicative multi-year phases of decreased water resource anomaly (deviation from mean), which may prime wide-scale water resources to be more susceptible to drought. This may be achievable either through extrapolating historical periodic trends, detected in existing water resource records, or through utilising long-range projections of the NAOI which are becoming increasingly available from GCMs (e.g., Athanasiadis et al., 2020; Dunstone et al., 2016).
3. A combination of the above two methods.

These potential methods would be based on historical relationships between the NAOI and water resources, which need to be detectable in existing records. So that a utility from these multiannual NAO periodicities can be applied to new scenarios, there is a requirement for a systematic understanding of how these periodicities are transformed by atmospheric, meteorological, and hydrological systems, to produce specific water resources behaviours over time and space. This is particularly important if these potential utilities are to be applied in climate change scenarios, as many of the interactions between these geophysical systems may change as a result of increasing global temperatures (Kjellström et al, 2013; Hagemann et al, 2013). Furthermore, hydrological drought is a wide-scale hazard (Hannaford et al, 2011) meaning that, in order for multiannual NAO periodicities (and their relationship with water resources) to have utility in drought management regimes, an understanding of wide-scale (e.g., catchment- to national-scale) water resources' sensitivity to NAO periodicities is required. For instance, the utility of these multiannual behaviours may be limited if they are only influential on a small number of water resources, or if this influence produces a minimal affect in water resource behaviour. These requirements can be summarised as an understanding of how water resources, at a broad scale and in variety of different geographical and hydrological characteristics, respond to multiannual periodicities in the NAO.

Much existing research into multiannual teleconnection influence on water resources in Europe has been exploratory, focusing on whether relationships are detectable or significant, and how these multiannual periodicities relate to historical water resource extremes (e.g., Neves et al, 2019; Holman et al, 2011). These studies generally use small sample sizes to produce case studies of historical relationships with the NAOI. This may be because most existing multiannual hydroclimate teleconnection studies have utilized computationally-demanding frequency analyses such as the wavelet transform (e.g., Kuss and Gurdak, 2011; Holman et al, 2011; Küçük, et al, 2009; Fritier et al, 2012; Velasco et al., 2015). The wavelet transform is often favoured over other frequency transforms, such as the Fourier transform (Nakken, 1999; Pasquini et al., 2006), for its ability to assess time-varying periodicities in noisy datasets such as

hydrological variables (Sang et al, 2013). Most multiannual teleconnection studies have focused on 10 sites or fewer (e.g., Holman et al, 2011; Neves et al, 2019; Mullon et al, 2013; Küçük,et al, 2009; Ouachani et al, 2013), meaning there is limited data to demonstrate the extent to which multiannual NAO periodicities are expressed across wide-scale water resource records. Furthermore, few studies have investigated the relationships between multiannual NAO periodicities in water resources and meteorological drivers such as rainfall or evapotranspiration. As such, the role of different atmospheric, meteorological or hydrological systems in modulating these relationships has not been assessed.

## 1.4 Aims and Objectives

The aim of this PhD thesis is to assess the feasibility of a relationship between the NAO and water resource variables, at multiannual periodicities, for indicating water resource behaviour (including extremes), at seasonal to multiannual timescales. Specifically, the objectives are to:

1. Characterise multiannual periodicities in a large dataset of water resource records and assess their relation to wide-scale recorded droughts.
2. Test the influence of catchment characteristics on the propagation of multiannual periodicities between rainfall and water resource response.
3. Evaluate the spatiotemporal stability in the relationship between the NAOI and European rainfall.
4. Assess the extent to which non-stationarities in the relationship between the NAOI and water resources, at multiannual periodicities, effect the feasibility of this relationship for indicating future water resource behaviour or extremes.

## 1.5 Structure of the thesis

This thesis is organised in a paper format consisting of this introductory chapter, five manuscript-chapters that has been published in (or submitted to) high-impact peer-reviewed journals, followed by a discussion, conclusion and future work chapter. An overview of each chapter is given as follows:

Chapter 2 provides a review of current literature on the relationship between teleconnection systems and multiannual groundwater variability in Europe. This focuses on the development of a conceptual model for expected modulations of multiannual periodicities between the NAO and water resources. This chapter is comprised of the following published article:

*Rust, W., Holman, I., Corstanje, R., Bloomfield, J., and Cuthbert, M.: A conceptual model for climatic teleconnection signal control on groundwater variability in Europe, Earth-Sci. Rev., 177, 164–174, 2018.*

Chapter 3 addresses research objective 1 by quantifying the multiannual periodic behaviour of groundwater resources using a large dataset of observation boreholes in the UK. This chapter is comprised of the following published article:

*Rust, W., Holman, I., Bloomfield, J., Cuthbert, M., and Corstanje, R.: Understanding the potential of climate teleconnections to project future groundwater drought, Hydrol. Earth Syst. Sci., 23, 3233–3245, 2019.*

Chapter 4 addresses research objective 2 by investigating the modulation of multiannual periodicity strength between rainfall and streamflow, and its dependence certain catchment characteristics. This chapter is comprised of the following published article:

*Rust, W., Cuthbert, M., Bloomfield, J., Corstanje, R., Howden, N., and Holman, I.: Exploring the role of hydrological pathways in modulating multi-annual climate teleconnection periodicities from UK rainfall to streamflow, Hydrol. Earth Syst. Sci., 25, 2223–2237, 2021a.*

Chapter 5 addresses objective 3 by assessing the degree of spatiotemporal non-stationarity of the relationship between the NAOI and European rainfall, and

examining its implications for water resource forecasting utilities. This chapter is comprised of the following published article:

*Rust, W., Bloomfield, J. P., Cuthbert, M. O., Corstanje, R., and Holman, I. P.: Non-stationary control of the NAO on European rainfall and its implications for water resource management, Hydrol. Process., 35, <https://doi.org/10.1002/hyp.14099>, 2021b.*

Chapter 6 addresses objective 4 by assessing the feasibility of the relationship between the NAOI and water resources, at multiannual periodicities, for indicating future water resource extremes. This involves investigating non-stationarities in this relationship and assessing its influence on water resources in the context of climate change projections.

*Rust, W., Bloomfield, J., Cuthbert, M., Corstanje, R., and Holman, I.: The importance of non-stationary multiannual periodicities in the NAO index for forecasting water resource extremes, Hydrol. Earth Syst. Sci. Discuss. [preprint], <https://doi.org/10.5194/hess-2021-572>, in review, 2021.*

Chapter 7 provides an integrated discussion that will draw together the outcomes from the five previous chapters and demonstrates how these produce a unified piece of research that addresses the aims and objectives of this thesis.

Chapters 8 and 9 conclude the research undertaken in this PhD thesis and provide an overview of the further work that is required to progress this discipline.

Finally, the text of chapters 2 to 6 is unchanged from the published manuscripts, except for section and figure numbering, which has been updated to be consistent across this thesis, and references to these numbers throughout the manuscript text. The reference lists from each of these papers have been combined into the final reference list of the thesis, which also contains references for the introduction and integrated discussion.

## **2 CHAPTER 2: LITERATURE REVIEW**

This chapter consists of the published article Rust et al (2018); “A conceptual model for climatic teleconnection signal control on groundwater variability in Europe”. The following sections are sections taken directly from this manuscript.

### **2.1 Abstract**

The ability to predict future variability of groundwater resources in time and space is of critical importance to drought management. Periodic control on groundwater levels from oscillatory climatic systems (such as the North Atlantic Oscillation) offers a potentially valuable source of longer-term forecasting capability. While some studies have found evidence of the influence of such climatic oscillations within groundwater records, there is little information on how periodic signals propagate between a climatic system and a groundwater resource.

This paper develops a conceptual model of this relationship for groundwater resources in Europe, based on a review of current research. The studies reviewed here reveal key spatial and temporal signal modulations between climatic oscillations, precipitation, groundwater recharge and groundwater discharge. Generally positive correlations are found between the NAO (as a dominant influence) and precipitation in northern Europe indicating a strong control on water available for groundwater recharge. These periodic signals in precipitation are transformed by the unsaturated and saturated zones, such that signals are damped and lagged. This modulation has been identified to varying degrees, and is dependent on the shape, storage and transmissivity of an aquifer system. This goes part way towards explaining the differences in periodic signal strength found across many groundwater systems in current research.

So that an understanding of these relationships can be used by water managers in building resilience to drought, several research gaps have been identified. Among these are improved quantification of spatial groundwater sensitivity to periodic control, and better identification of the hydrogeological controls on signal lagging and damping. Principally, research needs to move towards developing

improved predictive capability for the use of periodic climate oscillations as indicators of longer-term groundwater variability.

## **2.2 Introduction**

A number of studies have identified significant extra-annual periodic signals in long-term groundwater records (Holman et al., 2011, Holman, 2006, Kuss and Gurdak, 2014, Velasco et al., 2017, Cao et al., 2016, Dickinson et al., 2014). Such signals are understood to be ultimately driven by oscillatory climatic systems, such as the El-Niño Southern Oscillation (ENSO) and the North Atlantic Oscillation (NAO) (Kingston et al., 2006). Currently there is no conceptual model that describes how these extra-annual periodic signals are propagated and transformed by meteorological and hydrogeological processes. Thus, the spatial and temporal variability of low-frequency signal strength found in groundwater data cannot be systematically explained at present. These long-period signals offer a source of improved forecasting capability for hydrogeological response, thereby representing a potentially valuable area of development for systematic understanding of groundwater variability (Kingston et al., 2007, Kuss and Gurdak, 2014, Water UK, 2016, Kingston et al., 2006, Van Loon, 2013, Tallaksen et al., 2006).

Many operational assessments of hydrogeological resilience to drought are based on the premise that describing response to annual fluctuation in groundwater recharge is sufficient for resource management (Environment Agency, 2013, Kingston et al., 2006). Annual variability typically represents a large proportion of the total variance observed in long-term groundwater records (Holman et al., 2011). As such it is a useful component in identifying groundwater sensitivity to catchment characteristics (Rust et al., 2014). However, as a requirement of the predictive modelling used for many water resource investigations (Van Loon, 2015), statistical assessments of groundwater records often assume variance and autocorrelation are stationarity at extra-annual scales (Milly et al., 2008). Therefore, the systematic periodic controls on groundwater resources at extra-annual scales have not traditionally been considered



(Kingston et al., 2006, Currell et al., 2014, Alexander et al., 2005, Folland et al., 2015, Hanson et al., 2006, Kuss and Gurdak, 2014, Bloomfield et al., 2003).

While parts of the systematic linkage between climate and groundwater have been assessed in isolation by previous studies, the current lack of a unifying model means that existing information on these periodic controls cannot be readily used to inform groundwater management decisions. Given the potential for improved prediction of groundwater variability, this information should allow for more effective planning for social, ecosystem, and infrastructure resilience to drought (Kingston et al., 2006, Van Loon, 2013, Van Loon, 2015). This is of particular importance in Europe, which has received little focus in groundwater teleconnection literature to date. In this paper we review existing research on hydroclimatological linkages and signal propagation through the water cycle to produce a conceptual model of how periodic climatic variability drives sympathetic signals in groundwater systems in Europe.

### **2.3 Generalised conceptual model of periodic climatic signal propagation to groundwater resources**

A generalised conceptual model of the control linkages within the water cycle between periodic climate systems and groundwater response is shown in Figure 1. The first two stages of this figure conceptualise the generation and propagation of low-frequency climate and weather signals, while the last two stages conceptualise how those signals propagate through the land surface and groundwater system via groundwater recharge and discharge. By assessing the current evidence base in each of these four stages, here we develop a conceptual model for spatiotemporal signal propagation between climate and groundwater systems in Europe, and identify knowledge gaps. In the following sections we assess the spatial distribution of climatic systems in the North Atlantic region (Section 2.4), the evidence for signal generation and spatial propagation through coupled climate and weather systems (Section 2.5) and finally signal transformations through the groundwater system (2.6, Controls on periodic recharge signals; 2.7, Saturated zone influence on discharge signals).

### 1. Climate variability

Climatic systems comprising components of atmospheric and / or oceanic circulations, exhibiting low frequency variability.



### 2. Control on Periodic weather signals

Spatial distribution of precipitation, and temperature variability in the UK and Europe is, at least partly, driven by complex relationships with atmospheric and oceanic currents.



### 3. Control on periodic recharge signals

Signals of local variability in precipitation and evapotranspiration are converted to groundwater recharge through flow and storage processes in the surface, root and unsaturated zones.



### 4. Control on periodic discharge signals

Signals of groundwater recharge are captured across the spatial domain of an aquifer, and are converted to signals of groundwater level and discharge to springs or river base flow, through saturated zone processes.

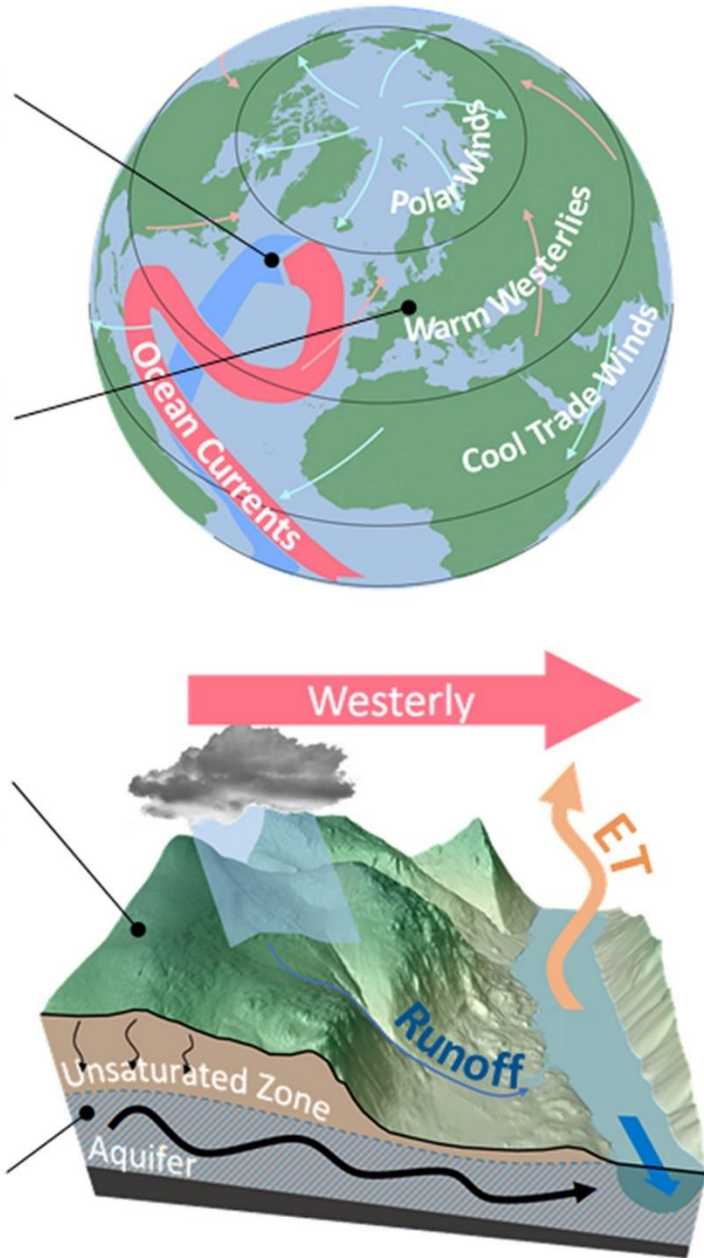


**Figure 1 Generalised conceptual model of low frequency signal propagation between climatic systems and groundwater level and discharge.**

## **2.4 Climatic variability and teleconnections**

### **2.4.1 Measures of climatic variability**

Research into hydroclimatology often relies on statistical assessments between climatic anomalies and hydrological datasets. Anomalies are defined as the difference between a measured climate variable (for instance sea level pressure (SLP)) and the normal state, usually the temporal mean, of that variable. They are therefore useful metrics for comparing measurements at different locations within a climate system (Hurrell et al., 2003).

Teleconnection (TC) indices are constructed from anomalies at different locations within a system of atmospheric or oceanic variability (such as the NAO), giving a spatial picture as to the state of the system. TC indices are often described in terms of their phase as departures from the mean, either a positive or negative phase. This indicates which anomaly is most dominant and therefore which mode the system is in. For instance the El Niño or La Niña mode in the case of the El Niño Southern Oscillation (ENSO). TC indices often exhibit multiscale periodic variability as a result of complex non-linear processes within atmospheric and oceanic dynamics (Hauser et al., 2015, Hurrell and Van Loon, 1997). These indices are therefore favoured by hydroclimatologists as a tool to measure hydrological sensitivity to climatic circulations. (Kingston et al., 2006, Loboda et al., 2006).

A broad range of TCs have been studied in the past such as NAO (Hurrell, 1995), ENSO (Wang and Kumar, 2015), Pacific Decadal Oscillation (Routson et al., 2016, Kuss and Gurdak, 2014), Atlantic Multidecadal Oscillation (Wyatt et al., 2012), and Arctic and Antarctic Oscillation (Tabari et al., 2014), as well as other indicators of climate and oceanic variability such as sea surface temperature (SST) (Wilby et al., 1997). While it is not the intention of this paper to provide an exhaustive review of TCs, here we focus on recent TC research of potential relevance to groundwater systems in Europe. Such circulations are described in the following sections.

#### **2.4.1.1 North Atlantic Oscillation (NAO)**

The NAO is a dipole of SLP anomalies between semi-permanent centres of action in the North Atlantic: the Azores (Sub Tropical) High and the Icelandic (Sub Polar) Low (Hurrell et al., 2003). The oscillation exhibits a principle periodicity of 8–9 years, and a secondary periodicity of 3–5 years, which are seen principally in winter index values (Hurrell and Deser, 2010). Its variability is understood to be partially driven by quasi-stationary planetary waves (Hurrell, 1995, Trenberth, 1993).

The NAO is the dominant mode of atmospheric behaviour throughout the year in the North Atlantic region (Dickson et al., 1999). It can account for up to 30% of the variability in SST (Shabbar et al., 2001) and 50% of winter weather variability in Europe (Hurrell and Van Loon, 1997, Cassou et al., 2003, Fritier et al., 2012). Although the NAO is principally influential on European regional climate, its influence extends, to a lesser extent, to Africa, China and the USA (López-Moreno et al., 2011, Lee and Zhang, 2011, Wang et al., 2015, Magilligan and Graber, 1996).

#### **2.4.1.2 East Atlantic pattern (EA)**

The East Atlantic (EA) pattern has a similar spatiotemporal structure to the NAO, but shifted southwest within the Atlantic region. The EA exhibits a strong multi-decadal mode of variability (Holman et al., 2011) and is the second most prominent mode of low frequency variability in the North Atlantic Region (Wallace and Gutzler, 1981). The effect of the EA on regional climate closely mirrors that of the NAO, however it has been shown to exhibit internal variability (Hauser et al., 2015, Tošić et al., 2016).

#### **2.4.1.3 Arctic Oscillation (AO)**

The Arctic Oscillation (AO) is also known as the Northern Hemisphere Annual Mode (Climate Prediction Centre, 2015a). It is characterised by pressure anomalies over the Arctic, with other anomalies centred on latitudes of 37–45° N (Givati and Rosenfeld, 2013). The temporal variability of the AO is similar to that of the NAO, with a November–April correlation of 0.95 (Deser, 2000). As a result

of this, the AO exhibits a similar modulation on moisture and heat exchange in Europe to the NAO. Wallace and Gutzler (1981) suggests that the NAO is a regional expression of the larger AO, however the majority of research accepts that the NAO and AO are internally variable, in some instances influencing each other (Dickson et al., 2000).

#### **2.4.1.4 Scandinavia pattern/Polar – Eurasian Pattern (POL)**

The Scandinavia pattern (SCAND), also referred to as the Eurasia-1 Pattern (Bramston and Livezey, 1987) or the Polar-Eurasian Pattern (POL), consists of a primary circulation centre over Scandinavia with weaker centres of opposite phase over Western Europe and eastern Russia/western Mongolia (Saunders et al., 2012, Wedgbrow et al., 2002, Climate Prediction Centre, 2005b). Although no strong periodicity is given in the literature, Holman et al. (2011) suggest that the Scandinavia pattern exhibits relatively large inter-seasonal, inter-annual and inter-decadal variability.

#### **2.4.2 Teleconnection independency**

Wyatt et al. (2012) and Walter and Graf (2005) found significant co-variances between all North Atlantic indices, suggesting that most individual TC systems are not internally variable and are driven by a wider system. Despite these findings, Lavers et al. (2010) and Cooper (2009) argue that any attempt to confine such complex non-linear systems to univariate or bivariate measures will always fail to account for true variability. Given this, they are still useful tools so long as their assumptions are well understood throughout their analysis (Hurrell et al., 2003).

## **2.5 Teleconnection controls on periodic weather signals**

The amount of recharge to a given groundwater store is related to the amount of precipitation (PPT) and evapotranspiration (ET) received. These two processes are therefore critical carriers of periodic signals between climatic systems and

groundwater response. In order to explain the character of extra-annual periodic signals found in groundwater stores, it is first necessary to assess the role of weather systems. In the following section we firstly review the causal relationships between climatic systems and moisture and thermal exchange, and secondly the subsequent impacts on PPT and ET across Europe.

### **2.5.1 Atmospheric currents and storm generation**

North Atlantic westerlies and the Arctic Polar Jetstream affect the distribution of storm activity and wider thermal and moisture exchange over Europe (Joyce et al., 2000, Alexander et al., 2005, Feser et al., 2015). For example, the strength and location of the Polar Jetstream has been shown to account for approximately a third of winter storm variability in Western Europe (Alexander et al., 2005).

Since the NAO represents a system of pressure distribution in the North Atlantic, it can directly modulate transatlantic pressure gradients and therefore westerly strength (Feser et al., 2015). Strong westerlies enhance the advection of warm moist air from the Atlantic, creating stronger and more frequent cyclones along the North Atlantic storm track (Trigo et al., 2002). Additionally, decreased atmospheric pressure over Iceland, seen in the NAO +, is associated with an increase in the meridional tilt of the North Atlantic storm track (Walter and Graf, 2005). Thereby, there is an increased likelihood of larger storms reaching north-western Europe and propagating into central Europe during a NAO +. For example, Trigo et al. (2004) shows that PPT in western Europe is coverable with the NAO's periodicities, at a minimal lag. The NAO's control on ET is typically lagged by 6 months, meaning a strong winter NAO can modulate European ET rates in the subsequent summer (Wedgbrow et al., 2002).

In southern Europe, this relationship is inversed. The region experiences anomalous anticyclonic activity during a NAO + due to the meridionally tilted storm track, the influence of which decays inland (Tabari et al., 2014, Türkeş and Erlat, 2003).

Although this model of NAO control on westerly storm tracks is well corroborated (Alexander et al., 2005, Sickmoller et al., 2000, Taylor and Stephens, 1998), the

NAO index only accounts for a portion of total atmospheric variability. For example, Walter and Graf (2005) suggest that teleconnection control on storm track strength can be better explained by accounting for higher geopotential heights in the mid to upper troposphere. This accounts for atmospheric blocking at higher altitudes, a process which has been shown to block storm development towards northern Europe in a 'traditional' NAO +, skewing correlation analyses (Shabbar et al., 2001, Peings and Magnusdottir, 2014). Despite this, the original NAO definition is more widely used in research due to its fewer data requirements.

Extra-Atlantic TC systems, such as ENSO, have a negligible control on storm propagation across Europe (Alexander et al., 2002). As such these have not been reviewed in any further detail.

### **2.5.2 Oceanic currents and thermal exchange**

The dominant mechanism of oceanic influence on thermal exchange in Europe is the Gulf Stream (Frankignoul et al., 2001). It accounts for increased winter temperatures and an enhanced storm path in western Europe (Ezer, 2015, Davis et al., 2013). The Gulf Stream exhibits control over both PPT frequency and potential evapotranspiration (PET) in the region (Seager et al., 2002). Zonal heat transfer, seen in oceanic systems such as the Gulf Stream, can be viewed as the oceanic counterpart to westerly and storm track moisture transfers.

The NAO (in particular the Subpolar Low) modulates the Gulf Stream strength through extraction of heat from the Subpolar Gyre and Labrador Sea (Delworth and Zeng, 2016). A positive NAO (NAO +) increases deep water formation (DWF) thereby steepening thermal gradients across the Atlantic and enhancing the Gulf Stream (Chaudhuri et al., 2011, Delworth and Zeng, 2016, Walter and Graf, 2005, Drinkwater et al., 2014). This increase in DWF in the Polar Regions has also been shown to increase the meridional tilt of the Gulf Stream, extending the enhanced thermal exchange further into northern Europe (Bakke et al., 2008).

The long-term average NAO phase is more influential on the Gulf Stream than its finer-scale fluctuations, due to the oceanic system's ability to filter high-frequency variability from external drivers (Hurrell and Deser, 2010). As a result of this memory capacity, the NAO's influence on the Gulf Stream strength and tilt can be lagged by an average of 1–2 years (Taylor, 1995, Joyce et al., 2000, Frankignoul et al., 2001), and up to 7 years (Wyatt et al., 2012, Hurrell and Deser, 2010).

Other patterns, such as the EA and AO, have been shown to have similar influences on the Gulf Stream, predominantly through spatiotemporal covariance with the NAO signal (Wedgbrow et al., 2002). The similarity of control between the NAO, EA and AO further validates the assertion of Walter and Graf (2005) and Wedgbrow et al. (2002) who suggest that these systems are regional expressions of a more complex, vertically heterogeneous, air-sea system over the North Atlantic. Additionally, Principle Component Analysis (PCA) of Gulf Stream data has revealed no periodicities > 10 years, making a systematic control of thermal exchange over Europe from non-NAO-like systems unlikely (Chaudhuri et al., 2011). Since drivers of groundwater recharge (PPT and ET) are primarily influenced by the NAO and NAO-like oscillations (such as the EA pattern and the AO), the remainder of this paper will focus on NAO-like signal propagation through groundwater systems.

### **2.5.3 Spatial distribution of periodic precipitation anomalies**

Figure 2 shows a synthesis of spatial correlation data from published studies between winter NAO index values and PPT or Palmer Drought Severity Index (PDSI). Studies that give point, gridded or regional correlation values between 0 and 1 (such as R) were used. The spatially aggregated data can be considered a generalised correlation between NAO and moisture availability (either directly as PPT or as measured by PDSI). Direct ET correlation data has not been included due to paucity of research. Voronoi polygons were used to distribute the correlation data across a map of Europe shown in Figure 2.



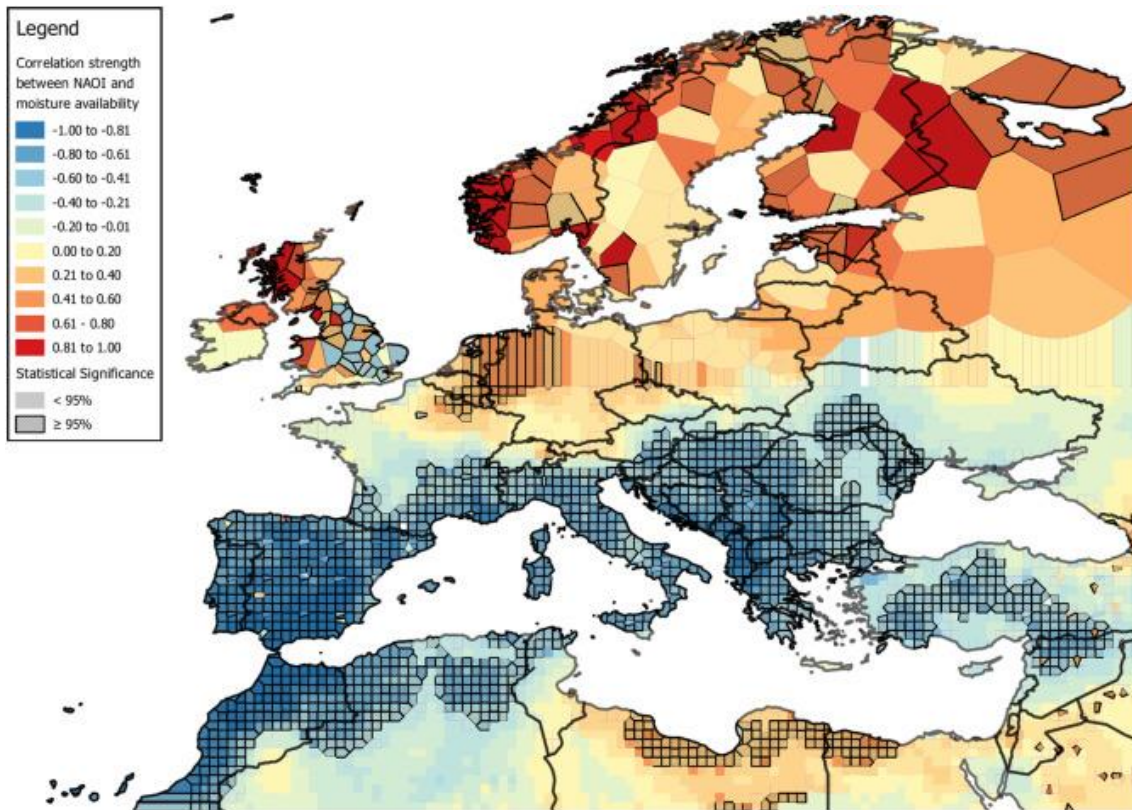


**Figure 2 Correlation between Winter NAO and Precipitation and PDSI. (based on correlation coefficients from Brandimarte et al., 2010, Cullen and DeMenocal, 2000, Fowler and Kilsby, 2002, Hurrell, 1995, Lopez-Bustins et al., 2008, Luković et al., 2015, Lavers et al., 2010, López-Moreno et al., 2011, Murphy and Washington, 2001, Queralt et al., 2009, Rogers et al., 2001, Soediono, 1989, Tabari et al., 2014, Türkeş and Erlat, 2003, Uvo, 2003, Wang et al., 2015, Wilby et al., 1997).**

Four primary spatial patterns can be described from figure 2:

1. There is a positive correlation between a winter NAO index and PPT/PDSI in northern regions of Europe, including the UK and the Scandinavian countries. Highest correlations can be seen in areas dominated by orographic rainfall (for instance Wales, northwest England, and Scotland), and western coastlines (such as the Scandinavian Mountains in Norway). This reflects the NAO's control on the Gulf Stream and Atlantic Storm Track strength and tilt.

2. The only area which appears to exhibit an opposite trend to wider northern Europe is central and south east England. At this location, wetter conditions have a weak negative correlation with the winter NAO. This may be the result of orographic rainfall to the west imposing a barrier to storm progression (Wilby et al., 1997), or a sensitivity of this region to the NAO's sub-tropical component (Wedgbrow et al., 2002).
3. Southern and Mediterranean Europe show a strong negative correlation between the winter NAO and PPT/PDSI. As such these areas are dryer during a positive winter NAO. This is most likely the result of the increased meridional tilt of the westerly storm track in a positive NAO, which limits moisture transport to south Europe.
4. In general, the strength of the correlation is low in the intermediate zone between positive and negative correlation and diminishes eastward or with distance from the coastline.

It should be noted that the data aggregated in figure 2 are from multiple studies which have used separate methodologies and have differing levels of confidence. As such this figure should be considered a general representation of winter NAO influence on catchment wetness.

The ability of TC systems to control PPT and ET independently over time and space is critical for determining control on the total water available for recharge. In central Europe, the NAO and NAO-like systems are more capable of driving ET than they are of PPT (Trigo et al., 2002, Mares et al., 2002). This is possibly due to the decay of NAO-driven storm tracks with distance from the Atlantic, while anticyclonic systems are able to drive ET further inland. The result is a dominant NAO control on ET towards central Europe (Merino et al., 2015, López-Moreno et al., 2011, Türkeş and Erlat, 2003, Bozyurt and Özdemir, 2014). For example, Ghasemi and Khalili (2008) and Tabari et al. (2014) found a greater NAO control on Reference ET in Iran, compared to PPT. The independent control of PPT and ET is still unclear in current research due the effect of local topography, differing study methodologies or the influence of external forcing beyond the TC systems under consideration (Wedgbrow et al., 2002).

## **2.6 Controls on periodic recharge signals**

The nature of teleconnections and their control on weather is spatially variable, as shown in Section 2.5. However, a wide range of intrinsic catchment characteristics, for example land cover, soil or geological properties, modify the propagation of potential recharge signals by varying degrees (Nimmo, 2005, Rust et al., 2014). Here we discuss the current understanding of how the influence of catchment characteristics, and the distribution of such parameters, affect the propagation of low-frequency periodic signals from PPT and ET through to aquifer recharge.

### **2.6.1 Land surface processes and recharge**

The land surface and root zones provide the interface between meteorological processes and infiltration. These include the effect of vegetation, actual ET, surface storage, soil type, and soil storage. While climatic and weather systems are shown to control anomaly signals in both PPT and ET at multiple time scales, the surface and root zones mediate the actual volumes of water that infiltrate into the unsaturated zone. Indeed long-term changes in these near-surface processes may confound low frequency signal propagation towards groundwater recharge (Ferguson and Maxwell, 2010, Healy, 2010).

While shallow soil horizons and surface stores have been shown to filter finer-scale variability (hourly–daily) from incoming signals (Baram et al., 2012), surface processes have minimal impact on the propagation of long-period signals (Bakker and Nieber, 2009, Dickinson et al., 2014). For example, Rust et al. (2014) showed that vegetation type can affect annual and seasonal climate signal propagation into groundwater recharge with little effect on extra-annual scales. It is therefore considered that surface processes bear little impact within the presented conceptual model of long period climate signal propagation.

### **2.6.2 Unsaturated zone influence on recharge signals**

Signal propagation below the root zone is one of the most poorly quantified components of the hydrological cycle. This is, in part, because of the complex

nonlinear relationship between flow, water content, and hydraulic diffusivity (Cuthbert et al., 2010). While this is an area of much ongoing research, the development of periodic signals through the unsaturated zone is still an area of much research paucity. There is an established literature, however, on drought development through the water cycle (Van Loon, 2013, Van Loon et al., 2012, Van Loon et al., 2014, Peters et al., 2003, Peters et al., 2006, Di Domenico et al., 2010, Peters, 2003, Tallaksen et al., 2006, Tallaksen et al., 2009, Bloomfield and Marchant, 2013, Mishra and Singh, 2010). These focus on the propagation of episodic negative anomalies in PPT through to groundwater level and are a useful parallel to periodic signal propagation.

Van Loon (2015) provides a comprehensive text on drought propagation between meteorology and groundwater, in which four signal modulations are characterised. These are i) Pooling of meteorological droughts into prolonged groundwater drought; ii) Attenuation of PPT deficits in surface stores; iii) Lags in the onset of drought between meteorological, soil moisture, and groundwater systems; and finally, iv) Lengthening of droughts when moving between soil moisture and groundwater drought, as a result of attenuation. Features i, iii and iv can be considered descriptions of the unsaturated zone's ability to dampen incoming signals in PPT and ET.

The ability of a groundwater system to propagate, or dampen, drought signals from PPT and ET is often related to properties of the unsaturated zone, such as storage or thickness (Bloomfield and Marchant, 2013, Van Loon, 2015, Van Loon et al., 2014). For example, Bloomfield and Marchant (2013) identified lags and lengthening of drought signals between PPT and groundwater level, similar to those described by Van Loon (2015). They propose that long autocorrelations seen in the Standardised Groundwater Index for multiple boreholes across the UK may be explained by the unsaturated zone's ability to filter out higher autocorrelation frequencies in PPT, while allowing longer-period signals to pass. This is corroborated well by Kumar et al. (2016), who showed that groundwater head anomalies at locations of thicker unsaturated

zones achieved higher correlations with SPI at longer accumulation periods, when compared with thinner unsaturated zones.

As an indicator of available storage in an unsaturated zone, soil type is an important characteristic in modulating the degree of signal damping. Dickinson et al. (2014) describes a greater damping rate (with depth) for periodic signal propagation through clayey soils, compared to sandy soils. They concluded that soils with lower hydraulic diffusivity (such as clay soils) filter out sinusoidal frequencies more effectively than soils with greater diffusivity (such as sandy soils). They also propose that extra-annual periodic signals are unlikely to reach steady state through an unsaturated zone, meaning these signals will persist through to recharge. These findings are supported by Velasco et al. (2017).

In addition to damping incoming infiltration signals, the unsaturated zone is conceptualised to lag signal perturbations between infiltration and groundwater recharge (Gurdak et al., 2007, Crosbie et al., 2005, Cao et al., 2016, Dickinson, 2004, Cuthbert and Tindimugaya, 2010). Despite this, very few studies have quantified this lag for unsaturated zones in Europe. Holman et al. (2011) found significant transient lagged correlations between the NAO index and groundwater level data in the UK. Highest correlations were found at 4 year and 16-year period scales. Although lag times were not directly quantified in the study, phase-shifts were presented as tending towards 180° for the NAO signal, indicating a 2- to 8-year lag provided by unsaturated zones in the UK.

While there has been little quantification of periodic signal damping and lagging through unsaturated zones in Europe, many groundwater resources globally provide a clearer view of the dampening capability of the unsaturated zone. For example, Kuss and Gurdak (2014) found an (up to) 93% dependence between groundwater variability on PDO-like signals, at a lag of between 11 and 46 years, in the USA High Plains aquifer. By undertaking a lag correlation between a coupled PDO-like periodic component of rainfall and groundwater level, they attributed the damping detected to the varying thickness of the unsaturated zone. Similar results have been found by Cao et al. (2016) in assessing recharge in the North China Plain aquifer, finding that an increase in unsaturated thickness

> 30 m, results in a reduction in maximum recharge rate of up to 70%. It is worth noting that the North China Plain and the High Plains aquifers cover considerably larger spatial domains compared to those found in Europe. It is not clear, at present, to what extent the strength of these recorded signals is a result of larger aquifer domains or the influence of different TC patterns in these locations, for instance the PDO or ENSO.

While the geometry and storage of an unsaturated zone can affect the amount of signal damping, this effect is not absolute. For example, Velasco et al. (2017) described the degree of damping through an unsaturated zone is also dependent on the periodicity of the boundary oscillation itself. They report that at an example depth of 10 m, between 100% (for sandy soils) and ~ 70% (for silty clay loam) of an NAO-like boundary flux is preserved. They conclude that rate of signal damping with depth decreases with increasing period length of a boundary condition, and that this is modulated by soil type and infiltration rate. This is corroborated with other research in this area (Bakker and Nieber, 2009, Cao et al., 2016, Dickinson et al., 2014, Ataie-Ashtiani et al., 1999, Nimmo, 2005, Currell et al., 2014, Bloomfield and Marchant, 2013, Van Loon, 2015, Van Loon et al., 2014).

There are still significant knowledge gaps in describing low-frequency periodic signals progress through the unsaturated zone in Europe. Principally, the quantification of NAO-like signal lags and attenuation through spatially varying soil and geological materials. Despite this, four conceptual effects of surface and unsaturated zone parameters on periodic signal propagation can be described at present:

1. The unsaturated zone dampens signals between PPT and recharge. The damping capacity of an unsaturated zone becomes greater with increased depth to the water table and/or lower hydraulic diffusivity. Increased damping results in a decreased amplitude in signals at the water table. Damping appears proportional to unsaturated zone thickness, meaning periodic recharge signals tend towards steady-state with increased

- damping capacity. This is comparable to the attenuation described by Van Loon (2015); resulting in a smoothing of the incoming PPT signal.
2. Shorter periodic recharge signals are more sensitive to damping. This is true of compound periodic signals, such as those found in the NAO index. In the case of the NAO, it would be expected that the secondary periodicity of 3–4 years would be dampened to a greater extent than the primary periodicity of 8–9 years. This is again comparable to Van Loon (2015); however, period-dependent damping rates appear to be a character specific to periodic signal progression.
  3. The unsaturated zone acts to lag periodic signals between PPT and recharge. The lag provided by the unsaturated zone is a function of its damping capacity and is driven by the same characteristics. Measured lags range from 5 to 75 years for different periodic signals, highlighting the sensitivity and variability of lag to unsaturated zone characteristics (Kuss and Gurdak, 2014, Holman et al., 2011). Lag is independent of signal periodicity and amplitude. Here there is a strong parallel with ‘Lagging’ as described by Van Loon (2015), with periodic signals showing a lagging of a perturbation within the signal.
  4. The unsaturated zone does not stretch periodic signals, meaning periodicity of recharge signals is preserved (Dickinson et al., 2014). As such, ‘Lengthening’, as described in Van Loon (2015), is not considered to occur for periodic signals.

### **2.6.3 Spatial sensitivity of recharge signal damping**

As concluded in Section 2.6.2, unsaturated zone signal damping is dependent, in part, on unsaturated zone thickness. Here we have produced an indicative map (Figure 3) to show the expected effects of periodic NAO control on recharge to aquifers in Europe, based unsaturated zone thickness. Thicker unsaturated zones are considered to provide greater damping and lagging (and produce signals closer to steady state). Figure 3 combines the spatial distribution of NAO control on PPT and PDSI given in Figure 2, with modelled unsaturated zone thickness at 0.5° resolution published in Fan et al. (2013). This figure does not

account for textural effects of the soil and geology, which are known to modulate signal propagation (Dickinson et al., 2014, Velasco et al., 2017), as there is as yet incomplete understanding of the spatial distribution of these controls. As such this figure should be considered a generalised view of groundwater recharge sensitivity to the NAO.

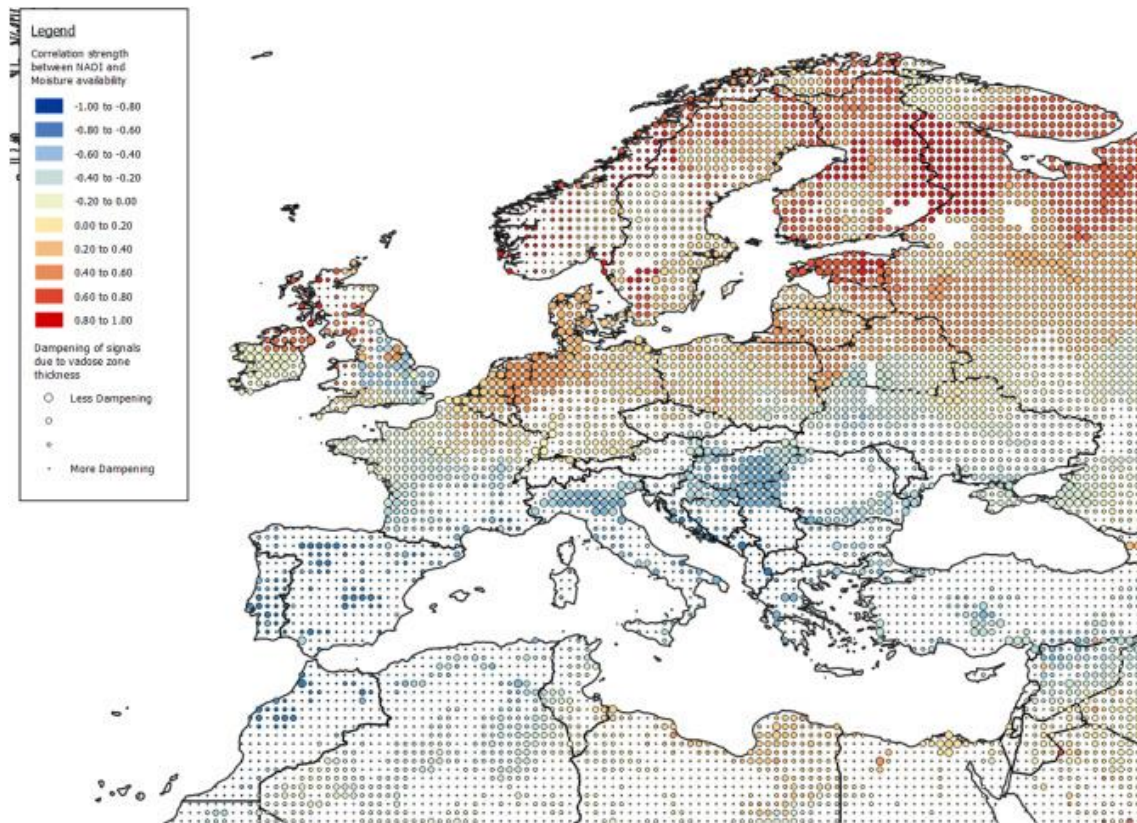


**Figure 3 Composite plan combining NAO correlation with PPT and PDSI (Figure 1) into a 0.5° point grid, and expected damping capacity of the unsaturated zone inferred from modelled depth-to-groundwater data produced by Fan et al. (2013), where size of circles is proportional to expected damping capacity.**

Mid- to high-latitude Europe generally shows reduced thickness of the unsaturated zone, resulting in greater amplitude of NAO signals arriving at the saturated zone. Local areas of minimal signal damping can be seen in the UK, Netherlands, northern Italy, Hungary, Estonia and eastern Scandinavia. Some areas with the strongest correlations, such as the western Norwegian coast and much of Spain, are expected to receive a greater damping and lagging of the NAO signal due to the relatively thick unsaturated zone. A similar divide is seen



in the UK, with larger depths to water table producing damped NAO signals in Scotland. The primary chalk aquifer in England, despite showing a generally weaker correlation with the NAO, is expected to receive a greater exposure to NAO signals in recharge due to relatively shallow aquifers in the region. It can also be seen that the Chalk is potentially subject to varying teleconnection control across its domain, as a result of anomalous moisture control seen in south east England. Stronger NAO correlations are expected in the Triassic Sandstone in central England, with minimal signal damping. These findings may explain results from Holman et al. (2011) which show varying strength of covariance between borehole data from across the UK and the NAO index.

## **2.7 Saturated zone influence on discharge signals**

In Section 2.6, we discussed that the distribution of unsaturated zone properties is likely to generate a spatially varied damping effect on TC signals propagation to the water table. Unlike the unsaturated zone, the saturated zone exhibits dominant flow vectors orthogonal to the surface of groundwater saturation. Therefore, it can display complex cumulative interactions with spatially distributed recharge, hydrogeological properties, and discharge boundary conditions (Simpson et al., 2013). We therefore expect that the saturated zone will display considerable local- and wide-scale spatial sensitivity when compared to the unsaturated zone. Here we discuss the current understanding of how periodic signals progress through the saturated zone. A synthesis of the principal modulations of TC-like signal propagation through the saturated zone will be given.

The saturated zone produces a damping effect on signals between recharge and discharge. The extent of damping is dependent on the characteristic aquifer length and properties such as transmissivity and storage (Bloomfield and Marchant, 2013, Cuthbert et al., 2009, Cuthbert et al., 2010, Cuthbert et al., 2016, Cook et al., 2003, Simpson et al., 2013, Van Loon, 2015). Specifically, aquifer response to periodic recharge is proportional to the ratio between the

aquifer response time ( $t$ ), calculated from  $t = L^2S/T$  (where  $L$  is the length of the aquifer [L],  $S$  is the Storativity [-],  $T$  is the Transmissivity [ $L^2/T$ ]), and the period of the sinusoidal boundary flux,  $P$  [T] (Townley, 1995, Dickinson, 2004). Even for a small aquifer length of 1km,  $t$  can range from days for highly hydraulically diffuse aquifers to decades for lower diffusivity geological material (Bricker, 2017, Townley, 1995). Where  $t:P \gg 1$ , an aquifer response is too slow to reach equilibrium with the periodic forcing meaning any periodic recharge signals are significantly damped and attenuated at the point of groundwater discharge. Where  $t:P \ll 1$ , an aquifer responds quickly to a boundary flux and is therefore close to equilibrium at any instance in time (Townley, 1995). Where  $t:P \approx 1$ , the response of an aquifer is comparable to the periodicity of the boundary flux and therefore may produce more complex phase-shifted, or out-of-phase, responses (Currell et al., 2014).

The damping response of an aquifer, as represented by the ratio  $t:P$ , is not necessarily constant across its catchment. For example Townley (1995) showed that for aquifers with  $t:P \geq 1$  or  $t:P > 1$  the amplitude of a periodic signal is increased close to the downstream boundary. This is considered to be due to the inability of the aquifer to carry larger lateral flows near the boundary. Farther away from the downstream boundary, this effect is diminished (Townley, 1995).

The propagation of perturbations in recharge signals throughout an aquifer may also be controlled by aquifer properties such as transmissivity and storage (Van Loon, 2013). Such progressions can provide useful information regarding the hydrogeological controls on signal damping. For example, Cook et al. (2003) shows that aquifer discharge responses can dampen to 95% and 10% of the perturbation at 1 km and 30 km aquifer length, respectively, within 200 years of the original recharge perturbation. They also show that the magnitude of this effect is most sensitive to aquifer transmissivity and the distance between the perturbation point and discharge area. This is in agreement with other research that indicates that response times can extend into geological timescales (Schwartz et al., 2010, Rousseau-Gueutin et al., 2013, Cuthbert et al., 2017). Again, parallels can be drawn here between the damping expected in periodic

signal propagation through saturated rock, and the processes of 'Attenuation' and 'Lagging' of episodic drought signals described by Van Loon (2015). The extent of 'Lengthening' and 'Pooling' of incoming signals to groundwater resources, as discussed by Van Loon (2015), are currently unknown for periodic signals.

Given the dependence of signal dampening on aquifer transmissivity and storage, it can be said that the spatial distribution of aquifer properties is critical in determining the spatial structure of teleconnection signal propagation (Yu and Lin, 2015, Simpson et al., 2013). While this is understood conceptually, it is rarely known how such characteristics are distributed across an aquifer. Therefore it can be difficult to characterise how signals may spatially propagate through an aquifer (Peters et al., 2006).

Groundwater flow rates typically show a linear relationship with groundwater levels close to downstream boundaries of the aquifer. At these locations, discharge can be fixed irrespective of aquifer properties or groundwater head (Peters, 2003). For groundwater catchments with slower response rates, these boundary conditions allow for an additional degree of spatial variability in responsiveness, as the groundwater system can contain both slow-responding and quick-responding components. Peters et al. (2006) discuss that such catchments are more responsive to short-term variations in recharge close to discharge boundaries. Although periodic signals are not directly discussed in this research, a comparison can be made for short-frequency and long-frequency periodic signals. It is therefore expected that areas close to points of discharge may be more sensitive to shorter-period components of climatic signals (for instance, the secondary 3–4 year component of the NAO), compared to the wider aquifer (Peters et al., 2006, Peters, 2003).

Symmetry between positive and negative anomalies is informative in that it provides information on the geological modulation of teleconnection signals. Analysis of the asymmetry of the relationship is equally informative as it sheds light on the connectivity between the signal and surface stores. For instance, Eltahir and Yeh (1999) describe that during a positive ground water anomaly, water table connectivity with surface drainage (such as rivers) is

increased, allowing groundwater to be drained away more efficiently. Therefore, negative anomalies tend to persist for longer than positive anomalies.

Groundwater discharge provides springflow and river baseflow. While many studies have related total river flow to signals of climatic circulations, showing detectable correlations between climatic circulations, hydrogeological properties and baseflow (Singh et al., 2015, Bloomfield et al., 2009), relevantly little research has been undertaken which directly assesses mechanistic propagations of climate signals through to spatial and temporal variability in baseflow and spring flow.

Recent research has introduced the concept of climate-induced groundwater abstraction, resulting in a human-influenced exacerbation of periodic climate signal presence within groundwater resources (Gurdak, 2017). For example, Russo and Lall (2017) have shown that groundwater resources in the USA display a greater coherence with indices of climatic oscillations (such as NAO and ENSO) in areas of agricultural land use (and therefore heavier groundwater abstraction). Conceptually, these influences are expected to exacerbate the negative anomaly component between recharge and discharge. Similar results have been found by Asoka et al. (2017) between monsoon precipitation and groundwater storage in India. There is currently a paucity of information as to the impacts of climate-induced abstraction in Europe, however existing research for other areas indicates the importance of a human component within the conceptual model of climate-groundwater teleconnections.

## **2.8 Current understanding of climatic teleconnection signal control on groundwater variability**

Presently there exists no comprehensive, unified understanding of how teleconnection signals propagate through to spatiotemporal variability in groundwater levels and flows. Through a review of hydroclimatological and hydrogeological literature, we present a conceptual model of teleconnection

signal propagation through to groundwater variability based. This conceptual model is given as an overview, with the NAO as an example, in Figure 4.

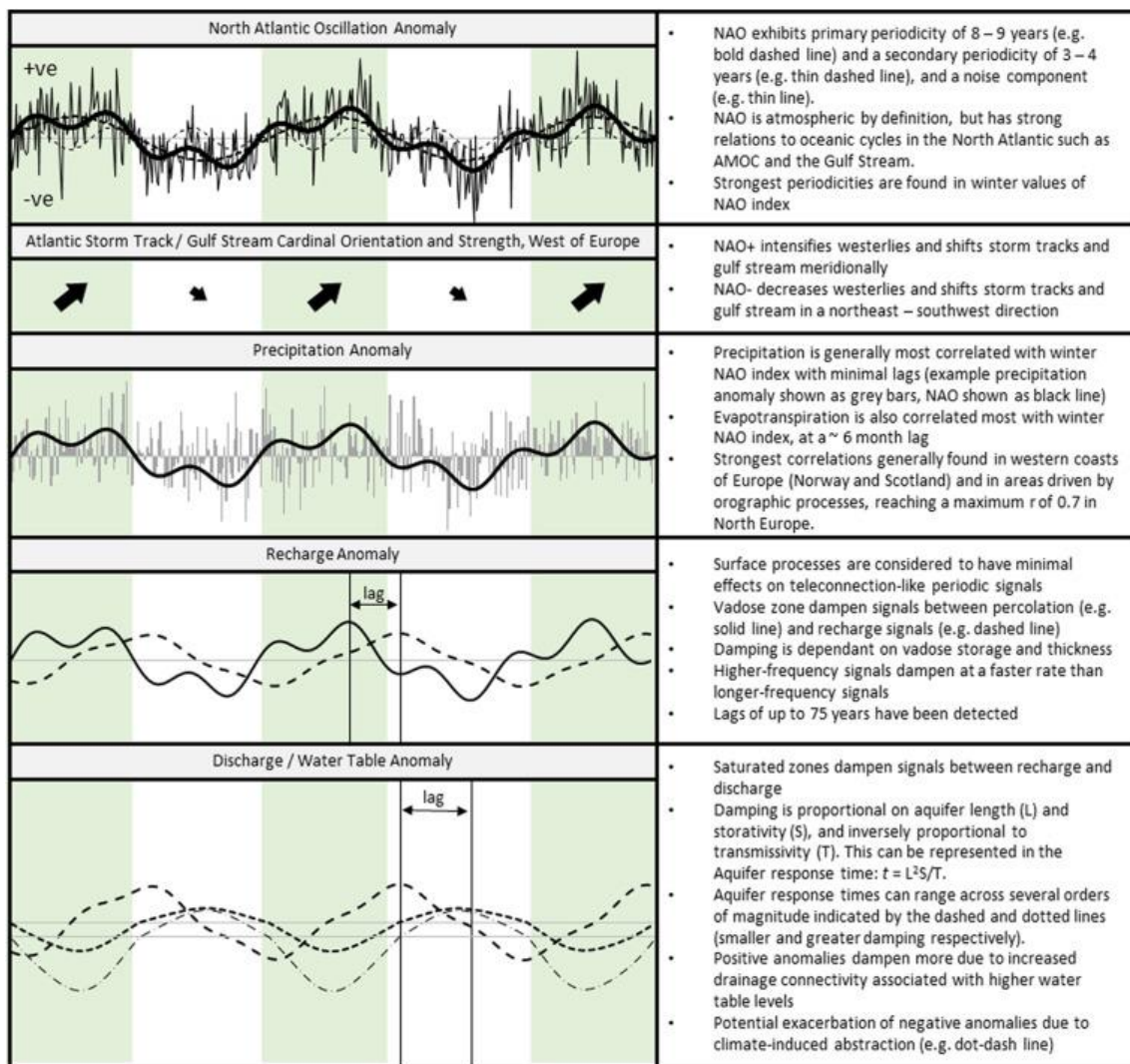


**Figure 4 Conceptual model of signal propagation from Teleconnection through to groundwater discharge, using the NAO in the UK as an example.**

The mechanics of signal propagation of teleconnection signals through to atmospheric and oceanic variability is relatively well understood. However, the terrestrial water cycle is shown to exhibit complex non-linear spatial relationships as a result of distributed hydraulic properties of the unsaturated and saturated zone. While a few principal characteristics of periodic flow progression have been reviewed in this paper, there are still many knowledge gaps. Specifically, regarding how teleconnection processes, such as the NAO, manifest in

spatiotemporal groundwater variability. As a result of the developed conceptual model, we have identified the following research gaps:

1. *Hydrogeology and periodic signals*. There is currently limited research that quantifies the propagation of teleconnection signals through an entire aquifer system. For instance, from PPT and ET to groundwater discharge. In order for information on teleconnection dependency to be of practical use for water resource managers, further quantification of damping and lagging effects for a range of aquifers is required.
2. *Distributed signal sensitivity*. Existing studies that have looked at groundwater sensitivity to a teleconnection control are generally based on limited point measurements. Therefore, at present, limited comment can be made on the spatial distribution of this sensitivity and how this influences flow across an aquifer catchment.
3. *Importance of multiple or confounding signals*. Much hydroclimatology research in the North Atlantic focuses on the NAO, which does not account for the influence of other teleconnection signals. In addition, the method of teleconnection indexing is critical to how well the true variability of a system is represented. This is shown in the NAO, in which the typical index does not account for atmospheric blocking which can lead to significant alteration of moisture variability across Europe. This may represent an important modulation of teleconnection control on groundwater variability. In addition, the anthropomorphic influence of climate-induced abstraction may also lead to important signals modulations. Despite this, the quantification of these mechanisms in Europe is limited in the existing literature.

Teleconnection control on periodic groundwater variability offers an indicator for near-future resource availability. This is therefore a useful tool for water companies and water managers to address the lack of longer-term forecasting of droughts (Water UK, 2016). This paper has shown, there is a developing conceptual understanding of the atmospheric, hydrological and hydrogeological

controls on such periodic variability. However, there is insufficient knowledge at present to enable the use of teleconnection systems as predictors of spatiotemporal groundwater variability.

So that an understanding of such control-linkages can produce useful tools for improved water resource management, current research needs to move beyond detection of teleconnection signal presence, towards the development of indicative or predictive capabilities across a range of groundwater catchments.

## **2.9 References**

The reference list for this paper has been combined with the final reference section for this thesis in chapter 10.

.

# 1 **3 CHAPTER 3 MULTIANNUAL PERIODICITIES IN WATER**

## 2 **RESOURCES**

3 This chapter consists of the published article Rust et al (2019); “Understanding the  
4 potential of climate teleconnections to project future groundwater drought”. This  
5 chapter will address research objective 2.

6

### 7 **3.1 Abstract**

8 Predicting the next major drought is of paramount interest to water managers, globally.  
9 Estimating the onset of groundwater drought is of particular importance, as  
10 groundwater resources are often assumed to be more resilient when surface water  
11 resources begin to fail. A potential source of long-term forecasting is offered by  
12 possible periodic controls on groundwater level via teleconnections with oscillatory  
13 ocean-atmosphere systems. However, relationships between large-scale climate  
14 systems and regional to local-scale rainfall, ET and groundwater are often complex  
15 and non-linear so that the influence of long-term climate cycles on groundwater  
16 drought remains poorly understood. Furthermore it is currently unknown whether the  
17 absolute contribution of multi-annual climate variability to total groundwater storage is  
18 significant. This study assesses the extent to which multi-annual variability in  
19 groundwater can be used to indicate the timing of groundwater droughts in the UK.  
20 Continuous wavelet transforms show how repeating teleconnection-driven 7-year and  
21 16-32 year cycles in the majority of groundwater sites from all the UK’s major aquifers  
22 can systematically control the recurrence of groundwater drought; and we provide  
23 evidence that these periodic modes are driven by teleconnections. Wavelet  
24 reconstructions demonstrate that multi-annual periodicities of the North Atlantic  
25 Oscillation, known to drive North Atlantic meteorology, comprise up to 40% of the total  
26 groundwater storage variability. Furthermore, the majority of UK recorded droughts in  
27 recent history coincide with a minima phase in the 7-year NAO-driven cycles in  
28 groundwater level, providing insight into drought occurrences on a multi-annual  
29 timescale. Long-range groundwater drought forecasts via climate teleconnections  
30 present transformational opportunities to drought prediction and its management  
31 across the North Atlantic region.



32

33

### 3.2 Introduction

34 Multi-annual variability detected in hydrometeorological datasets has long been  
35 associated with systems of atmospheric-oceanic (climatic) oscillation, such as El Niño  
36 Southern Oscillation (ENSO) and the North Atlantic Oscillation (NAO). Such periodic  
37 teleconnection signals have been detected in rainfall (Luković et al. 2014),  
38 evapotranspiration (Tabari et al. 2014), air temperature (Faust et al. 2016), and river  
39 flow (Su et al. 2018; Dixon, et al. 2011); however these periodicities are often weak  
40 when compared to the finer-scaled (daily to seasonal) variability that is typical of  
41 hydrometeorological processes (Meinke et al. 2005). By contrast, groundwater  
42 systems are expected to be particularly susceptible to multi-annual teleconnection  
43 influence, given their sensitivity to long-term changes in rainfall and evapotranspiration  
44 (Bloomfield & Marchant 2013a; Forootan et al. 2018; Van Loon 2015; Folland et al.  
45 2015), and their ability to filter fine-scale variability in recharge signals (Dickinson et  
46 al. 2014; Velasco et al. 2015; Townley 1995). Consequently, recent studies have  
47 focused on the detection of long-term periodic cycles in groundwater levels in Europe  
48 (e.g. Holman et al. 2009; Holman et al. (2011); Folland et al. (2015); and Neves et al.  
49 (2019)), North America (e.g. Tremblay et al. (2011); Kuss & Gurdak (2014)) and  
50 globally (e.g. Wang et al. (2015); Lee & Zhang (2011)), and their relationships with  
51 climatic oscillations. An understanding of multi-annual periodicity strength in  
52 groundwater level may provide an improvement in long-lead forecasting of  
53 hydrogeological extremes (Rust et al. 2018; Meinke et al. 2005; Kingston et al. 2006),  
54 in part, by enabling such cyclical behaviour to be projected into the future. This is  
55 particularly apparent of groundwater drought, which is known to result from multi-  
56 annual moisture deficits (Van Loon 2015; Van Loon et al. 2014; Peters et al. 2006).  
57 Therefore, it is critical to quantify the absolute strength of all periodicities within  
58 groundwater levels so that the strength of multi-annual cycles, the influence of  
59 teleconnections, and their contribution towards groundwater droughts can be  
60 understood.

61 Existing studies into groundwater teleconnections use quantitative methods to detect  
62 periodic behaviour in groundwater datasets and often their relationship with time series  
63 of climate indices (used to measure the strength and state of climate oscillations).

64 Common quantitative methods range from temporal correlation analysis (Knippertz et  
65 al. 2003; Szolgayova et al. 2014) to more complex periodicity detection and  
66 comparison. These latter methods include Fourier transform, (Nakken, 1999, Pasquini  
67 et al. 2006), singular spectrum analysis (SSA) (Kuss & Gurdak 2014; Neves et al.  
68 2019) and wavelet transformations (Fritier et al. 2012; Holman et al. 2011; Tremblay  
69 et al. 2011). The wavelet transform (WT) has been shown to be particularly skilful at  
70 detecting multi-annual periodic behaviour in noisy hydrogeological datasets; detecting  
71 the influence of the NAO, ENSO and Atlantic Multidecadal Oscillation (AMO) on North  
72 American groundwater levels (Kuss & Gurdak 2014; Velasco et al. 2015), and the  
73 NAO, East Atlantic pattern (EA) and Scandinavian pattern on European groundwater  
74 level variability (Holman et al. 2011; Neves et al. 2019). However, in order to enhance  
75 multi-annual periodicity detection, many studies have used data processing methods  
76 that remove or suppress variability at the higher end of the frequency spectrum (e.g.  
77 winter or annual averaging or conversion of time series to cumulative departures from  
78 mean (Weber & Stewart 2004)). Due to this data modification, it is currently unknown  
79 whether the absolute contribution of multi-annual climate variability to total  
80 groundwater storage is significant. This limitation makes assessment of systematic  
81 linkages between climatic oscillations and groundwater level response problematic  
82 (Rust et al. 2018). As a result, the fundamental question of whether multi-annual  
83 teleconnection cycles in groundwater level are sufficiently strong to influence  
84 hydrogeological drought remains largely unanswered. Given the potential for improved  
85 long-lead forecasting, quantification of multi-annual variability in groundwater level  
86 represents an opportunity to support efficient infrastructure investment, systems of  
87 water trading (Rey et al. 2018) and robust planning for groundwater drought.

88 The aim of this paper is to assess the extent to which periodic behaviour in  
89 groundwater level produced by teleconnections, may be used as an indicator for the  
90 timing of groundwater droughts. In doing so, this paper develops and applies an  
91 improved method to describe and characterise the absolute strength of periodic  
92 behaviour in groundwater level and its drivers (rainfall and evapotranspiration). This  
93 aim will be met by addressing the following research objectives:

- 94 1. Characterise dominant intra- and multi-annual periodicities in groundwater level  
95 records across a range of aquifer types

- 96 2. Quantify the absolute strength of these multi-annual periodic groundwater level  
97 oscillations compared to the total variability in groundwater levels  
98 3. Qualitatively assess evidence for the control of climate teleconnections on  
99 identified multi-annual periods  
100 4. Assess the extent to which the timing of the multi-annual periodic groundwater  
101 level oscillations align with recorded groundwater droughts

102 These objectives will be implemented on UK hydrogeology records, given the  
103 considerable coverage of recorded groundwater level data in time and across the  
104 country (Marsh & Hannaford 2008) however the methodologies developed can be  
105 applied to any regions.

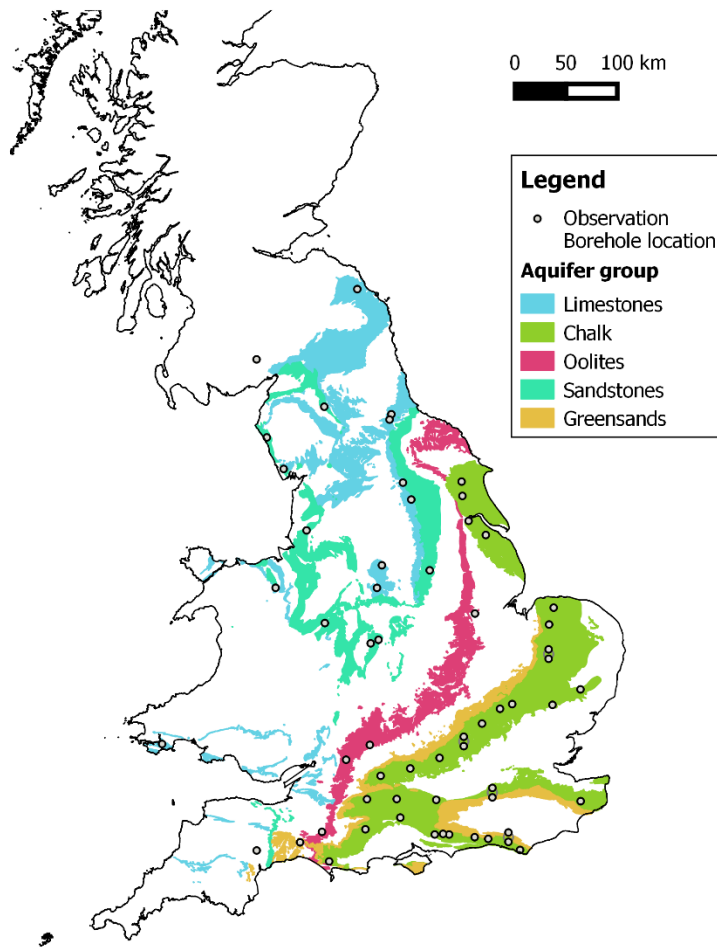
106

### 107 **3.3 Data and Methods**

#### 108 **3.3.1 Groundwater data**

109 Groundwater level time series from 59 reference boreholes covering all of the major  
110 UK aquifers, with record lengths of more than 20 years and data gaps no longer than  
111 24 months, have been assessed in the study. These recorded groundwater level  
112 hydrographs range from 21 to 181 years in length, with an average length of 53 years.  
113 The sites are part of the British Geological Survey's Index Borehole network and, in  
114 addition to their data coverage, have been chosen as they exhibit representative and  
115 naturalistic hydrographs with minimal impact from abstractions. They cover a range of  
116 unconfined and confined consolidated aquifer types and have been categorised into 5  
117 main aquifer groups; 34 records in Chalk, a limestone aquifer comprising of a dual  
118 porosity system with localized areas where it exhibits confined characteristics; 8  
119 records in Limestone, characterised by fast-responding fracture porosity; 3 records in  
120 Oolite characterised by highly fractured lithography with low intergranular permeability;  
121 12 sites in Sandstone, comprised of sands silts and muds with principle inter-granular  
122 flow but fracture flow where fractures persist; and 2 records in Greensands,  
123 characterised by intergranular flow with lateral fracture flow depending on depth and  
124 formation (Marsh & Hannaford 2008).

125



126

127 **Figure 5 Location of the observation borehole locations used in this study. Boreholes**  
 128 **within 0.5 km of another have been displaced and denoted on a grey circle for visibility.**

### 129 **3.3.2 Rainfall**

130 Rainfall time series from the Centre of Ecology and Hydrology’s CEH-GEAR 1km  
 131 gridded rainfall dataset (Tanguy et al. 2016), which is based on spatio-temporal  
 132 interpolation of daily rain gauge totals between 1890 and 2017, was used. However,  
 133 relatively few rainfall stations exist prior to 1950 that were used for this interpolation;  
 134 as such data prior to 1950 was not used in this analysis. Monthly rainfall series have  
 135 been calculated for each borehole from the 1km grid cell in which they are located, as  
 136 geospatial data on areas of groundwater recharge connected to specific observation  
 137 boreholes does not exist. This dataset may contain artefacts as a result of the spatio-  
 138 temporal interpolation, in comparison to station data. However the use of rainfall data  
 139 in this study is to provide a broad understanding of rainfall periodicities to supplement

140 those from groundwater level data. As such, this interpolated dataset is deemed  
141 appropriate.

142

### 143 **3.3.3 Potential Evapotranspiration (PET)**

144 Monthly PET series for each borehole have been derived from the Centre of Ecology  
145 and Hydrology's CHES-PE 1km gridded dataset of calculated daily PET values. The  
146 PET values, between 1960 and 2015, were calculated using the Penman-Monteith  
147 equation, with meteorological data taken from the CHES gridded meteorological  
148 dataset. Details on the underlying observation datasets and interpolation methods can  
149 be found in Robinson et al. (2016). This data has been used previously to study long-  
150 term trends in hydrological variability (Robinson et al. 2017).

151

### 152 **3.3.4 Methods**

#### 153 **3.3.4.1 Data pre-processing**

154 In this study we use the continuous wavelet transform (CWT) to produce a time-  
155 averaged frequency spectrum for each borehole hydrograph and co-located rainfall  
156 and PET time series.

157 For all datasets, gaps less than two years were infilled using a cubic spline to produce  
158 a complete time series for the CWT. This interpolated information was later removed  
159 from the time-frequency transformation (prior to time-averaging) to ensure that the  
160 data infilling had minimal effect on the final spectrum. For time series with gaps greater  
161 than two years, the shortest time period before or after the data gap was removed to  
162 produce one complete record. Individual rainfall and PET time series were trimmed to  
163 match the length of the corresponding borehole level time series. All time series were  
164 centred on the long-term mean and normalized to the standard deviation to produce a  
165 time series of anomalies. Unlike most previous studies, no high- or low-band filtering  
166 was undertaken on the datasets, ensuring all information on periodic variability was  
167 preserved. This approach ensures that the Proportion of a periodicity to the variance  
168 (standard deviation) of the original dataset is not modified.

169 2.1.1. Continuous Wavelet Transform.

170 Following the data pre-processing steps, a CWT was applied to quantify the time-  
171 averaged frequency spectra of the rainfall, PET and groundwater datasets. The CWT  
172 has been used to assess long term trends and periodicities in many hydrological  
173 datasets including rainfall (Rashid et al. 2015), river flow (Su et al. 2017), and  
174 groundwater (Holman et al. 2011; Kuss & Gurdak 2014). We use the package  
175 “WaveletComp” produced by Rosch & Schmidbauer (2018) for all transformations in  
176 this paper.

177 The continuous wavelet transform,  $W$ , consists of the convolution of the data  
178 sequence  $(x_t)$  with scaled and shifted versions of a mother wavelet (daughter  
179 wavelets):

$$W(\tau, s) = \sum_t x_t \frac{1}{\sqrt{s}} \psi^* \left( \frac{t - \tau}{s} \right) \quad (\text{Eq. 1})$$

180 where the asterisk represents the complex conjugate,  $\tau$  is the localized time index,  $s$   
181 is the daughter wavelet scale and  $dt$  is increment of time shifting of the daughter  
182 wavelet. The choice of the set of scales  $s$  determines the wavelet coverage of the  
183 series in its frequency domain. The Morlet wavelet was favoured over other candidates  
184 due to its good definition in the frequency domain and its similarity with the signal  
185 pattern of the environmental time series used (Tremblay et al. 2011; Holman et al.  
186 2011).

187 The CWT produces a time-frequency wavelet power spectrum for each time series.  
188 Within the time-frequency spectra, a cone of influence (COI) is used to denote those  
189 parts that are affected by edge-effects, where estimations of spectral power are less  
190 accurate. Therefore only data from within COI were averaged over time to produce a  
191 time-average wavelet power spectrum for frequency bands from 6 months up to 64  
192 years. Wavelet power spectra were then normalised to the maximum average wavelet  
193 value so that the frequency distribution of each site can be directly compared. The  
194 normalized average wavelet power spectra (herein referred to as the wavelet power  
195 spectra) provide a comparative measure of the strength of the range of periodicities  
196 within frequency space.

### 197 3.3.4.2 Significance testing

198 As Allen and Smith (1996) demonstrate, geophysical datasets can exhibit pseudo-  
199 periodic behaviour as a result of their lag-1 autocorrelation (AR1) properties. Datasets  
200 with greater AR1 tend to have spectra biased towards low frequencies, thus they are  
201 described as containing red noise (Allen et al. 1996; Meinke et al. 2005; Velasco et al.  
202 2015). In order to assess the likelihood that a periodic signal is the result of internal  
203 (red) noise within the data, significance of the red noise null hypothesis was tested.  
204 For this, 1000 randomly constructed synthetic series with the same AR1 as the original  
205 time series were created using Monte Carlo methods. Wavelet spectra maxima from  
206 these represent periodicity strength that can arise from a purely red noise process.  
207 Wavelet powers from the original dataset that are greater than these “red” periodicities  
208 are therefore considered to be driven by a process other than red noise, thus rejecting  
209 the null hypothesis. Here, while a 95% Confidence Interval (CI) ( $\leq 0.05$  alpha values)  
210 is identified, we report on the full range of alpha results to provide a detailed  
211 assessment of the likelihood of external forcing on periodic behaviour.

### 212 3.3.4.3 Time reconstruction

213 In order to assess the characteristics of periodicities over time, we employ a reversal  
214 of the wavelet transform (wavelet reconstruction) to convert selected periodic domains  
215 back into a time series of normalised anomalies. Period bands were selected where  
216 the frequency spectra identified shared wavelet power (and significance) between  
217 groundwater, rainfall and PET, indicating a wide-spread signal presence at these  
218 bands.

219 The reverse wavelet transform is given by:

$$(x_t) = \frac{dj \cdot dt^{1/2}}{0.776 \cdot \psi(0)} \sum_s \frac{Re(W(.,s))}{s^{1/2}} \quad (\text{Eq. 2})$$

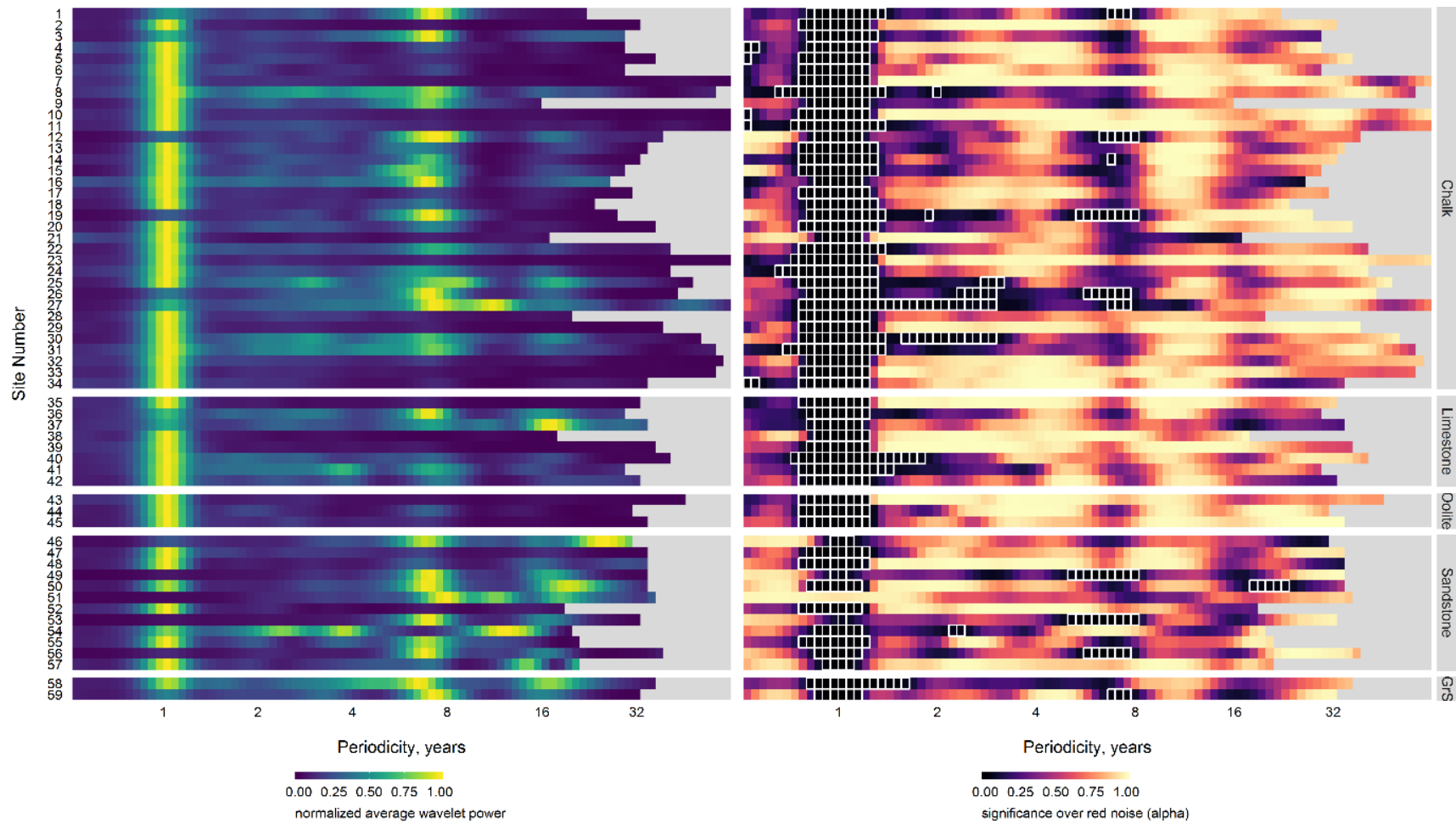
220 Where  $dj$  is the frequency step and  $dt$  is the time step.

221 Negative phases of these time-reconstruction anomaly time series were compared to  
222 episodes of recorded wide-scale hydrogeological drought (provided by Marsh et al.  
223 (2007) and Todd et al. 2013)), to assess the relationships between multi-annual  
224 variability in groundwater and groundwater droughts.

#### 225 **3.3.4.4 Periodicity strength quantification**

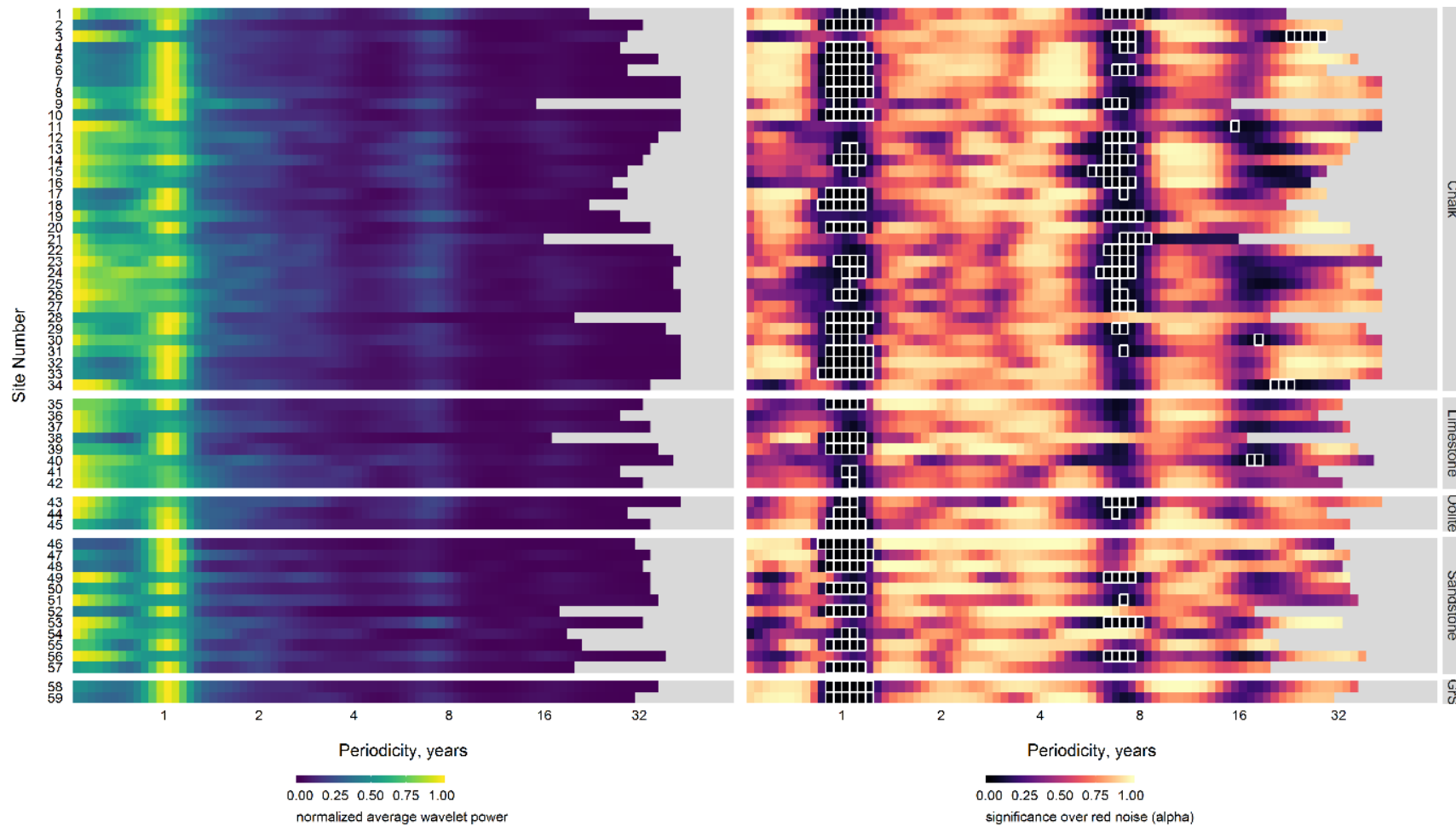
226 While the wavelet power spectra from the CWT provide an estimate of the relative  
227 strength of periodicities compared to the total frequency spectra, they do not provide  
228 an absolute measure of a periodicities contribution to total groundwater variability  
229 (which includes noise and non-periodic information). As such the percentage  
230 contributions of each time-reconstruction have been calculated. Since the datasets  
231 were normalised to the standard deviation of the raw data prior to the CWT, the  
232 standard deviations of the reconstructed anomaly time series represent the proportion  
233 of the original standard deviation as a decimal percentage.





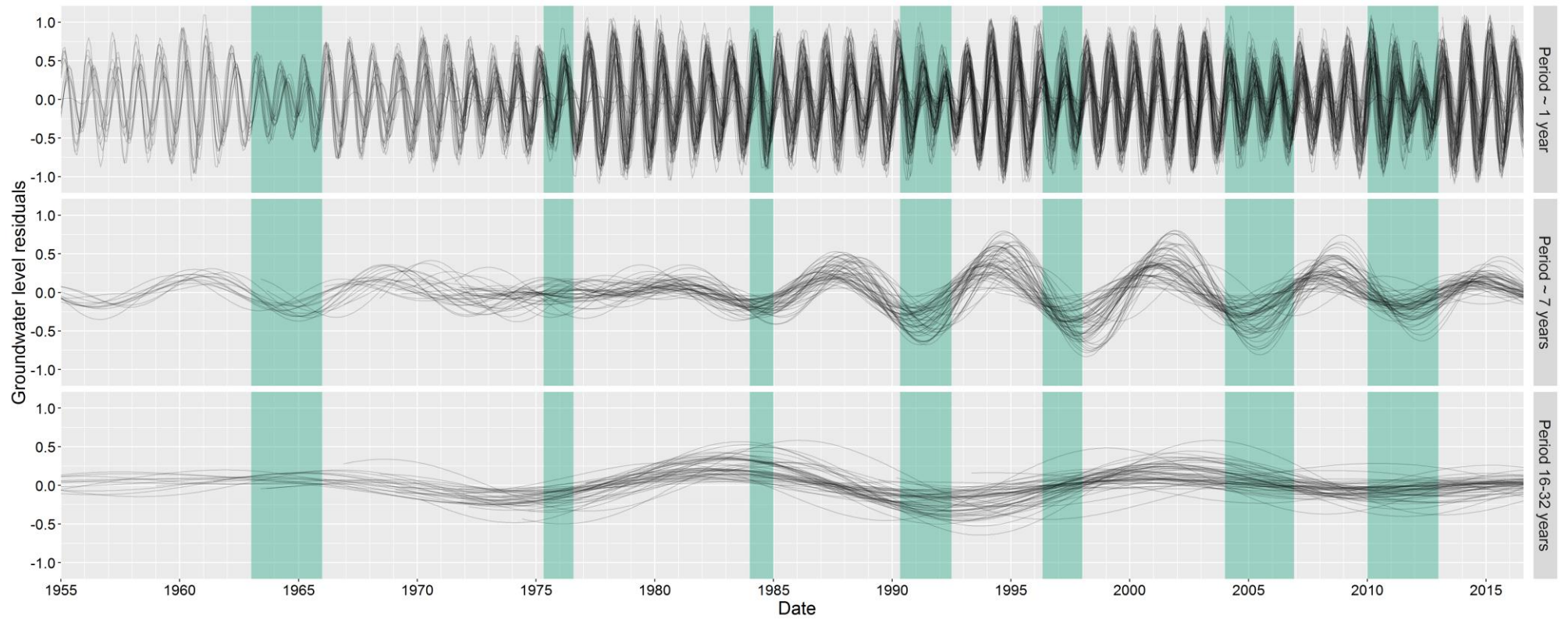
234

235 **Figure 6 Normalised average wavelet power spectra (left) and wavelet power significance alphas (right) for monthly groundwater levels**  
 236 **in the 59 index boreholes (grouped by aquifer type). In the right-hand figure, boxes outlined in white are those powers that are**  
 237 **significant over red noise to a 95% confidence interval ( $\alpha \leq 0.05$ ).**



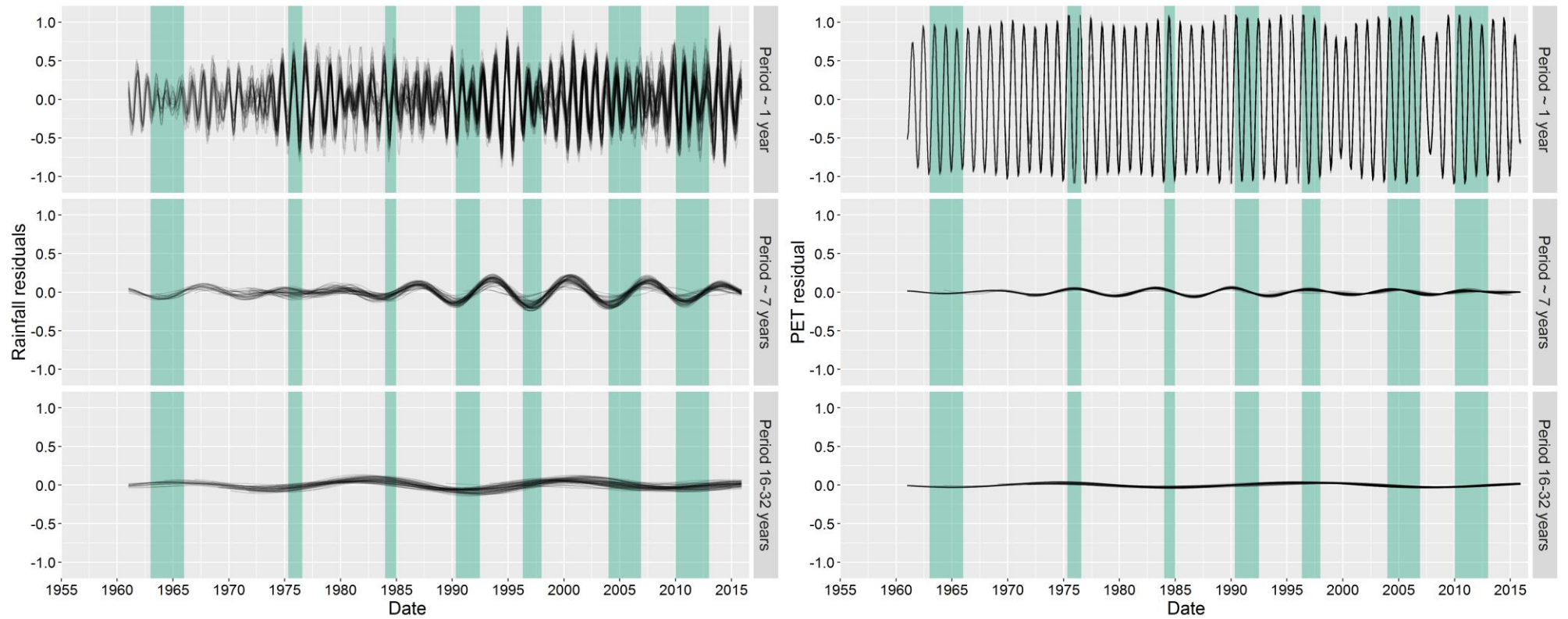
238

239 **Figure 7 Normalised average wavelet power spectra (left) and wavelet power significance alphas (right) for monthly rainfall time series**  
 240 **for co-locations of the 59 index boreholes. In the right-hand figure, boxes outlined in white are those powers that are significant over**  
 241 **red noise to a 95% confidence interval ( $\alpha \leq 0.05$ ).**



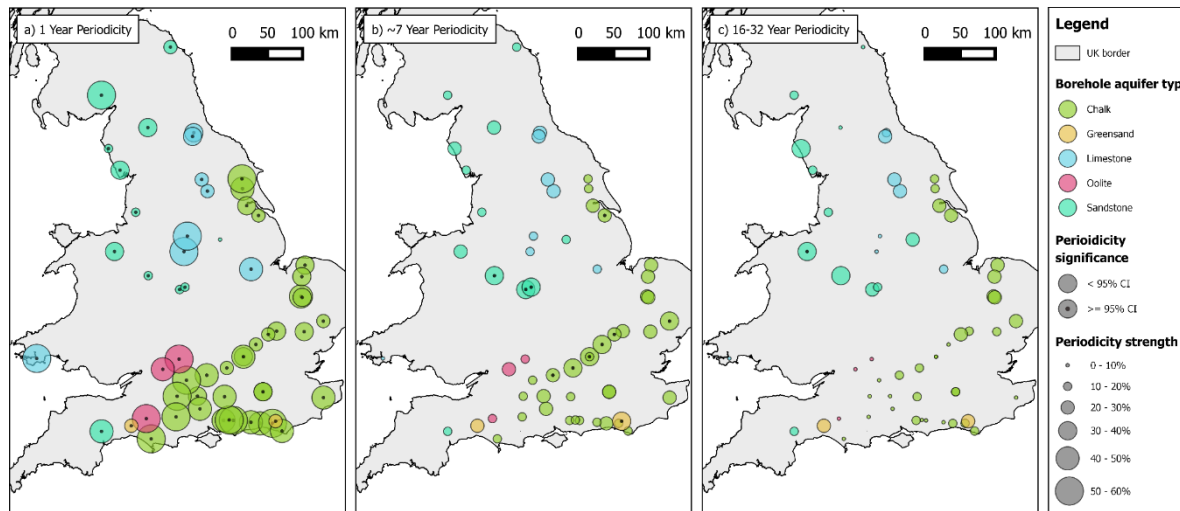
242

243 **Figure 8** Overlaid reconstructions of the three key periodic domains found across the 59 groundwater wavelet spectra are shown. All  
 244 **periods (both significant and non-significant) within these bands have been displayed to allow for comparison of period strength and**  
 245 **phase over time. Areas shaded blue represent approximate periods of significant droughts in the UK. Only reconstructions between**  
 246 **1955 and 2017 are shown to allow clearer comparison.**



247

248 **Figure 9 Overlaid rainfall (left) and PET (right) reconstructions of the three key periodic domains are shown. All periods (both significant**  
 249 **and non-significant) within these bands have been displayed to allow for comparison of period strength and phase over time. Areas**  
 250 **shaded blue represent approximate periods of significant droughts in the UK. Only reconstructions between 1955 and 2017 are shown**  
 251 **to allow clearer comparison.**



252

253 **Figure 10 Maps showing strength (percentage of the original time series standard deviation) and significance of the a) 1 year, b) ~7**  
 254 **year and c) 16-32 year periodicity bands. No periodicity strength was found to be above 60% of the original signal.**

255

## 3.4 Results

### 256 3.4.1 Time-averaged wavelet power and significance over red noise

257 Wavelet power spectra (frequency strength) and alpha values (significance) for each  
258 of the 59 groundwater level and rainfall time series are displayed in figures 6 and 7  
259 respectively. Wavelet power is analogous to the strength of the periodicity compared  
260 to other frequencies. Periodicities with alpha values less than or equal to 0.05 (95%  
261 CI) are highlighted. Bands of greater wavelet power and lower alpha values at  
262 periodicities of 1, ~7 and 16-32 year(s) can be seen across the majority of the  
263 groundwater and rainfall spectra for the 59 sites (herein referred to as P1, P7 and P16-  
264 32 respectively). PET wavelet spectra were found to have no notable or significant  
265 periodicity beyond seasonality (indicative of the UK's temperate climate), and are  
266 displayed in the supplementary material.

267

268 The annual cycle (P1) exhibited the greatest power across 43 of the 59 observation  
269 borehole spectra, with normalised wavelet powers ranging from 0.03 to 1 (mean of  
270 0.84). Alpha values for P1 in the observation boreholes also showed the greatest  
271 likelihood of external forcing when compared to the other identified periodic domains  
272 (alpha values ranging from 0.00 to 0.94, mean of 0.017). All but one observation  
273 borehole (site 51) showed significant (95%) alpha values for P1 wavelet power. Lower  
274 than average P1 wavelet powers were most prevalent in the Sandstone lithology (6  
275 out of 12 sandstone sites), Greensands (1 out of 2 sites) and to some extent, the Chalk  
276 (6 out of 35 sites). It should be noted, however, that the relatively small sample sizes  
277 of Greensand and Oolite aquifers makes interpretation of systematic differences at  
278 these lithographies difficult. P1 wavelet power was generally lower across all the  
279 corresponding rainfall time series, which is expected given rainfall's established bias  
280 towards high-frequency variability (Meinke et al. 2005). Of those boreholes with lower  
281 P1 power in groundwater, most (e.g. 35, 59) show greater P1 powers in rainfall (and  
282 PET) indicating hydrogeological processes as the mechanism for weaker P1  
283 periodicity. However, a small number (e.g. 38, 40 and 42) had similarly low P1  
284 periodicity in the corresponding rainfall, indicating meteorological drivers for poor  
285 annual strength at these observation boreholes (considering that PET showed little

286 variance in P1 strength across the observation boreholes). PET spectra and alpha  
287 values showed a universally high P1 wavelet power.

288 The second greatest wavelet power across the groundwater boreholes was between  
289 6 and 9 years, roughly centred on the 7 year periodicity (P7)). Maximum normalised  
290 groundwater wavelet powers ranging from 0.01 to 1 (average of 0.52) between  
291 boreholes were detected, and a corresponding band of lower than average alpha  
292 values (ranging from 0.01 to 0.99, mean of 0.34), indicating that this periodicity is likely  
293 to be driven by an external variance. Average P7 wavelet power values were greatest  
294 for Sandstone (0.68) and Greensands (1.00), and lower for Limestone (0.39) and  
295 Oolite (0.17). Chalk showed intermediate strength with the greatest range (0.01 to  
296 1.00, mean of 0.50). Ten groundwater sites showed significant (95%) P7 wavelet  
297 powers (sites 1, 12, 14, 19, 26, 27, 49, 53, 55 and 59). While the P7 wavelet power in  
298 the corresponding rainfall data was considerably lower than those detected in  
299 groundwater level (ranging from 0.014 to 0.35, mean of 0.16), the alpha values are  
300 comparable with the P7 signal strength in groundwater. This indicates that P7 signals  
301 in rainfall are weak, but likely driven externally. Generally lower alpha values for P7 in  
302 rainfall, compared to groundwater, are also likely a result of rainfall's lower  
303 autocorrelation. Negligible wavelet powers and no significance was shown at the P7  
304 band for corresponding PET data.

305

306 The final and second mode of common multi-annual wavelet power was the band  
307 between 16 years and 32 years (P16-32). P16-32 had an average wavelet power of  
308 0.28 across all boreholes; ranging between 0.01 and 1. Similar to P7, the greatest  
309 wavelet power of P16-32 was found in the Sandstone (average of 0.58) and the  
310 Greensand (average of 0.64) aquifer types. Whereas Chalk, Limestone and Oolite  
311 showed relatively weaker signals (averages of 0.18, 0.32 and 0.03 respectively). Only  
312 one site in the groundwater (site 50) and five rainfall time series (sites 3, 11, 30, 34,  
313 40) showed 95% significance over red noise in this periodicity band.

314

### 315 **3.4.2 Reconstructed anomaly time series**

316 The three main common period domains identified by the wavelet transform (P1, ~7  
317 and 16-32 years) were reconstructed into anomaly time series using the reversed  
318 wavelet transform and are presented in figure 8 for groundwater levels and figure 9 for  
319 rainfall and PET. This was undertaken to allow investigation and comparison of  
320 periodic behaviour over time and to assess how these reconstructed periodic signals,  
321 within multiple sites across multiple aquifers, align with periods of historical  
322 groundwater drought. The behaviour of the multiple reconstructed groundwater level,  
323 precipitation and PET anomaly time series (in all three periodicity domains) were  
324 shown to be well-aligned in time, with positive (maxima) and negative (minima) phases  
325 occurring within comparable time. The only exception to this pattern was seen  
326 between 1970 and 1980 in the P7 reconstructions, where phases in the P7  
327 reconstructions become misaligned. This was predominantly apparent in groundwater  
328 and to a lesser extent in rainfall. Positive and negative phases of the P7  
329 reconstructions in PET were well-aligned for the entire time series.

330 Notable episodes of groundwater droughts in the UK were overlaid onto the  
331 reconstructed periods in figure 9 between 1955 and 2016. With the exception of the  
332 1975-6 event, every episode of drought in this time period coincides with a negative  
333 phase of the reconstructed P7 groundwater anomalies. The 1975-6 drought (often  
334 used as a benchmark drought in the UK due to its wide-reaching impacts (Marsh et al.  
335 2007)) occurred at a time of notable minima/maxima misalignment of the P7 period  
336 across all groundwater sites, and a period of negative anomaly in the P16-32  
337 reconstructions. Most recorded major droughts in the UK appeared to occur  
338 irrespective of the state of the P16-32 anomaly, with droughts occurring in minima and  
339 maxima of this reconstruction.

### 340 **3.4.3 Percentage standard deviation**

341 The percentage of the standard deviation in the original groundwater level signal  
342 represented by each reconstructed periodicity band is shown in figure 10 for all the  
343 observation boreholes. The percentages are representative of the absolute strength  
344 of the periodicity compared to the recorded data variance (standard deviation).



345 P1 represents the greatest average contribution to groundwater variability across all  
346 the aquifer groups (Chalk: 41%, Limestone: 40%, Oolite: 52%, Sandstone: 26%,  
347 Greensand: 28%). While most sites show that P1 accounts for the greatest proportion  
348 of the standard deviation, P7 is the dominant periodicity at 11 of the 59 sites (5 within  
349 Sandstone, 5 within Chalk and 1 within Greensand), and P16-32 is the strongest cycle  
350 in 3 of the 59 sites (3 within Sandstone and 1 within Limestone). P1 strength in the  
351 Chalk appears to be greatest in the South of England, with weaker strengths in the  
352 South East and East. Aside from the Chalk, there are no clear spatial patterns in P1  
353 strength. P7 accounts for an average of 21.7% of signal strength across all aquifer  
354 groups, ranging from 3.8% to 40% across the observation boreholes. Spatial variance  
355 in P7 signal strength is less when compared to P1, although there is a noted area of  
356 significance in Chalk of South East England (e.g. the Chiltern Hills and  
357 Cambridgeshire), and a smaller cluster of P7 significance in the Sandstone of the  
358 central England, where the greatest P7 strengths are found. P16-32 strengths are  
359 spatially focused in Eastern England for the Chalk, and the central and north-western  
360 England for the Sandstone. No clear patterns for the remaining aquifer groups is  
361 apparent for the 16-32 year periodicity band.

362

## **3.5 Discussion**

### **3.5.1 Characterisation of signal presence and strength in groundwater level**

Many studies have focused on the role of seasonality in defining groundwater variability, and the onset and severity of groundwater drought (Jasechko et al. 2014; Hund et al. 2018; Mackay et al. 2015; Ferguson & Maxwell 2010). While we show that the annual cycle is an important component of groundwater response, it is often not representative of overall behaviour, accounting for (on average) less than half of total groundwater level variability. Conversely, we show that multi-annual periodicities form an unprecedented proportion of total groundwater variability; with 41% of sites (24 out of 59) exhibiting multi-annual periodicity strength that is comparable to (within 10%), or greater than, seasonality. It is expected that the strength of multi-annual cycles in groundwater level will vary according to signal strength in recharge drivers (e.g. rainfall and evapotranspiration) and hydrogeological processes that lag or attenuate long-term changes in these recharge signals (Van Loon 2013; Van Loon 2015; Townley 1995; Dickinson et al. 2014). These two processes may explain the local differences in signal strength between sites in aquifer types and geographically across the UK, as displayed in the results. For instance, pronounced multi-annual variability (significant 7 year cycles and stronger 16-32 year cycles) in the Chalk sites is generally associated with catchments of thicker unsaturated zones, larger interfluves or areas of weaker corresponding seasonality in rainfall (for example, the Chiltern Hills in South East England). These catchment properties have been shown to dampen higher frequency variability between rainfall and groundwater response due to storage buffers, thereby producing a sensitivity to multi-annual variability (Peters et al. 2006; Van Loon 2013). Multi-annual cycles are also generally strong for the granular porosity aquifers (Sandstone and Greensand); which is to be expected given the influence of lower hydraulic diffusivity (typical of granular porosity flow) on the suppression of high-frequency variability (Townley 1995). This also agrees with Bloomfield & Marchant (2013) who

document sensitivity to long-term accumulation in rainfall in UK Sandstone aquifers. Conversely, the Limestone and Oolite aquifer types exhibit weaker multi-annual periodicities in groundwater level, with strong seasonality. Townley (1995) and Price et al. (2005) document that, due to their faster-responding fracture porosity with low storativity, limestone lithographies have a lower damping capacity of finer-scale variability in recharge, meaning they are able to respond in-time to the strong seasonality in PET and rainfall. The results typically show lower percentage contributions of multi-annual periodicities to total groundwater level variability than some previous international studies (Kuss & Gurdak 2014; Neves et al. 2019; 389; Velasco et al. 2015). This can be explained by potentially weaker periodicities in driving climatic circulations over Europe compared to North America (as indicated by Kuss & Gurdak (2014)), or UK-specific hydrogeological properties such as smaller aquifer size compared to North America or continental Europe, which may affect teleconnection strength (Rust et al, 2018). However, we also expect lower percentage contributions of multi-annual periodicities due to the use of unmodified groundwater level datasets prior to spectral decomposition (wavelet transform). Using unmodified level data has enabled us to represent the absolute contribution of multi-annual variability to groundwater level behaviour at each site.

### **3.5.2 Evidence for teleconnection control on multi-annual groundwater variability**

Here, we discuss the evidence that the multi-annual variability present in UK groundwater level records (as previously discussed) is the result of teleconnection influences with climatic oscillations. The conceptualisation of groundwater teleconnections of Rust et al (2018) suggests that a teleconnection between the oscillatory climate systems and groundwater level would be associated with;

- a) an apparent and coherent multi-annual periodicity band within groundwater sites across a wide geographical area, that aligns with known

- multi-annual variability in indices of climatic oscillations (for instance, the 7-year periodicity of the NAO (Hurrell et al. 2003),
- b) increased likelihood that this periodicity band is the result of an external influence, and not the result of internal red-noise variability of the groundwater level time series (as indicated by Allen et al. (1996) and Meinke et al. (2005))
  - c) comparable signals in rainfall as established drivers for multi-annual groundwater variability, and
  - d) broad alignment of minima and maxima of time-reconstructed multi-annual periodicities. Some fine-scale misalignment in groundwater periodicities is expected as a result of unsaturated and saturated zone lags between rainfall and groundwater response (Van Loon 2013; Peters et al. 2006; Dickinson et al. 2014; Cuthbert et al. 2019).

The majority of groundwater level hydrographs and corresponding rainfall profiles showed a coherent band of increased periodicity strength and periodicity significance principally around the 7-year frequency range and, to a lesser extent, the 16-32 year range. The 7 year periodicity closely compares to the principle 7-year periodicity documented in the strength of the NAO's atmospheric dipole, which has been associated with multi-annual periodicities in rainfall (Meinke et al. 2005) and groundwater globally (Tremblay et al. 2011; Kuss & Gurdak 2014; Holman et al. 2011; Neves et al. 2019). Additionally, the time-reconstructions show clear temporal alignment of minima (with the exception of the 1975-6 period, which will be discussed later), indicating the wide-spread coherent influence of a climatic teleconnection. As such, we corroborate with existing research that documents the control of the NAO on UK rainfall (Alexander et al. 2005; Trigo et al. 2004), and show new evidence of the wide-spread propagation of multi-annual variability in rainfall through to spatio-temporal multi-annual groundwater variability, conceptualised by Rust et al (2018).

While the NAO is known to be the dominant mode of winter climate variability in Europe (López-Moreno et al. 2011; Alexander et al. 2005; Hurrell & Deser 2010), the second strongest is provided by the East Atlantic (EA) pattern (Wallace &

Gutzler 1981). The EA is similar in frequency structure to the NAO but shifted southward, however it has been shown to exhibit its own internal variability (Hauser et al. 2015; Tošić et al. 2016; (Moore et al., 2013). Importantly, the EA has been shown to exhibit a 16-32 year periodicity (Holman et al, 2011), and therefore aligns with the second strongest mode of multi-annual variability in groundwater and rainfall documented in this study. As such, the increased strength, significance and minima-alignment of the 16-32 year periodicity range detected in groundwater levels in this paper may be explained through a teleconnection between the EA pattern and European winter climate variability.. While the EA has received little focus in climate variability research compared to the NAO, the findings here support Krichak & Alpert (2005) who document a multi-decadal control on UK and European precipitation through shifting phases of the EA, and Holman et al (2011) who detected weak relationships between the EA and groundwater levels in the UK. Comas-Brua and McDermotta (2014) suggest that much of the multi-decadal climate variability (temperature and precipitation) in the North Atlantic region can be explained by a modulation of the NAO by the EA, which may contribute to the spatial and temporal variability seen in both the ~7 year and 16-32 year reconstructions across the borehole sites. In summary, the modes of multi-annual variability detected in the majority of UK groundwater level hydrographs and rainfall time series appear to be best explained via a teleconnection with the NAO and EA's principle periodicities.

### **3.5.3 Teleconnections as indicators for groundwater extremes**

The final objective of this paper was to assess the extent to which the timing of multi-annual periodic groundwater level oscillations align with the timing of recorded groundwater droughts. To achieve this, documented periods of groundwater drought have been compared to reconstructed periodicities within groundwater level. We show principally, that every documented groundwater drought between 1955 and 2014 occurs during a negative phase of the ~7 year cycle detected in the majority of UK groundwater boreholes, with the exception of the 1975-6 drought.

Groundwater droughts are typically the result of multi-annual accumulation of rainfall deficits, with the specific timing and duration of drought (for a particular site) also driven by sub-annual rainfall and evapotranspiration (Van Loon et al. 2014; Peters 2003). Marsh et al. (2007) identify a multi-annual decline in rainfall for the majority of droughts in the UK over the past 60 years, with rainfall deficits reaching a critical accumulation period of 2-3 years in the lead-up to drought commencement (Folland et al. 2015). It is therefore to be expected that the majority of droughts are captured within the negative phases of the ~7 year cycle in the groundwater level anomalies, as this cycle (along with the 16-32 year cycle) represents groundwater's multi-annual response to the land-atmosphere water flux. The 1975-6 drought does not fit this pattern as we show a clear disruption to the ~7 year cycle during this period. This is of particular interest as this event is generally acknowledged to be anomalous for the UK. The severity of this event has been solely attributed to a short-term meteorological state (i.e. high-pressure atmospheric blocking) in existing literature, with very little long-term decline in groundwater levels (Rodda & Marsh, 2011; Bloomfield & Marchant 2013). It is therefore to be expected that the 1975-6 drought did not occur during a coherent negative phase of the ~7 year cycle detected in groundwater levels, and that we see a more pronounced suppression of seasonality during this time. Furthermore, we note that most droughts do not perfectly align with the minima of this ~7 year cycle. As previously stated, the commencement of a drought is dependent a combination of on multi-annual land-atmosphere water fluxes and particular sub-annual hydrological conditions (Van Loon et al. 2014). Therefore, this ~7 year fluctuation could be considered a cycle of increased drought risk, where groundwater resources may be more sensitive to sub-annual hydrological conditions. The 16-32 year periodicity, while also a representation of groundwater's multi-annual response to moisture balance, represents a smaller proportion of total groundwater behaviour and as such appears less representative of drought timings. Despite this, it is likely that this signal still has a role in modulating the severity of the ~7 year component.

The NAO and EA's control on long-term rainfall deficits in the UK and Europe has previously been identified by many studies (López-Moreno et al. 2011; Fowler & Kilsby 2002; Hurrell 1995). Here, we provide evidence to suggest that the NAO teleconnection with long-term rainfall volumes, in particular, propagates to detectable modes of groundwater level behaviour, creating episodes of increased drought risk in-line with the NAO's principal periodicity of approximately 7 years. While the effects of (non-) stationarity between the NAO, EA and UK hydrogeology have not been assessed in this study, these detected cycles may yield improved foresight into future episodes of increased drought risk in the UK. This is especially important given the proportion of groundwater level variability these cycles represent. We also note that teleconnections are not persistent and can be disrupted as exemplified by the 1975-6 drought. The findings here agree with Parry et al (2011) who found no relationship with this drought and the NAO phase or strength. Peings & Magnusdottir (2014) suggest that atmospheric blocking prohibits the expected effects of the NAO on UK and European rainfall, which may explain both the 1975-6 drought and the disruption to the 7-year periodicity in UK groundwater (Rodda & Marsh 2011). This therefore further highlights the importance of atmospheric blocking in regulating groundwater variability in the UK (Shabbar et al. 2001).

### **3.6 Conclusions**

This paper assesses the role of multi-annual variability and ocean-atmosphere systems in influencing groundwater drought. We quantify the absolute contribution of multi-annual cycles to groundwater variability, and provide new evidence for the influence of the NAO's control of European rainfall on UK groundwater drought over the past 60 years.

The wavelet transformation was used to identify and evaluate bands of periodic external influence on UK groundwater level hydrographs. We document the strength of multi-annual behaviour that align with the NAO's principal periodicity (approximately 7 years) and the EA's principal periodicity (16-32 years). We find

that seasonality accounts for an average of 39% of groundwater level variance across boreholes; with 7-year cycle accounting for an average of 21%, and 16-32 years accounting for 15%. Furthermore, we show the majority of UK droughts align with a negative phase of the 7-year cycle indicating periods of increase drought risk as part of this periodicity. In the UK, the economic regulator has implemented several measures to promote the trading of water between water supply companies to enable a more robust water supply system (OfWAT 2019; Deloitte LLP 2015). Here, we show that recursive patterns in groundwater contribute to a considerable proportion of the total groundwater level variability and therefore may provide new insights to allow undertakers of water supply to trade water further into the future, depending on teleconnection sensitivities. Such forecasted planning could help to reduce the ecological and human impacts of groundwater drought by allowing more time to plan and organised the required water transfers from areas less susceptible to teleconnection-driven drought. It is clear from the results here that long-range groundwater drought forecasts via climate teleconnections present transformational opportunities to drought prediction and its management across the North Atlantic region.

### **3.7 References**

The reference list for this paper has been combined with the final reference section for this thesis in chapter 10.



## **4 CHAPTER 4: CATCHMENT CONTROLS ON CYCLE PROPAGATION**

This chapter consists of the published article Rust et al (2021a); “Exploring the role of hydrological pathways in modulating multi-annual climate teleconnection periodicities from UK rainfall to streamflow”. This chapter will address research objectives 2.

### **4.1 Abstract**

An understanding of multi-annual behaviour in streamflow allows for better estimation of the risks associated with hydrological extremes. This can enable improved preparedness for streamflow-dependant services, such as freshwater ecology, drinking water supply and agriculture. Recently, efforts have focused on detecting relationships between long-term hydrological behaviour and oscillatory climate systems (such as the North Atlantic Oscillation – NAO). For instance, the approximate 7 year periodicity of the NAO has been detected in groundwater-level records in the North Atlantic region, providing potential improvements to the preparedness for future water resource extremes due to their repetitive, periodic nature. However, the extent to which these 7-year, NAO-like signals are propagated to streamflow, and the catchment processes that modulate this propagation, are currently unknown. Here, we show statistically significant evidence that these 7-year periodicities are present in streamflow (and associated catchment rainfall), by applying multi-resolution analysis to a large data set of streamflow and associated catchment rainfall across the UK. The results presented here provide new evidence for spatial patterns of NAO periodicities in UK rainfall, with areas of greatest NAO signal found in southwest England, south Wales, Northern Ireland and central Scotland, and show that NAO-like periodicities account for a greater proportion of streamflow variability in these areas. Furthermore, we find that catchments with greater subsurface pathway contribution, as characterised by the baseflow index (BFI), generally show increased NAO-like signal strength and that subsurface response times (as characterised by groundwater response time – GRT), of between 4 and 8 years,

show a greater signal presence. The results provide a foundation of understanding for the screening and use of streamflow teleconnections for improving the practice and policy of long-term streamflow resource management.

## **4.2 Introduction**

Meteorological conditions in many parts of the world are modulated by large-scale ocean–atmosphere systems, such as the Pacific Decadal Oscillation (PDO) and El Niño–Southern Oscillation (ENSO) in the western US (DeFlorio et al., 2013) and the North Atlantic Oscillation (NAO) in Europe (Trigo et al., 2002; Hurrell and Van Loon, 1997), with important multi-annual periodicities (Labat, 2010; Kuss and Gurdak, 2014). The NAO, a dipolar system of atmospheric pressure in the North Atlantic region (Hurrell and Deser, 2010), has been shown to account for the majority of European rainfall variability during the winter months and is particularly influential in western Europe (West et al., 2019; Uvo, 2003; Alexander et al., 2005; López-Moreno et al., 2011). This is achieved through a modulation of westerly storm tracks (Trigo et al., 2002; Dawson et al., 2004) and Gulf Stream strength (Frankignoul et al., 2001; Chaudhuri et al., 2011; Watelet et al., 2017) by the winter state of the NAO. As such, the NAO has been shown to drive hydrological variability in Europe, including river flow (Kingston et al., 2011; Svensson et al., 2015) and groundwater systems (Rust et al., 2019; Neves et al., 2019; Holman et al., 2011).

In addition to sub-annual variability, the NAO has been shown to exhibit a weak multi-annual cycle of between 6 and 9 years, often described as pseudo-periodic due to its varying strength (Hurrell et al., 2003; Zhang et al., 2011; Olsen et al., 2012). Despite this reported weakness, many hydroclimatology studies have identified a relationship between the NAO index (NAOI) and groundwater-level records, at multi-annual frequencies, in the USA (e.g. Kuss and Gurdak, 2014), continental Europe (e.g. Neves et al., 2019) and the UK (e.g. Holman et al., 2011). The strength of these detected cycles in groundwater records is often considerably stronger than those found in the NAOI, indicating that the 6–9 year periodicity of the NAO may still yield a considerable modulation on hydrological systems that are sensitive to long-term changes in water fluxes, such as

groundwater stores. (Bloomfield and Marchant, 2013; Forootan et al., 2018; Van Loon, 2015). Rust et al. (2019) compared NAO-like periodicities in composite rainfall records and groundwater levels in the UK's principal aquifers, demonstrating the degree to which multi-annual periodic signals (similar to those in the NAO) can be modulated through part of the hydrological cycle. Given the presence of these multi-annual cycles in both UK rainfall and groundwater records, it follows that these signals may be propagated to streamflow, particularly in groundwater-dominated streams such as those found in many parts of southern and eastern England (Bloomfield et al., 2009). High baseflow streams are often critical for the function of public water supply and freshwater ecosystems and provide a greater amenity value for surrounding areas (Acreman and Dunbar, 2004). Therefore, an understanding of the catchment processes that modulate multi-annual cycles in streamflow may provide a new opportunity to better manage the long-term use and sustainability of these streamflow-dependant services (Acreman and Dunbar, 2004; Chun et al., 2009). While existing studies have shown that the winter-averaged NAO can modulate streamflow in the UK at an annual scale (Kingston et al., 2006), the strength and spatiality of multi-annual cycles in streamflow, and the catchment processes that modulate them, have yet to be assessed.

Hydrological pathways are often used to conceptualise the propagation of effective rainfall signals (rainfall minus evapotranspiration) through a catchment to streamflow (Misumi et al., 2001; Bracken et al., 2013; Crossman et al., 2014; Lane et al., 2019). For example, surface pathways are the result of infiltration- or saturation-excess runoff from the land surface and provide a direct response to rainfall of the order of hours or days (Nathan and McMahon, 1990; Gericke and Smithers, 2014; Kronholm and Capel, 2016). Subsurface pathways (such as the travel of water through the unsaturated zone and groundwater flow paths to channel baseflow) exhibit generally lower celerities than surface pathways and can produce a protracted response to rainfall of the order of months or years, where faster subsurface pathways dominate (Carr and Simpson, 2018; Hellwig and Stahl, 2018), but range to decades or even millennia for longer, deeper groundwater flow pathways with low hydraulic diffusivity (Rousseau-Gueutin et

al., 2013; Cuthbert et al., 2019). Existing research into periodic NAO teleconnections with groundwater resources has highlighted the importance of subsurface pathway responsiveness in modulating NAO-like signals in groundwater stores (Kuss and Gurdak, 2014; Neves et al., 2019; Rust et al., 2019). Where a groundwater resource receives a periodic recharge signal (such as those from a climatic teleconnection), Townley (1995) suggests that pathways with response times shorter than the period length will propagate these signals to baseflow more effectively and with minimal damping. Conversely, groundwater pathways with response times longer than the period length cannot convey these signals to the stream at a sufficient rate, meaning that the amplitude of the periodic signal is damped as it passes through the aquifer. Therefore, in the case of streamflow, we may expect the following:

- The propagation of multi-annual periodic signals from rainfall to streamflow that is dependent on the relative contribution of surface and subsurface (e.g. groundwater) hydrological pathways within a catchment.
- Response times of subsurface pathways will modulate the amplitude of multi-annual periodic signals in streamflow where they are propagated by subsurface pathways.

Finally, these effects (modulation of NAO signal propagation by hydrological pathways) may be expected to differ between winter and summer streamflow. Catchments in the UK have been shown to receive the strongest NAO signals in winter rainfall (Alexander et al., 2005; Hurrell and Deser, 2010; West et al., 2019). However, given the degree of fine-scale variability seen in precipitation records (Meinke et al., 2005), winter streamflow may contain a relatively low signal-to-noise ratio as surface (and some subsurface) hydrological pathways respond to rainfall within the same winter season. Conversely, slower subsurface pathways provide a protracted response to winter rainfall signals and are generally accepted to filter finer-scale variability (Bloomfield and Marchant, 2013). As such, we may expect the NAO teleconnection to have a greater influence on summer streamflow in permeable catchments which have a greater contribution from subsurface pathways (baseflow) and proportionally less contribution from surface

pathways. In these instances, we may expect the teleconnection between NAO and UK streamflow may be asymmetric between summer and winter. If multi-annual periodic signals in streamflow are present via a teleconnection with the NAO, their use for improving the long-term projection of hydrological extremes will rely on an understanding of the catchment processes that modulate the strength of these signals and their seasonal sensitivities.

The aim of this paper is to assess the extent to which NAO-like multi-annual signals are propagated from rainfall to streamflow across the UK and to assess how this is modulated by the relative contribution of faster and slower hydrological pathways. We define NAO-like as those multi-annual cycles in hydrometeorological records that cover a wide spatial domain and are similar in length to the 6–9 year periodicity reported in the NAO, which we might expect given the control between the NAO and hydrological systems (Svensson et al., 2015).

This aim will be met by addressing the following research objectives:

1. characterising the strength, statistical significance and spatial distribution of NAO-like multi-annual periodicities in rainfall and associated UK streamflow; and
2. quantifying the relationship between catchment pathway contribution and response times and the NAO teleconnection by comparing NAO-like periodicity strength in summer and winter streamflow.

## **4.3 Data and Methods**

### **4.3.1 Streamflow Data**

Monthly streamflow data and catchment metadata from the UK National River Flow Archive (NRFA; Dixon et al., 2013; <http://nrfa.ceh.ac.uk/>, last access: 14 July 2020) has been used in this study. Gauging stations with more than 20 years of continuous streamflow data (and coincident catchment rainfall,

discussed in the following section) and no data gaps greater than 12 months were initially selected. Where there were multiple gauging stations in a single named river catchment, only the sites with the largest catchment area were taken forward. This produced a final list of 705 streamflow gauging stations for use in this study. These streamflow records range from 20 to 128 years in length, with a median length of 44.6 years (536 months). These sites provide a representative sample of sites from across the UK, with minimal bias towards the south of England, as indicated by Figure 11. It should be noted that, ideally, streamflow that has minimal influence from human factors should be used in hydroclimate studies to avoid confounding mechanisms; however, no such large-scale data set exists for the UK. Furthermore, over the period of analysis and the broad scale of this assessment, inconsistencies in the way water resource management practices are implemented is expected to result in noise to the observations rather than some systematic signal or bias that would affect the results of this paper.

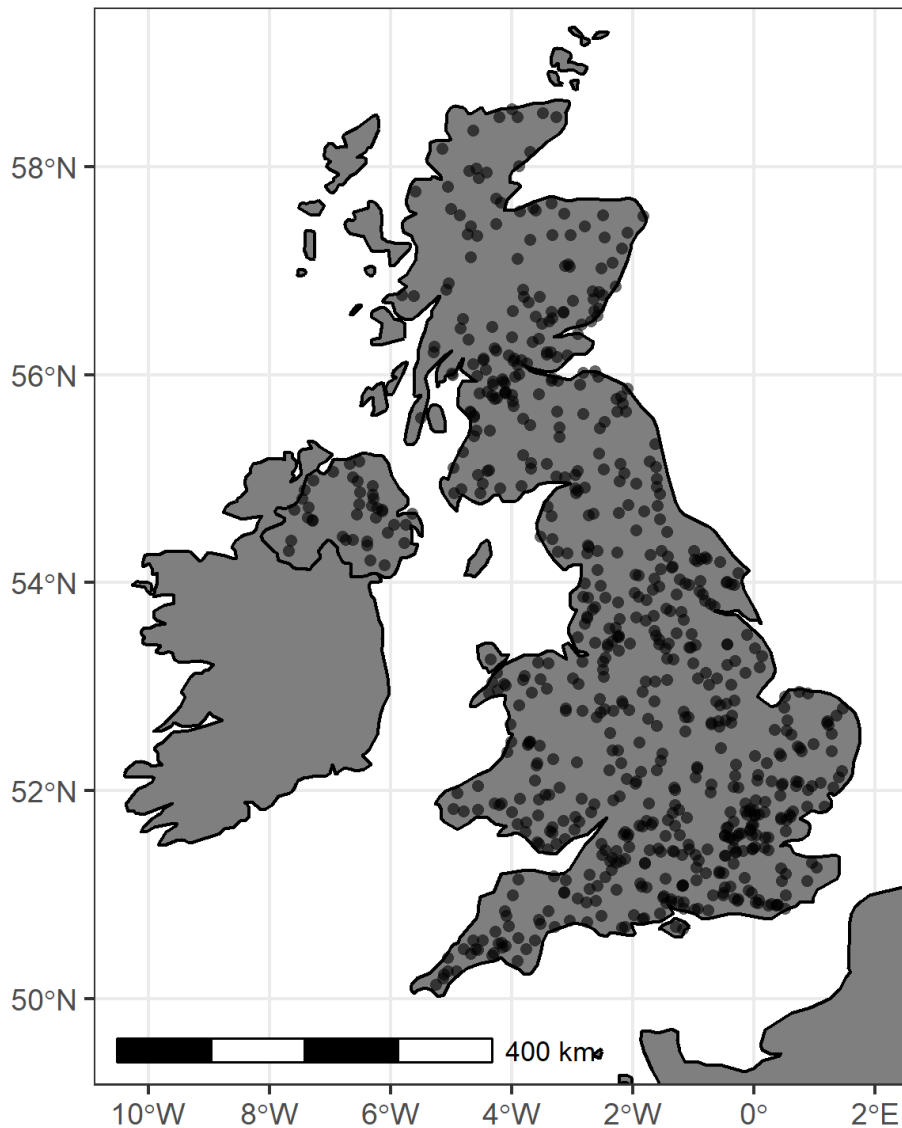


**Figure 11** Locations of streamflow gauges used in this study.

### 4.3.2 Catchment Rainfall Data

In order to categorise the relative influence of surface and subsurface hydrological pathways on streamflow, the baseflow index (BFI) from the NRFA has been used for each streamflow gauge (Gustard et al., 1992). The BFI is a calculated proportion of the flow hydrograph (ranging from 0 to 1) that is derived from slower subsurface pathways such as groundwater-driven baseflow, where 1 is entirely baseflow. While empirical, BFI has been shown to be effective in

relating physical catchment pathway processes to streamflow behaviour (Bloomfield et al., 2009; Chiverton et al., 2015) in addition to catchment storage. Figure 12a shows the spatial distribution of BFI across the UK. Higher BFI values are generally found in catchments with greater groundwater influence, such as those in southern and eastern England which are dominated by the UK's chalk aquifer (Marsh and Hannaford, 2008). Areas of moderate BFI can also be found where there are substantial superficial or glacial deposits, such as western England, central Wales and eastern Scotland. In this study, BFI has been grouped into low (0–0.25), medium (0.25–0.5), high (0.5–0.75) and very high (0.75–1). Bins at 0.25 intervals have been generated to test the relationship between varying BFI and multi-annual signal presence. While this potentially produces a non-normal distributed categorisation, it is necessary to effectively test a spread of BFI values. This non-normal distribution is mitigated by the choice of significance test described in the methods section.

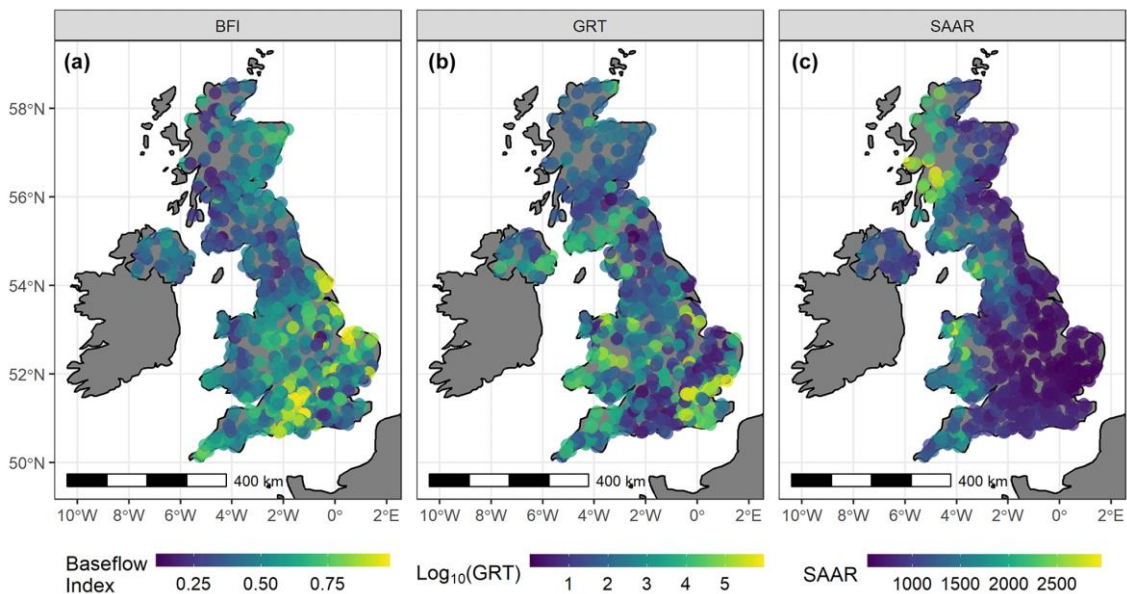


**Figure 12 Spatial distribution of (a) baseflow index (BFI), (b) log<sub>10</sub>(GRT) and (c) standard average annual rainfall (SAAR) for each streamflow record.**

In addition to the BFI, the global data set of groundwater response times (GRTs), developed by Cuthbert et al. (2019), has been used in this study to estimate the responsiveness of unconfined subsurface pathways. GRT (T) can be



conceptualised as a measure of the time required for a groundwater store to return to equilibrium after a perturbation in recharge, and it is given by the following:

$$\text{GRT} = \frac{L^2 S}{\beta T} \quad (\text{Eq.3})$$

where  $\beta$  is a dimensionless constant,  $T$  is transmissivity ( $L^2T^{-1}$ ),  $S$  is storativity (-) and  $L$  is the characteristic groundwater flow path length approximated for unconfined groundwater systems by the distance between perennial streams ( $L$ ). In this study, the mean GRT was taken for each of the NRFA catchment boundaries for each streamflow gauge.  $\text{Log}_{10}$  of GRT is displayed in Figure 12b for clarity purposes as the GRT ranges from approximately 1 year to approximately a million years (e.g. in very low permeability geological formations) for gauge catchments used in this study. While the mapping of GRT was carried out using global data sets with their inherent uncertainties, it should nevertheless enable categorisation of the likely timescales of groundwater response sufficiently well for the purposes of this paper. GRT is seen to be lowest (indicating shorter response times) in areas similar to areas of higher BFI, i.e. southern and eastern England but excluding the most southeasterly regions which show some of the highest GRT values (indicating longer response times). Lower GRT values are also seen in northern England. While BFI and GRT appear inversely similar in spatial extent, their correlation is low ( $r=-0.304$ ). This is to be expected as they measure different aspects of the catchment process. Unlike BFI, which is an empirical measure of the degree to which slower pathways contribute to streamflow variability (which may encompass groundwater and throughflow), GRT is an estimate of the responsiveness of groundwater stores. In this study, GRT is grouped into five categories, namely 0–4 years, 4–8 years, 8–16 years, 16–32 years and greater than 32 years.

Finally, standard average annual rainfall (SAAR) for the period 1961–1990 is also provided as metadata in the NRFA. While not used in the analysis, it is provided here to aid later discussion. There is a clear zonal divide in SAAR distribution in

the UK, with greater values on the west coast and lower values found on the east coast of the UK and central England; the greatest values are found in western Scotland.

### 4.3.3 Methods

#### 4.3.3.1 Data pre-processing

In this study, we follow a similar pre-processing methodology to that set out in Rust et al. (2019). The following pre-processing steps were undertaken. First, all time series were centred on the long-term mean and normalised to the standard deviation to produce a time series of anomalies. This is to allow spectra between rainfall and streamflow (and between sites across the UK) to be directly compared. From these anomalies, three time series were created for both streamflow and rainfall, namely monthly, winter-averaged (December, January and February – DJF) data and summer-averaged (June, July and August – JJA) data.

#### 4.3.3.2 Continuous wavelet transform (CWT) and identification of multi-annual periodic signals

The continuous wavelet transform (CWT) is a multi-resolution analysis use to quantify the amplitude of periodic components of a time series. It has been used increasingly on hydrological data sets to extract information on non-stationary periodic behaviours in rainfall (Rashid et al., 2015), river flow (Su et al., 2017) and groundwater (Holman et al., 2011; Kuss and Gurdak, 2014). We use the package of WaveletComp, produced by Rosch and Schmidbauer (2018), for all transformations in this paper. The wavelet power,  $W$ , represents a dimensionless, absolute measure of periodic amplitude at a time index,  $t$ , and scale index,  $s$ , through a convolution of the data sequence ( $x_t$ ) with scaled and time-shifted versions of a wavelet as follows:

$$W(\tau, s) = \frac{1}{s} \left| \sum_t x_t \frac{1}{\sqrt{s}} \psi * \left( \frac{t - \tau}{s} \right) \right|^2 \quad (\text{Eq. 4})$$

where the asterisk represents the complex conjugate,  $t$  is the localised time index,  $s$  is the wavelet scale, and  $dt$  is the increment of the time shifting of the wavelet. The choice of the set of scales,  $s$ , determines the wavelet coverage of the series in its frequency domain. The Morlet wavelet was favoured over other candidates due to its good definition in both the time and frequency domains (Tremblay et al., 2011; Holman et al., 2011). Since all data sets have been converted to anomalies prior to the CWT, the calculated wavelet power represents the relative strength of periodicities within the frequency spectra of the anomaly data set. CWT was undertaken on all three data set time resolutions (monthly, winter average and summer average) to gain an understanding of the periodicities within UK seasonal hydrological data.

#### **4.3.3.3 Wavelet significance testing**

Environmental data sets generally exhibit non-zero lag-1 autocorrelations (AR1) due to system storages (Meinke et al., 2005). As a result, they can produce low frequencies as a function of internal variance rather than an external forcing (Allen and Smith, 1996; Meinke et al., 2005; Velasco et al., 2015). In order to assess whether the periodicities detected as part of the CWT are likely to be the result of noise within the data set, a red noise (AR1) significance test has been carried out on all wavelet transforms. For this, 1000 randomly constructed synthetic series with the same AR1 as the original time series were created using Monte Carlo methods. Wavelet spectra maxima from these represent periodicity strength that can arise from a purely red noise process. Wavelet powers from the original data set that are greater than these red periodicities are, therefore, considered to be driven by a process other than red noise, thus rejecting the null hypothesis. It is important to note that this does not test the significance of a relationship with the NAO but simply the probability that any periodicity detected is the result of internal variance. Teleconnection processes are often noisy, meaning that the identification of significant periodic behaviours in hydrological data sets can be problematic (Rust et al., 2019). While we highlight any periodicities equal to or above a 95 % confidence interval (CI) ( $\leq 0.05$  p values, due to convention), we also report the full range of p-value results in order to accrue an understanding of periodic forcing across the large data set.

#### **4.3.3.4 Identification of common multi-annual period strengths in rainfall and streamflow**

An exploratory approach was undertaken to identify the most prominent, common multi-annual periodicity across the streamflow records. The wavelet powers of defined peaks in the wavelet power spectrum, greater than 1 year, were identified since the NAO is expected to produce a dominant, widespread multi-annual periodicity similar to those found in UK groundwater-level records (Rust et al., 2019). Where no peak multi-annual periodicity was found (this occurred in 20 data sets; ~3 % of the total data), the maximum wavelet power was identified from within the 25th and 75th percentile of the identified peak wavelet powers from the rest of the streamflow data set. These bounds were used to calculate peak multi-annual periodicities in rainfall data sets for the winter and summer streamflow time resolutions. In order to isolate the relationship between catchment responsiveness and multi-annual signal strength, the effect of spatially varying signal powers in rainfall needs to be minimised. As such, a residual wavelet power was calculated for each of the streamflow gauges by subtracting the rainfall multi-annual wavelet power from the streamflow multi-annual wavelet power. This is, therefore, also a measure of how signal strength is modulated between rainfall and streamflow. For the summer streamflow NAO powers, a pragmatic decision was made to construct the residual using summer streamflow and winter rainfall, given the dominant control of the NAO on winter rainfall totals, the perennial nature of all UK catchments in this study and the expectation that winter recharge will be a dominant driver for summer baseflow (Hannaford and Harvey, 2010). It is important to note that modulation, in this case, refers to a change in the spectral strength of specific periods between rainfall and streamflow and not a measure of change in the amplitude of a temporally periodic behaviour between rainfall and streamflow.

#### **4.3.3.5 Testing the relationship between NAO-like signal strength and hydrological pathway characteristics**

In order to test the significance of the relationship between the BFI and GRT groups and NAO-like signal presence, the Mann–Whitney U test (MWU) was undertaken. The MWU tests the null hypothesis that it is equally likely that a randomly selected value from one population will be different to a randomly selected value from a second population. We use this test here to investigate whether populations from each successive pair of ordinal groups (e.g. low to medium for BFI) have significantly different distributions. The MWU is appropriate for non-normally distributed BFI and GRT data sets.

## **4.4 Results**

### **4.4.1 Average wavelet power and $p$ values**

Wavelet power spectra and  $p$  values for each of the 705 streamflow and catchment rainfall records are displayed in Figs. 3 and 4, respectively. Average wavelet power and  $p$  values across all sites are shown by the thick line in each plot. Wavelet power is a measure of the relative strength of periodic behaviour (periodicity) within a data set. It should be noted that these spectra are produced from normalised monthly, winter and summer data sets and, as such, represent signal presence relative to the variance of the individual data set. In the monthly streamflow and rainfall spectra figures, two discrete bands of periodicity can be seen in the average wavelet powers. These are centred on the 1-year and, approximately, 7-year periodicity, with average 1-year wavelet powers of 0.661 (range – 0.113–0.980) for streamflow and 0.284 (range – 0.051–0.621) for catchment rainfall and average 7-year wavelet powers of 0.056 (range – 0.002–0.360) for streamflow and 0.036 (range – 0.003 and 0.070) for rainfall. The ~7-year periodicity (P7) signal is also exhibited as discrete periodicities in the seasonal data, with mean P7 wavelet powers of 0.274 (0.029–0.582) and 0.198 (0.010–0.571) for winter and summer streamflow and 0.253 (0.015–0.472) and 0.107 (0.006–0.535) for winter and summer catchment rainfall, respectively.

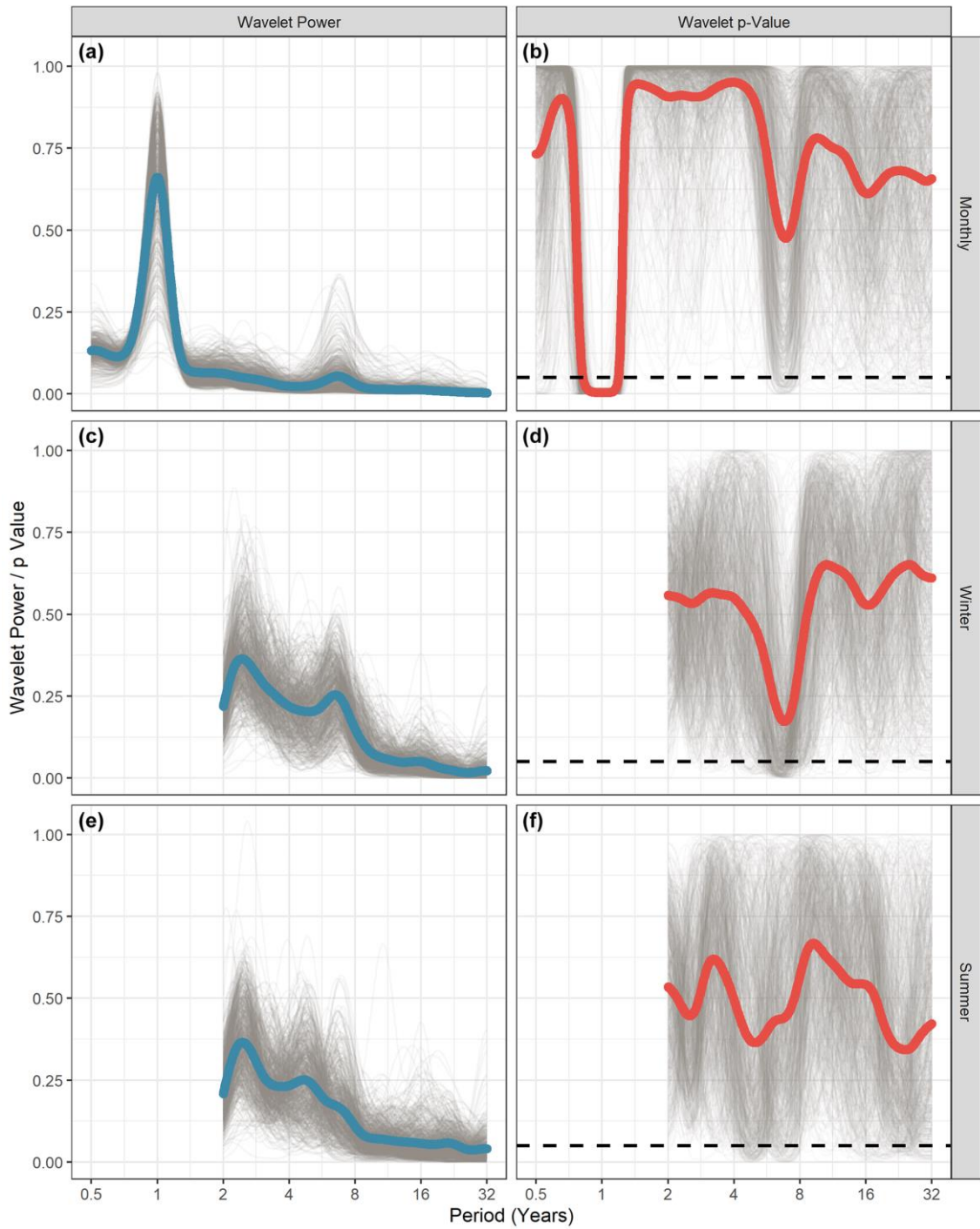


**Figure 13** Stacked streamflow wavelet spectra power (a, c, e) and p values (b, d, f) from the normalised monthly, winter and summer resolution data of 705 catchments. The 95% confidence interval is shown as a dashed black line in the right column figures. The opacity of each average spectra line has been lowered to allow general trends to be identified.

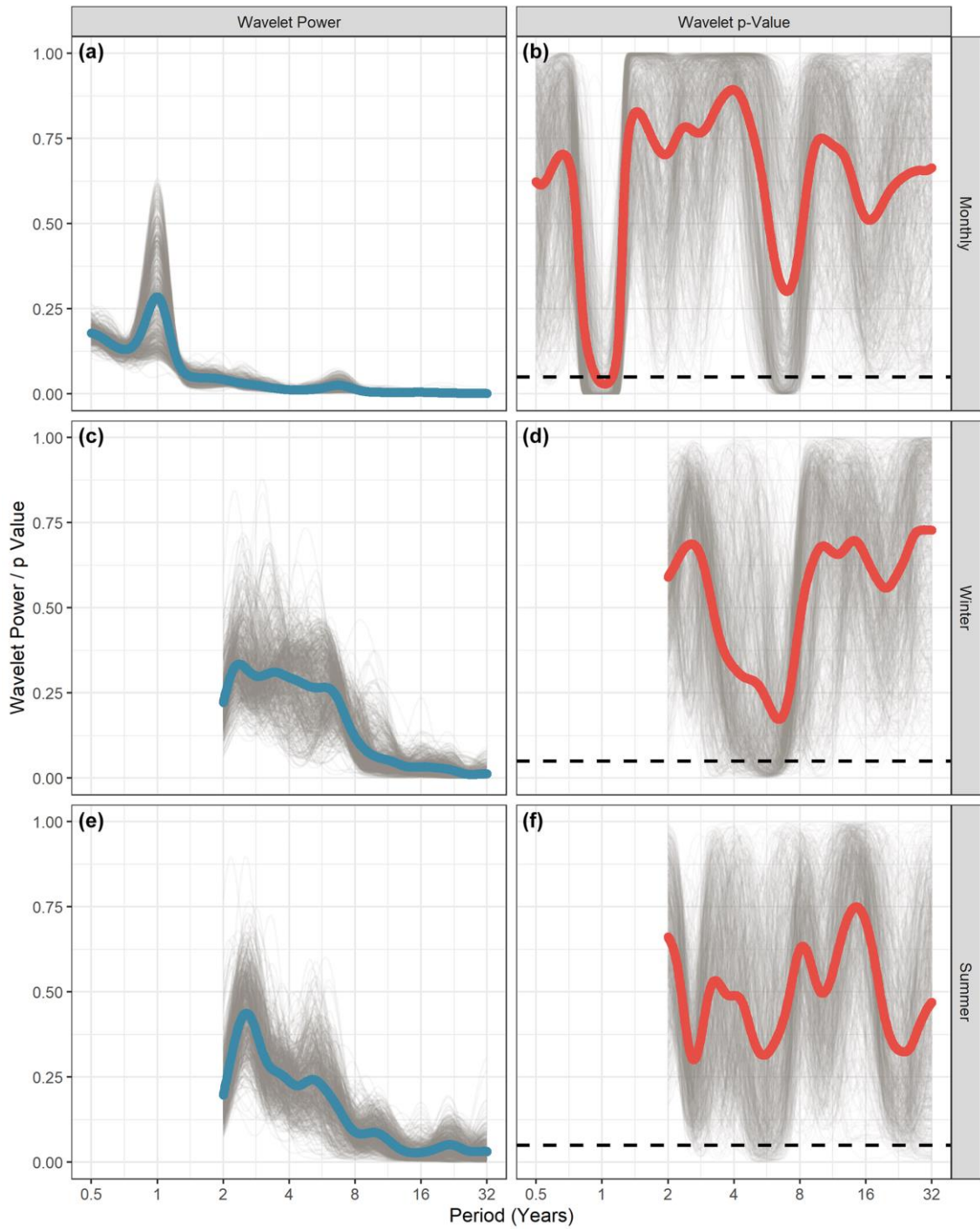


**Figure 14** As in Figure 13 but for catchment rainfall data.

These strengths are generally reflected in the wavelet  $p$  values, with bands of lower  $p$  values at the (approximately) 7-year periodicity in the monthly data and seasonal data and at the 1 year in the monthly data. Wavelet  $p$  values indicate the likelihood that the detected wavelet powers are not the result of external

forcing. As such, lower values indicate the increased significance of external forcing over the red noise null hypothesis. Wavelet  $p$  values are generally lower in the monthly catchment rainfall spectra (0.002–0.996; mean of 0.289) compared with monthly streamflow (0–0.995; mean of 0.443), but this may be an artefact of longer autocorrelations in streamflow records relative to rainfall. Wavelet  $p$  values are comparable for the seasonal spectra, with the exception of summer rainfall, which shows the lowest significance (winter rainfall – 0.003–0.995 and mean of 0.148; winter streamflow – 0.001–0.839 and mean of 0.129; summer rainfall – 0.005–0.992 and mean of 0.462; summer streamflow – 0.000–0.997 and mean of 0.348). Summer rainfall shows the weakest wavelet powers and greatest  $p$  values for the P7 band.

Discrete bands of decreased average wavelet  $p$  values can also be seen between 16 and 32 years for all the streamflow (monthly – 0.502; winter – 0.400; summer – 0.209) and rainfall data sets (monthly – 0.456; winter – 0.569; summer – 0.355). This periodicity band, however, exhibits negligible average wavelet power, indicating minimal influence on variability. In the winter- and summer-averaged power spectra, there is a band of increased strength at the 2–3 year periodicity. In the winter-averaged data, there is no comparably low  $p$  value, suggesting these higher powers are the result of noise within the averaged time series. However, all the summer spectra appear to exhibit some decreased  $p$  value at this 2–3 year band.

#### **4.4.2 Spatial distribution of wavelet powers**

The main multi-annual periodicity detected in the winter and summer river flow data (P7) was mapped for seasonal catchment rainfall and streamflow in Figure 15. The winter spatial distributions show three distinct areas of increased wavelet power and significance, which are shared between catchment rainfall and streamflow. The largest area is located in the southwest of England and south Wales, extending north into the Midlands and east into the southeast of England in the streamflow data. For rainfall, this area encompasses 101 of the 221 catchments, with significant (greater than 95 % CI) P7 wavelet power and 224 of the 262 significant sites in streamflow. The two other areas of increased



wavelet significance in rainfall and streamflow cover Northern Ireland (20 significant sites for rainfall; 12 for streamflow) and central Scotland (30 significant sites for rainfall; 25 for streamflow). There are also stronger P7 wavelet powers along the west coast of the UK in both winter rainfall and streamflow; however, most significant powers (>95 % CI) are found in England and Wales. Additionally, the location of the greatest wavelet powers differs between winter rainfall and streamflow. Winter rainfall shows higher wavelet powers along the southwestern peninsula of England and south Wales, whereas the greatest winter streamflow wavelet powers are found in south and southeastern England and appear to be co-located over the chalk and other principal aquifers (Allen et al., 1996).

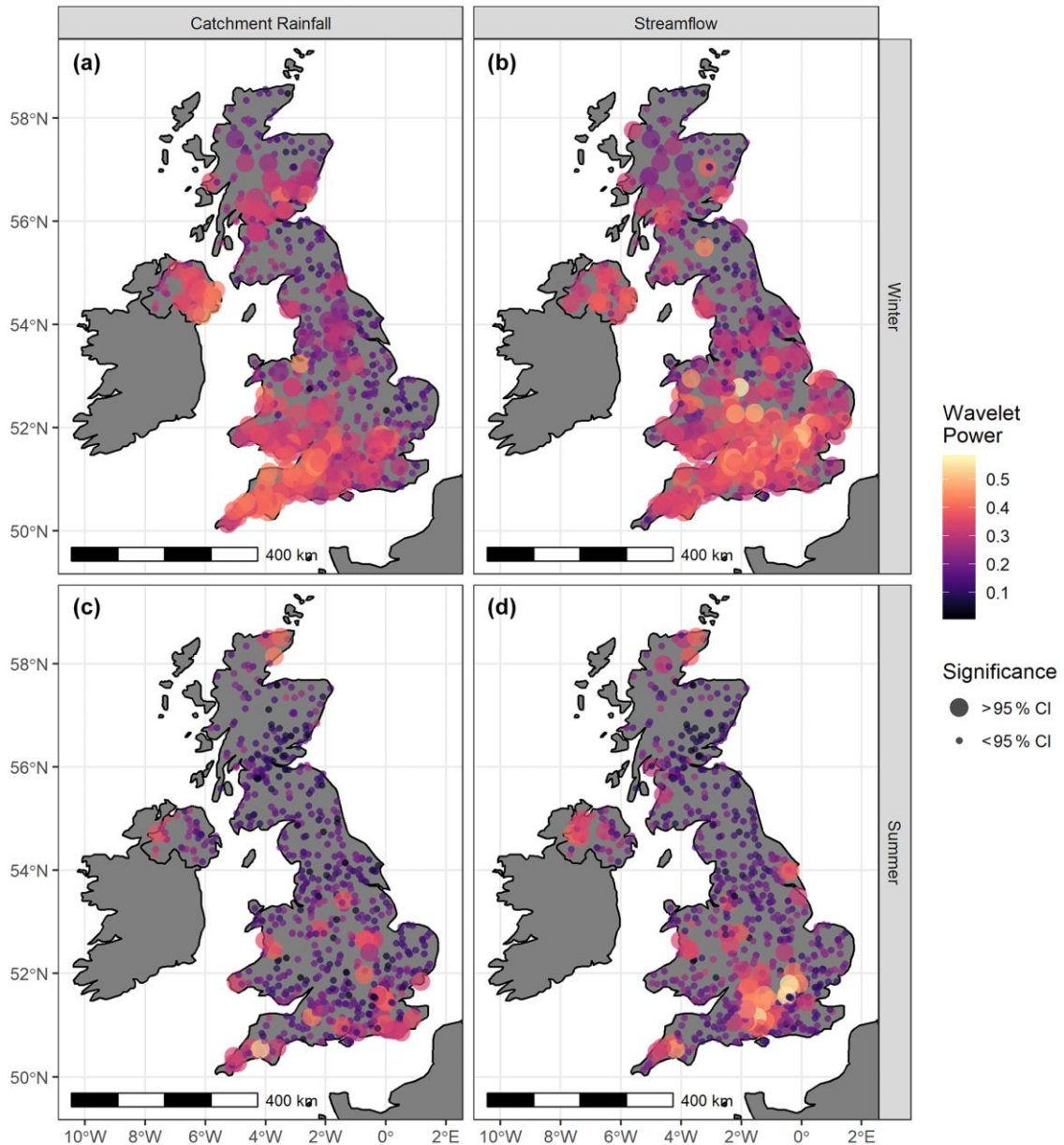


**Figure 15** Spatial distribution of P7 wavelet power and significance in catchment rainfall and streamflow for winter- and summer-averaged data sets.

Little spatial structure exists in P7 wavelet power and significance for the summer-averaged rainfall data. Some increased density in significance is seen towards the south coast of England; however, this may be due to the increased density of sites in this region, as seen in Figure 12, especially given the negligible average P7 wavelet strength displayed in Figure 14. Conversely, summer-averaged river flows show some clear spatial structure of wavelet power and

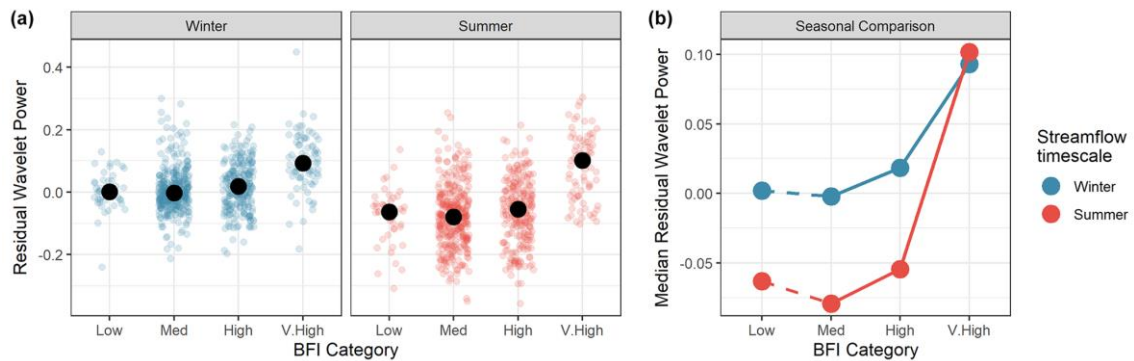
significance in the south of England, where 51 of the 70 sites with significant P7 powers are located. Again, these sites appear to be co-located over the chalk aquifer (Allen et al., 1996).

#### **4.4.3 Testing of hydrological pathways**

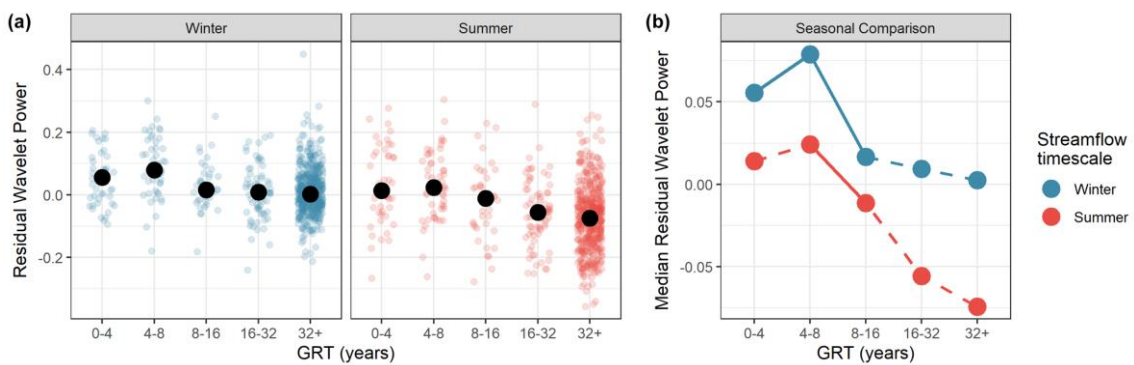
Figure 16 shows scatterplots of the P7 residual wavelet powers (RWPs) for winter and summer streamflow plotted by BFI category (Figure 16a) and a comparison of median P7 RWPs with significance results from the MWU (Figure 16b). Winter P7 median RWPs show a trend of increasing wavelet powers with increasing BFI category, with the exception between the low and medium categories (0.001, -0.002, 0.019 and 0.093 for low, medium, high and very high groups, respectively). A similar relationship is seen in the summer median P7 RWPs (-0.063, -0.079, and -0.054 for low, medium and high groups), with a notably steeper increase for the final group when compared to winter P7 residuals (increasing to 0.101). This brings the median P7 residual powers for summer streamflow to a comparable magnitude to winter streamflow. In general, winter median P7 residual powers are close to zero, except for the very high category, indicating minimal modulation of P7 signal strength between rainfall and streamflow in the catchments with low to high BFI. Summer P7 residuals are negative for low–high BFI catchments, indicating a reduction in P7 wavelet powers in streamflow compared to winter rainfall. The median P7 residual for sites in the very high BFI is the only positive residual for summer streamflow, indicating an increase in relative P7 signal strength between winter rainfall and summer streamflow for these sites.

Figure 17 shows P7 RWPs plotted against groundwater response time (GRT) groups, showing all gauges (Figure 17a) and median RWPs with significant results from the MWU (Figure 17b). Winter streamflow shows higher, positive median RWPs across all GRT groups (0.056, 0.079, 0.017, 0.009 and 0.002 for the 0–4, 4–8, 8–16, 16–32 and 32+ year groups, respectively), whereas summer streamflow only shows positive RWPs for catchments in the 0–4 and 4–8 year GRT groups (median RWP of 0.014 and 0.024, respectively). GRTs groups greater than or equal to 8 years all show negative median RWPs

(-0.011, -0.058 and -0.074 for 8–16, 18–32 and 32+ year groups, respectively). Both winter and summer streamflow show decreasing median RWPs with increasing GRT, with the exception of the 4–8 year GRT group, which shows the greatest median RWP in both winter and summer. Significant differences between GRT groups are found between 0–4 and 4–8 and 4–8 and 8–16 for winter streamflow and between 4–8 and 8–16 for summer streamflow.



**Figure 16 (a) Jittered scatterplots for residual wavelet powers in winter and summer, categorised by BFI; bold black points mark the average residual wavelet power for each BFI category. (b) Comparison of these median residual wavelet powers with significant changes between groups (shown as solid lines) and non-significant changes between groups (shown as dashed lines).**



**Figure 17 As in Figure 16 but for the groundwater response times (GRTs).**

## 4.5 Discussion

### 4.5.1 Detecting a teleconnection between the NAO and UK streamflow

Our results indicate that the dominant, common multi-annual periodicity in UK streamflow (and catchment rainfall) is that of an  $\sim 7$ -year cycle. This can be seen most clearly in the monthly and winter streamflow spectra (Figure 13a–d). This cycle compares to the 6–9 year pseudo-periodicity documented in the strength of the NAO's atmospheric dipole, which has been associated with multi-annual periodicities in hydrometeorological records globally (Labat, 2010; Rust et al., 2019; Tremblay et al., 2011; Kuss and Gurdak, 2014; Holman et al., 2011; Neves et al., 2019). We show here that this  $\sim 7$ -year cycle is widespread within rainfall and streamflow variability across the UK, with the majority of streamflow and rainfall records assessed here exhibiting a coherent band of increased periodicity strength and significance around this 7-year frequency range. This, combined with greater significance for this periodicity, and the wide spatial domain on which it is detected, indicates an external control on this multi-annual mode of variability. As such, we build upon evidence in existing research that documents the teleconnection between the NAO and rainfall in Europe and show new evidence of the propagation of the NAO's  $\sim 7$ -year cycle to UK streamflow variability. Additionally, we detect expected differences between signal presence in summer and winter rainfall, showing increased strength and spatial structure of NAO-like signals during the winter months and weaker summer values with little spatial structure (suggesting noise). This generally agrees with existing research showing that NAO's control over European rainfall is primarily expressed in winter months (Trigo et al., 2004; West et al., 2019). However, it should also be noted that there are multiple interacting climate systems that affect European weather (for instance, the East Atlantic and Scandinavia patterns; Bru and McDermott, 2014) that, while generally weaker than the NAO's influence in European weather variability, may have an additional or compounding influence on the cycles detected in streamflow and rainfall presented here. For the remainder of the paper, we will continue to refer to these cycles as NAO-like, however, given the

NAO's established dominant control on European weather variability (Hurrell and Van Loon, 1997).

#### **4.5.2 Controls on multi-annual signals in catchment rainfall**

We provide new evidence that NAO-like multi-annual periodicities in UK rainfall are seen in the winter months and are heavily localised to the southwest of England, south Wales, the east coast of Northern Ireland and the central band of Scotland (Figure 15). This is contrary to previous research that has typically found the strongest relationships between the NAOI and UK rainfall along the west coast of the UK, particularly on the west coast of Scotland (Murphy and Washington, 2001; Fowler and Kilsby, 2002; West et al., 2019). Rust et al. (2018) suggest that the NAO may have two pathways for its modulation on UK rainfall, namely a fine-scale (e.g. subannual or annual) atmospheric pathway via modulation of westerly storm tracks (Trigo et al., 2002; Parker et al., 2019; Woollings and Blackburn, 2012) or an oceanic pathway via long-term influences on the Gulf Stream (Taylor and Stephens, 1998; Chaudhuri et al., 2011; Watelet et al., 2017). As such, we may expect teleconnection studies that assess the annual relationship between the NAO and rainfall (such as existing research) to better capture the atmospheric pathway. Conversely, studies that assess a longer-term influence (such as the wavelet analysis used here), may better capture the oceanic pathway for NAO control on rainfall (i.e. via the Gulf Stream). Haarsma et al. (2015) show that precipitation in the southwest of England exhibits the strongest negative correlation in the UK ( $\sim -0.4$ ) with modelled variability in the Atlantic Meridional Overturning Current (of which the Gulf Stream is part). As such, the increased strength in NAO-like signals in winter rainfall shown here in the southeast of England could be explained by the NAO's long-term control on the Gulf Stream.

#### **4.5.3 Hydrological drivers for signal strengths**

We have shown that NAO-like periodicities are localised to specific regions in the UK in winter rainfall (Figure 15a) and are negligible in summer rainfall (Figure 15c). This suggests that NAO-like periodicities in summer streamflow do not originate from summer rainfall and that catchment processes that drive winter

rainfall signal propagation to summer streamflow (e.g. subsurface pathways, Haslinger et al., 2014; Folland et al., 2015; Barker et al., 2016) may inform an understanding of catchment controls on the NAO teleconnection with streamflow. Here, we provide statistically significant evidence that multi-annual periodic signals in rainfall are propagated to streamflow differently between winter and summer months, depending on the contribution from different hydrological pathways (and their response times). Furthermore, we provide evidence that pathways of specific response times propagate these periodic signals to UK streamflow more effectively than others, highlighting the catchment properties that may produce a sensitivity to the NAO teleconnection with streamflow. Below, we discuss how these relationships align with current hydrological understanding.

Rust et al. (2019) establish that multi-annual, NAO-like periodicities in groundwater-level records are considerably stronger than those in co-located rainfall records. Groundwater behaviour generally exhibits longer autocorrelations than rainfall with negligible fine-scale variability (noise), due to the damping effect of subsurface hydrological pathways (Townley, 1995; Dickinson, 2004; Gnann et al., 2020). As such, groundwater can express a greater signal-to-noise ratio for low-frequency variations (such as those produced by the NAO teleconnection; Holman et al., 2009; Rust et al., 2018). By comparison, rainfall, which generally contains more fine-scale (hourly–daily) variability, exhibits a lower signal-to-noise ratio which suppresses the proportional strength of multi-annual, NAO-like signals (Meinke et al., 2005; Brown, 2018). A parallel can be drawn here with hydrological pathway influence on streamflow, as surface pathways more closely reflect rainfall variability, and subsurface pathways more closely reflect groundwater variability (Ockenden and Chappell, 2011; Kamruzzaman et al., 2014; Mathias et al., 2016; Gnann et al., 2020).

Streamflow driven primarily by surface processes (e.g. BFI <0.5) exhibits close-to-zero median RWP in winter (Figure 16b), indicating that surface pathways affect a minimal modulation of NAO periodicity strength from winter rainfall to winter streamflow; this is likely due to their relatively short response times

(minutes to days; Mathias et al., 2016). This also explains why the spatial footprint of NAO-like periodicities in winter streamflow (Figure 15b) generally matches that of winter rainfall (Figure 15a) as a greater proportion of surface pathways are active in response to greater in-season rainfall (due to more infiltration- or saturation-excess runoff from the land surface; Ledingham et al., 2019). Summer streamflow, where driven by surface pathways, shows minimal sensitivity to NAO periodicities in winter rainfall (negative median RWPs), due to fewer catchment storage mechanisms available convey winter rainfall signals to summer streamflow (Barker et al., 2016) and the weaker NAO teleconnection with UK summer rainfall (as noted by Alexander et al., 2005; Hurrell and Deser, 2010; West et al., 2019, and indicated here). Conversely, streamflow that is dominated by subsurface pathway influence (e.g. BFI > 0.75) exhibits the greatest NAO periodicities (Figure 16b). We also see significant increases in NAO periodicity strength with increasing BFI in all but the lowest two BFI categories (low to medium). We, therefore, confirm the expectation that NAO periodicities in groundwater are propagated to streamflow via subsurface pathways. This relationship is also seen in the spatial footprints of NAO periodicities in winter (Figure 15b) and summer streamflow (Figure 15d). Gauges with the strongest NAO-like periods in summer and winter streamflow are found in catchments that are within, or that drain, the chalk outcrop in south-central England. These catchments are known to be heavily driven by groundwater behaviour (Marsh and Hannaford, 2008). In Figure 15b, we see that the spatial footprint of NAO periodicities in summer streamflow is localised to these chalk-dominated catchments. Permeable catchments such as those on the chalk aquifer are known to slowly respond to winter rainfall at a seasonal timescale (Hellwig and Stahl, 2018). As such, these catchments have sufficient subsurface pathway contributions to protract NAO periodicities in winter rainfall through to summer streamflow. Conversely, Figure 15 also shows some areas of the chalk with relatively low NAO-like periods, such as the southern coast of England. Similarities can be seen here with Marchant and Bloomfield (2018), who identify discrete regions of groundwater-level behaviour within the chalk aquifer, with varying autocorrelations. The chalk of the south coast of England tends to have



thinner superficial deposits and negligible glacial deposits (unlike those in the area of the chalk outcrop), producing a faster recharge response to rainfall with shorter autocorrelations (Marsh and Hannaford, 2008; Marchant and Bloomfield, 2018). Dickinson et al. (2014) highlight the importance of unsaturated zone thickness in modulating periodic signal progression, which may explain why catchments in the southern chalk exhibit lower signal-to-noise ratios for NAO periodicities.

While the relationship between NAO periodicities and streamflow BFI indicates the importance of subsurface pathway contribution to teleconnection strength, properties of the subsurface pathways themselves are expected to modulate periodic signal propagation from rainfall to streamflow (Rust et al., 2018). We show streamflow in catchments with shorter groundwater response times (GRTs) exhibit stronger NAO-like periodicities, but the strongest NAO periodicity is found in catchments with GRTs between 4 and 8 years. Townley (1995) shows that where the groundwater response time of a subsurface store is longer than a periodicity in recharge, the system will exhibit larger periodic variations in groundwater head but a greater attenuation of periodic discharges at a streamflow boundary. This is because the pathway cannot equilibrate the periodic recharge to its hydraulic boundaries at a sufficient rate. Conversely, where the pathway response time is shorter than that of a periodicity in recharge, groundwater discharge will show greater periodic variations as the entire pathway is able to convey this signal. This may explain the reduction in NAO periodicities seen as GRT increases in Figure 16b. Where subsurface pathway response times are longer than the principal P7 of the NAO, we may expect the pathway to dampen the signal propagation to baseflow (Townley, 1995; Dickinson, 2004). However, this process fails to explain the reduced NAO periodicity strength seen in the results, where GRT is less than the ~7-year NAO periodicity (seen principally in the winter streamflow data). As suggested by Najafi et al. (2017) and Wilby (2006), faster pathways can exhibit a weaker signal-to-noise ratio when compared to slower pathways which are known to smooth signal propagation (Barker et al., 2016). As such, streamflow in catchments with the shortest GRT (i.e. 0–4 years) may exhibit greater response to finer-scale

variability in rainfall, which suppresses the relative strength of the NAO periodicity. This would also explain why summer streamflow does not show a similarly reduced NAO-like period strength for the 0–4 years GRT band, as summer streamflow generally would be expected to exhibit greater signal-to-noise ratios due to a greater proportion of slow pathway contribution. As such, the results suggest that, in addition to the described periodic signal modulations in Townley et al. (1995), there is an ideal range of subsurface pathway response times that are long enough to produce a greater signal-to-noise ratio but sufficiently short so that there is minimal damping.

These results may have important implications for streamflow management, as we show that readily available estimates of BFI and GRT may be used to screen or identify catchments where further work may be necessary to understand long-term cyclical behaviour in streamflow. This may be particularly important for ensuring the sustainable, ongoing use of water resources, such as abstraction for water supply and ecosystem management. This is particularly important for summer streamflow, where streamflow services are often vulnerable to drought conditions (Visser et al., 2019). Furthermore, there is a need for consideration of these cycles within water management policy and practice in the UK. For instance, stochastic or probabilistic approaches often used for water resource planning periods may need to be augmented in order to account for the cyclical, non-stationary variability reported here and for their potential benefits to be realised.

## **4.6 Conclusions**

This paper assesses the degree to which the principal multi-annual periodicity (P7) of the NAO is present in streamflow and catchment rainfall records using the continuous wavelet transform to identify multi-annual periodicities. We provide new evidence for the role of oceanic and atmospheric pathways in propagating NAO periodicities to catchment rainfall by identifying spatial patterns of statistically significant NAO-like periodicities in UK catchment rainfall and streamflow. This may help further explicate the varying spatial extent of the NAO influence over Europe and the North Atlantic region. Furthermore, we identify

specific streamflow catchment characteristics that are most responsive to the NAO periodicities in catchment rainfall. We find that streamflow that is driven predominantly by subsurface pathway contributions often exhibits greater NAO-like periodicities and that subsurface pathways with response times comparable in length to the P7 of the NAO produce the greatest sensitivity to the NAO teleconnection. These findings build on the fundamental understanding of periodic signal propagation through hydrological pathways and can aid in the identification of catchments with sensitivities to multi-annual control, for instance, those found in climatic teleconnections. The ability to screen catchments for their potential teleconnection-driven multi-annual variability may have direct implications for water management decision-making, for example, the permitting of surface water abstractions and their implications for ecologically sensitive streamflow systems. Such information may help to protect vulnerable habitats or aid appropriate investment in surface water abstraction infrastructure. The results here take necessary steps towards a greater understanding of how climatic teleconnections can be used to improve water resource management practices.

## **4.7 References**

The reference list for this paper has been combined with the final reference section for this thesis in chapter 10.



## **5 CHAPTER 5: NON-STATIONARITY BETWEEN NAO AND EUROPEAN RAINFALL**

This chapter consists of the published article Rust et al (2021b); “Non-stationary control of the NAO on European rainfall and its implications for water resource management”. This chapter will address research objectives 3.

### **5.1 Introduction**

Water resource forecasting generally centres on understanding hydrological variability over coming months or years, so that water managers can prepare for extremes such as droughts or floods (Chang and Guo 2020; Hao et al., 2018). Some forecasting systems seek to project further into the future to allow long-term planning of infrastructure and resilience to extremes and climate change (Svensson et al., 2015). These systems can rely directly or indirectly on outputs from Global Climate Models (GCMs) (such as gridded reanalysis datasets) to forecast hydrological conditions (Bhatt et al., 2015; Ionita et al., 2020). In the North Atlantic region, in particular Western Europe, the North Atlantic Oscillation (NAO) is used as an indicator for hydrometeorological conditions given its leading control on winter rainfall totals (Scaife et al., 2008; 2014; Hurrell & Deser, 2010). A dipole of pressure anomalies over the North Atlantic, the NAO’s positive phase (greater than average pressure gradient; NAO+) results in wetter conditions in northwest Europe with dryer conditions in southwest Europe (Trigo et al., 2004; Rust, Holman, Corstanje, Bloomfield & Cuthbert, 2018). Its negative phase (weaker than average pressure gradient; NAO-) results in the inverse effect on rainfall (Folland et al., 2015; and as shown by the correlation coefficients in Figure 18). Given this relationship, and, considering the role of winter rainfall variability in groundwater drought development (e.g. reduced winter recharge) and generation of late winter / early spring floods, the NAO offers a potential explanatory variable when understanding the behaviour of some hydrological extremes.

Many studies have investigated the relationship between the NAO Index (NAOI) and recorded hydrological variables in Europe, including river flow (Burt & Howden, 2013), groundwater (Lavers et al, 2015), and seasonal rainfall (West et al, 2019), or calculated water resource variables such as the Standardised Precipitation Index (Moreira et al, 2016). Furthermore, a growing number of studies have detected multi-annual periodicities in hydrological variables (river flow and rainfall (Rust, et al., 2020), and groundwater level (Neves et al, 2019) that align with weak periodicities detected in the NAOI (Hurrell & Van Loon, 1997), suggesting that multi-annual cycles in the NAO may affect the occurrence of floods and droughts in Western Europe.

GCMs have historically been ineffective at predicting NAO dynamics within future scenarios (Smith et al, 2016); however, recent developments in high-performance computing have enabled forecasting of NAOI effects at seasonal (Świerczyńska-Chłaściak & Niedzielski, 2020) or decadal (Athanasiadis et al; 2020; Dunstone et al., 2016) timescales. Furthermore, with high-resolution hydrometeorological datasets becoming more readily available (Sun et al., 2018), regression analyses between the NAOI and climate variables for forecasting purposes is more achievable. As such, there is a renewed interest from the water resources community in developing medium- to long-term water resource forecasting systems using the NAOI, with the aim of improving preparedness for hydrological extremes and water resource planning (Hall & Hanna, 2018; Svensonn et al; 2016). This is particularly useful in water-scarce regions such as southern England (Folland et al., 2015), and the Iberian Peninsula (Moreira et al., 2016) where long-range forecasting has the largest potential benefit to strategic water resource planning (Stein et al., 2016).

The current use of relationships between NAOI and winter rainfall (herein referred to as NAOI-P) relies heavily on the assumption that the strength and direction of the relationship is sufficiently stationary to be applicable in future scenarios. However, research into the dynamics of the NAO itself have shown the NAOI-P relationship to be non-stationary at multi-decadal timescales (Vicente-Serrano & López-Moreno, 2008). Furthermore, there has yet to be an assessment of their

utility from a water resource perspective, at decadal or multi-decadal timescales relevant to current water resource projections. We discuss the non-stationarity of the NAOI-P relationship in Western Europe from a water resource forecasting perspective, by undertaking a rolling 10-year window correlation between the NAOI and gridded winter rainfall estimates for the period the past 125 years (1889 – 2016) across Western Europe. Furthermore, we identify five zones across Europe with similar non-stationary behaviours that provide insight for the application of the NAOI-P relationship for future water management.

## 5.2 Data Methods

Two datasets have been used in this paper; NAOI data from the NCAR Climate Analysis Section (Hurrell, 2003), and precipitation data from the Global Precipitation Climate Centre (Schneider et al., 2018) have been used. The NAOI data are the Hurrell station-based winter (DJFM) index (Hurrell, 2003). This dataset covers the period 1864 to 2019. The precipitation data are taken from the GPCP's Full Data Monthly Product Version 2018 which is an estimated, gridded precipitation dataset at 0.5° resolution (Schneider, Becker, Finger, Meyer-Christoffer & Ziese, 2018). The dataset is specifically generated to investigate long-term climatological relationships and covers the period 1891 to 2016. The precipitation data have been processed according to the same winter (DJFM) used by the Hurrell winter NAOI dataset for use in the correlation analysis. Grid cells between -13-20° Longitude and 35-70° Latitude were used to represent Western Europe. A simple Pearson's  $r$  correlation between NAOI and winter rainfall has been produced for the full-period of data (Figure 18).

A rolling 10-year correlation analysis between winter rainfall and winter NAOI was calculated for each grid cell in Western Europe for the period 1891-2016, using the Pearson's correlation coefficient with the  $n-9$  to  $n$ -year period representing the  $n$ -year correlation coefficient. A k-medoids cluster analysis (analogous to k-means for the median case) was then undertaken on the rolling-window correlation-series. Each rolling-window correlation series was not normalised

prior to clustering as the Pearson's correlation coefficient is a normalised metric, and the analysis (in-part) is aiming to understanding how the directional control is characterised across Western Europe. Clustering has been undertaken to draw together generalised areas that have similar strength and direction of NAOI-winter rainfall correlation that may be useful for planning purposes. Five clusters were chosen as this gave the greatest spatial coherence between clusters, thereby indicating the regions where it may or may not be appropriate to use the NAOI-P to inform water resource decision making. Medoids (analogous to median centroids) have been calculated for each cluster.

A dissimilarity matrix was also calculated for the rolling-window correlation series using an inverse Pearson's correlation coefficient. The dissimilarity of the rolling correlation series has been assessed to understand the range and extremes (most dissimilar) of NAO control on winter rainfall within selected nation-based regions. These are regions that represent characteristic NAOI-P relationships from either full-period correlation (Figure 18) or clustered rolling correlations (Figure 19) within their domain.

Significance thresholds have been calculated for all correlations (full-period and 10-year rolling) to the 95% confidence interval. Means and variances of the cluster medoids and dissimilar pairs have been calculated which, in addition to a qualitative assessment of temporal variability of the NAOI-P relationship, will be used to assess non-stationarity.



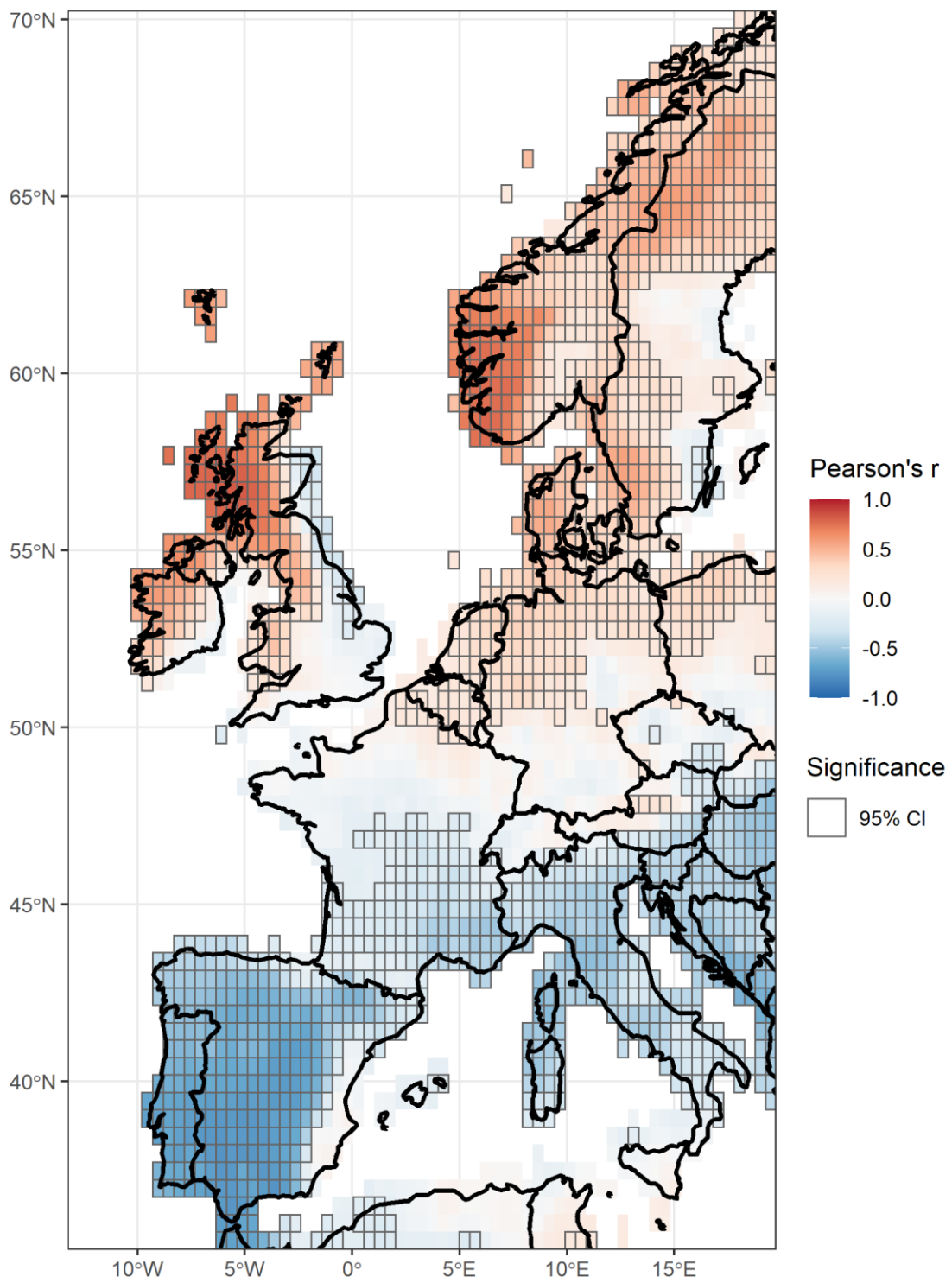


**Figure 18 Pearson's r correlation between NAOI and rainfall using 1991 to 2016 winter data (DJFM)**

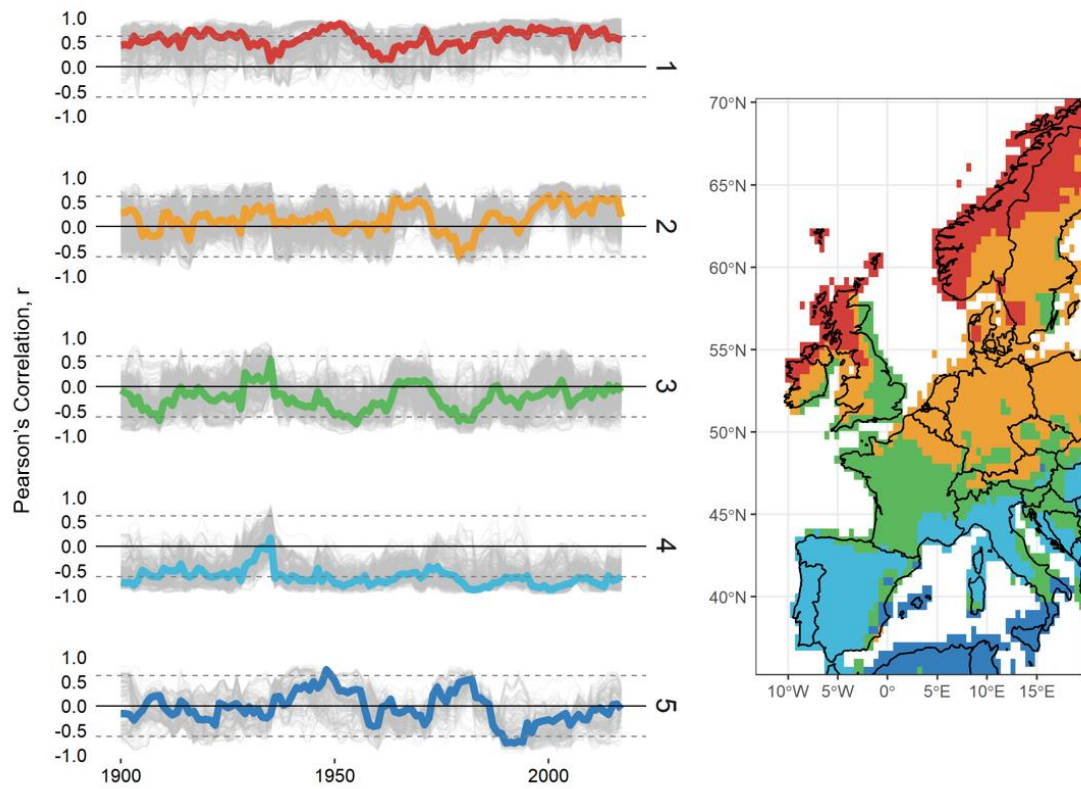


**Figure 19 Cluster analysis of 10-year rolling correlation series for Western Europe. Grey lines represent the individual rolling correlation series in each cluster while the coloured lines represent the centroids (medoids) of each cluster. Dotted grey lines represent the 95% CI.**

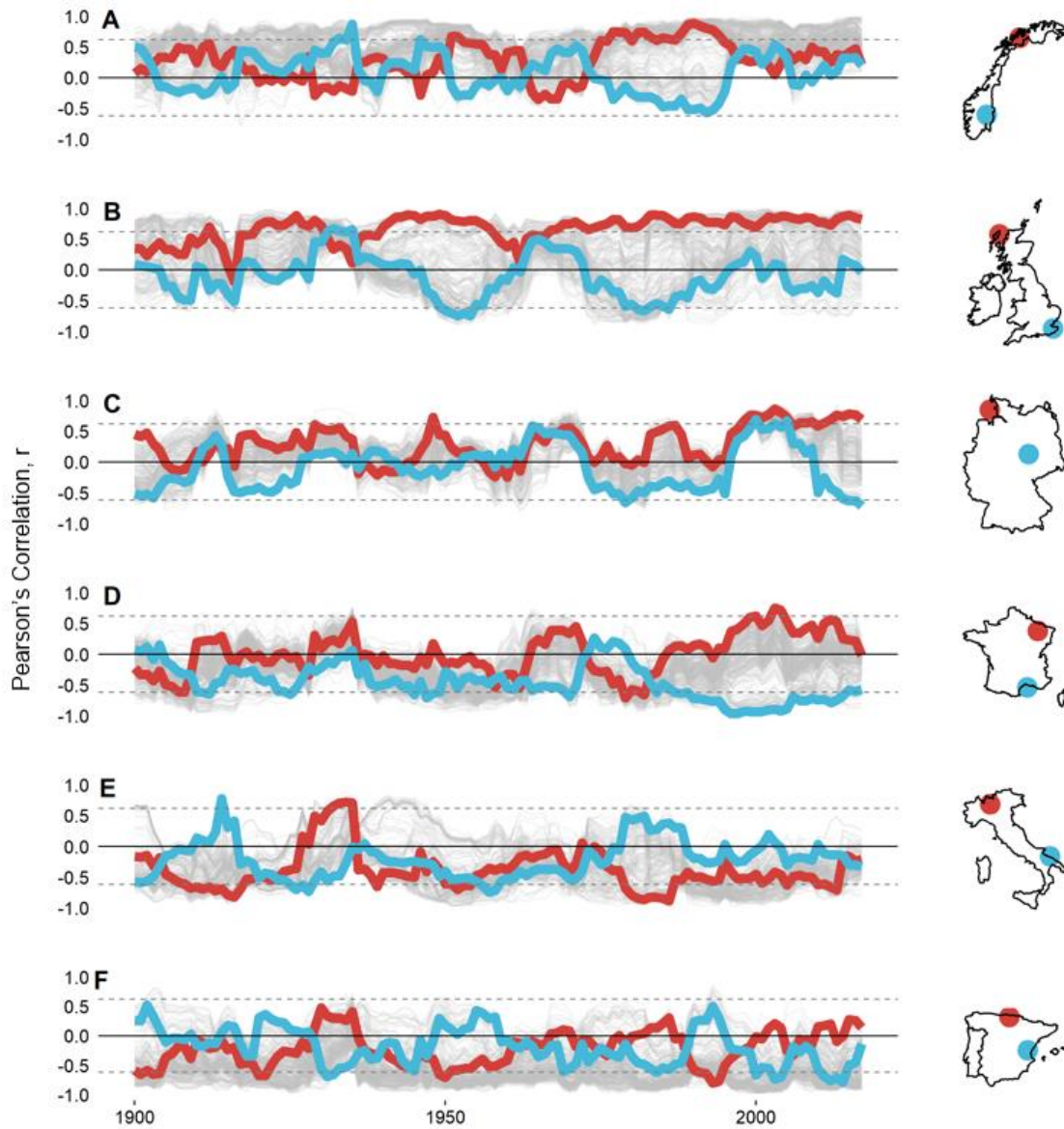


**Figure 20** 10 year moving correlation analysis for selected Western Europe nation-based regions. The two most dissimilar (inverse Pearson's correlation) rolling correlation series are displayed with the colours lines and their location is displayed on the inset map. Dotted grey lines represent the 95% CI.

### 5.3 Results

The clustered rolling correlation series (Figure 19) indicate regions with similar behaviour of the NAOI-P relationship. Clusters show that NAOI-P correlation varies considerably over time and space, transitioning from positive in higher latitudes (e.g. clusters 1 and 2), to negative in lower latitude (e.g. clusters 3 and 4). This is consistent with the full-period correlation results (Figure 18).

Additionally, we can categorise these clusters into three distinct responses:

1. Relative temporal stability of NAOI-P correlation, containing 2 clusters:
  - i. Cluster 1 (centroid mean: 0.57, var: 0.03) representing a positive correlation found in northwest regions of Scotland, Ireland and Scandinavia
  - ii. Cluster 4 (centroid mean: -0.64, var: 0.03) representing the Iberian Peninsula and northern and central Italy, Sardinia and southeastern France with a stronger negative NAOI-P correlation.
2. Transitional regions with greater NAOI-P temporal variance, containing 2 clusters:
  - i. Cluster 2 (centroid mean: 0.16, var: 0.07) representing a variable, often positive, correlation in western England, Wales, central Ireland, central Scandinavia and most of Germany, Belgium and the Netherlands.
  - ii. Cluster 3 (centroid mean: -0.24, var: 0.06) representing a variable, often negative correlation in east and southeast England and France.
3. Highly variable NAOI-P relationship, containing only cluster 5 (centroid mean: -0.04, var: 0.1) covering Sicily, and northern Africa.

While the clustering analysis indicates regions with a similar NAOI-P relationship, the dissimilarity pairs (Figure 20) indicate that considerable variance is still found within these regions. These pairs are consistent with the clustering analysis in showing the greatest difference between NAOI-P response is found on a latitudinal gradient. Dissimilarity pairs in the northwest and southwest of Europe

appear to show relative temporal stability for the majority of the period assessed (such as northwest Scotland (mean: 0.67, var: 0.045) and south of France (mean: -0.46, var: 0.01), whereas others show greater deviations and transience in the direction of the NAOI-P correlation (such as southeast England (mean: -0.11, var: 0.0.12), or eastern Spain (mean: -0.19, var: 0.102)). The individual dissimilarity series with the greatest variance is found in southeast England (var: 0.123). Individual 10-year-correlations range from 0.92 to -0.57 for Norway; 0.90 to -0.75 for the UK and Ireland; 0.92 to -0.63 for Germany; 0.78 to -0.97 for France; 0.58 to -0.96 for Italy and 0.52 to -0.80 for Spain and Portugal.

## **5.4 Discussion and Conclusions**

This paper seeks to question whether the relationship between winter NAOI and winter precipitation (NAOI-P) is sufficiently stationary for application to water resource forecasting in Western Europe. Results indicate few regions in Western Europe where the NAOI-P relationship may be considered stationary at a decadal scale. Given the degree to which this relationship has been utilised in water resource studies, we find that such non-stationarity has direct implications for the efficacy of water resource forecasting in Western Europe.

Previous research into the NAOI-P relationship has consistently highlighted the northwest and southwest of Europe as having the strongest correlation (Tsanis et al., 2019; Hurrell & Deser, 2010). The results generally agree with these areas: for example, Cluster 1 (NW Scotland, Ireland and Norway) remains in a strong, positive correlation for the majority of the period assessed, and Cluster 4 (Portugal and Spain), remain in a similarly strong but negative correlation. In NW UK and Ireland, where winter rainfall is some of the highest in Europe (Tetz, Tziperman, Coumou, Pfeiffer, & Cohen, 2017) and water is in abundance, the NAOI-P relationship has more utility for flood risk and high-flows management, rather than drought. In Portugal and Spain, some of the most water-scarce areas in Europe (Estrela, Pérez-Martin, & Vargas, 2012), the relative stationarity of the NAOI-P relationship shown in Cluster 4 supports use of this relationship for water

management purposes in these regions. However, generalisation of these regions (particularly Spain) as entirely stationary at a multi-decadal timescale may not be appropriate as shown by the dissimilarity pairs in figure 19f, where we see considerable fluctuations in the correlation, suggesting caution should still be taken when applying the NAOI-P relationship over large areas in these regions.

While we show that some regions agree with existing research (as mentioned previously), the results show that most of Western Europe exhibits a non-stationary NAOI-P relationship. This has the greatest implications in water-scarce regions where there is a demand for new approaches to manage water scarcity, such as southern England (Bryan, Ward, Barr & Butler, 2019; Folland et al., 2015). Recent research (e.g. Svensson et al., 2015; Prudhomme et al., 2017) has focused on developing new forecasting systems to allow prediction of water resource variables (rainfall, river flow, groundwater level) for one or more years into the future, many of which rely (at least in part) on the NAOI-P relationship in these regions.

Our results show that Clusters 2, 3 and 5, which cover most of Europe, are transitional regions that exhibit stronger non-stationarity than those of relative stationarity (Clusters 1 and 4). Previous work shows many of these areas to have weak to moderate, yet often significant, NAOI-P correlations; such as for western and northern England (West et al., 2019), northern Germany (Riaz, Iqbal & Hameed, 2017), southern France (Massei et al., 2007). Indeed, many studies in these regions have found skilful prediction of winter rainfall (and other water resource variables) through use of the historical NAOI-P relationship, despite the nonstationary reported here (Scaife et al., 2015; Ionita & Nagavciuc, 2020; Svensson et al., 2015; Rasouli et al., 2020; Moreira et al., 2016; Rousi, Rust, Ulbrich, & Anagnostopoulou, 2020). This apparent contradiction with the non-stationary correlation results at decadal timescales and results from other studies for multi-decadal timescales (Vicente-Serrano & López-Moreno, 2008; Pauling, Luterbacher, Casty, & Wanner, 2006) can be explained by the common multi-decadal periods of relative stability in the results, despite general non-stationarity

throughout the rolling correlation series. For example, increased stationarity can be seen in the Cluster 3 medoid, and in the dissimilarly pairs for the UK (figure 19b), the south of France (figure 19c), and Italy (figure 19e), between 1970 and present. As mentioned previously, existing water resource forecasting systems rely on high-resolution, often gridded, hydrometeorological datasets for calibration of the NAOI-P relationship, many of which are only available for recent decades (Sun et al., 2018). Such forecasting systems may be using a calibration period of relative stability in the NAOI-P relationship that is not representative of the true non-stationarity shown here. This naturally draws into question the longer-term validity of many existing studies that seek to utilize the NAOI-P relationship, without accounting for its non-stationary nature.

Counter to this, there are many areas in Europe where utility of the NAOI-P relationship has been discounted for water resource forecasting due to poor average correlation (Figure 18): for instance, south Germany (Riaz et al., 2017), northern France (Massei et al., 2007) and southeast England (Hall & Hanna, 2018). However, the results here suggest the NAOI-P correlation can remain in the same direction for up to 30 years, and stay in a state of significance (95% CI) for up to 5 years (for example, southeast England) in some areas with a weak average NAOI-P correlation. This suggests that if the mechanisms for this relationship inversion are understood, the NAOI could still be a powerful indicator for future (short to medium-term) water resource variability in areas that have historically been ruled out due to poor average correlation. However, water management policy and practice will need to be sufficiently flexible, such as employing frequent reviews of forecasts, to allow for utilization of this changing control.

Variability of the NAO has been a subject of ongoing focus in atmospheric sciences, as has the behaviour of the NAO's control on winter rainfall variability in Europe. In investigating non-stationarity of the NAOI-P relationship at multidecadal (30 year) timescales, Vicente-Serrano & López-Moreno (2008) suggest inversions of correlation direction may be the result of an eastward shift of the NAO's southern pressure centre (Azores) towards the eastern

Mediterranean. Atmospheric literature seems to agree that interannual to multi-decadal eastward shifts of the NAO are due to Rossby wave dynamics (Peterson, Lu & Greatbatch, 2003; Luo & Gong, 2006; Zhang, Jin, Chen, Guan & Li, 2011), the exact mechanics of which are still being explored in GCMs (Huang et al., 2018). If systems for water resource forecasting are to use the NAOI-P relationship, it is critical to account for the apparent NAOI-P non-stationarity. For this to happen, more research is required to understand the full extent of this non-stationarity within different regions and time periods across Europe, and most importantly, research is required to fully understand the mechanisms by which the NAOI-P relationship is inverted and how this can be represented in GCMs. Further, these non-stationary relationships may shed further light on existing uncertainties in hydrometeorological understanding, which are summarised by Bloesch et al. (2019). With an improved understanding of non-stationarities between European weather and driving climate systems, we may be better positioned to answer questions around non-stationarity of the hydrological cycle (e.g. question 1 of the paper), questions on how drought- and flood-rich periods arise (e.g. question 9), or how hydrological models can be adapted to extrapolate changing climate conditions (e.g. question 19). Answers to these questions are critical for continued sustainable use of water resource in a changing climate.

## **5.5 References**

The reference list for this paper has been combined with the final reference section for this thesis in chapter 10.



# 1 **6 CHAPTER 6: IMPLICATIONS OF NONSTATIONARY NAO** 2 **PERIODICITIES FOR FORECASTING OF WATER** 3 **RESOURCE EXTREMES**

4 This chapter consists of the article (currently in under review) Rust et al (2021c); “The  
5 importance of non-stationary multiannual periodicities in the NAO index for forecasting  
6 water resource extremes” This chapter will address research objective 4

## 7 **6.1 Abstract**

8 Drought forecasting and early warning systems for water resource extremes are  
9 increasingly important tools in water resource management, particularly in Europe  
10 where increased population density and climate change are expected to place greater  
11 pressures on water supply. In this context, the North Atlantic Oscillation (NAO) is often  
12 used to indicate future water resource behaviours (including droughts) over Europe,  
13 given its dominant control on winter rainfall totals in the North Atlantic region. Recent  
14 hydroclimate research has focused on the role of multiannual periodicities in the NAO  
15 in driving low frequency behaviours in some water resources, suggesting that notable  
16 improvements to lead-times in forecasting may be possible by incorporating these  
17 multiannual relationships. However, the importance of multiannual NAO periodicities  
18 for driving water resource behaviour, and the feasibility of this relationship for  
19 indicating future droughts, has yet to be assessed in the context of known non-  
20 stationarities that are internal to the NAO and its influence on European meteorological  
21 processes. Here we quantify the time-frequency relationship between the NAO and a  
22 large dataset of water resources records to identify key non-stationarities that have  
23 dominated multiannual behaviour of water resource extremes over recent decades.  
24 The most dominant of these is a 7.5-year periodicity in water resource extremes since  
25 approximately 1970 but which has been diminishing since 2005. Furthermore, we  
26 show that the non-stationary relationship between the NAO and European rainfall is  
27 clearly expressed at multiannual periodicities in the water resource records assessed.  
28 These multiannual behaviours are found to have modulated historical water resource  
29 anomalies to an extent that is comparable to the projected effects of a worst-case  
30 climate change scenario. Furthermore, there is limited systematic understanding in  
31 existing atmospheric research for non-stationaries in these periodic behaviours which

32 poses considerable implications to existing water resource forecasting and projection  
33 systems, as well as the use of these periodic behaviours as an indicator of future water  
34 resource drought.

35

## 36 **6.2 Introduction**

37 Oscillatory ocean-atmosphere systems (such as El Nino Southern Oscillation (ENSO),  
38 North Atlantic Oscillation (NAO) and Pacific Decadal Oscillation (PDO)) are known to  
39 modulate hydrometeorological processes over a large domain, often driving  
40 multiannual periodicities in hydrological records (Kuss and Gurdak, 2014; Labat, 2010;  
41 Trigo et al., 2002). As such, indices of these systems can be useful when explaining  
42 decadal-scale variations in water resource behaviour in Europe (Svensson et al, 2015;  
43 Kingston et al, 2006), North America (Coleman and Budikova, 2013) and Asia (Gao et  
44 al, 2021). In the North Atlantic region, the NAO represents the principal mode of  
45 atmospheric variability and is a leading control on European winter rainfall totals  
46 (Hurrel, 1995; Hurrel and Deser, 2010). As such, many studies have found strong and  
47 significant relationships between the winter NAO Index (NAOI) and hydrological  
48 variables across Europe (Wrzesinski and Paluszkiewicz, 2011; Brady et al, 2019; Burt  
49 and Howden, 2013), leading to the development of seasonal and long-lead forecasting  
50 systems of hydrological behaviour (Svensson et al, 2015, Bonaccorso et al, 2015).

51 A growing number of studies have identified stronger relationships between the NAOI  
52 and certain water resource variables at multiannual periodicities (Holman et al, 2011;  
53 Neves et al, 2019; Uvo et al, 2021), than at an annual scale. This is particularly  
54 apparent where longer hydrological response times predominate (Rust et al 2021a).  
55 For instance, Neves et al (2019) identified significant relationships between the NAOI  
56 and groundwater level in Portuguese aquifers and at approximately 6- and 10-year  
57 periodicities, with associations to episodes of recorded groundwater drought.  
58 Furthermore, Liesch and Wunsch (2019) found significant coherence between NAOI  
59 and groundwater level at approximately 6- to 16-year periodicities across the UK,  
60 Germany, Netherlands and Denmark. Rust et al (2019; 2021a) identified a similar  
61 significant 6- to 9-year cycle across a large dataset of groundwater level (59  
62 boreholes) and streamflow (705 gauges) in the UK, which was associated with the  
63 principal periodicity of the NAO (of a similar length (Hurrell et al., 2003; Zhang et al.,

64 2011)). In the instance of groundwater level, this periodicity was found to represent a  
65 notable portion of overall behaviour (40% the standard deviation), and minima in the  
66 cycle were shown to align with recorded instances of wide-spread groundwater  
67 drought (Rust et al, 2019). Given their association with recorded droughts across  
68 Europe, these studies highlight the potential benefit of an *a priori* knowledge of  
69 multiannual NAO periodicities in water resources for improving preparedness for water  
70 resource extremes in Europe. Here we use extremes to describe water resource deficit  
71 (i.e., drought) and periods of anomalously high water resource stores. This is distinct  
72 from hydrological extremes, which infers the drought – flood continuum.

73 However, the value of a multiannual relationship between the NAO and European  
74 water resources has yet to be assessed in the context of reported non-stationarities in  
75 hydroclimate systems. For instance, the NAO is an intrinsic mode of atmospheric  
76 variability (Deser et al, 2017), but can also be influenced by multiple other  
77 teleconnection systems such as the Madden-Julien Oscillation, Quasi-Biennial  
78 Oscillation (Feng et al 2021) or El-Nino Southern Oscillation (Zhang et al, 2019). As  
79 such it is currently unclear whether periodicities in the NAOI are emergent behaviours  
80 or the result of external forcing. This has been compounded by a relatively weak  
81 signal-to-noise ratio for NAO periodicities, making confident multiannual signal  
82 detection difficult (O'Reilly et al, 2018; Hurrell et al, 1997). While stronger NAO-like  
83 multiannual periodicities have been detected in water resource variables, due to the  
84 high-band filtering function of hydrological processes (van Loon, 2013), the degree to  
85 which these behaviours are sufficiently stable to enable development of predictive  
86 utilities is currently unclear. Furthermore, existing research has shown that the sign of  
87 the relationship between NAOI and European rainfall is non-stationary at decadal  
88 timescales (Rust et al, 2021b); Vicente-Serrano and López-Moreno (2008)). This is  
89 expected to add a degree of uncertainty to the detection of lead times between  
90 multiannual periodic components in the NAO and water resource response, which is  
91 necessary in the development of early warning systems for water resource extremes.  
92 While some studies have ascribed lags to this multiannual relationship for European  
93 water resources (Neves et al, 2019; Holman et al, 2011), the extent to which this non-  
94 stationarity is present at multiannual periodicities has yet to be assessed.

95 Finally, a critical application of early warning systems for water resource extremes is  
96 in the design of drought management regimes for existing and projected climate

97 change (Sutanto et al, 2020). While some studies have quantified the degree of  
98 modulation that multiannual ocean-atmosphere systems can have on water resources  
99 (Kuss and Gurdak, 2014; Neves et al., 2019; Velasco et al., 2015), few have compared  
100 these to the expected modulations from projected climate change scenarios. As such  
101 the benefit of incorporating multiannual NAO periodicities into early warning systems  
102 for improving preparedness for water resource extremes in climate change scenarios  
103 has not been assessed.

104 The aim of this paper is to assess the utility of multiannual relationships between the  
105 NAO and water resources for improving preparedness for future water resource  
106 extremes. This aim will be met by addressing the following research objectives:

- 107 1. Quantify significant covariances between multiannual periodicities in the NAOI  
108 and water resource extremes, and assess the extent to which these  
109 periodicities are stable over time
- 110 2. Assess multiannual periodicity phase differences between the NAOI and  
111 water resources over time, to understand the extent to which annual-scale  
112 non-stationarities between the NAO and European rainfall are expressed at  
113 multiannual scales
- 114 3. Quantify the modulations of water resource variables caused by key  
115 multiannual periodicities in the NAO, during the dry season, and compare this  
116 with projected modulations of water resources due to climate change.

117 These objectives will be implemented on UK water resource records, given the  
118 considerable coverage of recorded water resource data in time and across the space  
119 (Marsh and Hannaford, 2008); however, the methodologies developed can be applied  
120 to any regions.

121

## 122 **6.3 Data**

### 123 **6.3.1 Water resource data**

124 The National Groundwater Level Archive (NGLA) and National River Flow Archive  
125 (NRFA) provide high-resolution spatiotemporal coverage of groundwater level records  
126 and streamflow across the UK.

127 **6.3.1.1 Groundwater data**

128 Monthly NGLA groundwater level data from 136 boreholes covering all of the major  
129 UK aquifers, with record lengths of more than 20 years and data gaps no longer than  
130 24 months, have been used (Figure 21).". While some meta-analysis was conducted  
131 on monthly data, the primary analysis was undertaken on seasonally averaged data,  
132 meaning a data gap of no more than two points. They cover a range of unconfined  
133 and confined consolidated aquifer types and have been categorised into generalised  
134 aquifer groups of Chalk (78 sites), Limestone (12 sites), Oolite (12 sites), Sandstone  
135 (34) and variably cemented mixed clays and sands (Lower Greensand Group, Allen  
136 et al., 1997) (3 sites). Given the spatially heterogenous response of the Chalk aquifer  
137 to droughts (Marchant and Bloomfield, 2018), Chalk sites have been subdivided into  
138 four groups based on aquifer region: Lincolnshire basin (8 sites), East Anglian basin  
139 (17 sites), Thames and Chiltern basin (29 sites) and Southern basin (21 sites) (Allen  
140 et al., 1997; Marchant and Bloomfield, 2018).

141 Broad aquifer groups can be described as follows: Chalk, a limestone aquifer  
142 comprising of a dual porosity system with localized areas where it exhibits confined  
143 characteristics; characterised by fast-responding fracture porosity (Bloomfield, 1996);  
144 Oolite characterised by a highly fractured lithology with low intergranular permeability;  
145 Sandstone, comprised of sands silts and muds with principle inter-granular flow but  
146 fracture flow where fractures persist; and Lower Greensand, characterised by  
147 intergranular flow with lateral fracture flow depending on depth and formation (Allen et  
148 al, 1997).

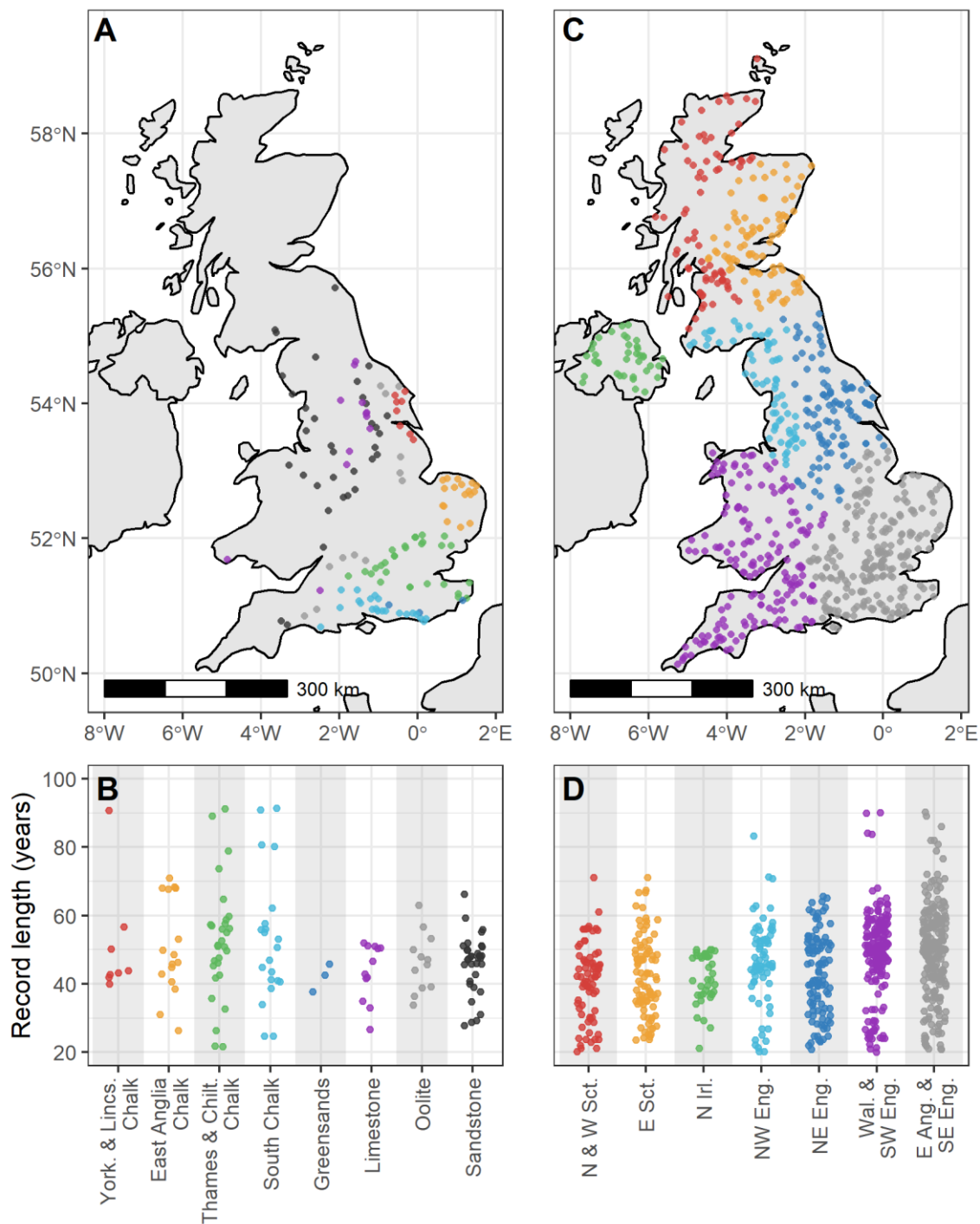
149 **6.3.1.2 Streamflow data**

150 Monthly streamflow data from the UK National River Flow Archive (NRFA; Dixon et  
151 al., 2013: <http://nrfa.ceh.ac.uk/>) has been used. Gauging stations with more than 20  
152 years of continuous streamflow data and no data gaps greater than 24 months were  
153 initially selected. Sites serving the largest catchment were selected where there are  
154 multiple sites within a single river catchment. This produced a final list of 767  
155 streamflow gauging stations for use. To understand broad spatial relationships across  
156 the streamflow dataset, records have been divided into groups based on the NRFA  
157 river drainage basin (RDB). These are grouped by seven generalised regions of the  
158 UK; North and West Scotland (75 records), East Scotland (89 records), Northern

159 Ireland (38 records), North-west England (70 records), North-east England (102  
160 records), Wales & South-west England (170 records), East Anglia & South-east  
161 England (223 records). Streamflow with minimal influence from human factors is often  
162 used in hydroclimate studies to avoid confounding mechanisms, however no such  
163 large-scale dataset exists for the UK. Furthermore, over the period of analysis and the  
164 broad scale of this assessment, inconsistencies in the way water resource  
165 management practices are implemented is expected to result in noise to the  
166 observations rather than some systematic signal or bias that would affect the results  
167 of this paper.

### 168 **6.3.2 North Atlantic Oscillation data**

169 Monthly North Atlantic Oscillation Index (NAOI) data calculated by the National Centre  
170 for Atmospheric Research (NCAR) using the principal component (PC) method for the  
171 period 1989 – 2021 has been used. The PC NAOI is a time series of the leading  
172 empirical orthogonal functions (EOFs) of sea level pressure grids across the north  
173 Atlantic region (20°-80°N, 90°W-40°E).



174

175 **Figure 21 - Spatial and temporal distributions of water resource records; a) location of**  
 176 **groundwater boreholes coloured by associated aquifer group, b) jitter plot of**  
 177 **groundwater record lengths within each aquifer group, c) location of streamflow**  
 178 **gauges coloured by associated regional group, d) jitter plot of streamflow record**  
 179 **lengths within each regional group**

180

## 6.4 Methods

### 181 6.4.1 Data Pre-processing

182 In this study we use the continuous and cross-wavelet transform to understand  
183 behaviours and relationships across different periodicities within the different water  
184 resource variable time series.

185 For all datasets, gaps less than two years were infilled to a monthly time step using a  
186 cubic spline to produce a complete time series for the wavelet transform. For time  
187 series with gaps greater than two years, the shortest time period before or after the  
188 data gap was removed. The records were not trimmed to obtain a common period of  
189 data coverage. Instead, all data was trimmed to start at a minimum of 1930. This was  
190 to allow the analysis of the fewer records that cover a longer time period while still  
191 capturing a time periods with adequate record coverage. All of the time series were  
192 standardised by dividing by their standard deviation and subtracting their mean.

### 193 6.4.2 Quantifying wide-spread water resource extremes

194 In order to meet objective 1, we produced a time series which describes the behaviour  
195 of wide-spread water resource extremes across each resource variable (i.e.,  
196 groundwater or streamflow). In this study we have assessed water resource extremes  
197 using a drought threshold methodology proposed in Peters (2003). While other  
198 measures of drought are available (e.g., Standardised Precipitation Index (SPI) and  
199 Standardised Groundwater Index (SGI)) (Bloomfield and Marchant, 2013), a threshold  
200 approach has been adopted as its can be easily applied to both streamflow and  
201 groundwater variables.

202 To calculate a drought series from monthly groundwater level and streamflow series,  
203 we first used the threshold methodology given by equation 4.3 in Peters (2003):

204

$$\int_0^M (x_t(c) - x(t))_+ dt = c \int_0^M (\bar{x} - x(t))_+ dt \quad (\text{Eq. 5})$$

205 Where:



206

$$x_+ = \begin{cases} x & \text{if } x \geq 0 \\ 0 & \text{if } x < 0 \end{cases}$$

207

208

209

210

211

212

213

and  $M$  is the full length of the data series. Here we use a threshold level of  $c = 0.3$  for groundwater level and  $c = 0.01$  for streamflow. Peters et al (2003) found that a value of 0.3 for groundwater level was comparable to other commonly used thresholds. A value of 0.01 for streamflow was chosen as it produced a similar distribution of drought events as the groundwater drought series. The chosen value of  $c$  for either variable is not expected to affect the outcomes of the study as the focus is on the frequency structure of water resource extremes, rather than magnitude.

214

215

216

217

218

219

220

For each measurement site, the monthly time series of drought status (whether in drought according to the threshold criteria or not) was converted into a yearly series describing whether that site experienced a drought in the calendar year. Then, for each year, the number of sites that experienced drought were summed and divided by the number of sites with coverage of that year. This produced a time series of the proportion of sites experiencing drought each year, for groundwater level and streamflow variables. This is referred to as the drought coverage time series.

221

### 6.4.3 Frequency Transformations

222

#### 6.4.3.1 Continuous Wavelet Transform (CWT)

223

224

225

226

227

The Continuous Wavelet Transform (CWT) was performed on the drought coverage time series for groundwater and streamflow to understand the frequency behaviour of wide-spread water resource extremes over time. The CWT is often used in geoscience to understand non-stationarities of a variable over time and frequency space (Sang, 2013).

228

229

The cross-wavelet transform,  $W$ , consists of the convolution of the data sequence  $(x_t)$  with scaled and shifted versions of a mother wavelet (daughter wavelets):

$$W(\tau, s) = \sum_t x_t \frac{1}{\sqrt{s}} \psi^* \left( \frac{t - \tau}{s} \right) \quad (\text{Eq. 6})$$

230

231

where the asterisk represents the complex conjugate,  $\tau$  is the localized time index,  $s$  is the daughter wavelet scale and  $dt$  is increment of time shifting of the daughter

232 wavelet. The choice of the set of scales  $s$  determines the wavelet coverage of the  
233 series in its frequency domain. The Morlet wavelet was favoured over other candidates  
234 due to its good definition in the frequency domain and its similarity with the signal  
235 pattern of the environmental time series used (Tremblay et al. 2011; Holman et al.  
236 2011).

237 The modulus of the transform can be interpreted as the continuous wavelet power  
238 (CWP):

$$P(\tau, s) = |W(\tau, s)| \quad (\text{Eq. 7})$$

239 We use the package “WaveletComp” produced by Rosch & Schmidbauer (2018) for  
240 all wavelet transformations in this paper.

#### 241 **6.4.3.2 Cross-Wavelet Transform (XWT)**

242 The bivariate XWT was applied between the NAOI and each of the water resources  
243 records (groundwater level (GWL) and streamflow (SF)). This produces a cross-  
244 wavelet power which is analogous to the covariance between the two variables over  
245 a time and frequency spectrum. This has been selected over the cross-wavelet  
246 coherence (analogous to correlation) as this metric requires a high degree of spectral  
247 smoothing, making the resultant coherence spectra sensitive to the choice of  
248 smoothing approach (Rosch & Schmidbauer (2018)) Here we use the covariance  
249 spectrum to compare against the drought series frequency spectrum to understand  
250 where strong coherences are reflective of dominant behaviours in water resource  
251 extremes.

252 In order to calculate cross-wavelet power (XWP) for the bivariate case, it is first  
253 necessary to calculate the continuous wavelet transform (CWT) for each of the  
254 variables separately. The XWT between variables  $x$  and  $y$  is given by:

$$W.xy(\tau, s) = \frac{1}{s} \cdot W.x(\tau, s) \cdot W.y^*(\tau, s) \quad (\text{Eq. 8})$$

255 The modulus of the transform can be interpreted as the cross-wavelet power (XWP):

$$P.xy(\tau, s) = |W.xy(\tau, s)| \quad (\text{Eq. 9})$$

256

### 257 **6.4.3.3 Wavelet Significance**

258 Lag-1 autocorrelations (AR1) in environmental datasets can produce emergent low  
259 frequency behaviours, making the detection of externally-forced behaviours more  
260 difficult (Allen and Smith, 1996; Meinke et al., 2005; Velasco et al., 2015). In this study,  
261 a significance test was undertaken to test the red-noise null hypothesis that wavelet  
262 powers calculated are the result of the recorded variables' AR1 properties. This was  
263 based on 1000 synthetic Monte Carlo series with the original AR1 values. In this paper  
264 we test significance to the 95% CI.

265 The significance spectra for the XWT for each variable pair (e.g., GWL and NAOI) form  
266 the primary results for the XWT method in this paper, since the cross-wavelet power  
267 is heavily dependent on the individual series and its frequency composition. The  
268 overall relationship between the NAOI and water resources as a whole are  
269 investigated by showing the proportion of sites over time and frequency that exhibit a  
270 significant relationship with the NAOI (95% CI). This average significance spectrum is  
271 produced by summing the significance matrices across each resource (groundwater  
272 level or streamflow) and dividing by the number of records used in year each.

273

### 274 **6.4.3.4 Phase Difference**

275 In the bivariate case, the instantaneous phase difference for the XWP spectrum  
276 (between wavelets pairs from the CWT spectrum for each variable) can also be  
277 calculated as:

$$278 \text{Angle}(\tau, s) = \text{Arg}(W_{xy}(\tau, s)) \quad (\text{Eq. 10})$$

278

279 This is the difference of the individual phases from both variables at an instantaneous  
280 time and frequency (period), converted to an angle between  $-\pi$ , and  $\pi$ . Values close  
281 to 0 indicate the two series move in-phase, with absolute values close to  $\pi$  indicating  
282 an out-of-phase relationship. Values between 0 and  $\pi$  indicate degrees of phase  
283 difference or phase shift. Phase differences between 0 and  $\pi$  can indicate the degree  
284 to which variable x is leading variable y, however a phase difference between 0 and -  
285  $\pi$  can either indicate that variable y is leading variable x, or that variable x is leading

286 by more than half the phase rotation (period length). The degree to which a certain  
287 variable is leading is analogous to a lag between the two variables.

288

#### 289 **6.4.4 Modulation measurement**

290 In order to understand the degree of modulation that the NAO teleconnection has on  
291 water resources, an absolute and relative modulation value has been calculated for  
292 each series. Here, we use modulation to describe the degree to which the NAO (or  
293 other process) has increased or decreased a water resource measure from its mean.  
294 This has been derived by reconstructing a specific principal periodicity range from the  
295 cross-wavelet powers using the following equation:

$$(x_t) = \frac{dj \cdot dt^{1/2}}{0.776 \cdot \psi(0)} \sum_s \frac{Re(W(., s))}{s^{1/2}} \quad (\text{Eq. 11})$$

296 Where  $dj$  is the frequency step and  $dt$  is the time step.

297 This produces a periodic reconstruction of a component of the original dataset that  
298 conforms to the set of periodicities (scale steps) selected. The mean and maximum  
299 amplitude of this periodic reconstruction was calculated from the absolute values of  
300 minima and maxima. Since the data were standardised by dividing by the standard  
301 deviation prior to the wavelet transform, this calculated mean and maximum amplitude  
302 are also relative to the sd of the original data. Multiplying the calculated amplitude by  
303 the original sd converts this back into a real-valued measurement. This was only done  
304 for groundwater, since streamflow is highly dependent on catchment size. In the case  
305 of streamflow, amplitudes are reported as relative to the standard deviation of the  
306 streamflow record. All calculated modulations were produced using reconstructed  
307 wavelets from after 1970 where the majority of records are present in both  
308 groundwater and streamflow variables. This was done to mitigate the effect of differing  
309 record lengths.

310

311

## 6.5 Results

### 312 6.5.1 Multiannual water resource extremes covariance with NAOI

313 Figure 22 shows the NAOI covariance significance spectrum (fig 2a and 2b) and  
314 drought frequency spectrum (fig 2c and 2d) for the groundwater level records. These  
315 have been plotted together to allow for easier interpretation and comparison of the  
316 results. Black lines in the spectral plots show the 95% CI. The calculated drought  
317 series (fig 2e) and record coverage (fig 2f) have also been plotted alongside for  
318 comparison.

319 Figure 22a shows the results from the XWT significance testing between the NAOI  
320 and the 136 groundwater level records. Results are displayed as contours showing  
321 the percentages of sites that exhibited a significant (0.05  $\alpha$ ) XWP within the time-  
322 frequency spectrum. There are five localised regions within the NAOI x GWL XWP  
323 spectrum that denote a wide-spread significance between the GWL records and the  
324 NAOI. The greatest significance contours of these regions (referred to here as focal  
325 points (FPs)) are labelled on figure 22a as: FP 1: 1934 at the 4.2 years periodicity  
326 (80% of records); FP 2: 1974 at the 8.5 years periodicity (40% of records); FP 3: 1995  
327 at 5.4 years (80% of records); FP 4: 2005 at 7 years (90% of records) and; FP 5: 2012  
328 at 2.9 years (60% of records).

329 These focal points are grouped into three larger regions within the 10% contour;  
330 between 1933 – 1940 spanning the 3- to 5-year periodicity; 1964 – 2020 spanning the  
331 4- to 12-year periodicity and; 2007 – 2017 spanning the 2- to 4-year periodicity. There  
332 is a single peak in the time-averaged percentage plots (figure 22b) at the 7.5-year  
333 periodicity (average of 26% of records)

334 Figure 22c shows the results from the CWT of the groundwater drought series (shown  
335 in Fig 2e). There are five regions of significant wavelet power in the groundwater  
336 drought frequency spectrum that are labelled in figure 22c as follows; region 1: 1930 -  
337 1950 in the 4- to 8-year periodicity range (greatest power at 4.8 years); region 2: 1930  
338 – 1945 in the 10- to 13-year periodicity range (greatest power at 11.7 years); region 3:  
339 1960 – 1965 in the 2.5- to 3.5-year periodicity range (greatest power at 2.8 years);  
340 region 4: 1960 – 1990 centred at the 12- to 17-year periodicity range (greatest power  
341 at 15.4 years); and region 5: 1980 to 2020 at the 6- to 8-year periodicity range (greatest

342 power at 7 years). There is a sixth significant region starting in 2019 and covering  
343 periods between 2 and 5 years, however this is very close to the end of the record and  
344 may be subject to edge effects. As such this region has not been taken forward for  
345 discussion.

346 There are also two notable non-significant regions of medium strength wavelet power  
347 ( $\geq 0.4$ ); 1930 - 2000 at the 14- to 23-year periodicity range (centred at 16 years), and  
348 between 1960 and 1970 at the 8- to 16-year periodicity range (centred at 9 years).  
349 There are two notable peaks in time-averaged wavelet power for the GWL drought  
350 series (figure 22d); the greatest at the 7-year periodicity (average wavelet power of  
351 0.38), and the second at the 14-year periodicity (average wavelet power of 0.24).

352 Figure 23 shows the same as Figure 22 but for the streamflow (SF) case. There are  
353 six localised regions within the NAOI x SF XWP spectrum that denote a wide-spread  
354 significance between the SF records and the NAOI. FPs of these regions are labelled  
355 on figure 22a; FP 1: 1940 at the 6.7-year periodicity (30% of records); FP 2: 1962 at  
356 the 5.2-year periodicity (50% of records); FP 3: 1975 at the 8.5-year periodicity (40%  
357 of records); FP 4: 1994 at the 5.2-year periodicity (80% of records); FP 5: 2007 at the  
358 7-year periodicity (90% of records) and; FP 6: 2011 to 2015 at the 3.2-year periodicity  
359 (60% of records). These centres are grouped into larger regions within the 10%  
360 contour; these are between 1933 – 1947 spanning the 5.5- to 8-year periodicity; 1960  
361 – 1970 spanning the 4- to 8-year periodicity; 1965 – 1990 spanning the 7- to 11-year  
362 periodicity; 1988 – 2000 spanning the 4- to 5.5-year periodicity; 1995 – 2020 spanning  
363 the 4.5- to 11-year periodicity and 2007 – 2017 spanning the 2.5- to 4.5-year  
364 periodicity. There is a single peak in the time-averaged percentage plots (figure 23b)  
365 at the 7.5-year periodicity (average of 29% of records)

366 Figure 23c shows the results from the CWT of the streamflow drought series (shown  
367 in Fig 3e). There are three regions of significant wavelet power in the groundwater  
368 drought frequency spectrum that are labelled on Figure 23c; region 1: 1930 – 1935 in  
369 the 21 year periodicity (this region appears clipped by the record start date, so the  
370 strongest wavelet power for this region may not be captured); region 2: 1930 - 1937 in  
371 the 2.5- to 6.5-year periodicity range (strongest power at 4.3 years) and; region 3:  
372 1930 – 1960 in the 11- to 15-year periodicity range (strongest power at 13 years);

373 There are four non-significant regions of medium strength wavelet power ( $\geq 0.4$ );  
374 1935 – 1945 at the 2- to 3-year periodicity; 1955 – 1965 at the 2- to 4-year periodicity;  
375 1960 – 2015 at the 5.5- to 8-year periodicity; and 2000 – 2005 at the 2- to 5-year  
376 periodicity. The time-averaged wavelet power for the SF drought series (figure 23d)  
377 contains multiple peaks suggesting no dominant periodicity. The greatest peak is at  
378 the 7-year periodicity with an average wavelet power of 0.21.

### 379 **6.5.2 Cross-wavelet phase difference**

380 The cross-wavelet phase difference ( $\phi$ ) between water resource variables and the  
381 NAOI at the 7.5-year periodicity has been displayed in figure 24 for the GWL records  
382 and figure 25 for the streamflow records. The phase difference is a circular  
383 measurement where 0 indicates an in-phase relationship (analogous to zero lag) and  
384  $\pm \pi$  indicates an out-of-phase relationship between the selected periodicity within the  
385 two variables (analogous to half a periodicity lag (3.75-years)). The purpose of these  
386 plots of phase differences are to visualise and understand the difference in phase  
387 between the NAO and water resources. Records have been split by their aquifer group  
388 in Figure 24, and by catchment region in figure 25, to understand if there are any  
389 general differences between regions.

390 The majority of groundwater level records cover the period 1970 to present, meaning  
391 general trends are more clearly presented for this time period. The phase difference  
392 of most GWL records can be defined by a sudden shift at approximately 1990 (figure  
393 24). Values of  $\phi$  generally range from between  $-1/4\pi$  and  $-3/4\pi$  (-0.76 to -2.36 rads;  
394 generally anti-phase) for the period 1975 to 1990 to between  $+1/4\pi$  and  $+3/4\pi$  (0.76  
395 to 2.36 rads; generally in-phase) for the period 1990 to 2019 across all sites. This is  
396 with the exception of 17 sites across the South Chalk and Thames & Chiltern Chalk  
397 which have shorter ~anti-phase periods (between approximately 1985 and 1990).  
398 Average  $\phi$  values for the period 1970 – 1990 (1990 – 2020) for each aquifer region  
399 are: -1.26 (1.41) in East Anglian Chalk; -2.25 (1.21) in Lincolnshire Chalk, 0.52 (0.83)  
400 in South Chalk, -1.37 (0.83) in Thames & Chiltern Chalk, 1.51 (1.21) in Greensands, -  
401 0.78 (0.66) in Limestone, -1.36 (1.09) in Oolite, -0.70 (1.35) in Sandstone. As such  
402 most aquifer regions experience an average reversal of polarity at 1990. Greensand  
403 GWL show no reversal when assessing average  $\phi$  values, however 1 of the 3 sites in  
404 this aquifer group does show this reversal.

405 Similar to the GWL records, most SF records exhibit a shift in phase difference at  
406 approximately 1990, with catchment groups in the north of the UK showing minimal  
407 shifts (i.e., NW Scotland, E Scotland, NI, and NW England) (figure 25). In the southern  
408 catchment groups, values of  $\phi$  generally range from between  $-1/2\pi$  and  $\pm\pi$  (generally  
409 anti-phase) for the period 1970-1990 (approximately prior to the shift) to between 0  
410 and  $+3/4\pi$  (generally in-phase) for the period 1990 to 2020 (approximately after the  
411 shift). Furthermore, catchment groups in the east of the UK (i.e., E Scotland, NE  
412 England, East Anglia & SE England) during the in-phase period (1990-2020) exhibit a  
413 notable transition to increased phase difference (to approximately  $+3/4\pi$ ) between  
414 2000 and 2010 before decreasing to approximately  $+1/4\pi$  in 2020. Average  $\phi$  values  
415 for the period 1970 – 1990 (1990 – 2020) for each catchment region are: -0.21 (0.14)  
416 in North and West Scotland, 0.49 (0.86) in East Scotland, -0.43 (0.46) in Northern  
417 Ireland, -0.44 (0.47) in NW England, 2.32 (1.08) in NE England, 0.77 (0.64) in Wales  
418 and SE England, and 2.53 (0.99) in East Anglia and SE England.

### 419 **6.5.3 Modulation of dry season water resources**

420 Figure 26 shows two boxplots for each aquifer group, representing the distribution of  
421 mean (in blue) and maximum (in red) dry-season GWL deviation as a result of the 7.5-  
422 year periodicity (over the length of each of the record). Median values from each of  
423 these mean and maximum boxplots are described below, and are referred to as  
424 med.mean and med.max respectively.

425 The 7.5 year periodicity accounts for the greatest deviation of-dry season GWL in the  
426 Chalk aquifer regions, with the Thames & Chiltern basin GWL showing the greatest  
427 modulation of all groups showing med.mean of 0.94m and a med.max of 1.38m. Two  
428 other Chalk groups showed similarly strong modulations; the South Chalk basin GWL  
429 (med.mean: 0.7m, med.max: 1.07m); and the Lincolnshire Chalk GWL  
430 (med.mean: .56m, med.max: 0.77m). The East Anglia GWL show lowest modulation  
431 of the Chalk (med.mean: 0.16m, med.max: 0.34m), similar to GWL in the Limestone  
432 (med.mean: 0.35m, med.max: 0.51m) and the Oolite (med.mean: 0.21m, med.max:  
433 0.33m). Lowest overall modulations are found in the Sandstone (med.mean: 0.15m,  
434 med.max: 0.25m) and Greensands aquifers (med.mean: 0.12m, med.max: 0.17m).

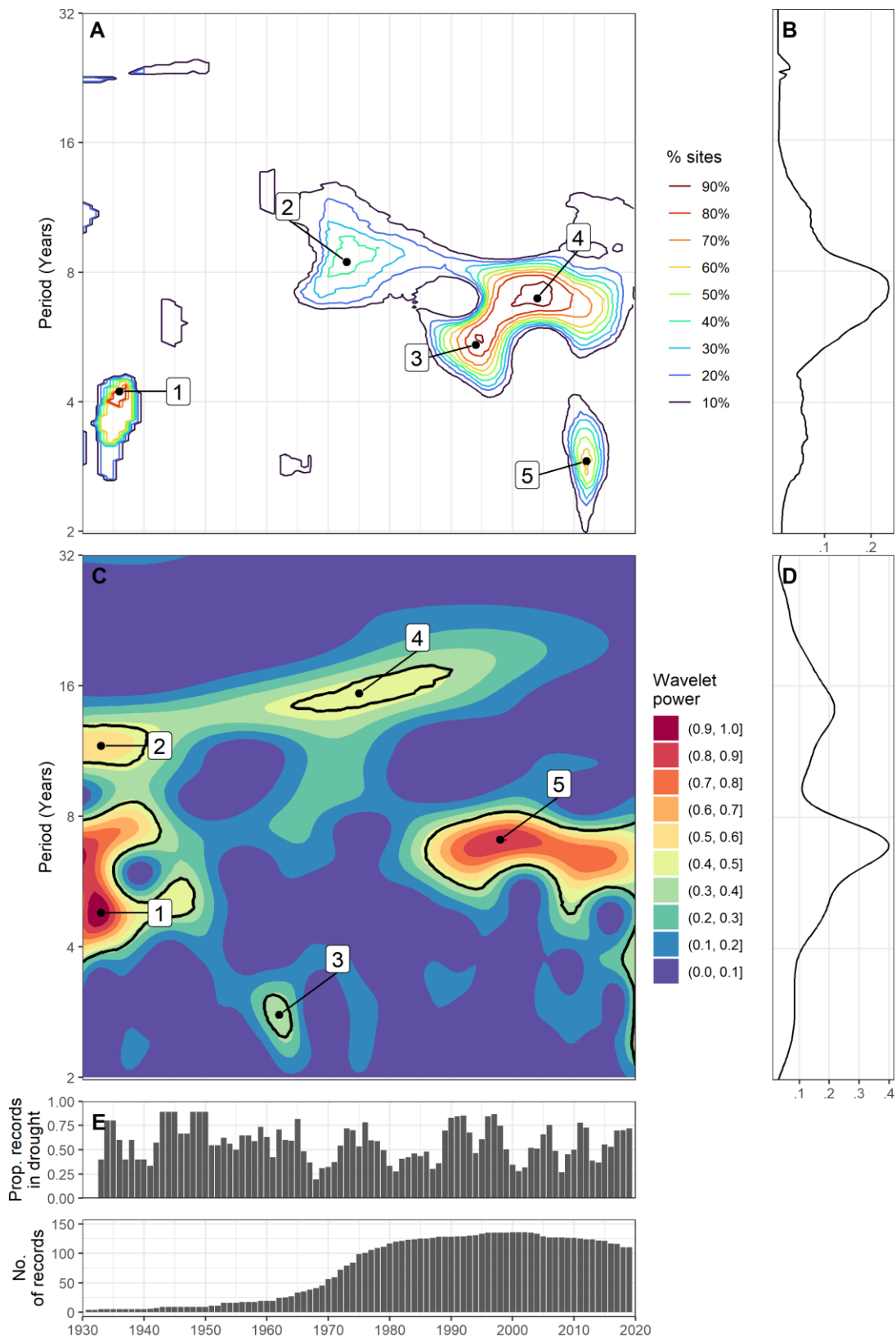
435 Figure 27 shows the same as figure 26 but for the streamflow case. Streamflow  
436 modulations are measured as relative to the standard deviation of each record.



437 Modulation of streamflow for each catchment group are (in descending order of  
438 med.mean); Wales & south-west England (med.mean: 0.32, med.max: 0.50); East  
439 Anglia & south-east England (med.mean: 0.31, med.max: 0.53); Northern Ireland  
440 (med.mean: 0.29, med.max: 0.50); West Scotland (med.mean: 0.27, med.max: 0.46);  
441 north-east England (med.mean: 0.27, med.max: 0.47), north-west England  
442 (med.mean: 0.26, med.max: 0.46), east Scotland (med.mean: 0.21, med.max: 0.39).

443

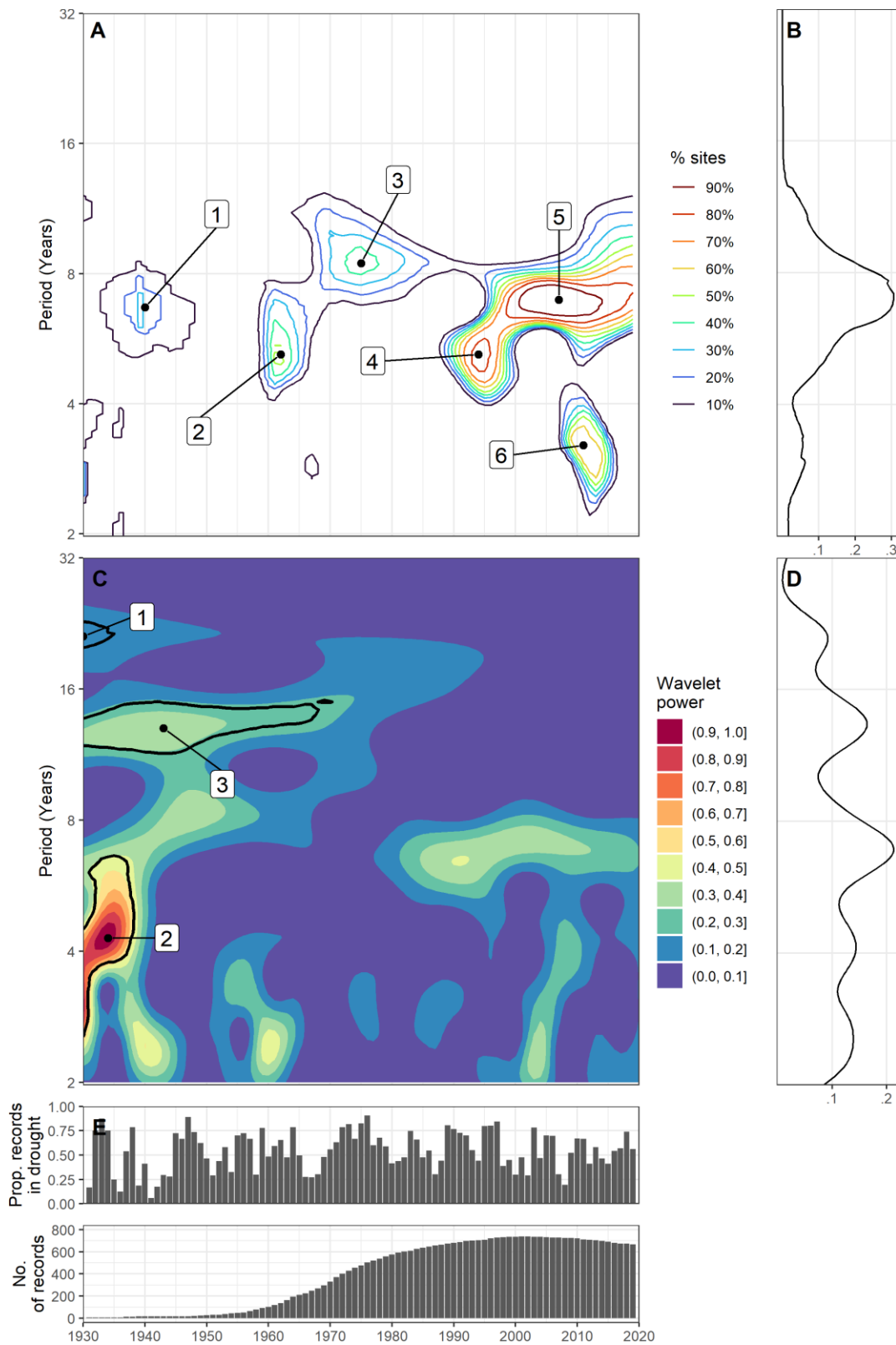
444



445

446 **Figure 22 - a) Significance (95% CI) contours between GWL and NAOI, b) time-averaged**  
 447 **proportion of gw1 records with a significant XWP with the NAOI (measured as a decimal**  
 448 **fraction), c) wavelet (spectral) power of GWL drought series, d) time-averaged wavelet**

449 (spectral) power of GWL drought series, e) GWL drought coverage time series, f)  
450 temporal coverage of records.  
451

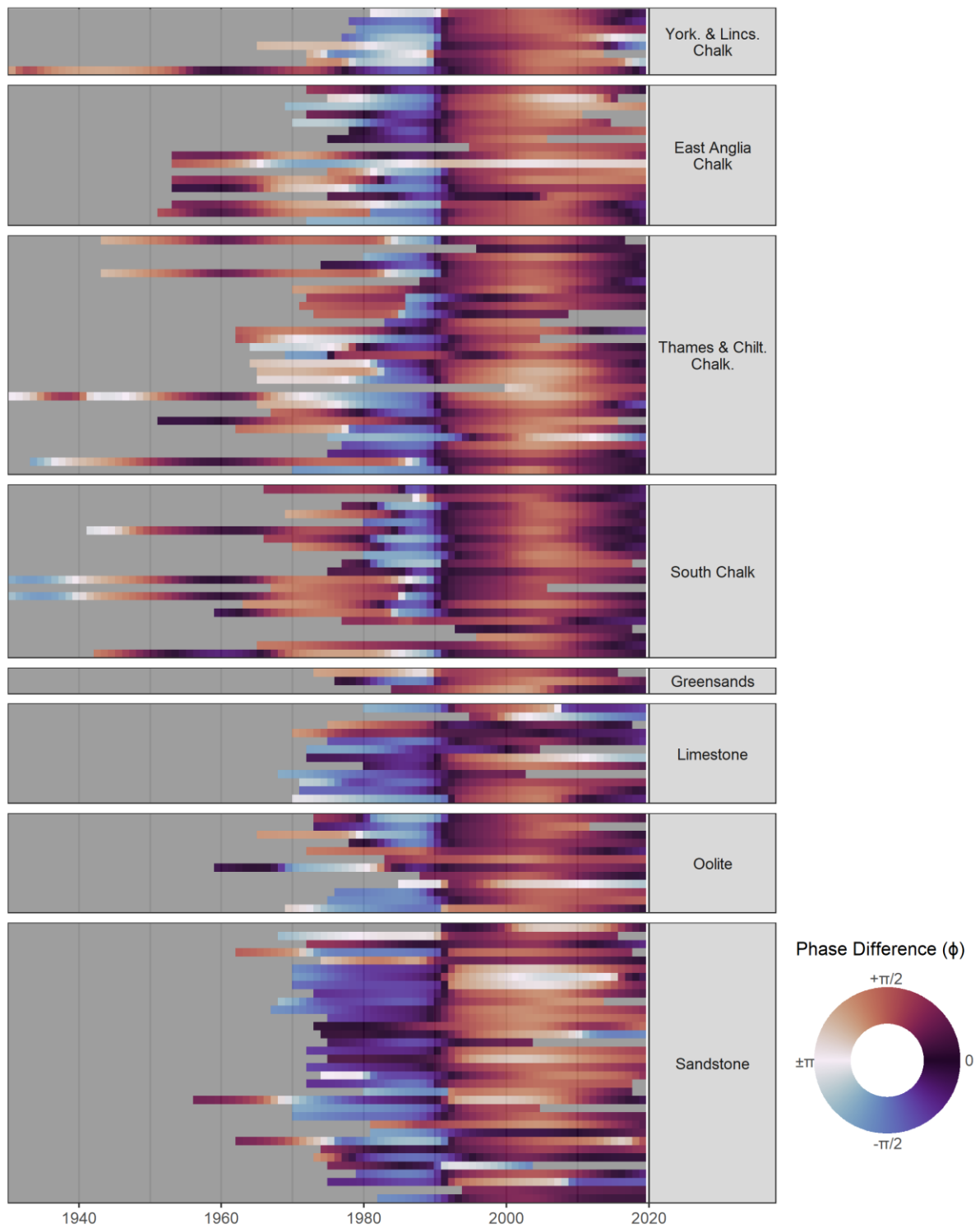


452

453 **Figure 23 - a) Significance (95% CI) contours between SF and NAOI, b) time-averaged**  
 454 **proportion of SF records with a significant XWP with the NAOI (measured as a decimal**  
 455 **fraction),c) wavelet (spectral) power of SF drought series, d) time-averaged wavelet**

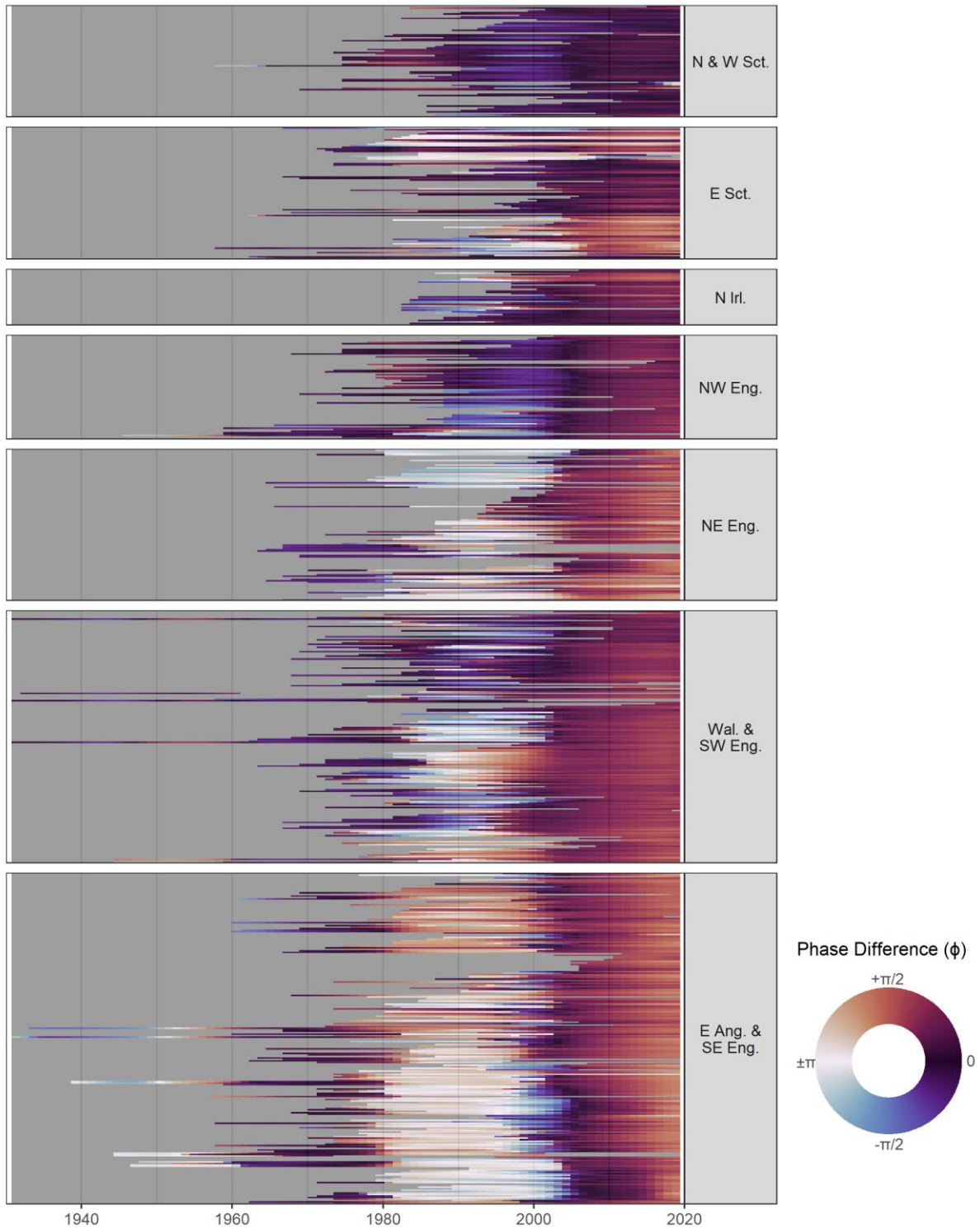
456 (spectral) power of SF drought series, e) SF drought series showing proportion of  
457 records in drought each year, f) temporal coverage of records.

458



459

460 **Figure 24 - Phase difference between the NAOI and each GWL record for the GWL**  
 461 **record period. Results are grouped by aquifer regions.  $\phi = 0$  is equivalent to an in-**  
 462 **phase relationship and  $\phi = \pm\pi$  is equivalent to an antiphase relationship.**

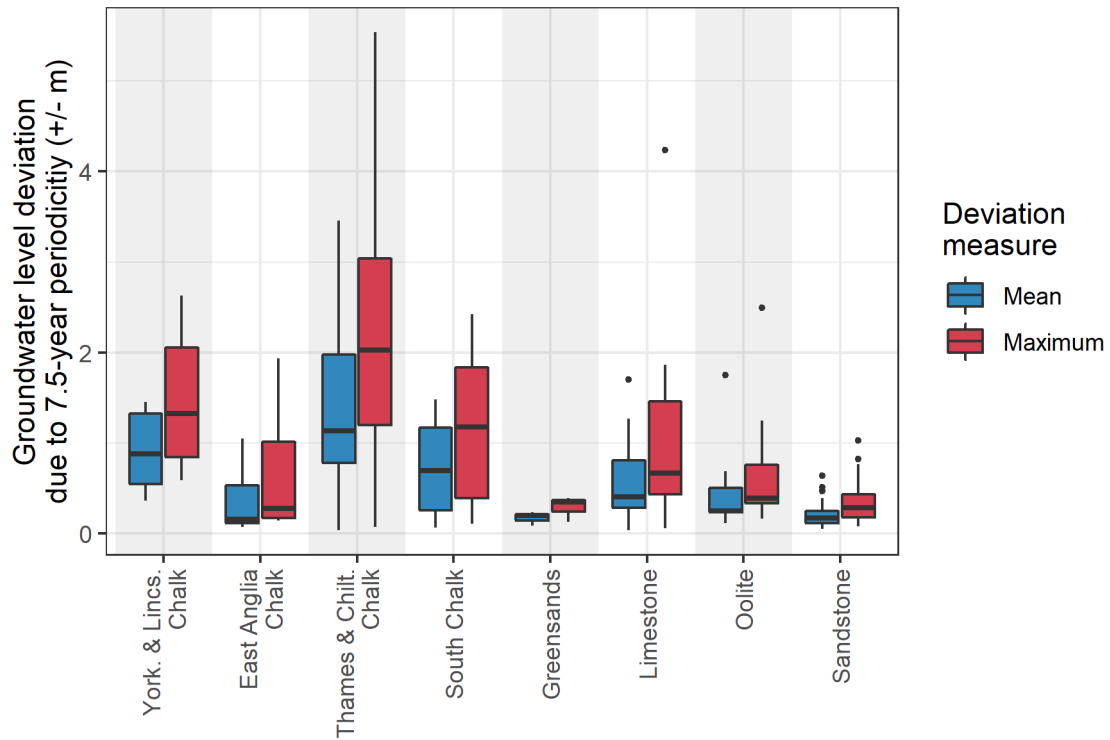


463

464 **Figure 25 - Phase difference between the NAOI and each streamflow record for the**  
 465 **streamflow record period. Results are grouped by aquifer regions.  $\phi = 0$  is equivalent**  
 466 **to an in-phase relationship and  $\phi = \pm\pi$  is equivalent to an antiphase relationship.**

467

468

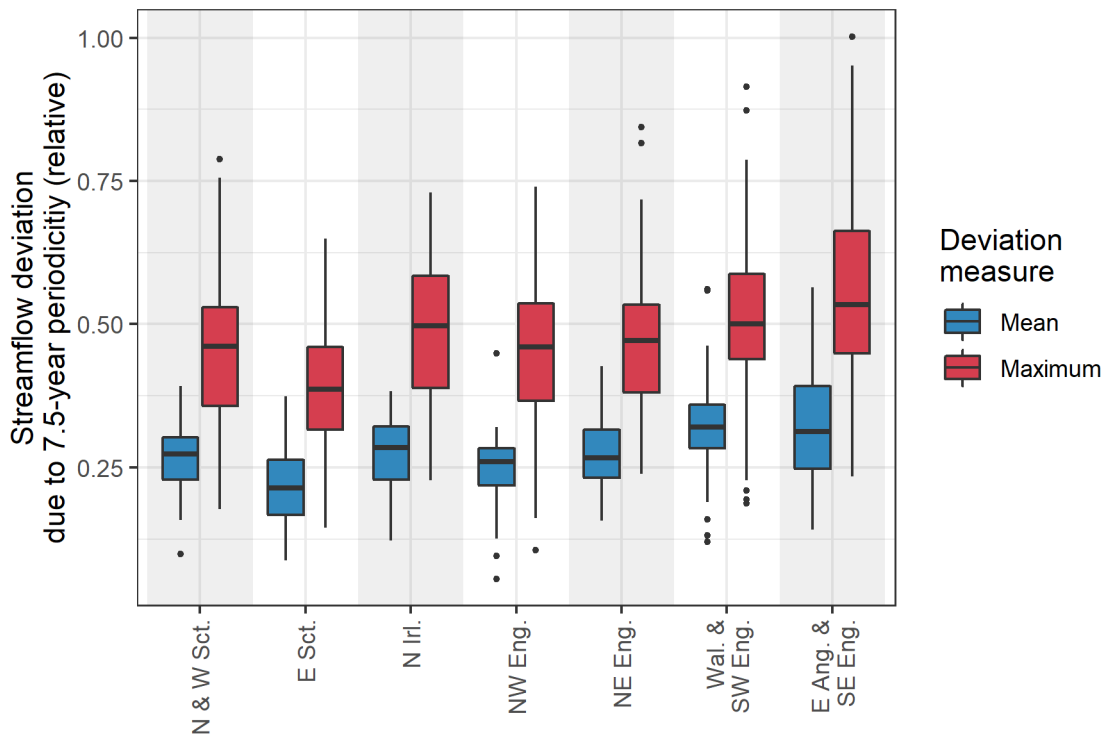


469

470 **Figure 26 - Distribution of absolute mean and maximum modulation of summer**  
 471 **groundwater level as a result of the principal cross-wavelet periodicity between the**  
 472 **NAOI and winter Groundwater level by aquifer region**

473





474

475 **Figure 27 - Modulation of summer streamflow (relative to record standard deviation) as**  
 476 **a result of the principal cross-wavelet periodicity between the NAOI and winter**  
 477 **streamflow.**

478 **6.6 Discussion**

479 **6.6.1 Historical covariances between the NAOI and water resources at**  
 480 **multiannual periodicities**

481 Our results show that the dominant mode of multiannual covariance between the NAOI  
 482 and UK water resources is at the ~7.5-year periodicity. This is apparent in the time-  
 483 averaged covariance significance plots for groundwater (figure 22b) and streamflow  
 484 (figure 23b). The same 7.5-year periodicity is also the strongest average mode of  
 485 periodic behaviour in water resource extremes. Periodicities of similar lengths have  
 486 previously been detected in European GWL records, such as those in the UK (Rust et al  
 487 al, 2018 Holman et al, 2011), Hungary (Garamhegyi et al, 2016), Spain (Luque-  
 488 Espinar et al, 2008), Italy (De Vita et al 2011), and Germany (Liesch and Wunsch,  
 489 2019); and European streamflow records, for example in the UK (Rust et al 2021; Burt  
 490 and Howden, 2013) and Sweden (Uvo et al, 2021). The results therefore are

491 consistent with principal periodicities detected in wider European water resources and  
492 highlight the NAO's wide-scale control on water resource extremes.

493 Despite the prominence of the average 7.5-year periodicity in water resource  
494 variables, the wider time-frequency spectra show that the NAO's multiannual control  
495 on water resources is subject to considerable transience and non-stationarity across  
496 time and frequency. For instance, the percentage of water resource records with a  
497 significant covariance with the NAOI at the 7.5-year periodicity remains below 10%  
498 until between 1960 and 1965, with significance becoming abruptly widespread (> 30%)  
499 between 1980 and 1985. As such this suggests that the NAO's control on water  
500 resources, at the 7.5-year periodicity, has only been prominent over the past four to  
501 five decades. Furthermore, prior to this mode of behaviour, an approximate 16-year  
502 periodicity predominated the water resource extremes record that did not covary with  
503 NAOI. Previous studies have associated a minimum in this 16-year cycle in water  
504 resources with the wide-scale 1976 drought (Rust et al, 2019) that affected most UK  
505 water resources, particularly in the south of the country (Rodda and Marsh, 2011).  
506 These findings are also consistent with Barker et al (2019) who demonstrate longer  
507 duration drought events in the UK for the period 1940 to 1980 (approximately), and  
508 comparatively shorter drought durations for the period 1980 to present. This may be  
509 explained by a more prominent low-frequency influence on water resources and  
510 extremes during this period, causing longer negative anomalies on drought indices.  
511 Finally, Holman et al (2011) linked a 16-year periodic behaviour in groundwater  
512 records with the East Atlantic pattern, the second-most dominant mode of atmospheric  
513 variability in the North Atlantic region. The results here could be interpreted as  
514 suggesting an abrupt shift towards increased frequency of water resource extremes  
515 around 1970 to 1980 as a result of a transition of periodic control from the EA to the  
516 NAO. This interpretation may expand on findings from Neves et al (2019) who  
517 demonstrate that historical droughts in southwest Europe are better explained with a  
518 combination of NAO and EA influence.

519

520 Multiple studies have noted a marked change in European hydrological drought trends  
521 since the 1970s, often in the context of the ongoing effects of climate change on water  
522 resources (Tanguy et al 2021; Rodda and Marsh, 2011; Bloomfield et al., 2019). These

523 impacts vary depending on the water resource and region but can include changing  
524 drought frequency (Spinoni et al, 2015; Bloomfield et al., 2019; Chiang et al, 2021),  
525 severity (Hanel et al, 2018; Bloomfield et al., 2019), and increasing divergence of  
526 drought characteristic across Europe (Cammalleri et al, 2020). We show here that a  
527 dominant 7.5-year periodicity, driven by the NAO, has occurred coincident to these  
528 reported changing trends, and proceeded a secondary periodicity of approximately 16  
529 years. As such the results here suggest that some of the change in drought frequency  
530 that has been noted to have occurred since the 1970s, may be in-part driven by the  
531 NAO's increased periodic control on water resources. Hydroclimate studies often  
532 highlight that the interaction between climate change, ocean-atmosphere processes  
533 and land-surface processes may be complex, resulting in non-linear hydrological  
534 responses to increasing global temperatures (Rial et al 2004, Wu et al, 2018). As such,  
535 the abrupt emergence of a 7.5-year periodicity between the NAO and water resource  
536 extremes between 1980 and 1985, and its weakening since 2005, may be evidence of  
537 this type of non-linear response. While there have been many studies assessing the  
538 impact of climate change projections on the NAO (e.g. Rind et al (2005); Woolings and  
539 Blackburn (2012)), there have been few that have investigated potential interactions  
540 between climate change and multiannual periodicities in the NAO. As such, the role of  
541 climate change in affecting the non-stationary periodicities (detected in this study) is  
542 currently unknown.

543 Yuan et al (2017) highlight the importance of suitable calibration period selection for  
544 the development of drought early warning systems, particularly in climate change  
545 scenarios. Many of these systems in Europe (e.g. Hall and Hanna, 2018; Svensson et  
546 al., 2015) rely on high-resolution hydrometeorological datasets for calibration of  
547 historical relationships, many of which are only available for recent decades (Rust et  
548 al, 2021b, Sun et al 2018). We show here that frequency statistics potentially used as  
549 calibration bases for water resource early warning systems can exhibit both  
550 multidecadal periods of stability and abrupt sub-decadal non-stationarities, driven by  
551 multiannual behaviours in the NAO. Furthermore, we show a weakening of the  
552 dominant 7.5-year periodicity since 2005, suggesting a different frequency structure  
553 may predominate water resource extremes from the 2020s. This further highlights the  
554 need for continuous recalibration of critical forecasting utilities, and the potential

555 benefit of including the NAOI as a covariate when understanding multiannual periodic  
556 variability in European water resources.

557

558 **6.6.2 Phase difference between NAO and water resource records at 7.5-**  
559 **year periodicity**

560 The quantification of lead times between meteorological processes and water  
561 resource response is critical in the development of early warning systems for water  
562 resource management. As such, hydroclimate studies have sought to investigate  
563 temporal lags between multiannual periodicities in the NAO and water resource  
564 variables across Europe (Uvo et al, 2021, Neves et al 2019, Holman et al 2011).  
565 However, previous research has highlighted that the relationship strength and sign  
566 between the NAO and European rainfall is non-stationary at sub-decadal to decadal  
567 timescales (Rust et al 2021, Vicente-Serrano & López-Moreno, 2008). The extent to  
568 which this non-stationarity is projected to multiannual periodicities in water resources  
569 was previously unknown. Sign change is synonymous with a phase difference shift of  
570 approximately  $\pi$  between periodic components of the NAO and water resources, and  
571 as such has the potential to disrupt the projection of lead times into future scenarios.  
572 Here we assess the phase difference between the NAO and water resources at a  
573 country scale to identify the extent to which this non-stationary is present at  
574 multiannual periodicities.

575 Most water resources records exhibit an abrupt shift in phase difference of  
576 approximately  $-\pi$  around 1990. An earlier shift (of approximately  $+\pi$ ) is also apparent  
577 between 1970 and 1980, however this is less temporally aligned across the fewer  
578 records that cover this period. This suggests that, for the period of approximately 1970  
579 to 1990, the relationship sign between the NAO and water resources was inverted.  
580 Furthermore, the timing of this period of inversion generally aligns with reported  
581 periods of sign inversion in existing studies between the NAO and UK rainfall (Rust et  
582 al 2021, Vicente-Serrano & López-Moreno, 2008). It is interesting to note that this  
583 period of inversion is notably shorter for some groundwater level records of the Chalk  
584 (e.g., those in South Chalk and Thames and Chiltern Chalk). Rust et al (2021b)  
585 showed the south and south east of the UK was subject to the increased non-  
586 stationarity of the NAO-precipitation relationship when compared to other regions,  
587 which may explain these relatively short periods of relationship inversion. A similar  
588 spatial pattern is shown in the streamflow records, with minimal phase difference shifts

589 in northwest England, Scotland, and Northern Ireland where more stable signs have  
590 been found by Rust et al (2021b).

591 Localisation of this non-stationarity between the NAO and water resources at  
592 multiannual periodicities suggests it is possible to identify a discrete time period of  
593 sufficient stationarity from which to calculate lead-in times for early warning systems  
594 (for instance, between 1990 and 2020). However, phase differences for this period  
595 also show a degree of non-stationarity, varying by up to approximately  $\pm\frac{1}{4}\pi$ . Some of  
596 this variance may be due to changing storage dynamics within a catchment over time  
597 (Rust et al, 2014; Beverly and Hocking, 2012), but also the introduction of red noise  
598 from reconstructing from non-significant wavelets. This also explains the increased  
599 variance seen in aquifer groups characterised by higher autocorrelation (e.g.,  
600 Sandstone) (Bloomfield and Marchant, 2013), and the relatively low variance seen in  
601 streamflow records which often have lower autocorrelation when compared to  
602 groundwater level (Hannaford et al, 2021). While this can be minimised by calculating  
603 phase difference from significant wavelets only, we have shown in the previous section  
604 that the significance between the NAO and water resources and multiannual  
605 periodicities is also subject to notable non-stationarity.

606 Finally, in order to calculate accurate lead-in times between periodicities in the NAO  
607 and water resources in future scenarios, a sufficient systematic understanding of the  
608 NAO sign non-stationarity is required. However, there is limited research that has  
609 investigated the causes for these modes of multiannual non-stationarity. Vicente-  
610 Serrano & López-Moreno (2008) suggest that an eastward shift of the NAO's southern  
611 centre of action may account for a portion of this variability, but highlight that further  
612 work is required for this to be a sufficient explanation of a changing correlation between  
613 the NAO and European rainfall. As such, existing non-stationarities between the NAO  
614 and water resources at multiannual periodicities remains a considerable barrier to its  
615 application in improving preparedness for future water resource extremes.

### 616 **6.6.3 NAO multiannual modulations on water resources in future** 617 **scenarios**

618 Water resource management systems are in place across Europe to improve planning  
619 and preparedness for the projected effects of climate change. As such, in order for  
620 multiannual NAO modulations of water resources to have sufficient utility for water

621 management systems in future scenarios, they need to exhibit a comparable influence  
622 on water resources to the projected effects of climate change. Here, we present  
623 historical modulations of summer water resource variables from the principal NAO  
624 periodicity alongside expected impacts on water resources from climate change  
625 projections in order to discuss their comparative influence.

626 Jackson et al (2015) estimated median groundwater level change due to climate  
627 change in 24 boreholes across Chalk, limestone, sandstone and greensand aquifer  
628 groups in the UK for the 2050s under a high emission scenario for September (as a  
629 typical annual minima of groundwater levels in the UK). Median level from each site in  
630 Jackson et al (2015) have been regrouped and averaged across the broad aquifer  
631 groups used in this study to allow comparison with historical deviations in water  
632 resource results as a result of the NAO's 7.5-year periodicity. This comparison is  
633 provided in Table 1. A mapping table of this comparison is available in the  
634 supplementary material.

635





<b>Aquifer group</b>	<b>50<sup>th</sup> %ile gwl change due to climate change ( m)</b>	<b>Gwl deviation due to 7.5-year NAO periodicity (<math>\pm</math> m) (med.mean)</b>	<b>Gwl deviation due to 7.5-year NAO periodicity (<math>\pm</math> m) (med.max)</b>
Chalk (East Anglia)	-0.21	0.16	0.31
Chalk (Lincolnshire)	-0.31	0.71	1.03
Chalk (South)	-0.64	0.73	1.08
Chalk (Thames / Chilterns)	-0.69	0.86	1.33
Limestone	-0.28	0.35	0.51
Oolite	-0.36	0.21	0.33
Sandstone	-0.07	0.15	0.25
Greensands	-0.10	0.12	0.17

**Table 1 - Synthesis of Table 3 from Jackson et al (2015). Median results from the absolute teleconnection modulation on groundwater level from Figure 3 of this paper are also presented for the mean and maximum modulation cases. NAO teleconnection modulations greater than the reported 50<sup>th</sup> percentile climate change modulation are shaded in grey.**

Historical modulations in groundwater level due to multiannual periodicities in the NAO were greater than projected GWL modulation from a high emissions climate change scenario, in all but two aquifer groups for mean NAO modulation (East Anglia Chalk, Oolite), and all but one for maximum NAO modulation (Oolite). Similar degrees of GWL modulation from climate change scenarios have been shown for wider European aquifer systems (e.g., Dams et al, 2011), and the results for NAO modulations of GWL are of a similar degree to those reported by Neves et al (2019) for aquifers in the Iberian Peninsula. While few studies have looked at multiannual NAO modulations of groundwater level across Europe, the results here suggest a similar response across Western Europe, where the NAO has a greater influence on precipitation (Trigo et al, 2002). However, existing

studies notable uncertainties in the future trends of groundwater level change due to climate change. For instance, Yusoff et al. (2002) demonstrated that it was not possible to predict whether groundwater level would rise or fall between 2020s and 2050s, Bloomfield et al. (2003) showed that groundwater levels were expected to rise in the 2020s but fall in the 2050s, and, Jackson et al (2015) showed reductions in annual and average summer levels but increases in average winter levels by the 2050s. For streamflow, Kay et al (2020) give estimated modulations to low flows (Q95) as a result of climate change (2050 horizon). While no Scottish catchments were used in the study, percentage modulations for low flows were found to be mostly between 0 to -20% change with some catchments showing up to -40% change for catchments in the West and South West of the UK. Schnieder et al (2013) show similar low flow modulations across Europe as a result of climate change, ranging from +20% for northwest Europe to -40% in the Iberian Peninsula. As such, the results for streamflow (Figure 27) indicate that multiannual NAO modulation of streamflow has been, on average, comparable to the expected change due to climate change scenarios. NAO modulations in streamflow are notably less than those found in groundwater level, as may be expected given the established sensitivity of groundwater processes to long-term changes in meteorological fluxes (Forootan et al., 2018; Van Loon, 2015; Folland et al., 2015).

Given the scale of multiannual NAO influence on water resource compared to the estimated effects of climate change, the NAO may have the potential to impact the projected trend of water resource variability in certain future scenarios more than was previously understood, and therefore effect the required adaptive management response. However, existing research has shown that that current GCMs do not fully replicate low frequency behaviours in the NAO that have been historical recorded (Eade et al, 2021). Given the importance of multiannual periodicities the NAO in defining water resource behaviour, demonstrated here and in other research (e.g., Uvo et al, 2021; Neves et al, 2019), this raises notable uncertainties in the use of GCMs outputs for projecting European water resource behaviour into future scenarios. Findings reported here suggest that current projections from these GCMs may contain error that is comparable to the current

projected effect of climate change on water resources. This therefore highlights the need for improved low frequency representation in GCMs, and for an understanding of the non-stationary atmospheric behaviours are can considerably influence wide-scale water resource behaviour.

Rust et al (2018) set out a conceptual model for how multiannual modulations of water resources due to the NAO may provide a system for improving water resource forecasts and management regimes. This model highlights the need for a systematic understanding of how multiannual periodicities affect water resources over time, including temporal lags and amplitude modulation between the NAO and water resources. We demonstrate that the degree to which the NAO's 7.5-year periodicity has modulated historical water resources is of a similar order of magnitude to the estimated impacts on water resource variables from climate change projections. These results further show the importance of including the influence of multiannual NAO periodicities on water resources in the understanding of future extremes, as they have the potential to affect the required management regime for certain resources in climate change scenarios. However, we also show that there are notable non-stationarities in NAO periodicities over time and their relationship with water resource response, for which there is limited systematic understanding in existing hydroclimate literature.

## **6.7 Conclusions**

This paper assesses the utility of the relationship between the NAO and water resources, at multiannual periodicities, for improving preparedness of water resource extremes in Europe. We review this relationship in the context of non-stationary dynamics within the NAO and its control on UK meteorological variables, as well as its potential impact on water resources in climate change scenarios. We provide new evidence for the time-frequency relationship between the NAO and water resources in western Europe showing that a wide-spread 7.5-year periodicity, which predominates the multiannual frequency structure of many European water resources, is the result of a non-stationary control from the NAO

between approximately 1970 and 2020. Furthermore, we show that known non-stationarities of the relationship sign between the NAOI and European rainfall at the annual scale are present in water resources at multiannual scales. A current lack of systematic understanding of both these forms of non-stationarity, in existing atmospheric or meteorological literature, is a considerable barrier to the application of this multiannual relationship for improving preparedness for future water resource extremes. However, we also show that the degree of modulation from multiannual NAO periodicities on water resources can be comparable to modulations from a worst-case climate change scenario. As such multiannual periodicities offer a valuable explanatory variable for ongoing water resource behaviour that have the potential to heavily impact the required management regimes for individual resources in climate change scenarios. Therefore, we highlight knowledge gaps in atmospheric research (e.g. the ability of climate models to simulate NAO non-stationarities) that need to be addressed in order for multiannual NAO periodicities to be used in improving early warning systems or improving preparedness for water resource extremes.

## **6.8 References**

The reference list for this paper has been combined with the final reference section for this thesis in chapter 10.

# **7 CHAPTER 7 INTEGRATED DISCUSSION**

## **7.1 Introduction**

Hydroclimate studies have linked multiannual periodicities detected in European water resource records with long-term behaviours in the NAO (e.g., Holman et al, 2011; Uvo et al, 2021), and have shown that multiannual NAO periodicities may influence the occurrence of water resource drought (e.g., Neves et al, 2019). As such, these studies often highlight the potential of multiannual NAO periodicities as an indicator of future water resource behaviours, which may allow for improved preparedness of certain water resource extremes (e.g., Neves et al, 2019; Liesch and Wunsch, 2019).

However, prior to the papers presented in this thesis, few studies had investigated - in detail - how this relationship is expressed across varied or large hydrometeorological datasets. Therefore, there was limited data to investigate the character of multiannual NAO influence on water resources at a spatial scale that is appropriate for water management applications (Perveen, 2012). Furthermore, little was known of the broad physical processes that influence this multiannual relationship, meaning its feasibility for improving preparedness of water resource extremes had not been fully assessed.

This integrated discussion will show how the papers presented in this PhD thesis combine to address these knowledge gaps. The aim of this thesis is to assess the extent to which multiannual connections between the NAO and water resources may have utility for water resource forecasting and for improving preparedness for water resource extremes. The following will discuss the results from the individual papers presented here and demonstrate how these address the overarching aim and the research objectives of this thesis.

## **7.2 Influence of multiannual NAO periodicities on recorded water resource behaviour**

Results presented in this thesis demonstrate that an approximately 7-year periodicity represents a fundamental component of the UK water cycle. This

behaviour permeates many hydrometeorological processes, including rainfall (Rust et al 2018, 2021a), streamflow (Rust et al 2021a, 2021c) and groundwater (Rust et al. 2018, 2021c), and aligns with similar periodicities found in other European water resources (e.g., Garamhegyi et al, 2016; Luque-Espinar et al, 2008; De Vita et al 2011; Liesch and Wunsch, 2019; Burt and Howden, 2013). Rust et al (2021c) shows that this mode of multiannual behaviour is significantly related to the NAOI (at a 7.5-year periodicity), thereby contributing to the existing body of evidence for how multiannual periodicities in ocean-atmosphere systems effect water resources globally (e.g., Kuss and Gurdak, 2011; Forootan, et al, 2018; Holman et al, 2011). Furthermore, instances of wide-scale recorded groundwater drought in the UK, since the 1960s, have been found to align with minima in this ~7-year cycle in groundwater level (Rust et al, 2019). This relationship is further shown in Rust et al (2021c), where a strong association between the NAOI and calculated wide-spread groundwater drought was demonstrated. These findings are consistent with Neves et al, 2019 who demonstrated links between multiannual behaviour in the NAO and recorded hydrological droughts in Portugal, as well as adding to the body of evidence for the NAO's more general influence of European water resource extremes (e.g., Kingston et al, 2015; Bonaccorso et al, 2015; Lee and Zhang, 2011). This ~7-year periodicity was found to represent a large portion of overall water resource behaviour in many of the water resource records assessed, effecting regional groundwater level anomalies by a median of up to 2m in the Chalk of the Thames and Chilterns (equating to approximately 0.71sd), and streamflow anomalies by up to 0.55sd in some regions of the UK (i.e., East Anglia and the South East), during the dry season (Rust et al, 2021c).

Rust et al (2021c) demonstrated that the frequency structure of water resources and droughts, and their relationships with multiannual NAO periodicities, can exhibit notable non-stationarity. Specifically, that the ~7-year periodicity detected in wide-scale water resources (i.e., Rust et al, 2019, 2021a) has only been dominant since the 1970s and has been weakening since approximately 2005. Given the established control of the NAO (and its periodicities) on European hydrometeorological variables (e.g., Rust et al, 2021b, Trigo et al, 2002, Leisch

and Wusch et al 2019), these findings have important implications for existing studies of water resource behaviour across Europe. For instance, they highlight the degree to which a study's time horizon selection (and the assumption of stationarity this produces) can bias the assessment of water resource behaviour. Often, time horizons are limited due to data availability, with many high-resolution datasets used in water resource research starting after the 1970s (Sun et al 2018; Dixon et al, 2013). These potential biases may be of greatest impact to studies that have assessed water resource trends or the frequency of hydrological droughts in Europe over recent decades (e.g., Oikonomou et al, 2020; Hisdal et al, 2001; Spinoni et al, 2015; González-Hidalgo et al, 2018). Furthermore, some existing hydroclimate teleconnection studies have assessed water resource behaviour predominantly over this period of relatively stationary frequency behaviour (e.g., Neves et al, 2019; Uvo et al, 2021), meaning generalised findings from such assessments may not be representative of future water resource behaviours. As such, this thesis further emphasises the need for longer hydrological records in order to minimise bias induced by assumptions of stationarity in hydrological studies (Mahmoudi et al, 2019; Wu et al, 2005). Finally, these findings also have important implications for existing water resource modelling systems, which will be discussed in section 7.4.1.

Non-stationarities between the NAOI and water resources, identified here, are consistent with Eade et al (2021), who demonstrated an increased autocorrelation in the NAOI since the 1960s, and furthermore with Iles and Hegerl (2017) who showed that similar behaviours in the NAOI had a notable effect on extratropical hydrometeorological variables between 1960s and 1990s. Furthermore, results presented in this thesis demonstrate that non-stationarities in the annual-scale relationship between the NAOI and European rainfall (demonstrated in Rust et al, 2021b and Vicente-Serrano and López-Moreno, 2008) have considerable influence on the multiannual periodicities of wide-scale water resources (Rust et al, 2021c).

Stronger ~7-year periodicities in wide-scale water resources from the 1970s are also partially coincident with the ongoing effects of climate change on water

resource behaviour, many of which have been noted since the late 1980s or early 1990s (e.g., Padron et al, 2020; Barker et al, 2019). However, it is currently unclear the extent to which the frequency structure of ocean-atmosphere systems in the north Atlantic region (such as the NAO) are affected by increasing global temperatures (Olsen et al, 2012). Given the importance of these periodicities in driving water resource behaviour, as shown in Rust et al (2019; 2021c) and others (e.g., Uvo et al, 2021; Liesch and Wunsch et al, 2019) and their relationship with systems such as the NAO, this represents a considerable uncertainty for the use of projected water resources in climate change scenarios, especially considering the comparable influence on water resources between multiannual NAO periodicities and climate change projections (as demonstrated in Rust et al, 2021c). This is discussed further in section 7.4.1.

### **7.3 Controls on multiannual signal propagation from the NAO to water resources**

The first part of the conceptual model for multiannual NAO control on water resources, proposed in Rust et al (2018), is concerned with the linkages between the NAO and meteorological processes (i.e., rainfall and PET), which are key drivers for long term water resource behaviours. Rust et al (2019 and 2021a) demonstrated significant ~7-year periodicities in catchment rainfall and negligible periodicities in catchment PET. This suggests that precipitation is a critical pathway for multiannual periodicity propagation between the NAO and water resources, which may be expected given the strong relationship between the NAOI and European rainfall demonstrated in existing research (e.g., West et al, 2019; Rust et al, 2021b; Trigo et al, 2002). Despite the paucity of multiannual periodicities detected here in catchment PET, existing hydroclimate research has shown correlations between PET in Europe and the NAOI (e.g., Criado-Aldeanueva et al, 2014). Rust et al (2021a) suggests two pathways for the NAO's control on UK meteorological processes; an atmospheric pathway (i.e., the westerly jet stream), facilitating the NAO's influence on annual-scale rainfall and PET; and an oceanic pathway (i.e., the Gulf Stream) responsible for propagating low-frequency periodicities from the NAO to rainfall. This explanation is consistent



with Chiacchio and Wild, (2010) who demonstrate an atmospheric pathway for the NAO's control on surface solar radiation, a key driver for PET.

The relationship between the NAO and UK rainfall was explored in a broader context in Rust et al (2021b), which showed notable non-stationarities in the sign and strength of the NAO's wintertime correlation with European precipitation. Furthermore, Rust et al (2021c) demonstrated, for the first time, the extent that this non-stationarity is propagated through to multiannual periodicities in water resource records. Vicente-Serrano and López-Moreno (2008) investigated this non-stationarity, at multidecadal scales, and associated phases of sign shift with an eastward shift of the NAO's southern pole, but highlighted that further research is required for this to fully explain this behaviour. Indeed, this phenomenon has received little to no attention in wider hydroclimate research to date, meaning there is no general consensus in existing literature of the mechanisms for this behaviour. However, it is worth reiterating that the NAO is conceptual representation of wider, complex atmospheric variability in the North Atlantic region (Deser et al, 2017) and as such only represents a portion of atmospheric variance. Therefore, there may be insufficient information captured either in the conceptual NAO, or the measured NAOI, to sufficiently explore this non-stationarity.

The second part of the conceptual model describes how multiannual signals in rainfall may be modulated by surface and subsurface hydrological processes. Rust et al (2021a) contributes new information showing that surface processes contribute minimal attenuation of ~7-year periodicities in rainfall, whereas subsurface pathways (such as unsaturated and groundwater flow) can attenuate ~7-year signals in winter rainfall through to the summer stream baseflow, where groundwater influence is dominant. Furthermore, a significant association was demonstrated between the strength of ~7-year periodicities in streamflow and the response times of groundwater pathways, with strongest signals found in catchments with response times similar to 7 years. These results are consistent with the mathematical model proposed by Towney (1995) for how periodic signals are expected to propagate through the saturated zone and provide the first

empirical evidence for this model in the UK. Similarly, results from groundwater level analyses (e.g., Rust et al (2019 and 2021c)), show that groundwater pathways with longer response times than 7 years (such as in Sandstone aquifers), exhibit the strongest ~7-year periodicities in groundwater level since they cannot propagate periodic behaviours through to discharge at the same rate as they are received in recharge (Towney 1995, Bakker and Nieber, 2009).

Rust et al (2021a) did not explicitly test unsaturated zone properties (such as thickness) as a control on multiannual periodicity propagation, due to a lack of a spatially distributed dataset for unsaturated zone characteristics in the UK. However, stream baseflow can be indicative of the influence of both unsaturated and saturated zone dynamics on streamflow (Bloomfield et al., 2009; Tashie et al, 2018). As such, findings from Rust et al (2021a) are consistent with existing studies into the effects of the unsaturated zone on periodicity propagation (e.g., Dickenson et al, 2014), showing that subsurface storage (e.g., unsaturated zone thickness) is an important controlling variable for multiannual periodicity propagation from rainfall to stream baseflow. As such, there may be benefit in assessing the role of unsaturated zone characteristics on water resource sensitivity to multiannual NAO periodicity, in addition to saturated zone characteristics, which has not been conducted here.

## **7.4 Implications of multiannual periodicities in water resources for forecasting**

### **7.4.1 Implications of findings for existing water resource forecasting systems**

As discussed in Rust et al (2021b and 2021c), existing water resource forecasting systems in Europe (such as for drought warning) are often calibrated to water resource records collected after the 1970s, due to the limited availability of high-resolution data prior to this time (Dixon et al, 2013). While Rust et al (2021c) focused on data from the UK, the influence of the NAO on hydrometeorological

variables across Europe has been established in existing research, including the effect of multiannual periodicities (e.g., Liesch and Wunsch, 2019) and non-stationaries (e.g., Rust et al, 2021b). As such, the considerable degree to which water resources have been influenced by non-stationary multiannual NAO periodicities (demonstrated in Rust et al, 2019 and 2021c) has important implications for existing water resource forecasting systems not only in the UK, but may also effect similar systems across Europe. For instance, Rust et al (2021c) demonstrates that multiannual periodicities in water resources can abruptly change strength or frequency over a relatively short period (approximately 5 years), suggesting the frequency structure of water resource variables may be notably different in future scenarios. As such existing water resource forecasting systems, which may be used for planning or to inform drought preparation, may misrepresent future water resource metrics, such as the likelihood of drought, given these non-stationary frequency dynamics. Salas (2017) highlights, in general, the need for a greater understanding of hydrological non-stationarities if forecasting systems are to make skilful estimates of future water resource extremes. Here, we demonstrate a new mode of non-stationarity that further highlights this importance and may provide an *a priori* understanding for new assessments of water resource behaviour.

Existing water resource forecasting systems may also be impacted by the broader findings presented here. Eade et al (2021) showed that GCM projections poorly replicate low frequency behaviour that has been historically detected in the NAOI. Findings from the papers presented here demonstrate that multiannual periodicities in the NAO can have a controlling influence on the behaviours of water resources and their extremes. This influence is shown to affect water resource anomalies by up to 0.71sd in some regions, and a mean of 0.31sd across all groundwater level and streamflow records assessed. Given this, and the findings of Eade et al (2021), GCMs may be poorly suited for use in projecting water resource behaviour since they do not recreate these important modes of multiannual periodicity. Furthermore, these estimates of multiannual influence on water resource anomalies provide an indication as to the amount of behaviour information that may not be captured when using current GCM projections. These

anomalies are also shown to be comparable to the estimated impacts of climate change on water resource behaviour, and so further emphasise the uncertainties of existing water resource projections (e.g., Bisselink et al, 2020 or HR Wallingford, 2020). These findings highlight that further work is required to develop appropriate projections of water resources in climate change scenarios, that better replicate the dynamics of multiannual periodic teleconnections in the North Atlantic region.

#### **7.4.2 Implications of findings for the application of multiannual NAO periodicities in new forecasting systems**

The findings presented here demonstrate two modes of non-stationarity (i.e., of periodicities within the NAOI, and of the relationship between the NAOI and European rainfall at an annual scale), for which there is limited mechanistic understanding in existing hydroclimate research. As such, these modes pose considerable challenges to the application of multiannual NAO periodicities for estimating likely future water resource behaviour. For instance, there is inconclusive evidence presented here to suggest whether multiannual periodicities in the NAO are externally forced (and therefore theoretically predictable) or are emergent behaviours from internal noise (and therefore not predictable). The NAO itself is an intrinsic part of atmospheric variability in the North Atlantic and as such requires no external forcing (Deser et al, 2017). Conversely, the NAO can also be influenced by other atmospheric or oceanic processes such as QBO and ENSO (Feng et al 2021; Zhang et al, 2019). The non-stationary behaviours detected in Rust et al (2021c) do not rule out these periodicities as emergent properties of stochastic processes in North Atlantic atmospheric processes. Therefore, this represents an ongoing knowledge gap that may require collaborative effort between hydrology, climate, and atmospheric disciplines to address. Sufficient predictability of multiannual periodicities in the NAO will need to be demonstrated by future research in order to justify the use of these behaviours as feasible for water resource forecasting applications. Recent research has demonstrated improved predictability of multiannual behaviour in the NAO using external drivers such as solar activity (Drews et al,

2021) or other teleconnection systems (Pan et al, 2019), suggesting that further improvements may be possible in the future or with further research.

An improved understanding of multiannual periodicities in the North Atlantic region may also explain the second mode of non-stationarity, i.e., in the sign and strength of the correlation between the NAOI and rainfall across Europe (Rust et al, 2021b). Vicente-Serrano and Lopez-Moreno (2008) suggest that this non-stationarity may be related to an eastward shift of the NAO's southern pole, but highlight that further work is required to understand the mechanisms behind these decadal non-stationarities, and that caution should be taken when applying the correlation between the NAOI and European rainfall in forecasting applications.

Despite these challenges, it remains evident that the NAO influences multiannual behaviour in water resources, even if the frequency and strength of these behaviours may change or be unpredictable at present. As such there may still be some utility to an *a priori* understanding of these behaviours in water resource management. For instance, understanding the current, or near-future, frequency structure of water resource extremes may help to better manage water usage between different resources. In the case of the UK, existing water resource management policy requires water companies to develop a Water Resource Management Plan every 5 years. These describe how a water company plans to balance their water supply and demand over the coming 25-year period and as such typically involve the projection of water resource to understand future availability (DEFRA, 2017). Furthermore, Drought Plans are also required to describe how water companies plan to prepare for, and respond to, drought conditions (DEFRA, 2021). Existing methodologies used by water companies to estimate future water resource behaviour are often time-independent or probabilistic, which may not be easily adapted to include multiannual periodic fluctuations from wetter and dryer periods. This is further confounded by the detected non-stationarities of these multiannual periodicities. However Rust et al (2021b) showed these behaviours may remain stable at a sub-decadal timescale, meaning there may still be useful information in these modes of behaviours that can be assimilated into water company's 5-year plans. For instance, an

awareness of the current phase of multiannual water resource behaviour (i.e., whether a surplus or deficit phase) may be useful in priming a water resource management plan to expect more, or less, of certain extremes. Despite this, the application of multiannual NAO periodicities to estimate water resource quantities at a seasonal to multi-year scale is currently prohibited by the two modes of non-stationarity demonstrated in the papers of this thesis (e.g., Rust et al, 2021b and 2021c).

## 8 CHAPTER 8: CONCLUSIONS

The aim of this PhD thesis was to assess the feasibility of a relationship between the NAO and water resource variables, at multiannual periodicities, for indicating water resource behaviour (including extremes), at seasonal to multiannual timescales. This has been achieved through four published manuscripts (and one submitted) in high-impact, peer reviewed journals, and an integrated discussion. Research presented here provides new contributions to the discipline of hydroclimate teleconnections, and to the understanding of water resource behaviour over recent decades. The following key findings have been made:

1. A dominant periodicity, of approximately 7 years, has been demonstrated to be present in UK rainfall, groundwater and streamflow records, with associations to instances of wide-spread groundwater drought over the past 60 years. This mode of behaviour can be comparable to the strength of seasonality and can have a defining influence on water resource behaviour.
2. The propagation of ~7-year periodicities from rainfall to water resources is controlled, in part, by subsurface pathway length (or pathway response time) within a catchment. Furthermore, pathways with response times similar in length to 7 years (such as some groundwater pathways) propagate this signal with minimal dampening, meaning some resources are more sensitive to 7-year signals in rainfall than others. Sensitivity to these multiannual periodicities may now be screened using these catchment characteristics.
3. The sign and strength of the NAO's control on rainfall (and therefore water resources) is temporally non-stationary across the UK and Europe, and there is limited understanding of the mechanisms that drive this. As such there is current uncertainty in how the NAO may be used to indicate future water resources, since the nature of the relationship is likely to change.
4. The ~7-year periodicity detected in UK groundwater and streamflow shares a significant, but non-stationary, relationship with the NAO. This 7-year periodicity also extends to the frequency of groundwater droughts,

and streamflow (but to a lesser degree). This 7-year periodicity-relationship between the NAOI and water resources has been relatively stable from the 1970s to present and has been weakening since 2005.

The findings from the four empirical papers presented here have major implications for the study of hydroclimate teleconnections in the North Atlantic region, as they demonstrate that the multiannual relationship between the NAO and water resources may not be predictable, given current atmospheric or climatological understanding. Furthermore, findings presented here demonstrate two ways in which these multiannual periodicities may affect the use of existing water resource forecasting systems. The first considers whether existing water resource datasets covering the period between the 1970s and 2020 are representative, since they do not exhibit the non-stationary frequency structure (and its abrupt shifts) that is demonstrated in longer datasets. This calls into question the applicability of water resource forecasting systems that have been calibrated using data collected since the 1970s, when these non-stationary periodicities became dominant. The second is regarding the appropriateness of existing water resource projections using GCMs, as existing research has demonstrated their poor skill in replicating multiannual behaviours in systems such as the NAO. The findings here demonstrate the importance of these multiannual periodicities in defining wide-scale water resource behaviour (and extremes), and therefore the potential inaccuracy of water resource projections using current GCMs.

Finally, while we demonstrate considerable challenges to the use of multiannual NAO periodicities as indicators for water resource forecasting, we also identify ways in which these behaviours may be used alongside existing policy for water resource planning, and the preparation for water resource extremes by allowing water managers to better understand which of their resources may be more sensitive to these behaviours, and the degree to which (and the timescales over which) these resource may be modulated by multiannual NAO periodicities.



## 9 CHAPTER 9: FUTURE WORK

Several knowledge gaps or areas for further work have been identified throughout this thesis. These include further work that is required in order to progress the application of multiannual NAO periodicities as indicators for water resource behaviour, as well as other work that may be useful in improving understanding wide-scale water resource variability. These are:

1. The driving mechanisms for a non-stationary sign and strength of the correlation between the winter NAOI and rainfall. Findings in this thesis have demonstrated that this non-stationarity has a notable affect at multiannual periodicities, meaning the direction or magnitude of water resource response to multiannual NAO periodicities cannot currently be predicted. This may require more collaborative research between atmospheric and climatological sciences.
2. The origin of multiannual periodicities in the NAO, and their non-stationarity. At present it is unclear whether multiannual periodicities in the NAO are emergent from internal variances or the result of an external forcing. In understanding this, it is likely that non-stationarities of the multiannual connection with water resources (as I have described in this thesis) will be elucidated.
3. The role of the unsaturated zone in modulating multiannual signal propagation from rainfall to water resources. While the controls of broad catchment characteristics on multiannual periodicity sensitivity have been assessed in this thesis, further detail on the role of the unsaturated zone in modulating these controls may aid the development of relationships between water resources and multiannual NAO periodicities for forecasting purposes. While this has been addressed to a degree in this thesis, the lack of a distributed dataset of unsaturated zone properties has meant that a broad-scale assessment of these processes has yet to be undertaken.
4. This thesis has focused on the role of the NAO, but the research presented here has highlighted that other ocean-atmosphere teleconnection systems

may also have an important influence on UK water resources that may modulate the NAO's control. For instance, the East Atlantic or Scandinavia pattern. While these modes of atmospheric variability and their influence on water resources may be better understood by addressing knowledge gap 2, an investigation into their unique influences may also prove beneficial in developing improved preparedness for water resource extremes.

5. Interactions between increasing global temperatures (i.e., climate change) and multiannual periodicities in the NAO (or other ocean/atmosphere systems) is not currently understood for the North Atlantic region. This is also reflected in the lack of skill, currently exhibited by GCMs, in projecting multiannual atmospheric variability the north Atlantic oscillation. Any application of multiannual NAO periodicities for improving preparedness of water resource extremes will need to include the effects of an increasing global temperature of hydroclimatological processes.

As highlighted above, a cross-discipline effort between hydrologists, meteorologists and climatologist may be required to answer many of these knowledge gaps, given the complex interactions of oscillatory ocean-atmosphere systems on water resources demonstrated in this thesis. Given the challenges facing water resource managers over coming years (e.g., from climate change and population pressures), having more approaches for improving preparedness for natural hazards such as water resource drought will become increasingly important. While current understanding of how multiannual NAO periodicities affect water resources may fall short of what is necessary for predictive applications, some improvement to water resource management is still possible through an *a priori* understanding of the importance of multiannual behaviours on water resources. This information may aid water managers understand likely periods of wetter or dryer conditions in the near future, or to better explain historical water resource behaviour in order to improve existing forecasting approaches.

## 10 CHAPTER 10: REFERENCE LIST

Acreman, M. C. and Dunbar, M. J.: Defining environmental river flow requirements – a review, *Hydrol. Earth Syst. Sci.*, 8, 861–876, 2004.

Alexander, M.A., Blade, I., Newman, M., Lanzante, J.R., Lau, N.C., Scott, J.D. The atmospheric bridge: the influence of ENSO teleconnections on air-sea interaction over the global oceans. *J. Clim.* 15, 16, 2205–2231. 2002.

Alexander, L.V., Tett, S.F.B., Jonsson, T. Recent observed changes in severe storms over the United Kingdom and Iceland. *Geophys. Res. Lett.* 32, 13, 1–4. 2005.

Allen, D.J., Brewerton, L.J., Coleby, L.M., Gibbs, B.R., Lewis, M.A., MacDonald, A.M., Wagstaff, S.J., Williams, A.T.: The physical properties of major aquifers in England and Wales. British Geological Survey, 333pp, BGS Report WD/97/034, 1997

Allen, M.R., Smith, L.A.: Monte Carlo SSA: Detecting irregular oscillations in the Presence of Colored Noise. *Journal of Climate*, 9, 3373–3404, 1996.

Allen, R. J. and Anderson, R. G.: 21st century California drought risk linked to model fidelity of the El Niño teleconnection, *npj Climate and Atmospheric Science*, 1, 1–14, 2018.

Asoka, A., Gleeson, T., Wada, Y., Mishra, V. Relative contribution of monsoon precipitation and pumping to changes in groundwater storage in India. *Nat. Geosci.* 10, 109–117. 2017.

Ataie-Ashtiani, B., Volker, R.E., Lockington, D.A. Numerical and experimental study of seepage in unconfined aquifers with a periodic boundary condition. *J. Hydrol.* 222, 1, 4, 165–184. 1999.

Athanasiadis, P J., Yeager, S., Kwon, Y., Bellucci, A., Smith, D. W., and Tibaldi, S. Decadal Predictability of North Atlantic Blocking and the NAO. *Npj Climate and Atmospheric Science*, 3, 20. 2020.

Bakke, J., Lie, Ø., Dahl, S.O., Nesje, A., Bjune, A.E. Strength and spatial patterns of the Holocene wintertime westerlies in the NE Atlantic region. *Glob. Planet. Chang.* 60, 2, 28–41. 2008.

Bakker, M., Nieber, J.L. Damping of sinusoidal surface flux fluctuations with soil depth. *Vadose Zone J.* 8, 1, 119. 2009.

Baram, S., Kurtzman, D., Dahan, O. Water percolation through a clayey vadose zone. *J. Hydrol.* 424–425, 165–171. 2012.

Barker, L. J., Hannaford, J., Chiverton, A., and Svensson, C.: From meteorological to hydrological drought using standardised indicators, *Hydrol. Earth Syst. Sci.*, 20, 2483–2505, 2016.

Barros, A. P. and Bowden, G. J.: Toward long-lead operational forecasts of drought: An experimental study in the Murray-Darling River Basin, *J. Hydrol.*, 357, 349–367, 2008.

Barnston, A.G., Livezey, R.E. Classification, seasonality and persistence of low frequency atmospheric circulation patterns. *Mon. Weather Rev.* 115, 6, 1083–1126. 1987.

Becker, R. A.: *Water Use and Conservation in Manufacturing: Evidence from U.S. Microdata*, US Census Bureau Center for Economic Studies, 2016.

Bergstrom, D. M., Wienecke, B. C., van den Hoff, J., Hughes, L., Lindenmayer, D. B., Ainsworth, T. D., Baker, C. M., Bland, L., Bowman, D. M. J. S., Brooks, S. T., Canadell, J. G., Constable, A. J., Dafforn, K. A., Depledge, M. H., Dickson, C. R., Duke, N. C., Helmstedt, K. J., Holz, A., Johnson, C. R., McGeoch, M. A., Melbourne-Thomas, J., Morgain, R., Nicholson, E., Prober, S. M., Raymond, B., Ritchie, E. G., Robinson, S. A., Ruthrof, K. X., Setterfield, S. A., Sgrò, C. M., Stark, J. S., Travers, T., Trebilco, R., Ward, D. F. L., Wardle, G. M., Williams, K. J., Zylstra, P. J., and Shaw, J. D.: Combating ecosystem collapse from the tropics to the Antarctic, *Glob. Chang. Biol.*, 27, 1692–1703, 2021.

Beverly, C. and Hocking, M.: Predicting Groundwater Response Times and Catchment Impacts from Land Use Change, *Australasian Journal of Water Resources*, 16, 29–47, 2012.

Bhatt, Diva, and R. K. Mall. "Surface Water Resources, Climate Change and Simulation Modeling." *Aquatic Procedia*, 4, 730–38. 2015.

Bisselink B., Bernhard J., Gelati E., Adamovic M., Guenther S., Mentaschi L., Feyen L., and de Roo, A. Climate change and Europe's water resources. European Commission. 2020.

Bloomfield, J.P., Marchant, B.P. Analysis of groundwater drought building on the standardised precipitation index approach. *Hydrol. Earth Syst. Sci.* 17, 12, 4769–4787. 2013.

Bloomfield, J.P.: The role of diagenesis in the hydrogeological stratification of carbonate aquifers: An example from the Chalk at Fair Cross, Berkshire, UK, *Hydrol. Earth Sys. Sci.*, 1, 19-33, 1997.

Bloomfield, J.P., Allen, D.J., Griffiths, K.J. Examining geological controls on baseflow index (BFI) using regression analysis: an illustration from the Thames Basin, UK. *J. Hydrol.* 373, 1–2, 164–176. 2009.

Bloomfield, J.P., Gaus, I., Wade, S.D. A method for investigating the potential impacts of climate-change scenarios on annual minimum groundwater levels. *Water Environ. J.* 17, 2, 86–91. 2003.

Bloomfield, J.P., Marchant, B.J., and McKenzie, A.A.:2019. Changes in groundwater drought associated with anthropogenic warming, *Hydrol. Earth Syst. Sci.*, 23, 1393–1408, 2019.

Blöschl, G., Bierkens, M. F. P., Chambel, A., Cudennec, C., Destouni, G., Fiori, A., Kirchner, J. W., McDonnell, J. J., Savenije, H. H. G., Sivapalan, M., Stumpp, C., Toth, E., Volpi, E., Carr, G., Lupton, C., Salinas, J., Széles, B., Viglione, A., Aksoy, H., Allen, S. T., Amin, A., Andréassian, V., Arheimer, B., Aryal, S. K., Baker, V., Bardsley, E., Barendrecht, M. H., Bartosova, A., Batelaan, O.,

Berghuijs, W. R., Beven, K., Blume, T., Bogaard, T., Borges de Amorim, P., Böttcher, M. E., Boulet, G., Breinl, K., Brilly, M., Brocca, L., Buytaert, W., Castellarin, A., Castelletti, A., Chen, X., Chen, Y., Chen, Y., Chiffard, P., Claps, P., Clark, M. P., Collins, A. L., Croke, B., Dathe, A., David, P. C., de Barros, F. P. J., de Rooij, G., Di Baldassarre, G., Driscoll, J. M., Duethmann, D., Dwivedi, R., Eris, E., Farmer, W. H., Feiccabrino, J., Ferguson, G., Ferrari, E., Ferraris, S., Fersch, B., Finger, D., Foglia, L., Fowler, K., Gartsman, B., Gascoin, S., Gaume, E., Gelfan, A., Geris, J., Gharari, S., Gleeson, T., Glendell, M., Gonzalez Bevacqua, A., González-Dugo, M. P., Grimaldi, S., Gupta, A. B., Guse, B., Han, D., Hannah, D., Harpold, A., Haun, S., Heal, K., Helfricht, K., Herrnegger, M., Hipsey, M., Hlaváčiková, H., Hohmann, C., Holko, L., Hopkinson, C., Hrachowitz, M., Illangasekare, T. H., Inam, A., Innocente, C., Istanbuluoglu, E., Jarihani, B., et al.: Twenty-three unsolved problems in hydrology (UPH) – a community perspective, *Hydrol. Sci. J.*, 64, 1141–1158, 2019. Bonaccorso, B., Cancelliere, A., and Rossi, G.: Probabilistic forecasting of drought class transitions in Sicily (Italy) using Standardized Precipitation Index and North Atlantic Oscillation Index, *J. Hydrol.*, 526, 136–150, 2015

Bozyurt, O., Özdemir, M.A. The relations between North Atlantic Oscillation and minimum temperature in Turkey. *Procedia Soc. Behav. Sci.* 120, 532–537. 2014.

Bracken, L. J., Wainwright, J., Ali, G. A., Tetzlaff, D., Smith, M. W., Reaney, S. M., and Roy, A. G.: Concepts of hydrological connectivity: Research approaches, Pathways and future agendas, *Earth-Sci. Rev.*, 119, 17–34, 2013.

Brady, A., Faraway, J., and Prosdocimi, I.: Attribution of long-term changes in peak river flows in Great Britain, *Hydrol. Sci. J.*, 64, 1159–1170, 2019.

Brandimarte, L., Di Baldassarre, G., Bruni, G., D'Odorico, P., Montanari, A., Relation between the North-Atlantic Oscillation and hydroclimatic conditions in Mediterranean areas. *Water Resour. Manag.* 25, 5, 1269–1279. 2010.

Bricker, S. Properties of the chalk aquifer in the Thames Basin. [ONLINE]. Available \_\_\_\_\_ at:

<http://www.bgs.ac.uk/research/groundwater/waterResources/thames/chalk.html>. [Accessed: 8th August 2017]. 2017.

Brown, S. J.: The drivers of variability in UK extreme rainfall, *Int. J. Climatol.*, 38, 119–130, 2018.

Bru, L. and McDermott, F.: Impacts of the EA and SCA Patterns on the European Twentieth Century NAO-Winter-Climate Relationships, *Q. J. Roy. Meteor. Soc.*, 140, 354–63, 2014.

Bryan, K., Ward, S., Barr, S. and Butler, D. “Coping with Drought: Perceptions, Intentions and Decision-Stages of South West England Households.” *Water Resources Management* 33, 1185–1202. 2019.

Burt, T. P., and Howden, N. J. K. “North Atlantic Oscillation Amplifies Orographic Precipitation and River Flow in Upland Britain.” *Water Resources Research* 49. 3504-3515. 2013.

Calado, G. G., Valverde, M. C., and Baigorria, G. A.: Use of Teleconnection Indices for Water Management in the Cantareira System - São Paulo – Brazil, 6, 413–431, 2019.

Cammalleri, C., Naumann, G., Mentaschi, L., Bisselink, B., Gelati, E., De Roo, A., and Feyen, L.: Diverging hydrological drought traits over Europe with global warming, *Hydrol. Earth Syst. Sci.*, 24, 5919–5935, 2020.

Cao, G., Scanlon, B.R., Han, D., Zheng, C. Impacts of thickening unsaturated zone on groundwater recharge in the North China Plain. *J. Hydrol.* 537, 260–270. 2016.

Carr, E. J. and Simpson, M. J.: Accurate and efficient calculation of response times for groundwater flow, *J. Hydrol.*, 558, 470–481, 2018.

Cassou, C., Terray, L., Hurrell, J.W., Deser, C. North Atlantic winter climate regimes: Spatial asymmetry, stationarity with time, and oceanic forcing. *J. Clim.* 17, 5, 1055–1068. 2003.

Chaudhuri, A.H., Gangopadhyay, A., Bisagni, J.J. Response of the Gulf Stream transport to characteristic high and low phases of the North Atlantic Oscillation. *Ocean Model* 39, 3–4, 220–232. 2011.

Chiacchio, M. and Wild, M.: Influence of NAO and clouds on long-term seasonal variations of surface solar radiation in Europe, *J. Geophys. Res.*, 115, 2010.

Chiang, F., Mazdidasni, O., and AghaKouchak, A.: Evidence of anthropogenic impacts on global drought frequency, duration, and intensity, *Nat. Commun.*, 12, 2754, 2021.

Chiverton, A., Hannaford, J., Holman, I. P., Corstanje, R., Prudhomme, C., Hess, T. M., and Bloomfield, J. P.: Using variograms to detect and attribute hydrological change, *Hydrol. Earth Syst. Sci.*, 19, 2395–2408, 2015.

Chang, F., Shenglian, G. *Advances in Hydrological Forecasting and Water Resource Management*. *Water*. 16, 6, 1819. 2020.

Chiew, F. H. S. and McMahon, T. A.: Global ENSO-streamflow teleconnection, streamflow forecasting and interannual variability, *Hydrol. Sci. J.*, 47, 505–522, 2002.

Chun, K. P., Wheeler, H. S., and Onof, C. J.: Streamflow estimation for six UK catchments under future climate scenarios, *Hydrol. Res.*, 40, 96–112, 2009.

Climate Prediction Centre. Arctic Oscillation (AO). [ONLINE] Available at: [http://www.cpc.ncep.noaa.gov/products/precip/CWlink/daily\\_ao\\_index/ao.shtml](http://www.cpc.ncep.noaa.gov/products/precip/CWlink/daily_ao_index/ao.shtml) [Accessed 1st April 2016]. 2005a.

Climate Prediction Centre. Scandinavian Pattern (SCAND). [ONLINE] Available at: <http://www.cpc.ncep.noaa.gov/data/teledoc/scand.shtml> [Accessed 1st April 2016]. 2005b.

Coleman, J. S. M. and Budikova, D.: Eastern U.S. summer streamflow during extreme phases of the North Atlantic oscillation, *J. Geophys. Res.*, 118, 4181–4193, 2013.



Cook, B.I., J.S. Mankin, and K.J. Anchukaitis. Climate change and drought: From past to future. *Curr. Clim. Change Rep.*, 4, 2, 164-170, 2018

Cook, P.G., Jolly, I.D., Walker, G.R., Robinson, N.I. From drainage to recharge to discharge: some timelags in subsurface hydrology. *Dev. Water Sci.* 50 (C), 319–326. 2003.

Cooper, M. Climate–river flow relationships across montane and lowland environments in northern Europe. *Hydrol. Process.* 985–996. 2009.

Criado-Aldeanueva, F., Soto-Navarro, F. J., and García-Lafuente, J.: Climatic Indices Influencing the Long-Term Variability of Mediterranean Heat and Water Fluxes: The North Atlantic and Mediterranean Oscillations, *Atmosphere-Ocean*, 52, 103–114, 2014

Crosbie, R.S., Binning, P., Kalma, J.D. A time series approach to inferring groundwater recharge using the water table fluctuation method. *Water Resour. Res.* 41, 1, 1–9. 2005.

Crossman, J., Futter, M. N., Whitehead, P. G., Stainsby, E., Baulch, H. M., Jin, L., Oni, S. K., Wilby, R. L., and Dillon, P. J.: Flow pathways and nutrient transport mechanisms drive hydrochemical sensitivity to climate change across catchments with different geology and topography, *Hydrol. Earth Syst. Sci.*, 18, 5125–5148, 2014.

Cullen, H.M., DeMenocal, P.B. North Atlantic influence on Tigris-Euphrates streamflow. *Int. J. Climatol.* 863, 853–863. 2000.

Currell, M., Gleeson, T., Dahlhaus, P. A new assessment framework for transience in hydrogeological systems. *Groundwater* 54, 1, 4–14,. 2014.

Cuthbert, M.O., Gleeson, T., Moosdorf, N., Befus, K.M., Schneider, A., Hartmann, J. and Lehner, B.: Global patterns and dynamics of climate–groundwater interactions. *Nature Climate Change*, 9, 137–141, 2019.

Cuthbert, M.O., Tindimugaya, C. The importance of preferential flow in controlling recharge in tropical Africa and implications for modelling the impact of climate change on groundwater resources. *J. Water Clim. Chang.* 1, 4, 234–245. 2010.

Cuthbert, M. O., Gleeson, T., Reynolds, S. C., Bennett, M. R., Newton, A. C., McCormack, C. J., and Ashley, G. M.: Modelling the role of groundwater hydro-refugia in East African hominin evolution and dispersal, *Nat. Commun.*, 8, 15696, 2017.

Cuthbert, M.O., Mackay, R., Tellam, J.H., Barker, R.D. The use of electrical resistivity tomography in deriving local-scale models of recharge through superficial deposits. *Q. J. Eng. Geol. Hydrogeol.* 42, 2, 199–209. 2009.

Cuthbert, M.O., Mackay, R., Tellam, J.H., Thatcher, K.E. Combining unsaturated and saturated hydraulic observations to understand and estimate groundwater recharge through glacial till. *J. Hydrol.* 391, 3–4, 263–276. 2010.

Cuthbert, M.O., Acworth, R., Anderson, M., Larsen, J., McCallum, A., Rau, G., Tallem, J. Understanding and quantifying focused, indirect groundwater recharge fluctuations from ephemeral streams using water table fluctuations. *Water Resour. Res.* 613–615. 2016.

Dams, J., Salvadore, E., Van Daele, T., Ntegeka, V., Willems, P., and Batelaan, O.: Spatio-temporal impact of climate change on the groundwater system, *Hydrol. Earth Syst. Sci.*, 16, 1517–1531, 2012.

Davis, X.J., Weller, R.A., Bigorre, S., Plueddemann, A.J. Local oceanic response to atmospheric forcing in the Gulf Stream region. *Deep-Sea Res. II Top. Stud. Oceanogr.* 91, 71–83. 2013.

Dawson, A., Elliott, L., Noone, S., Hickey, K., Holt, T., Wadhams, P., and Foster, I.: Historical storminess and climate “see-saws” in the North Atlantic region, *Mar. Geol.*, 210, 247–259, 2004.

DeFlorio, M. J., Pierce, D. W., Cayan, D. R., and Miller, A. J.: Western US Extreme Precipitation Events and Their Relation to ENSO and PDO in CCSM4, *J. Climate*, 26, 4231–4243, 2013.

Deloitte LLP: Water trading - scope, benefits and options - Final Report. Deloitte LLP, 117 pp, 2015.

Delworth, T., Zeng, F. The impact of the North Atlantic Oscillation on climate through its influence on the Atlantic meridional overturning circulation. *J. Clim.* 2, 1447–1462. 2016.

Department for Farming and Rural Affairs (DEFRA). Policy Paper: Water resources planning: how water companies ensure a secure supply of water for homes and businesses. <https://www.gov.uk/government/publications/water-resources-planning-managing-supply-and-demand/water-resources-planning-how-water-companies-ensure-a-secure-supply-of-water-for-homes-and-businesses>. [Accessed 21st Oct 2021]. 2017.

Department for Farming and Rural Affairs (DEFRA). Policy Paper: Drought: how water companies plan for dry weather and drought. <https://www.gov.uk/government/publications/drought-managing-water-supply/drought-how-water-companies-plan-for-dry-weather-and-drought>. [Accessed 21st Oct 2021]. 2021.

Demirel, M. C., Booij, M. J., and Hoekstra, A. Y.: Identification of appropriate lags and temporal resolutions for low flow indicators in the River Rhine to forecast low flows with different lead times, *Hydrol. Process.*, 27, 2742–2758, 2013.

Deser, C., Hurrell, J. W., and Phillips, A. S.: The role of the North Atlantic Oscillation in European climate projections, *Clim. Dyn.*, 49, 3141–3157, 2017.

Deser, C. On the teleconnectivity of the Arctic Oscillation. *Geophys. Res. Lett.* 27, 779–782. 2000.

De Vita, P., Allocca, V., Manna, F., and Fabbrocino, S.: Coupled decadal variability of the North Atlantic Oscillation, regional rainfall and karst spring

discharges in the Campania region (southern Italy), *Hydrol. Earth Syst. Sci.*, 16, 1389–1399, 2012.

Dickinson, J.E. Inferring time-varying recharge from inverse analysis of long-term water levels. *Water Resour. Res.* 40, 7, 1–15. 2004.

Dickinson, J.E., Ferré, T.P.A., Bakker, M., Crompton, B. A screening tool for delineating subregions of steady recharge within groundwater models. *Vadose Zone J.* 13, 6. 2014.

Dickson, R.R., Osborn, T.J., Hurrell, J.W., Meinke, J., Blindheil, J., Adlandsvik, B., Vinje, T., Alekseev, G.V., Maslowski, W., Meincke, J., Blindheim, J. The Arctic Ocean response to the North Atlantic Oscillation. *J. Clim.* 13, 15, 2671–2696. 1999.

Dickson, R.R., Osborn, T.J., Hurrell, J.W., Meinke, J., Blindheil, J., Adlandsvik, B., Vinje, T., Alekseev, G.V., Maslowski, W., Meincke, J., Blindheim, J.,. The Arctic Ocean response to the North Atlantic Oscillation. *J. Clim.* 13, 15, 2671–2696. 2000.

Di Domenico, A., Laguardia, G., Margiotta, M.R. Investigating the propagation of droughts in the water cycle at the catchment scale. In: *International Workshop Advances in Statistical Hydrology*, 1–10, 2010.

Dixon, H., Hannaford, J., and Fry, M. J.: The effective management of national hydrometric data: experiences from the United Kingdom, *Hydrol. Sci. J./J. Sci. Hydrol.*, 58, 1383–1399, 2013.

Drinkwater, K.F., Miles, M., Medhaug, I., Ottera, O.H., Kristiansen, T., Sundby, S., Gao, Y. The Atlantic Multidecadal Oscillation: its manifestations and impacts with special emphasis on the Atlantic region north of 60°N. *J. Mar. Syst.* 133, 117–130. 2014.

Drews, A., Huo, W., Matthes, K., Kodera, K., and Kruschke, T.: The Sun's role for decadal climate predictability in the North Atlantic, 2021.

Dunstone, N., Smith, D., Scaife, A., Hermanson, L., Eade, R., Robinson, N., Andrews, M., and Knight, J.: Skilful predictions of the winter North Atlantic Oscillation one year ahead, *Nat. Geosci.*, 9, 809, 2016.

Eltahir, E.A.B., Yeh, P.J.F. On the asymmetric response of aquifer water level to floods and droughts in Illinois. *Water Resour. Res.* 35, 4, 1199–1217. 1999.

Environment Agency, *Managing Water Abstraction*. Environment Agency, Bristol Available at: <https://www.gov.uk/government/publications/managing-waterabstraction>. [Accessed: 8th August 2017]. 2013.

Estrela, T., Pérez-Martin, M., and Vargas. E. “Impacts of Climate Change on Water Resources in Spain.” *Hydrological Sciences Journal*, 57, 1154–1167. 2012.

Eum, H.-I., Gupta, A., and Dibike, Y.: Effects of univariate and multivariate statistical downscaling methods on climatic and hydrologic indicators for Alberta, Canada, *J. Hydrol.*, 588, 125065, 2020.

Ezer, T. Detecting changes in the transport of the Gulf Stream and the Atlantic overturning circulation from coastal sea level data: the extreme decline in 2009–2010 and estimated variations for 1935–2012. *Glob. Planet. Chang.* 129, 23–36. 2015.

Fan, Y., Li, H., Miguez-Macho, G. Global Patterns of Groundwater Table Depth. *Science* 339, 6122, 940–943. 2013.

Faust, J.C., Fabian, K., Milzer, G., Giraudeau, J. and Knies, J.: Norwegian fjord sediments reveal NAO related winter temperature and precipitation changes of the past 2800 years. *Earth and Planetary Science Letters*, 435, 84–93, 2016.

Ferguson, I.M., Maxwell, R.M. Role of groundwater in watershed response and land surface feedbacks under climate change. *Water Resour. Res.* 46, 8, 1–15. 2010.

Feng, P.-N., Lin, H., Derome, J., and Merlis, T. M.: Forecast Skill of the NAO in the Subseasonal-to-Seasonal Prediction Models, *J. Clim.*, 34, 4757–4769, 2021.

Feser, F., Barcikowska, M., Krueger, O., Schenk, F., Weisse, R., Xia, L. Storminess over the North Atlantic and northwestern Europe—a review. *Q. J. R. Meteorol. Soc.* 141, 687, 350–382. 2015.

Feyen L., Ciscar J.C., Gosling S., Ibarreta D., Soria A. (eds). Climate change impacts and adaptation in Europe: JRC PESETA IV final report. European Commission. 2020.

Folland, C.K., Hannaford, J., Bloomfield, J.P., Kendon, M., Svensson, C., Marchant, B.P., Prior, J., Wallace, E. Multi-annual droughts in the English Lowlands: a review of their characteristics and climate drivers in the winter half-year. *Hydrol. Earth Syst. Sci.* 19, 5, 2353–2375. 2015.

Forootan, E., Khaki, M., Schumacher, M., Wulfmeyer, V., Mehrnegar, N., van Dijk, A.I.J.M., Brocca, L., Farzaneh, S., Akinluyi, F., Ramillien, G., Shum, C.K., Awange, J. and Mostafaie, A.: Understanding the global hydrological droughts of 2003–2016 and their relationships with teleconnections. *Science of the Total Environment*, 650, 2587-260, 2018.

Forzieri, G., Bianchi, A., Silva, F. B. E., Marin Herrera, M. A., Leblois, A., Lavalley, C., Aerts, J. C. J. H., and Feyen, L.: Escalating impacts of climate extremes on critical infrastructures in Europe, *Glob. Environ. Change*, 48, 97–107, 2018.

Fowler, H.J., Kilsby, C.G. Precipitation and the North Atlantic Oscillation: a study of climatic variability in northern England. *Int. J. Climatol.* 22, 7, 843–866. 2002.

Fowler, H. J. and Kilsby, C. G.: Precipitation and the North Atlantic Oscillation: a study of climatic variability in northern England, *Int. J. Climatol.*, 22, 843–866, 2002.

Fritier, N., Massei, N., Laignel, B., Durand, A., Dieppois, B., Deloffre, J., Links between NAO fluctuations and inter-annual variability of winter-months

precipitation in the Seine River watershed (north-western France). *Compt. Rendus Geosci.* 344, 8, 396–405. 2012.

Frankignoul, C., de Coëtlogon, G., Joyce, T.M., Dong, S. Gulf Stream variability and Ocean–Atmosphere interactions. *J. Phys. Oceanogr.* 31, 12, 3516–3529. 2001.

Gao, L., Deng, Y., Yan, X., Li, Q., Zhang, Y., and Gou, X.: The unusual recent streamflow declines in the Bailong River, north-central China, from a multi-century perspective, *Quat. Sci. Rev.*, 260, 106927, 2021.

Garamhegyi, T., Kovács, J., Pongrácz, R., Tanos, P., and Hatvani, I. G.: Investigation of the climate-driven periodicity of shallow groundwater level fluctuations in a Central-Eastern European agricultural region, *Hydrogeol. J.*, 26, 677–688, 2018.

Gericke, O. J. and Smithers, J. C.: Revue des méthodes d'évaluation du temps de réponse d'un bassin versant pour l'estimation du débit de pointe, *Hydrolog. Sci. J.*, 59, 1935–1971, 2014.

Ghasemi, A.R., Khalili, D. The association between regional and global atmospheric patterns and winter precipitation in Iran. *Atmos. Res.* 88, 2, 116–133. 2008.

Gibbons, S., Mourato, S., and Resende, G. M.: The Amenity Value of English Nature: A Hedonic Price Approach, *Environ. Resour. Econ.*, 57, 175–196, 2014.

Gimeno, L., Dominguez, F., Nieto, R., Trigo, R., Drumond, A., Reason, C. J. C., Taschetto, A. S., Ramos, A. M., Kumar, R., and Marengo, J.: Major Mechanisms of Atmospheric Moisture Transport and Their Role in Extreme Precipitation Events, *Annu. Rev. Environ. Resour.*, 41, 117–141, 2016.

Givati, A., Rosenfeld, D. The Arctic Oscillation, climate change and the effects on precipitation in Israel. *Atmos. Res.* 132–133, 114–124. 2013.

González-Hidalgo, J. C., Vicente-Serrano, S. M., Peña-Angulo, D., Salinas, C., Tomas-Burguera, M., and Beguería, S.: High-resolution spatio-temporal analyses of drought episodes in the western Mediterranean basin (Spanish mainland, Iberian Peninsula), *Acta Geophys.*, 66, 381–392, 2018.

Gnann, S. J., Howden, N. J. K., and Woods, R. A.: Hydrological signatures describing the translation of climate seasonality into streamflow seasonality, *Hydrol. Earth Syst. Sci.*, 24, 561–580, 2020.

Guilod, B. P., Jones, R. G., Dadson, S. J., Coxon, G., Bussi, G., Freer, J., Kay, A. L., Massey, N. R., Sparrow, S. N., Wallom, D. C. H., Allen, M. R., and Hall, J. W.: A large set of potential past, present and future hydro-meteorological time series for the UK, *Hydrol. Earth Syst. Sci.*, 22, 611–634, 2018.

Guimarães Nobre, G., Jongman, B., Aerts, J., and Ward, P. J.: The role of climate variability in extreme floods in Europe, *Environ. Res. Lett.*, 12, 084012, 2017.

Gurdak, J.J. Groundwater: climate-induced pumping. *Nat. Geosci.* 71, 10. 2017.

Gurdak, J.J., Hanson, R.T., McMahon, P.B., Bruce, B.W., McCray, J.E., Thyne, G.D., Reedy, R.C. Climate variability controls on unsaturated water and chemical movement, high Plains Aquifer, USA. *Vadose Zone J.* 6, 3, 533–547. 2007.

Gustard, A., Bullock, A., and Dixon, J. M.: Low flow estimation in the United Kingdom, IH Report No. 108, Institute of Hydrology, Wallingford, UK, 88 pp., <http://nora.nerc.ac.uk/id/eprint/6050> [Accessed: 14th July 2020], 1992.

Haarsma, R. J., Selten, F. M., and Drijfhout, S. S.: Decelerating Atlantic Meridional Overturning Circulation Main Cause of Future West European Summer Atmospheric Circulation Changes, *Environ. Res. Lett.*, 094007 , 2015.

Hanel, M., Rakovec, O., Markonis, Y., Máca, P., Samaniego, L., Kyselý, J., and Kumar, R.: Revisiting the recent European droughts from a long-term perspective, *Sci. Rep.*, 8, 9499, 2018.



Hanson, R.T., Dettinger, M.D., Newhouse, M.W. Relations between climatic variability and hydrologic time series from four alluvial basins across the southwestern United States. *Hydrogeol. J.* 14, 7, 1122–1146. 2006.

Hannaford, J. and Harvey, C.: UK seasonal river flow variability in near-natural catchments, regional outflows and long hydrometric records, in: BHS Third International Symposium, Managing Consequences of a Changing Global Environment, Newcastle, United Kingdom, 2010, 1–7, 2010.

Hannaford, J., Lloyd-Hughes, B., Keef, C., Parry, S., and Prudhomme, C.: Examining the large-scale spatial coherence of European drought using regional indicators of precipitation and streamflow deficit, *Hydrol. Process.*, 25, 1146–1162, 2011.

Hall, R J., and Hanna, E. “North Atlantic Circulation Indices: Links with Summer and Winter UK Temperature and Precipitation and Implications for Seasonal Forecasting.” *International Journal of Climatology*, 38, 660–677. 2018.

Hao, Z, Singh, V. P., and Xia, Y. “Seasonal Drought Prediction: Advances, Challenges, and Future Prospects.” *Reviews of Geophysics*, 56, 108–141, 2018.

Harris, G., Howard, T., Kaye, N., Kendon, E., Krijnen, J., Maisey, P., McDonald, R., McInnes, R., McSweeney, C., Mitchell, J., Murphy, J., Palmer, M., Roberts, C., Rostron, J., Sexton, D., Thornton, H., Tinker, J., Tucker, S., Yamazaki, K., and Belcher, S. UKCP18 Science Overview Report: UK Met Office. 2019.

Haslinger, K., Koffler, D., Schöner, W., and Laaha, G.: Exploring the link between meteorological drought and streamflow: Effects of climate-catchment interaction, *Water Resour. Res.*, 50, 2468–2487, 2014.

Hauser, T., Demirov, E., Zhu, J., Yashayaev, I. North Atlantic atmospheric and ocean inter-annual variability over the past fifty years — dominant patterns and decadal shifts. *Prog. Oceanogr.* 132, 197–219. 2015.

Healy, R. *Estimating Groundwater Recharge*. Cambridge University Press, London. 2010

Hellwig, J. and Stahl, K.: An assessment of trends and potential future changes in groundwater-baseflow drought based on catchment response times, *Hydrol. Earth Syst. Sci.*, 22, 6209–6224, 2018.

Hisdal, H., Stahl, K., Tallaksen, L. M., and Demuth, S.: Have streamflow droughts in Europe become more severe or frequent?, *Int. J. Climatol.*, 21, 317–333, 2001.

Holman, I.P. Climate change impacts on groundwater recharge — uncertainty, shortcomings, and the way forward? *Hydrogeol. J.* 14, 5, 637–647. 2006.

Holman, I.P., Rivas-Casado, M., Bloomfield, J.P., Gurdak, J.J. Identifying nonstationary groundwater level response to North Atlantic ocean-atmosphere teleconnection patterns using wavelet coherence. *Hydrogeol. J.* 19, 6, 1269–1278. 2011.

Holman, I.P., Rivas-Casado, M., Howden, N.J.K., Bloomfield, J.P. and Williams, A.T.: Linking North Atlantic ocean-atmosphere teleconnection patterns and hydrogeological responses in temperate groundwater systems. *Hydrological Processes*, 23, 3123–3126, 2009.

HR Wallingford. Updated projections of future water availability for the third UK Climate Change Risk Assessment. HR Wallingford Ltd. 2020.

Huang, Yu, Hong-Li Ren, Robin Chadwick, Zhigang Cheng, and Quanliang Chen. “Diagnosing Changes of Winter NAO in Response to Different Climate Forcings in a Set of Atmosphere-Only Timeslice Experiments.” *Atmosphere* 9, 10. 2018.

Hund, S. V., Allen, D.M., Morillas, L. and Johnson, M.S.: Groundwater recharge indicator as tool for decision makers to increase socio-hydrological resilience to seasonal drought. *Journal of Hydrology*, 563, 1119–1134, 2018.

Hurrell, J. Climate Analysis Section, NCAR, Boulder, USA. [Accessed 20<sup>th</sup> Dec 2020], 2003.

Hurrell, J.W. Decadal Trends in the North Atlantic Oscillation: regional temperature and precipitation. *Science* 5224, 269, 676–679. 1995.

Hurrell, J.W., Deser, C. North Atlantic climate variability: the role of the North Atlantic Oscillation. *J. Mar. Syst.* 79, 3–4, 231–244. 2010.

Hurrell, J.W., Van Loon, H. Decadal Variations in Climate Associated With the North Atlantic Oscillation. In: *Climatic Change at High Elevation Sites Vols. 36*, 3-4, 301–326. 1997.

Hurrell, J.W., Kushnir, Y., Ottersen, G., Visbeck, M. An Overview of the North Atlantic Oscillation. In: *The North Atlantic Oscillation: Climatic Significance and Environmental Impact*, 1–35, 2003.

Iles C, Hegerl G. Role of the North Atlantic Oscillation in decadal temperature trends. *Environ Res Lett.* 2017

Ionita, M. and Nagavciuc, V.: Forecasting low flow conditions months in advance through teleconnection patterns, with a special focus on summer 2018, *Sci. Rep.*, 10, 13258, 2020.

Jackson, C. R., Bloomfield, J. P., and Mackay, J. D.: Evidence for changes in historic and future groundwater levels in the UK, *Prog. Phys. Geogr.*, 39, 49–67, 2015.

Jasechko, S., Birks, S.J., Gleeson, T., Wada, Y., Fawcett, P.J., Sharp, Z.D., McDonnell, J.J. and Welker, J.M.: The pronounced seasonality of global groundwater recharge. *Water Resources Research*, 50, 8845–8867, 2014.

Jelena Luković, Branislav Bajat, Dragan Blagojević, M.K.: Spatial pattern of North Atlantic Oscillation impact on rainfall in Serbia. *Spatial Statistics.* 14, 39-52, 2014.

Joyce, T.M., Deser, C., Spall, M.A. The relation between decadal variability of subtropical mode water and the North Atlantic Oscillation. *J. Clim.* 13, 14, 2550–2569. 2000.

Kamruzzaman, M., Shahriar, M. S., and Beecham, S.: Assessment of short term rainfall and stream flows in South Australia, *Water*, 6, 3528–3544 , 2014.

Kane, R. P.: Quasi-Biennial and Quasi-Triennial Oscillations in some atmospheric parameters, *Pure Appl. Geophys.*, 147, 567–583, 1996.

Kashid, S. S., Ghosh, S., and Maity, R.: Streamflow prediction using multi-site rainfall obtained from hydroclimatic teleconnection, *J. Hydrol.*, 395, 23–38, 2010.

Kay, A. L., Watts, G., Wells, S. C., and Allen, S.: The impact of climate change on U. K. river flows: A preliminary comparison of two generations of probabilistic climate projections, *Hydrol. Process.*, 34, 1081–1088, 2020.

Kerr, R. A.: A north atlantic climate pacemaker for the centuries, *Science*, 288, 1984–1985, 2000.

Kim, J.-S., Seo, G.-S., Jang, H.-W., and Lee, J.-H.: Correlation analysis between Korean spring drought and large-scale teleconnection patterns for drought forecasting, 21, 458–466, 2017.

Kingston, D. G., Hannah, D. M., Lawler, D. M., and McGregor, G.: Regional Classification, Variability, and Trends of Northern North Atlantic River Flow, *Hydrol. Process.*, 25, 1021–1033, 2011.

Kingston, D.G., Lawler, D.M., McGregor, G.R. Linkages between atmospheric circulation, climate and streamflow in the northern North Atlantic: research prospects. *Prog. Phys. Geogr.* 30 (2), 143–174. 2006.

Kingston, D., McGregor, G., Hannah, D., Lawler, D. Large-scale climatic controls on New England River flow. *J. Hydrometeorol.* 8, 367–379. 2007.

Kjellström, E., Thejll, P., Rummukainen, M., Christensen, J. H., Boberg, F., Christensen, O. B., and Fox Maule, C.: Emerging regional climate change signals for Europe under varying large-scale circulation conditions, *Clim. Res.*, 56, 103–119, 2013.

Kloosterman, R. A., van der Hoek, J. P., and Herder, P.: Resilient Drinking Water Resources, *Water Resour. Manage.*, 35, 337–351, 2021.

Knippertz, P., Ulbrich, U., Marques, F. and Corte-Real, J.: Decadal changes in the link between El Niño and springtime North Atlantic oscillation and European–North African rainfall. *International Journal of Climatology*, 23, 1293–1311, 2003.

Kolusu, S. R., Shamsudduha, M., Todd, M. C., Taylor, R. G., Seddon, D., Kashaigili, J. J., Ebrahim, G. Y., Cuthbert, M. O., Sorensen, J. P. R., Villholth, K. G., MacDonald, A. M., and MacLeod, D. A.: The El Niño event of 2015–2016: climate anomalies and their impact on groundwater resources in East and Southern Africa, *Hydrol. Earth Syst. Sci.*, 23, 1751–1762, 2019.

Konapala, G., Mishra, A. K., Wada, Y., and Mann, M. E.: Climate change will affect global water availability through compounding changes in seasonal precipitation and evaporation, *Nat. Commun.*, 11, 3044, 2020.

Krichak, S.O. and Alpert, P.: Decadal Trends in the East Atlantic-West Russia Pattern and Mediterranean Precipitation. *International Journal of Climatology*. *International Journal of Climatology*, 25, 183–192, 2005.

Kronholm, S. and Capel, P.: Estimation of time-variable fast flow path chemical concentrations for application in tracer-based hydrograph separation analyses, *J. Am. Water Resour. As.*, 52, 6881–6896, 2016.

Küçük, M., Kahya, E., Cengiz, T. M., and Karaca, M.: North Atlantic Oscillation influences on Turkish lake levels, *Hydrol. Process.*, 23, 893–906, 2009.

Kumar, R., Musuuza, J.L., Van Loon, A.F., Teuling, A.J., Barthel, R., Broek, J. Ten, Mai, J., Samaniego, L., Attinger, S. Multiscale evaluation of the Standardized Precipitation Index as a groundwater drought indicator. *Hydrol. Earth Syst. Sci.* 1117–1131. 2016.

Kuss, A.M. and Gurdak, J.J.: Groundwater level response in U.S. principal aquifers to ENSO, NAO, PDO, and AMO. *Journal of Hydrology*, 519, 1939–1952, 2014.

Labat, D.: Cross Wavelet Analyses of Annual Continental Freshwater Discharge and Selected Climate Indices, *J. Hydrol.*, 385, 269–278, 2010.

Lane, R. A., Coxon, G., Freer, J. E., Wagener, T., Johnes, P. J., Bloomfield, J. P., Greene, S., Macleod, C. J. A., and Reaney, S. M.: Benchmarking the predictive capability of hydrological models for river flow and flood peak predictions across over 1000 catchments in Great Britain, *Hydrol. Earth Syst. Sci.*, 23, 4011–4032, 2019.

Lavers, D., Hannah, D., and Bradley, C. “Connecting Large-Scale Atmospheric Circulation, River Flow and Groundwater Levels in a Chalk Catchment in Southern England.” *Journal of Hydrology* 523, 179–189. 2015.

Lavers, D., Prudhomme, C., Hannah, D.M. Large-scale climate, precipitation and British river flows: identifying hydroclimatological connections and dynamics. *J. Hydrol.* 395, 3–4, 242–255. 2010.

Ledingham, J., Archer, D., Lewis, E., Fowler, H., and Kilsby, C.: Contrasting seasonality of storm rainfall and flood runoff in the UK and some implications for rainfall-runoff methods of flood estimation, *Hydrol. Res.*, 50, 1309–1323, 2019.

Lee, H.F. and Zhang, D.D.: Relationship between NAO and drought disasters in northwestern China in the last millennium. *Journal of Arid Environments*, 75, 1114–1120, 2011.

Liesch, T. and Wunsch, A.: Aquifer responses to long-term climatic periodicities, *J. Hydrol.*, 572, 226–242, 2019.

Loboda, N.S., Glushkov, A.V., Khokhlov, V.N., Lovett, L. Using non-decimated wavelet decomposition to analyse time variations of North Atlantic Oscillation, eddy kinetic energy, and Ukrainian precipitation. *J. Hydrol.* 322, 1–4, 14–24. 2006.

Lopez-Bustins, J.-A., Martin-Vide, J., Sanchez-Lorenzo, A. Iberia winter rainfall trends based upon changes in teleconnection and circulation patterns. *Glob. Planet. Chang.* 63,2–3, 171–176. 2008.

López-Moreno, J.I., Vicente-Serrano, S.M., Morán-Tejeda, E., Lorenzo-Lacruz, J., Kenawy, A. and Beniston, M.: Effects of the North Atlantic Oscillation (NAO)

on combined temperature and precipitation winter modes in the Mediterranean mountains: Observed relationships and projections for the 21st century. *Global and Planetary Change*, 77, 62–76, 2011.

Loucks, D. P. and van Beek, E.: Water Resources Planning and Management: An Overview, in: *Water Resource Systems Planning and Management: An Introduction to Methods, Models, and Applications*, edited by: Loucks, D. P. and van Beek, E., Springer International Publishing, Cham, 1–49, 2017.

Lowe, J., Bernie, D., Bett, P., Bricheno, L., Brown, S., Calvert, D., Clark, R., Eagle, K., Edwards, T., Fosser, G., Fung, F., Gohar, L., Good, P., Gregory, J., Luque-Espinar, J. A., Chica-Olmo, M., Pardo-Igúzquiza, E., and García-Soldado, M. J.: Influence of climatological cycles on hydraulic heads across a Spanish aquifer, *J. Hydrol.*, 354, 33–52, 2008.

Lü, A., Jia, S., Zhu, W., Yan, H., Duan, S., and Yao, Z.: El Niño-Southern Oscillation and water resources in the headwaters region of the Yellow River: links and potential for forecasting, *Hydrol. Earth Syst. Sci.*, 15, 1273–1281, 2011.

Luković, J., Blagojević, D., Kilibarda, M., Bajat, B., 2015. Spatial pattern of North Atlantic Oscillation impact on rainfall in Serbia. *Spat. Stat.* 14 Part A, 39–52.

Luo, D., and Gong, T. “A Possible Mechanism for the Eastward Shift of Interannual NAO Action Centers in Last Three Decades.” *Geophysical Research Letters* 33, L24815. 2006.

Luque-Espinar, J. A., Chica-Olmo, M., Pardo-Igúzquiza, E., and García-Soldado, M. J.: Influence of climatological cycles on hydraulic heads across a Spanish aquifer, *J. Hydrol.*, 354, 33–52, 2008. Mackay, J.D., Jackson, C.R., Brookshaw,

Mackay, J. D., Jackson, C. R., Brookshaw, A., Scaife, A. A., Cook, J., and Ward, R. S.: Seasonal forecasting of groundwater levels in principal aquifers of the United Kingdom, *J. Hydrol.*, 530, 815–828, 2015.

Magilligan, F.J., Graber, B.E. Hydroclimatological and geomorphic controls on the timing and spatial variability of floods in New England, USA. *J. Hydrol.* 178, 159–180, 1996.

Mahmoudi, P., Rigi, A., and Miri Kamak, M.: Evaluating the sensitivity of precipitation-based drought indices to different lengths of record, *J. Hydrol.*, 579, 124181, 2019.

Mahmood, S., Lewis, H., Arnold, A., Castillo, J., Sanchez, C., and Harris, C.: The impact of time-varying sea surface temperature on UK regional atmosphere forecasts, *Meteorol. Appl.*, 28, <https://doi.org/10.1002/met.1983>, 2021.

Marchant, B. P. and Bloomfield, J. P.: Spatio-temporal modelling of the status of groundwater droughts, *J. Hydrol.*, 564, 397–413 , 2018.

Mares, I., Mares, C., Mihailescu, M. NAO impact on the summer moisture variability across Europe. *Phys. Chem. Earth* 27, 1013–1017. 2002.

Marsh, T., Cole, G. and Wilby, R.: Major droughts in England, 1800 - 2006. *Weather*, 62, 2007.

Marsh, T. and Hannaford, J.: UK Hydrometric Register. Hydrological data UK series. Centre for Ecology and Hydrology, 214, 2008.

Massei, N., Durand, A., Deloffre, J., Dupont, J., Valdes, D., and Laignel, B. “Investigating Possible Links between the North Atlantic Oscillation and Rainfall Variability in Northwestern France over the Past 35 Years.” *Journal of Geophysical Research*, 112, D09121. 2007.

Massmann, C.: Reproducing different types of changes in hydrological indicators with rainfall-runoff models, 51, 238–256, 2020.

Mathias, S. A., McIntyre, N., and Oughton, R. H.: A study of non-linearity in rainfall-runoff response using 120 UK catchments, *J. Hydrol.*, 540, 423–436, 2016.



Meinke, H., de Voil, P., Hammer, G. L., Power, S., Allan, R., Stone, R. C., Folland, C., and Potgieter, A.: Rainfall variability of decadal and longer time scales: Signal or noise?, *J. Climate*, 18, 89–90, 2005.

Merino, A., López, L., Hermida, L., Sánchez, J.L., García-Ortega, E., Gascón, E., Fernández-González, S. Identification of drought phases in a 110-year record from Western Mediterranean basin: trends, anomalies and periodicity analysis for Iberian Peninsula. *Glob. Planet. Chang.* 133, 96–108, 2015.

Mideksa, T. and Kallbekken, S.: The impact of climate change on the electricity market: A review, *Energy Policy*, 38, 3579–3585, 2010.

Milly, P.C.D., Betancourt, J., Falkenmark, M., Hirsch, R.M., Kundzewicz, Z.W., Lettenmaier, D.P., Stouffer, R.J., Dettinger, M.D., Krysanova, V., On Critiques of “stationarity is Dead: Whither Water Management?”. *Water Resour. Res.* 51, 9, 7785–7789. 2008.

Mishra, A.K., Singh, V.P. A review of drought concepts. *J. Hydrol.* 391, 1–2, 202–216. 2010.

Misumi, R., Bell, V. A., and Moore, R. J.: River flow forecasting using a rainfall disaggregation model incorporating small-scale topographic effects, *Meteorol. Appl.*, 8, 297–305, 2001.

Moreira, E., Pires, C., and Pereira, L. “SPI Drought Class Predictions Driven by the North Atlantic Oscillation Index Using Log-Linear Modeling.” *WATER*, 8, 43, 2016.

Mullon, L., Chang, N.-B., Jeffrey Yang, Y., and Weiss, J.: Integrated remote sensing and wavelet analyses for screening short-term teleconnection patterns in northeast America, *J. Hydrol.*, 499, 247–264, 2013.

Murphy, S.J., Washington, R. United Kingdom and Ireland precipitation variability and the North Atlantic sea-level pressure field. *Int. J. Climatol.* 21, 8, 939–959. 2001.

Najafi, M. R., Zwiers, F. W., and Gillett, N. P.: Attribution of Observed Streamflow Changes in Key British Columbia Drainage Basins, *Geophys. Res. Lett.*, 44, 11012–11020, 2017.

Nathan, R. J. and McMahon, T. A.: Evaluation of automated techniques for base flow and recession analyses, *Water Resour. Res.*, 26, 1465–1473, 1990.

Naumann, G., Spinoni, J., Vogt, J. V., and Barbosa, P.: Assessment of drought damages and their uncertainties in Europe, *Environ. Res. Lett.*, 10, 124013, 2015.

Neves, M.C., Jerez, S. and Trigo, R.M.: The response of piezometric levels in Portugal to NAO, EA, and SCAND climate patterns. *Journal of Hydrology*, 568, 1105–1117, 2019.

Nimmo, J.R., 2005. Unsaturated Zone Flow Processes. *Encyclopedia of Hydrological Sciences*, pp. 24. Peings, Y., Magnusdottir, G. Forcing of the wintertime atmospheric circulation by the multidecadal fluctuations of the North Atlantic Ocean. *Environ. Res. Lett.* 9, 3, 34018, 2014.

NRFA: Streamflow and precipitation data, metadata, available at: <http://nrfa.ceh.ac.uk/> [last access: 14 July 2020], 2021.

OFWAT, Water Trading Report <https://www.ofwat.gov.uk/regulated-companies/markets/water-bidding-market/water-trading>. 2019.

Ockenden, M. C. and Chappell, N. A.: Identification of the dominant runoff pathways from data-based mechanistic modelling of nested catchments in temperate UK, *J. Hydrol.*, 402, 71–79, 2011.

Oikonomou, P. D., Karavitis, C. A., Tsesmelis, D. E., Kolokytha, E., and Maia, R.: Drought Characteristics Assessment in Europe over the Past 50 Years, *Water Resour. Manage.*, 34, 4757–4772, 2020.

Olsen, J., Anderson, N. J., and Knudsen, M. F.: Variability of the North Atlantic Oscillation over the past 5,200 years, *Nat. Geosci.*, 5, 808–812, 2012.

Ouachani, R., Bargaoui, Z., and Ouarda, T.: Power of teleconnection patterns on precipitation and streamflow variability of upper Medjerda Basin, *Int. J. Climatol.*, 33, 58–76, 2013.

Oschlies, A., Held, H., Keller, D., Keller, K., Mengis, N., Quaas, M., Rickels, W., and Schmidt, H.: Indicators and metrics for the assessment of climate engineering, *Earths Future*, 5, 49–58, 2017.

Padrón, R. S., Gudmundsson, L., Decharme, B., Ducharne, A., Lawrence, D. M., Mao, J., Peano, D., Krinner, G., Kim, H., and Seneviratne, S. I.: Observed changes in dry-season water availability attributed to human-induced climate change, *Nat. Geosci.*, 13, 477–481, 2020.

Parker, T., Woollings, T., Weisheimer, A., O'Reilly, C., Baker, L., and Shaffrey, L.: Seasonal Predictability of the Winter North Atlantic Oscillation from a Jet Stream Perspective, *Geophys. Res. Lett.*, 46, 10159–10167, 2019.

Pasquini, A.I., Lecomte, K.L., Piovano, E.L. and Depetris, P.J.: Recent rainfall and runoff variability in central Argentina. *Quaternary International*, 158, 127–139, 2006.

Pan, X., Wang, G., and Yang, P.: Introducing driving-force information increases the predictability of the North Atlantic Oscillation, *Atmospheric and Oceanic Science Letters*, 12, 329–336, 2019.

Pauling, A., Luterbacher, J., Casty, C., and Wanner, H. “Five Hundred Years of Gridded High-Resolution Precipitation Reconstructions over Europe and the Connection to Large-Scale Circulation.” *Climate Dynamics*, 26, 387–405. 2006.

Peings, Y. and Magnusdottir, G.: Forcing of the wintertime atmospheric circulation by the multidecadal fluctuations of the North Atlantic Ocean. *Environmental Research Letters*, 9, 34018, 2014.

Perveen, S.: Scale interactions and implications for water resources, hydrology, and climate, *J. Contemp. Water Res. Educ.*, 147, 1–7, 2012.

Peters, E. Propagation of Drought Through Groundwater Systems. PhD thesis Wageningen University. 2003.

Peters, E., Torfs, P.J.J.F., van Lanen, H.A.J., Bier, G. Propagation of drought through groundwater — a new approach using linear reservoir theory. *Hydrol. Process.* 17, 15, 3023–3040. 2003.

Peters, E., Bier, G., van Lanen, H.A.J., Torfs, P.J.J.F. Propagation and spatial distribution of drought in a groundwater catchment. *J. Hydrol.* 321, 1–4, 257–275, 2006.

Peterson, K. A, Lu, J., and Richard J. Greatbatch. “Evidence of Nonlinear Dynamics in the Eastward Shift of the NAO: The Eastward Shift of The Nao.” *Geophysical Research Letters*, 30, L1030. 2003.

Price, M., Downing, R.A. and Edmunds, W.M.: The chalk as an aquifer. In *The hydrogeology of the Chalk of North-West Europe*, Clarendon Press, Oxford, 2005.

Prudhomme, C., Hannaford, J., Harrigan, S., Boorman, D., Knight, J., Bell, V., Jackson, C., Svensson, C., Parry, S., Bachiller-Jareno, N., Davies, H., Davis, R., Mackay, J., McKenzie, A., Rudd, A., Smith, K., Bloomfield, J., Ward, R., and Jenkins, A.: Hydrological Outlook UK: an operational streamflow and groundwater level forecasting system at monthly to seasonal time scales, *Hydrol. Sci. J.*, 62, 2753–2768, 2017. Queralt, S., Hernández, E., Barriopedro, D., Gallego, D., Ribera, P., and Casanova, C.: North Atlantic Oscillation influence and weather types associated with winter total and extreme precipitation events in Spain, *Atmos. Res.*, 94, 675–683, 2009.

Ran, Y., Lannerstad, M., Herrero, M., Van Middelaar, C. E., and De Boer, I. J. M.: Assessing water resource use in livestock production: A review of methods, *Livest. Sci.*, 187, 68–79, 2016.

Rashid, M.M., Beecham, S. and Chowdhury, R.K.: Assessment of trends in point rainfall using Continuous Wavelet Transforms. *Advances in Water Resources*, 82, 1-15, 2015.

Rasouli, K., Scharold, K., Mahmood, T., Glenn, N., and Marks, D. "Linking Hydrological Variations at Local Scales to Regional Climate Teleconnection Patterns." *Hydrological Processes* 34, 5624–5641. 2020.

Rey, D., Pérez-Blanco, C.D., Escrivá-Bou, A., Girard, C. and Veldkamp, T.I.E.: Role of economic instruments in water allocation reform: lessons from Europe. *International Journal of Water Resources Development*, 35, 1–34, 2018.

Rial, J. A., Pielke, R. A., Sr, Beniston, M., Claussen, M., Canadell, J., Cox, P., Held, H., de Noblet-Ducoudré, N., Prinn, R., Reynolds, J. F., and Salas, J. D.: Nonlinearities, feedbacks and critical thresholds within the earth's climate system, *Clim. Change*, 65, 11–38, 2004.

Riaz, S., Iqbal, M., and Hameed, S. "Impact of the North Atlantic Oscillation on Winter Climate of Germany." *Tellus. Series A, Dynamic Meteorology and Oceanography*, 69, 1–10.1406263, 2017.

Riedel, T. and Weber, T. K. D.: Review: The influence of global change on Europe's water cycle and groundwater recharge, *Hydrogeol. J.*, 28, 1939–1959, 2020.

Robinson, E.L., Blyth, E., Clark, D.B., Comyn-Platt, E., Finch, J. and Rudd, A.C.: Climate hydrology and ecology research support system potential evapotranspiration dataset for Great Britain (1961 - 2015) [CHESS-PE], Centre for Ecology and Hydrology, 2016.

Robinson, E.L., Blyth, E.M., Clark, D.B., Finch, J. and Rudd, A.C.: Trends in atmospheric evaporative demand in Great Britain using high-resolution meteorological data, *Hydrology and Earth System Sciences*, 21, 1189-1224, 2017

Rodda, J. and Marsh, T.: The 1975-76 Drought - a contemporary and retrospective review. Centre for Ecology and Hydrology, 2011.

Rogers, A.N., Bromwich, D.H., Sinclair, E.N., Cullather, R.I. The Atmospheric Hydrologic Cycle over the Arctic Basin from Reanalyses. Part II: interannual variability. *J. Clim.* 14, 11, 2414–2429. 2001.

Rousi, E., Rust, H., Ulbrich, U., and Anagnostopoulou, C. “Implications of Winter NAO Flavors on Present and Future European Climate.” *Climate* 8, 13. 2020.

Rousi, E., Selten, F., Rahmstorf, S., and Coumou, D.: Changes in North Atlantic Atmospheric Circulation in a Warmer Climate Favor Winter Flooding and Summer Drought over Europe, *J. Clim.*, 34, 2277–2295, 2021.

Rousseau-Gueutin, P., Love, A.J., Vasseur, G., Robinson, N.I., Simmons, C.T., De Marsily, G. Time to reach near-steady state in large aquifers. *Water Resour. Res.* 49, 10, 6893–6908. 2013.

Routson, C.C., Woodhouse, C.A., Overpeck, J.T., Betancourt, J.L., McKay, N.P. Teleconnected ocean forcing of Western North American droughts and pluvials during the last millennium. *Quat. Sci. Rev.* 146, 238–250, 2016.

Rosch, A. and Schmidbauer, H.: *WaveletComp 1.1: a guided tour through the R package*, 2018.

Russo, T., Lall, U. Depletion and response of deep groundwater to climate-induced pumping variability. *Nat. Geosci.* 10, 105–108, 2017.

Rust, W., Corstanje, R., Holman, I.P., Milne, A.E. Detecting land use and land management influences on catchment hydrology by modelling and wavelets. *J. Hydrol.* 517, 378–389. 2014.

Rust, W., Holman, I., Corstanje, R., Bloomfield, J. and Cuthbert, M.: A conceptual model for climatic teleconnection signal control on groundwater variability in Europe. *Earth-Science Reviews*, 177, 164–174, 2018.

Rust, W., Holman, I., Bloomfield, J., Cuthbert, M., and Corstanje, R.: Understanding the potential of climate teleconnections to project future groundwater drought, *Hydrol. Earth Syst. Sci.*, **23**, 3233–3245, 2019.

Rust, W., Cuthbert, M., Bloomfield, J., Corstanje, R., Howden, N., and Holman, I.: Exploring the role of hydrological pathways in modulating multi-annual climate teleconnection periodicities from UK rainfall to streamflow, *Hydrol. Earth Syst. Sci.*, **25**, 2223–2237, 2021a.

Rust, W., Bloomfield, J. P., Cuthbert, M. O., Corstanje, R., and Holman, I. P.: Non-stationary control of the NAO on European rainfall and its implications for water resource management, *Hydrol. Process.*, **35**, 2021b.

Rust, W., Bloomfield, J., Cuthbert, M., Corstanje, R., and Holman, I.: The importance of non-stationary multiannual periodicities in the NAO index for forecasting water resource extremes, *Hydrol. Earth Syst. Sci. Discuss.* [preprint], <https://doi.org/10.5194/hess-2021-572>, in review, 2021.

Ryu, J. H., Svoboda, M. D., Lenters, J. D., Tadesse, T., and Knutson, C. L.: Potential extents for ENSO-driven hydrologic drought forecasts in the United States, *Clim. Change*, **101**, 575–597, 2010.

Sagir, S., Karatay, S., Atici, R., Yesil, A., and Ozcan, O.: The relationship between the Quasi Biennial Oscillation and Sunspot Number, *Adv. Space Res.*, **55**, 106–112, 2015.

Samaniego, L., Thober, S., Wanders, N., Pan, M., Rakovec, O., Sheffield, J., Wood, E. F., Prudhomme, C., Rees, G., Houghton-Carr, H., Fry, M., Smith, K., Watts, G., Hisdal, H., Estrela, T., Buontempo, C., Marx, A., and Kumar, R.: Hydrological Forecasts and Projections for Improved Decision-Making in the Water Sector in Europe, *Bull. Am. Meteorol. Soc.*, **100**, 2451–2472, 2019.

Sang, Y.-F.: A review on the applications of wavelet transform in hydrology time series analysis, *Atmos. Res.*, **122**, 8–15, 2013.

Saunders, K.M., Kamenik, C., Hodgson, D.A., Hunziker, S., Siffert, L., Fischer, D., Fujak, M., Gibson, J.A.E., Grosjean, M. Late Holocene changes in precipitation in northwest Tasmania and their potential links to shifts in the Southern Hemisphere westerly winds. *Glob. Planet. Chang.* 92–93, 82–91, 2012.

Scaife, A. A., Arribas, A., Blockley, E., Brookshaw, A., Clark, R. T., Dunstone, N., Eade, R., Fereday, D., Folland, C. K., Gordon, M., Hermanson, L., Knight, J. R., Lea, D. J., MacLachlan, C., Maidens, A., Martin, M., Peterson, A. K., Smith, D., Vellinga, M., Wallace, E., Waters, J., and Williams, A.: Skillful long-range prediction of European and North American winters, *Geophys. Res. Lett.*, 41, 2514–2519, 2014. Scaife, A. A., Folland, C. K., Alexander, L. V., Moberg, A., Brown, S., and Knight, J. R. European climate extremes and the North Atlantic Oscillation, *J. Climate*, 21, 72–83. 2008.

Schneider, C., Laizé, C. L. R., Acreman, M. C., and Flörke, M.: How will climate change modify river flow regimes in Europe?, *Hydrol. Earth Syst. Sci.*, 17, 325–339, 2013.

Schneider, U; Becker, A., Finger, P; Meyer-Christoffer, A. and Ziese, M. GPCP Full Data Monthly Product Version 2018 at 1.0°: Monthly Land-Surface Precipitation from Rain-Gauges built on GTS-based and Historical Data. 2018.

Schellekens, J., Heidecke, L., Nguyen, N., Spit, W.: The Economic Value of Water - Water as a Key Resource for Economic Growth in the EU Report. Ecorys. 2018.

Schwartz, F.W., Sudicky, E.A., McLaren, R.G., Park, Y.-J., Huber, M., Apter, M. Ambiguous hydraulic heads and 14C activities in transient regional flow. *Ground Water* 48, 366–379, 2010.

Seager, R., Battisti, D.S., Yin, J., Gordon, N., Naik, N., Clement, A., Cane, M. Is the Gulf Stream responsible for Europe's mild winters? *Q. J. R. Meteorol. Soc.* 128, 586, 2563–2586. 2002.



Shabbar, A., Huang, J., Higuchi, K. The relationship between the wintertime North Atlantic oscillation and blocking episodes in the North Atlantic. *Int. J. Climatol.* 21, 3, 355–369. 2001.

Sickmoller, M., Blender, R., Fraedrich, K. Observed winter cyclone tracks in the northern hemisphere in re-analysed ECMWF data. *Q. J. R. Meteorol. Soc.* 126, 591–620. 2000.

Simpson, M.J., Jazaei, F., Clement, T.P. How long does it take for aquifer recharge or aquifer discharge processes to reach steady state? *J. Hydrol.* 501, 241–248. 2013.

Singh, S., Srivastava, P., Abebe, A., Mitra, S. Baseflow response to climate variability induced droughts in the Apalachicola–Chattahoochee–Flint River Basin, U.S.A. *J. Hydrol.* 528, 550–561. 2015.

Smith, D M., Scaife, A., Eade, R., and Knight, J. “Seasonal to Decadal Prediction of the Winter North Atlantic Oscillation: Emerging Capability and Future Prospects: Seasonal to Decadal Prediction of the NAO.” *Quarterly Journal of the Royal Meteorological Society*, 142, 611–617. 2016.

Soediono, B. Impact of the North Atlantic Oscillation on river runoff in Poland Dariusz. *J. Chem. Inf. Model.* 53, 160. 1989.

Spinoni, J., Naumann, G., Vogt, J. V., and Barbosa, P.: The biggest drought events in Europe from 1950 to 2012, 3, 509–524, 2015.

Sprouse, T. W. and Vaughan, L. F.: Water Resource Management in Response to El Niño/Southern Oscillation (ENSO) Droughts and Floods, in: *Climate and Water: Transboundary Challenges in the Americas*, edited by: Diaz, H. F. and Morehouse, B. J., Springer Netherlands, Dordrecht, 117–143, 2003.

Stagge, J. H., Kingston, D. G., Tallaksen, L. M., and Hannah, D. M.: Observed drought indices show increasing divergence across Europe, *Sci. Rep.*, 7, 14045, 2017.

Stein, U., Özerol, G., Tröltzsch, J., Landgrebe, R., Szendrenyi, A., and Vidaurre, R. "European Drought and Water Scarcity Policies." In *Governance for Drought Resilience: Land and Water Drought Management in Europe*, edited by Hans Bressers, Nanny Bressers, and Corinne Larrue, 17–43. Springer International Publishing. 2016.

Su, L., Miao, C., Borthwick, A.G.L. and Duan, Q.: Wavelet-based variability of Yellow River discharge at 500-, 100-, and 50-year timescales. *Gondwana Research*, 49, 94–105, 2017.

Sun, Q., Miao, C., Duan, Q., Ashouri, H., Sorooshian, S., and Hsu, K "A Review of Global Precipitation Data Sets: Data Sources, Estimation, and Intercomparisons." *Reviews of Geophysics*, 56, 79–107. 2018

Sutanto, S. J., Van Lanen, H. A. J., Wetterhall, F., and Llort, X.: Potential of Pan-European Seasonal Hydrometeorological Drought Forecasts Obtained from a Multihazard Early Warning System, *Bull. Am. Meteorol. Soc.*, 101, E368–E393, 2020.

Svensson, C., Brookshaw, A., Scaife, A. A., Bell, V. A., Mackay, J. D., Jackson, C. R., Hannaford, J., Davies, H. N., Arribas, A., and Stanley, S.: Long-Range Forecasts of UK Winter Hydrology, *Environ. Res. Lett.*, 10, 064006, 2015.

Świerczyńska-Chłaściak, M. and Niedzielski, T. "Forecasting the North Atlantic Oscillation Index Using Altimetric Sea Level Anomalies." *Acta Geodaetica et Geophysica*, 55, 531–553. 2020.

Szolgayova, E., Parajka, J., Bloßchl, G. and Bucher, C.: Long term variability of the Danube River flow and its relation to precipitation and air temperature. *Journal of Hydrology*, 519, 871–880, 2014.

Tabari, H., Hosseinzadeh Talaei, P., Willems, P. Links between Arctic Oscillation (AO) and inter-annual variability of Iranian evapotranspiration. *Quat. Int.* 345, 148–157. 2014.

Tallaksen, L.M., Hisdal, H., Van Lanen, H.A.J. Propagation of drought in a groundwater fed catchment, the Pang in the UK. In: *Climate Variability and Change: Hydrological Impacts*, 128–133, 2006.

Tallaksen, L.M., Hisdal, H., van Lanen, H.A.J. Space-time modelling of catchment scale drought characteristics. *J. Hydrol.* 375, 3–4, 363–372. 2009.

Tashie, A., Scaife, C. I., and Band, L. E.: Transpiration and subsurface controls of streamflow recession characteristics, <https://doi.org/10.1002/hyp.13530>, 2018.

Tanguy, M., Dixon, H., Prosdocimi, I., Morris, D. and Keller, V.D.J.: Gridded estimates of daily and monthly areal rainfall for the United Kingdom (1890 - 2015) [CEH-GEAR]. NERC Environmental Information Data Centre, Wallingford, 2016.

Tanguy, M., Dixon, H., Prosdocimi, I., Morris, D. G., and Keller, V. D. J.: Gridded estimates of daily and monthly areal rainfall for the United Kingdom (1890–2017) [CEH-GEAR], NERC Environmental Information Data Centre, Wallingford, UK, 2019.

Tanguy, M., Haslinger, K., Svensson, C., Parry, S., Barker, L. J., Hannaford, J., and Prudhomme, C.: Regional Differences in Spatiotemporal Drought Characteristics in Great Britain, *Front. Environ. Sci. Eng. China*, 9, 67, 2021.

Taylor, A. North-south shifts of the Gulf Stream: Ocean-atmosphere interactions in the North Atlantic. *Int. J. Climatol.* 16, 559–583, 1995.

Taylor, A.H., Stephens, J.A. The North Atlantic oscillation and the latitude of the Gulf Stream. *Tellus* 50A, 134–142, 1998.

Todd, B., Macdonald, N., Chiverrell, R.C., Caminade, C. and Hooke, J.M.: Severity, duration and frequency of drought in SE England from 1697 to 2011. *Climatic Change*, 121, 673–687, 2013.

Tošić, I., Zorn, M., Ortar, J., Unkašević, M., Gavrilov, M.B., Marković, S.B. Annual and seasonal variability of precipitation and temperatures in Slovenia from 1961 to 2011. *Atmos. Res.* 168, 220–233, 2016.

Totz, S., Tziperman, E., Coumou, D., Pfeiffer, K., and Cohen, J. "Winter Precipitation Forecast in the European and Mediterranean Regions Using Cluster Analysis: Winter Precipitation Forecast." *Geophysical Research Letters*, 44, 418-426. 2017.

Townley, L.R. The response of aquifers to periodic forcing. *Adv. Water Resour.* 18, 3, 125–146, 1995.

Tremblay, L., Larocque, M., Anctil, F. and Rivard, C.: Teleconnections and interannual variability in Canadian groundwater levels. *Journal of Hydrology*, 410, 178–188, 2011.

Trenberth, K.E. Northern Hemisphere Climate Change: Physical Processes and Observed Changes. In: Mooney, H.A., Fuentes, E.R., Kronberg, B.I. (Eds.), *Earth System Responses to Global Change: Contrasts between North and South America*. Academic Press, 35–59, 1993.

Trigo, R.M., Osborn, T.J., Corte-real, J.M. The North Atlantic Oscillation influence on Europe: climate impacts and associated physical mechanisms. *Clim. Res.* 20, 9–17, 2002.

Trigo, R.M., Pozo-Vázquez, D., Osborn, T.J., Castro-Díez, Y., Gámiz-Fortis, S., EstebanParra, M.J. North Atlantic oscillation influence on precipitation, river flow and water resources in the Iberian Peninsula. *Int. J. Climatol.* 24, 8, 925–944. 2004.

Tsanis, I., and Tapoglou, E. "Winter North Atlantic Oscillation Impact on European Precipitation and Drought under Climate Change." *Theoretical and Applied Climatology* 135, 323–330. 2019.

Türkeş, M., Ertat, E. Precipitation changes and variability in Turkey linked to the North Atlantic oscillation during the period 1930–2000. *Int. J. Climatol.* 23, 14, 1771–1796, 2003

Turner, S., Barker, L. J., Hannaford, J., Muchan, K., Parry, S., and Sefton, C.: The 2018/2019 drought in the UK : a hydrological appraisal, *Weather*, 76, 248–253, 2021.

Uvo, C.B. Analysis and regionalization of northern European winter precipitation based on its relationship with the North Atlantic oscillation. *Int. J. Climatol.* 23, 10, 1185–1194. 2003.

Uvo, C. B., Foster, K., and Olsson, J.: The spatio-temporal influence of atmospheric teleconnection patterns on hydrology in Sweden, 34, 100782, 2021.

Van Loon, A.F. On the propagation of drought: How climate and catchment characteristics influence hydrological drought development and recovery. PhD thesis Wageningen University. 2013.

Van Loon, A.F. On the propagation of drought: How climate and catchment characteristics influence hydrological drought development and recovery. Ph.D thesis. Wageningen University, 2013.

Van Loon, A.F. Hydrological drought explained. *Wiley Interdiscip. Rev. Water* 2, 4, 359–392, 2015.

Van Loon, A.F., Van Huijgevoort, M.H.J., Van Lanen, H.A.J. Evaluation of drought propagation in an ensemble mean of large-scale hydrological models. *Hydrol. Earth Syst. Sci.* 16, 4057–4078, 2012.

Van Loon, A.F., Tijdeman, E., Wanders, N., Van Lanen, H.A.J., Teuling, A.J., Uijlenhoet, R. How climate seasonality modifies drought duration and deficit. *J. Geophys. Res.-Atmos.* 119, 8, 4640–4656, 2014.

Velasco, E.M., Gurdak, J.J., Dickinson, J.E., Ferré, T.P.A. and Corona, C.R.: Interannual to multidecadal climate forcings on groundwater resources of the U.S. West Coast. *Journal of Hydrology: Regional Studies*, 159, 16, 2015.

Vázquez, M., Nieto, R., Liberato, M., and Gimeno, L.: Global moisture transport and the role of major teleconnection patterns, EGU21–9326, 2021.

Vicente-Serrano, S M., and López-Moreno J. Nonstationary Influence of the North Atlantic Oscillation on European Precipitation. *Journal of Geophysical Research* 113 (D20). 2008.

Visser, A., Beevers, L., and Patidar, S.: The impact of climate change on hydroecological response in chalk streams, *Water*, 11, 596, 2019.

Wallace, J.M., Gutzler, D.S. Teleconnections in the Geopotential Height Field during the Northern Hemisphere Winter. *Mon. Weather Rev.* 109, 4, 784–812, 1981.

Walter, K., Graf, H.-F. The North Atlantic variability structure, storm tracks, and precipitation depending on the polar vortex strength. *Atmos. Chem. Phys.* 4, 5, 6127–6148, 2005.

Wang, H., Kumar, A. Assessing the impact of ENSO on drought in the U.S. Southwest with NCEP climate model simulations. *J. Hydrol.* 526, 30–41. 2015.

Wang, H., Chen, Y., Pan, Y., Li, W. Spatial and temporal variability of drought in the arid region of China and its relationships to teleconnection indices. *J. Hydrol.* 523, 283–296, 2015.

Water UK. Water Resources Long Term Planning Framework (2015–2065): Technical Report. Waker, UK Available at: <http://www.water.org.uk/waterresources-long-term-planning-framework>, [Accessed: 8th August 2017]. 2016.

Watelet, S., Beckers, J. M., and Barth, A.: Reconstruction of the Gulf Stream from 1940 to the present and correlation with the North Atlantic Oscillation, *J. Phys. Oceanogr.*, 47, 2741–2754, 2017.

Watts, G., Hisdal, H., Estrela, T., Buontempo, C., Marx, A., and Kumar, R.: Hydrological Forecasts and Projections for Improved Decision-Making in the Water Sector in Europe, *Bull. Am. Meteorol. Soc.*, 100, 2451–2472, 2019.

Weber, K. and Stewart, M.: A Critical Analysis of the Cumulative Rainfall Departure Concept, *Groundwater*, 42, 935-938, 2004.

Wedgbrow, R.L., Fox, H.R., O'Hare, G., Wilby, C.S. Prospects for seasonal forecasting of Summer Drought and Low River flow anomalies in England and Wales. *Int. J. Climatol.* 22, 219–236. 2002.

West, H., Quinn, N., and Horswell, M.: Regional rainfall response to the North Atlantic Oscillation (NAO) across Great Britain, *Hydrol. Res.*, 50, 1549–1563, 2019.

Wilby, R.L., O'Hare, G., Barnsley, N. The North Atlantic Oscillation and British Isles climate variability, 1865–1996. *Weather* 52, 9, 266–276. 1997

Wilby, R. L.: When and where might climate change be detectable in UK river flows?, *Geophys. Res. Lett.*, 33, L19407, 2006.

Woodhouse, C., A., Meko, D., M., Bigio, E., R., A Long View of Southern California Water Supply: Perfect Droughts Revisited. *Journal of the American Water Resources Association.* 56, 2, 212 – 230, 2020.

Woollings, T. and Blackburn, M.: The North Atlantic Jet Stream under Climate Change and Its Relation to the NAO and EA Patterns, *J. Climate*, 25, 886–902, 2012.

World Bank Group. High and Dry: Climate Change, Water and the Economy. International Bank for Reconstruction and Development / The World Bank. 2016.

Wrzesiński, D. and Paluszkiewicz, R.: Spatial differences in the impact of the North Atlantic Oscillation on the flow of rivers in Europe, 42, 30–39, 2011.

Wu, H., Hayes, M. J., Wilhite, D. A., and Svoboda, M. D.: The effect of the length of record on the standardized precipitation index calculation, *Int. J. Climatol.*, 25, 505–520, 2005.

Wu, Y., Zhang, G., Shen, H., and Xu, Y. J.: Nonlinear Response of Streamflow to Climate Change in High-Latitude Regions: A Case Study in Headwaters of Nenjiang River Basin in China's Far Northeast, *Water*, 10, 294, 2018.

Wyatt, M.G., Kravtsov, S., Tsonis, A.A. Atlantic Multidecadal Oscillation and Northern Hemisphere's climate variability. *Clim. Dyn.* 38, 5–6, 929–949, 2012.

Yuan, X., Zhang, M., Wang, L., and Zhou, T.: Understanding and seasonal forecasting of hydrological drought in the Anthropocene, *Hydrol. Earth Syst. Sci.*, 21, 5477–5492, 2017.

Yu, H.-L., Lin, Y.-C. Analysis of space–time non-stationary patterns of rainfall–groundwater interactions by integrating empirical orthogonal function and cross wavelet transform methods. *J. Hydrol.* 525, 585–597, 2015  
Zanchettin, D., Rubino, A., Traverso, P., and Tomasino, M.: Impact of variations in solar activity on hydrological decadal patterns in northern Italy, *J. Geophys. Res.*, 113, 2008.

Zhang, X. J., Jin, L. Y., Chen, C. Z., Guan, D. S., and Li, M. Z.: Interannual and interdecadal variations in the North Atlantic Oscillation spatial shift, *Chinese Sci. Bull.*, 56, 2621–2627, 2011

Zhang, W., Mei, X., Geng, X., Turner, A. G., and Jin, F.-F.: A Nonstationary ENSO–NAO Relationship Due to AMO Modulation, *J. Clim.*, 32, 33–43, 2019.







## APPENDICES

### Appendix A **Published Articles**

Rust, W., Hidden climate signals to improve water resource management. WWT Magazine. Faversham House Publishing. 2017.

Rust, W., Holman, I., Corstanje, R., Bloomfield, J., and Cuthbert, M.: A conceptual model for climatic teleconnection signal control on groundwater variability in Europe, *Earth-Sci. Rev.*, 177, 164–174, 2018.

Rust, W., Holman, I., Bloomfield, J., Cuthbert, M., and Corstanje, R.: Understanding the potential of climate teleconnections to project future groundwater drought, *Hydrol. Earth Syst. Sci.*, 23, 3233–3245, 2019.

Rust, W., Cuthbert, M., Bloomfield, J., Corstanje, R., Howden, N., and Holman, I.: Exploring the role of hydrological pathways in modulating multi-annual climate teleconnection periodicities from UK rainfall to streamflow, *Hydrol. Earth Syst. Sci.*, 25, 2223–2237, 2021a.

Rust, W., Bloomfield, J. P., Cuthbert, M. O., Corstanje, R., and Holman, I. P.: Non-stationary control of the NAO on European rainfall and its implications for water resource management, *Hydrol. Process.*, 35, 2021b.

Rust, W., Bloomfield, J., Cuthbert, M., Corstanje, R., and Holman, I.: The importance of non-stationary multiannual periodicities in the NAO index for forecasting water resource extremes, *Hydrol. Earth Syst. Sci. Discuss.* [preprint], <https://doi.org/10.5194/hess-2021-572>, in review, 2021.

Rust, W. Can we predict the UK's next major drought? *The Environment*. CIWEM. Syon Media. 2021.

## Appendix B Conference Papers

Rust, W. Understanding the potential of groundwater teleconnections to forecast hydrological extremes. EGU 2019, Vienna. 2019.

Rust, W. Understanding the potential of groundwater teleconnections to forecast hydrological extremes. 14th Groundwater Modellers' Forum and Darcy Lecture, Birmingham. 2016

Rust, W. Unearthing a hidden cycle in UK water extremes. CIWEM webinar, London. 2020.

Rust, W. Unearthing a hidden cycle in UK water extremes. BHS lunchtime webinar, London. 2021.

Rust, W. Exploring the role of hydrological pathways in modulating North Atlantic Oscillation (NAO) teleconnection periodicities from rainfall to streamflow. AGU 2020: Online Poster. 2020.

## Appendix C **Supplementary Material**

The following supplementary materials are associated with Rust et al (2019).

**Table 2 - Borehole sites used**

Site Number	Site ID	Borehole Name	Aquifer Group	Record length (months)	Number of gaps	Longest gap (months)
1	SP90/64	Ashley Green STW	Chalk	350	0	0
2	SY68/34	Ashton Farm	Chalk	516	2	4
3	TA10/63	Aylesby	Chalk	460	2	9
4	TQ21/161	Beeding Hill	Chalk	447	1	4
5	SU61/47	Catherington	Chalk	576	2	4
6	TQ01/133	Chantry Post Sullington	Chalk	456	5	17
7	SU81/1	Chilgrove House	Chalk	2,173	0	0
8	TQ25/86	Chipstead	Chalk	893	7	10
9	SU34/8D	Clanville Lodge Gate	Chalk	253	1	4
10	SU71/23	Compton House	Chalk	1,476	2	13
11	SE94/5	Dalton Holme	Chalk	1,537	0	0
12	TM15/112	Dial Farm	Chalk	585	3	5
13	TL79/25	Frying Pan Lodge	Chalk	545	3	4
14	SU47/141	Gibbet Cottages	Chalk	521	0	0
15	TL89/37	Grimes Graves	Chalk	449	3	8
16	TA02/104	Horkstow Road	Chalk	417	1	3
17	TQ31/46	Houdean Bottom	Chalk	481	1	3
18	SU33/12	Kings Somborne	Chalk	363	1	6
19	TL12/122	Lilley Bottom	Chalk	438	0	0
20	TR14/9	Little Bucket Farm	Chalk	553	1	4

21	ST07/10	Pant y Lladron	Chalk	262	1	5
22	TL44/12	Redlands Hall	Chalk	643	2	17
23	SU17/57	Rockley	Chalk	1,018	2	9
24	TL84/6	Smeetham Hall Cottages	Chalk	622	3	11
25	TF83/1	South Creake	Chalk	749	4	9
26	SU78/45A	Stonor Park	Chalk	670	1	3
27	TL33/4	Therfield Rectory	Chalk	1,610	2	48
28	SU74/40B	Tile Barn Farm	Chalk	544	1	121
29	SU04/2	Tilshead	Chalk	613	6	23
30	TF81/2A	Washpit Farm	Chalk	802	5	5
31	TQ25/13	Well House Inn	Chalk	888	5	4
32	TV59/7C	West Dean No. 3	Chalk	922	1	22
33	SU01/5B	West Woodyates Manor	Chalk	901	8	9
34	SE95/6	Wetwang	Chalk	544	1	3
35	SK15/16	Alstonefield	Limestone	513	1	5
36	SE44/80	Brick House Farm	Limestone	448	1	15
37	SE35/4	Castle Farm	Limestone	549	4	25
38	SN00/11	Greenfield Garage	Limestone	274	0	0
39	SK17/13	Hucklow South	Limestone	574	5	7
40	TF03/37	New Red Lion	Limestone	932	1	296
41	NZ22/53	Newton Aycliffe	Limestone	584	5	75
42	NZ21/29	Swan House	Limestone	556	1	33
43	SP00/62	Ampney Crucis	Oolite	699	0	0
44	ST88/62A	Didmarton 1	Oolite	472	4	7
45	ST51/57	Over Compton	Oolite	545	6	5
46	NY00/328	Brownbank Layby	Sandstone	487	5	26

47	SX99/37B	Bussels No. 7A	Sandstone	544	0	0
48	SD27/6B	Furness Abbey	Sandstone	526	4	21
49	SJ62/112	Heathlanes	Sandstone	547	4	7
50	SJ15/13	Llanfair Dyffryn Clwyd	Sandstone	540	0	0
51	SK67/17	Morris Dancers	Sandstone	568	1	9
52	NX97/2	Newbridge	Sandstone	287	0	0
53	SK00/41	Nuttalls Farm	Sandstone	510	1	8
54	NT94/3B	Royalty Observation	Sandstone	314	1	3
55	NY63/2	Skirwith	Sandstone	460	2	35
56	SK10/9	Weeford Flats	Sandstone	603	2	12
57	SD41/32	Yew Tree Farm	Sandstone	525	4	27
58	ST30/7	Lime Kiln Way	Greensand	578	2	8
59	TQ41/82	Lower Barn Cottage	Greensand	502	3	3

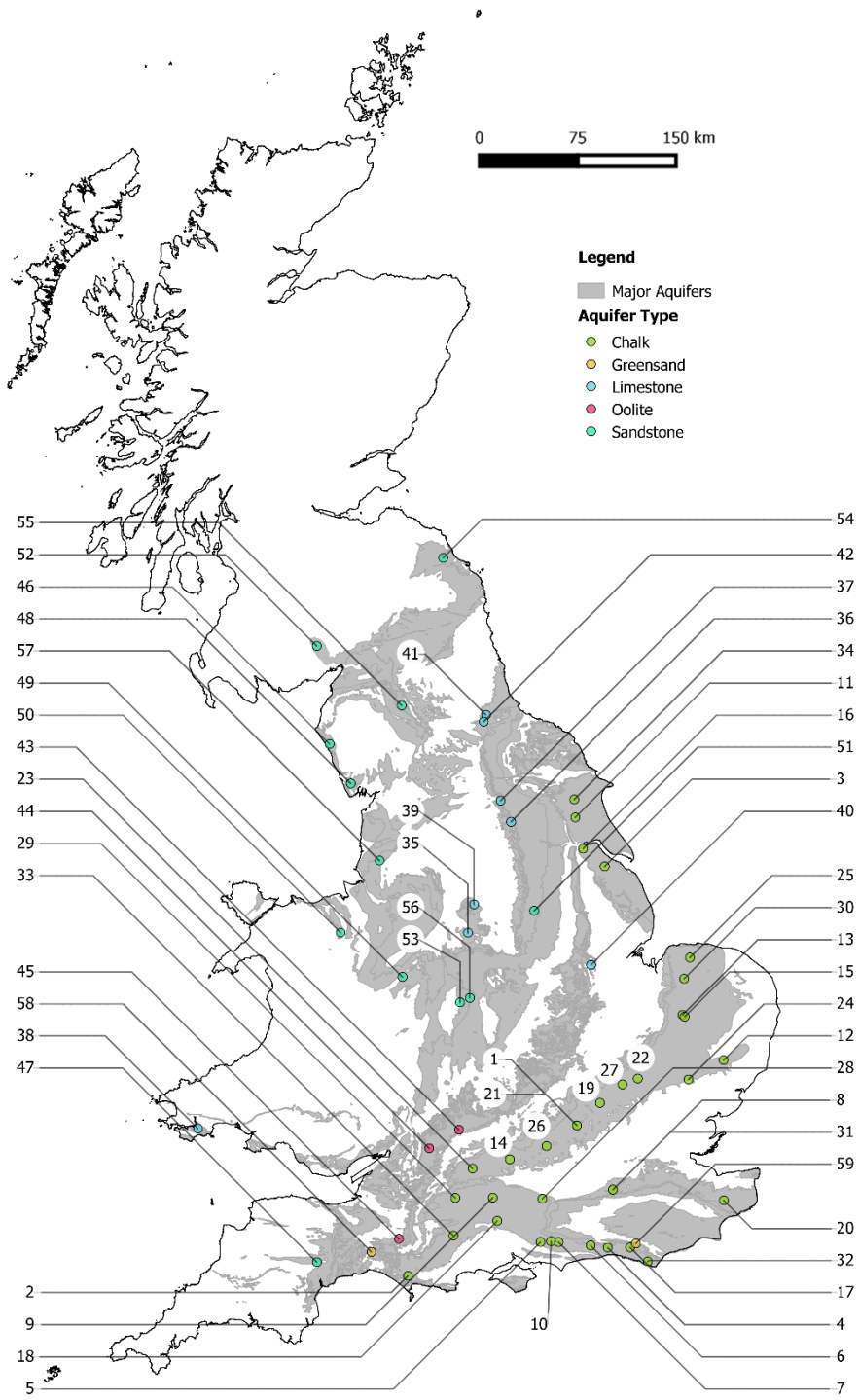


Figure 28 - Location of observation boreholes used in this study with their Site numbers, and major aquifers in the UK



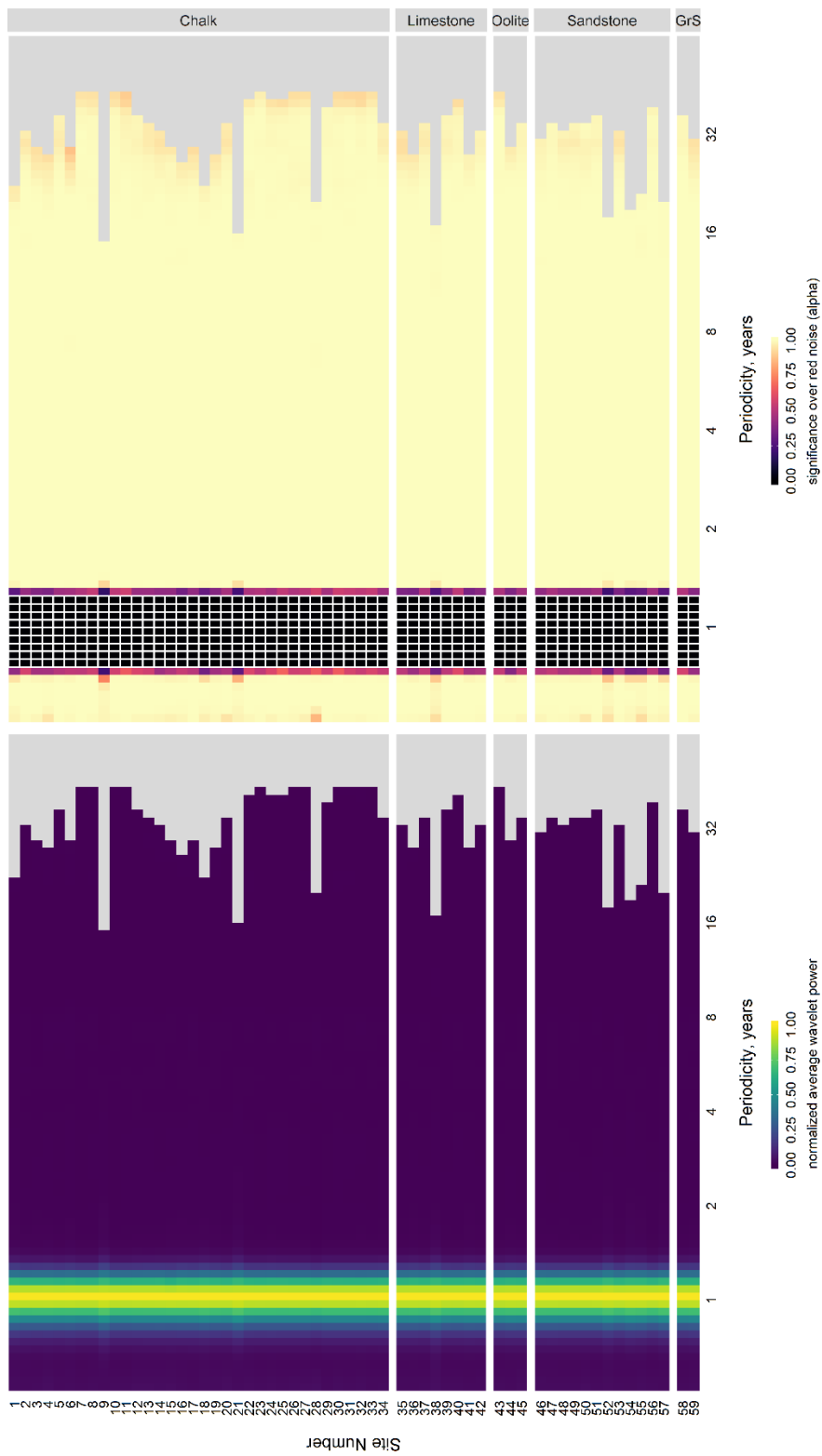


Figure 3 - Normalised average wavelet power spectra (left) and wavelet power significance alphas (right) for monthly PET time series for co-locations of the 59 index

boreholes. In the right-hand figure, boxes outlined in white are those powers that are significant over red noise to a 95% confidence interval ( $\alpha \leq 0.05$ ).